Steir. Beitr. z. Hydrogeologie / 43 / Seiten 9–158 / Graz 1992

Investigations with Natural and Artificial Tracers in the Karst Aquifer of the Lurbach System (Peggau–Tanneben–Semriach, Austria)

(H. BEHRENS, R. BENISCHKE, M. BRICELJ, T. HARUM, W. KÄSS, G. KOSI, H.P. LEDITZKY, Ch. LEIBUNDGUT, P. MALOSZEWSKI, V. MAURIN, V. RAJNER, D. RANK, B. REICHERT, H. STADLER, W. STICHLER, P. TRIMBORN, H. ZOJER, M. ZUPAN)

Content

1. Introduction

1.1. Scope of the Study (H. ZOJER)

The investigation area, the region between Semriach and Peggau, is the central part of the so-called "Central Styrian Karst". It comprises the basin of Semriach to the limestone areas of Eichberg via Tanneben east of the village Peggau.

The water disappearing east of the paleozoic limestone area in the Katzenbach, Eisgrube and the Lurbach sinkhole traverses the karst massif of Tanneben and re-emerges in the springs of the cave Lurgrotte – they are unified to a cave stream called Schmelzbach emerging at the lower entrance of the cave – and in the Hammerbach at the basis of the Peggauer Wand.

The area of Semriach–Peggau is closely linked with the progress of the artificial tracing technology. After intensive studies of the geological and speleological features it was tried for the first time in the year 1927 to clarify the subsurface drainage by means of artificial tracers (G. KYRLE, 1928). The experiment failed. So it was 1952, when an underground connection between the Lurbach sinkhole and the Hammerbach was proved (V. MAURIN, 1952). Further experiments were carried out in the following decades, starting in the seventies more intensively on the occasion of international courses.

Remembering these experiments it must also be stated, that the region of Semriach–Peggau was the first field area of the International Working Group for Tracer Hydrology, and the common results have been presented at the first tracer symposium ("Specialists' Conference on the Tracing of Subterranean Waters in Graz, March 28 – April 1, 1966"; H. BATSCHE et al., 1967). The combined field experiments are the basis for all future activities related to the comparison on the behaviour of artificial tracers. There, the karst area of Semriach–Peggau became of particular significance as it proved to be most suitable for tracing experiments afterwards. Thus, this karst area can be considered somehow as a test field for the development of artificial tracer technology and furthermore of environmental tracers too.

The individual karst investigations were integrated in several research programmes. It was the International Hydrological Decade in the early seventies, which permits to involve tritium measurements into the considerations of a first synopsis of artificial and natural tracers. In the middle of the eighties a programme was started with the support of the Government of Styria, the Ministry of Science and Research, the Waterworks of the City of Graz (Grazer Stadtwerke A.G.) and the Styrian Water Power Corporation (STEWEAG) in which especially stable isotope and hydrochemical investigations were included. Since about three years the basic funding of Joanneum Research allows to work to a high extent on the methodological progress in karst hydrogeology. The authors are pleased to express their gratitude for the support.

It is the objective of this investigation to clarify the transit of water in a karst massif applying classical hydrological as well as tracer methods. The intercomparison of both should show also the limits of each individual method considering the different boundary conditions. Special emphasis is directed to the analysis of single events, like floods or snow melt, which permits to separate runoff components and to calculate the underground storage. Also tracing experiments can be correlated with special events. Finally all these results should be included in mass transport models giving a better understanding of regularities in the regeneration of karst water.

1.2. Conventional Use of Terms (R. BENISCHKE)

In the following chapters all **topographic names** are based on the "Österreichische Karte 1 : 50.000, Bl. 164, Graz, rev. ed. 1985" (Topographic Map of Austria).

In some cases it was necessary to use local names not indicated in the official map, but they are either described or indicated in the hydrogeological map (Fig. 2.1).

In several other cases **geological nomenclature** uses an older style of writing topographic names.

The older style is used (e.g. Schöckl as topographic name and Schöckel limestone as geological unit) because names of stratigraphic units which are fixed in literature should not be changed.

Citations of caves are given in the same manner as they are registered in the **Austrian Cave Registry** with the corresponding registry number (subsequently referred as A.C.R. No.).

In the chapters treating mainly morphology, karsthydrogeology or modelling some terms are used which are explained here, because the use in anglo-american manner is somewhat different from that in other European particularly alpine areas. In many cases it is difficult to separate karst phenomena which show transitional conditions (e.g. transition from conduit flow to diffuse flow, or transitions of morphological elements).

The term **channel** is not only used descriptively for a bed with banks where a body of water flows or rests but is used generally also for a part along an active or inactive water-course, which bears the water in a trough, has banks, or in a big karst chamber, in a narrow subterranean canyon or in larger galleries or in any vadose or phreatic underground tube or conduit (as a water-filled part under hydraulic pressure). It is also used for a water-course through fissures or sediment fillings in caves.

Flow path is used generally for description of the way where water actually flows (like in a small stream) or more idealized where it is assumed that it is flowing (e.g. general flow directions in a tracing experiment, different paths through a sediment body or similar).

Flow system describes general hydrogeologic features as a complex network not distinguishing actual features like channels, conduits, flowpaths, shafts, galleries or joints and fissures.

Vadose zone means the unsaturated zone of a karst massif only with seepage water percolating along distinct predominantly aerated paths.

The **phreatic zone** summarizes all parts of the saturated aquifer (fissures and pores permanently or prevailing temporarily filled with water, with stagnant water or water which can be mobilized only under increased hydrostatic head). Here we do not use terms for the transition zone between permanent phreatic or permanent vadose parts. It should be clear from the text.

Karst water-table – a term stressed in long discussions from the last century to present days – is also used more descriptively than genetically to avoid disputations whether it is a surface (or interval) of a water body interconnected by communicating channels (s. above) of all kinds or it is a piezometric surface of one or more even separate aquifers established in the same altitudinal interval because of an uniform morphogenetic history.

1.3. Topographic Remarks (R. BENISCHKE)

The study area – about 15 km north of Graz – belongs to the "Central Styrian Karst" – originally "Mittelsteirischer Karst", a term introduced at first by H. BOCK (1913) – and has a total area of about 25 km² incl. the orographic catchment of the Lurbach, the karst massif of Tanneben between Badlgraben in the N, Mur valley in the W and Mitterbach–Taschen in the S and SE (Fig. 1.1). Whereas the northern

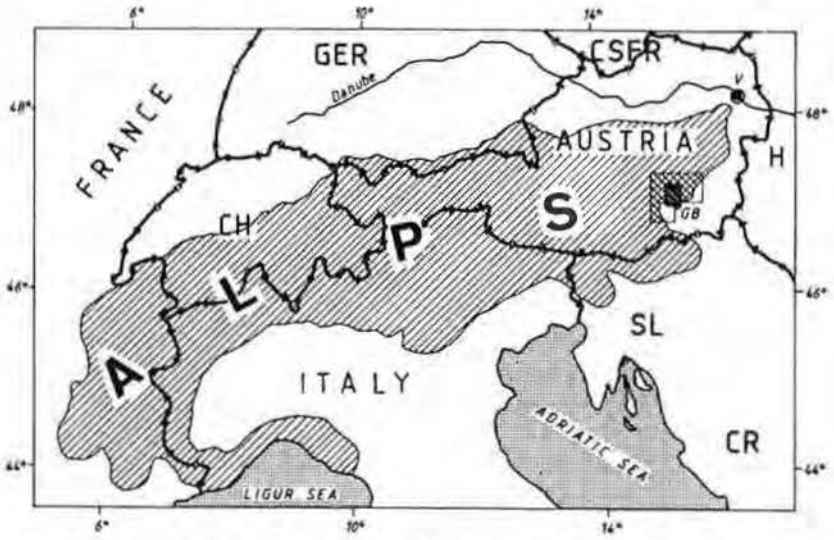

Fig. 1.1: Location map of the study area. GB = „Grazer Bergland" (V = Vienna).

margin (the narrow gorge-like valley called Badlgraben), the southern margin (valley of the small stream Mitterbach up to the Taschen, 814 m) and the western margin towards the Mur valley (the precipices of the Tanneben massif there are called Peggauer Wand in the southern section and Badlwand in the northern part) are well defined the eastern part of the study area is a transition zone between the karst massif and the Semriach basin.

The western side of the Mur valley is delimited by a rock wall called Feistritzer Felsenwand between Kugelstein (536 m) in the N and the church-hill (473 m) of the village Deutschfeistritz in the S.

Main summits on the Tanneben massif are the Angerleitenkogel (714 m), the Hochbrand (813 m) in the northern part, Bloderkogel (816 m), Schneiderkogel (824 m), Möstlkogel (901 m) in the central part and Hochglaserer (910 m) and Krienzerkogel (906 m) in the southern and eastern part. The central plateau is characterized by densely wooded hills and flat depressions (like Ertlhube at 763 m), dolines in some cases of considerable diameter and dry valleys like Brunngraben in the S.

To the E follows the basin of Semriach (main village, 709 m) and the catchment of the upper Lurbach (called Boden). The Lurbach drains this eastern part of the study area first in a EW-running course and then closely north of Semriach in a NS-direction. Some 100 m in the W of Semriach the Lurbach turns suddenly from NS

to EW, enters the karst area downstream of Semriach at about 666 m a.s.l and disappears at last into the cave Lurgrotte (A.C.R. No. 2836/1a). The last 100–200 m before it enters the cave the Lurbach flows through a gorge and finally through a large collapse doline called Lurkessel. The southern borderline of the Semriach basin is a low ridge between the latter and the EW-running Rötschgraben. The eastern margin is approximately the line Windhofkogel (1,064 m), the village of Anger (956 m), an unnamed summit at 1,009 m and the Rechbergkogel (1,020 m), and at the northern side the line between the latter and the highest summit of the study area called Fragnerberg (1,109 m). Between Fragnerberg and Tanneben massif the Eichberg rises up to 891 m a.s.l. belonging to the karst area too. At the northern flank of it sinkholes are situated about 300 m in the W of the small village Neudorf (790 m). Two of these sinkholes are larger dolines. One is called Eisgrube (A.C.R. No. 2836/4), which was in 1959 and 1985 injection place for tracing experiments. It is a doline with transition to a short steeply dipping passage, which is finally blocked by ceiling slabs and sediments. The other one is called Bachschwinde (A.C.R. No. 2836/64) and is used as a dump. From the Eisgrube a road leads through the wood to the village of Pöllau (741 m). About 500 m north of it immediately at the W-side of the road opens a small sinkhole called Katzenbachschwinde (A.C.R. No. 2836/65), which was injection point in 1966.

Since the orographic borderline in the N of the Tanneben massif is the Badlgraben and Bassgraben the karst area extends beyond this valley to the area of Lammkogel (759 m), Mühlbachgraben, Himmelreich, Mühlgraben, Schöneggkogel (772 m) and Schwarzkogel (906 m). For regional hydrologic considerations this area has to be included but has probably no significance for the water balance of the Lurbach catchment and the Tanneben massif. The southern borderline along Mitterbach up to Taschen is also a geological border as it will be described in the following chapter. South of this small valley there is a massif called Hiening with Draxlerkogel (806 m) and Hausberg (889 m) as highest summits. On the top of the latter are situated the ruins of Luegg.

2. Natural Background

2.1. Geology (V. MAURIN)

2.1.1. Lithostratigraphy

The most important factors for the type and spatial development of karstification are the petrography of the geological units of a region as well as the decomposition of the karstifiable rocks to permeable bedding-planes and tectonic diaclases.

The area of the Lurbach system shows a clear stratigraphic-lithologic subdivision of the strata into two groups with exceedingly unpermeable schists (Passail Group) of the Semriach basin and the extremely karstifiable Schöckel limestone (Fig. 2.1). These series of rocks belongs to the "**Tonschiefer-(Schöckelkalk)-Fazies**" (Shale/Schöckel limestone facies) of the Paleozoic of Graz (H.W. FLÜGEL, 1975, F. EBNER, 1983, H.W. FLÜGEL & F. NEUBAUER, 1984, L. WEBER, 1990, H. FRITZ, 1991).

This complex can be subdivided from the top to the basis (valid for the area between Peggau and Semriach) into:

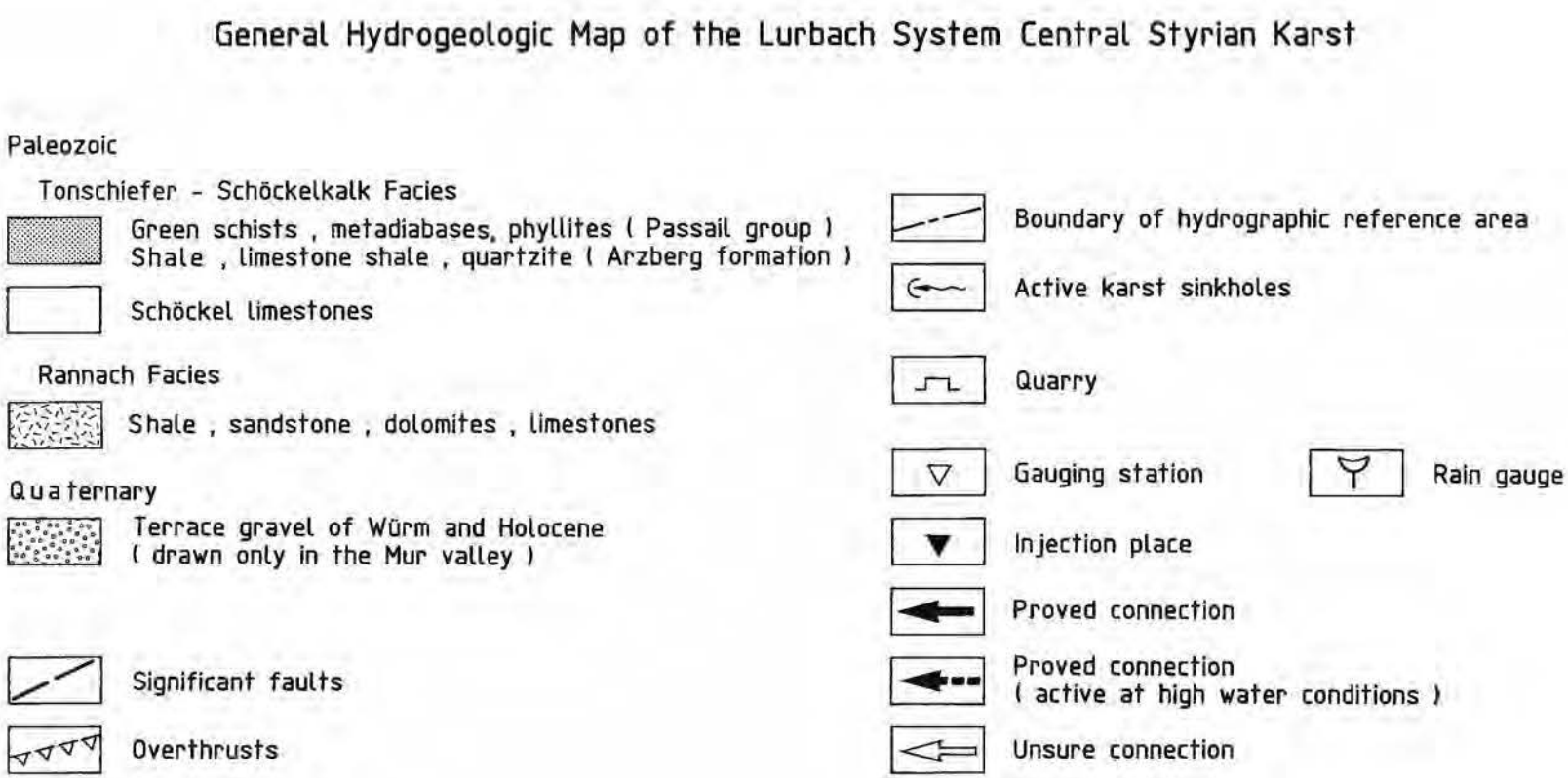

Fig. 2.1: Hydrogeological map of the study area Peggau–Tanneben–Semriach. E = Eisgrube, HB = Hammerbach spring, K = Katzenbachschwinde, L = Laurins spring, N = Neudorfer Schwinde, S = Schmelzbach, SU = Schmelzbach spring. *Continuation p. 17.*

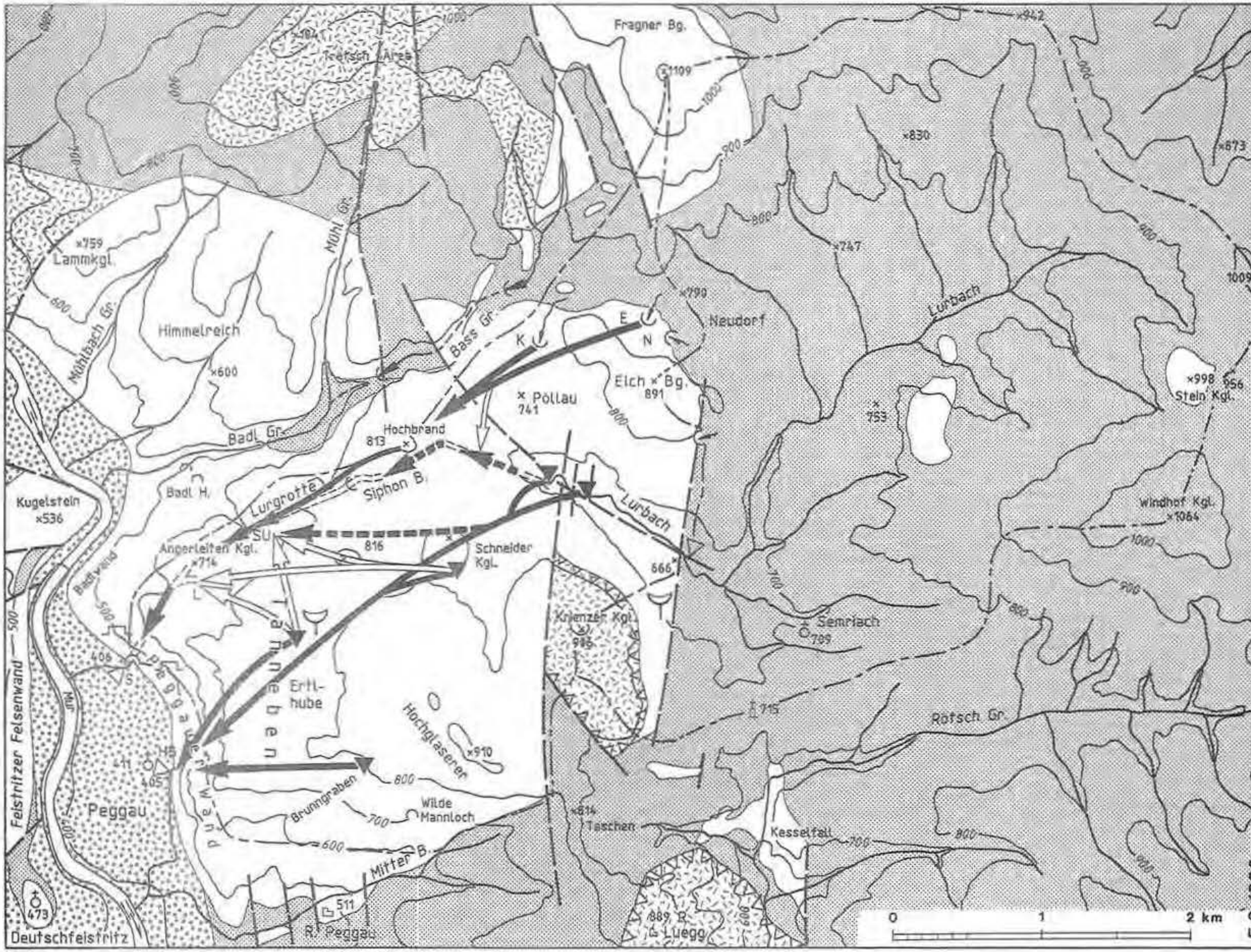

Fragner Bg.
1109
Trefsch Alm
Lammkgl.
759
Himmelreich
600
Mühlbach Gr.
Mühl Gr.
Bass Gr.
Neudorf
790
Eich Bg.
891
Pöllau
741
Hochbrand
813
Siphon B.
Lurgrotte
Badl Gr.
Badl H.
Kugelstein
536
Angerleiten Kgl.
714
SU
816
Schneider Kgl.
Lurbach
666
Kienzer Kgl.
Semriach
709
Tanneben
Ertl-hube
Hochglaserer
910
Peggauer Wand
Peggau
Brunngraben
Wilde Mannloch
Mitter B.
511
R. Peggau
Taschen
814
Kesselfall
889
R. Luegg
Rötsch Gr.
715
Windhof Kgl.
1064
Stein Kgl.
998
956
1009
830
747
753
673
942
Mur
Badlwand
Feistritzer Felsenwand
Deutschfeistritz
473
406
405
0
1
2 km
E.S 1992

A) Schöckel Group:

1. **Schöckel limestone** (Schöckel-Kalk): It is a grey, grayish-blue to white limestone-tectonite, very dense or micritic, oftenly straticulated, thickly stratified to plate-shaped, partly also massive. The primary thickness is probably some 100 m but shows often greater thickness because of tectonic compression.
   In the medium to upper stratigraphic parts it consists mostly of very pure limestones (up to more than 97% $CaCO_3$) and is only at few places dolomitized. In the deeper parts clay and sericite weighboards on bedding-planes, intercalations of dark or siliceous limestone layers and quartz hard-rocks are more frequent. These strata represent a transition to the underlying "Arzberg-Schichten" (Arzberg formation) and they belong therefore also to the Schöckel Group. Because of different mechanic properties the deformation by overthrust-tectonics lead to shear processes and an imbricate structured basis.
2. **Arzberg formation** (Arzberg-Schichten): It is a series of dark graphitic limestones or carbonatic schists, interbedded with black or sericite schists, partly with pyrites and intercalations of dark dolomites, sandy or quartzitic layers and quartz hard-rocks.
   In exploration boreholes (on Pb/Zn ore) in Peggau (H. SEELMEIER, 1944) they can be subdivided into a stratigraphic higher, more carbonatic complex and a lower one predominantly consisting of black schists, clayey shale and green schists. The primary thickness is about 200–300 m (H.W. FLÜGEL & F. NEUBAUER, 1984). The argentiferous Pb/Zn-Baryte mineralization in the region of Peggau–Deutschfeistritz is bound to that series. The higher, carbonate-rich parts of the Arzberg formation correspond to the older term "Grenzphyllit" (H.W. FLÜGEL et al., 1952).

B) Passail Group:

It is a epizonic-metamorphic, vulcanogene-sedimentary sequence with grey, violet or greenish sericite- or quartz-phyllites, sericite quartzite, carboniferous phyllites and greenstone as descendants of basic tuff, tuffites and basalt.
Because of repeated deformation, imbricate structures and fold tectonics the thickness is more than 1,000 m.

For a chronostratigraphic fixation of the entire complex in the region of Peggau–Semriach there are the Striatopora limestones (Striatoporenkalke) of the Arzberg formation, which are classified as Middle Devonian. Fossil localities are known from the "Blocksberg" in the Lurgrotte (H. BOCK, 1917), from the Badlgraben, the Lurkessel (upper entrance of the Lurgrotte) and from the pressure tunnel through the Kugelstein of the power plant Deutschfeistritz (F. HERITSCH & R. SCHWINNER, 1932). Recent investigations (W. TSCHELAUT, 1985) in the area around Guggenbach (in the W of Deutschfeistritz) brought a conodont fauna belonging to earliest Devonian. From regional geologic aspects it is assumed that the rocks of the Schöckel Group (Arzberg formation and Schöckel limestone) have Devonian age, those of the Passail Group (?)Ordovician, Silurian to (?)Early Devonian.

In the study area around the Krienzerkogel the Schöckel limestone of the Tanneben massif and in the S the schists of Taschen are overlayn by a tectonic nappe outlier of the **Rannach-Facies** (R. SCHWINNER, 1925, V. MAURIN, 1954). They start at the basis with light, friable, sandy schists with evenly surfaced fracture-planes, which are compared by F. EBNER & L. WEBER (1978) with the Kher formation (Schichten of Kher) in the W of the study area. A separation from the underlying schists of

Taschen is difficult because of poor exposure conditions. Above this sequence plate-shaped, crinoide-rich and coralliferous limestones follow and are overlayn by dolomitic sandstones and dolomites of the Dolomite-Sandstone-Stage. The tuff horizon is apparently not reached or developed. The entire series has Upper Silurian to Early Devonian age. For the development of the underground drainage system of the Lurbach this tectonic outlier has no significance.

Neogene sediments appear in the Semriach basin only in some remnants (R. SCHWINNER, 1925, V. MAURIN, 1954). They consist of bluish-green or gray, argillaceous-rich loam in the S and NW of Semriach, partly with carbonized relics of plants. They can be compared with miocene sediments of the Passail basin in the E. Their existence leads to the conclusion, that this intramontane neogene depression zone influenced also the region of Semriach. Moreover Pannonian gravel deposits can be found south of Semriach on the ridge to the Rötschgraben. These deposits and also the extensively wide-spread gravels on the Tanneben plateau and the sediments of quaternary terraces in the Mur valley will be discussed in more detail in chap. 2.2.

2.1.2. Tectonics

The region investigated is part of a complicated multiphased nappe structure of the whole Paleozoic of Graz on overfolding and thereby partly a duplication of the thickness of these limestones having occurred in the area of the Schöckel nappe. This explains the fact that the rocks of the lying Arzberg formation and of the Passail Group also occur as top of the Schöckel limestones (R. SCHWINNER, 1925, L. WEBER, 1990). The capping parts which are partly overfolded and in inverted order are known in literature as "Taschenschiefer" (Taschen schists) or "Obere Schiefer" (Upper schists), whereas the parts remained in the subjacent bed of the Schöckel limestones are known as "Untere Schiefer" (Lower schists).

According to L. WEBER the tectonic situation in the region of Peggau–Taschen is characterized by a NW-vergent compression fold-structure, which forces the Upper Schists into a flat syncline and presses them towards the fixed block of the Schöckel limestones in the N, whereat locally schists extend beyond the southern margin of the Tanneben block. In three structure drillings carried out in this area (T1–T3) between the upright Lower Schists and the invertedly lying Upper Schists no Schöckel limestones have been found.

The Schöckel limestone of the Tanneben massif was internally compressed by reverse faults and divided into flat synclines and anticlines. This tectonic structure can be well recognized when looking from the church hill of Deutschfeistritz at the steep rock wall called Peggauer Wand. A dislocation plane ascending 45° towards the N divides the whole rock wall into a slight syncline in the S and the subjacent part dipping gently towards NW (s. fig. 2.2). This corresponds well with the fact that at the southern end of the Peggauer Wand rocks of the Arzberg formation (dark limestones and clay schists) crop out whereas in the boreholes II and III in the Mur valley in front of the cave Lurgrotte and of the quarry of the cement works of Peggau the boundary zone between Schöckel limestone and Arzberg formation could not be found until 60–70 m below the valley floor.

On the whole the Schöckel limestones of the Tanneben massif in the SE are mostly lying very flat and plunge more and more towards the N and NW to Badlgraben and Badlenge of the Mur valley.

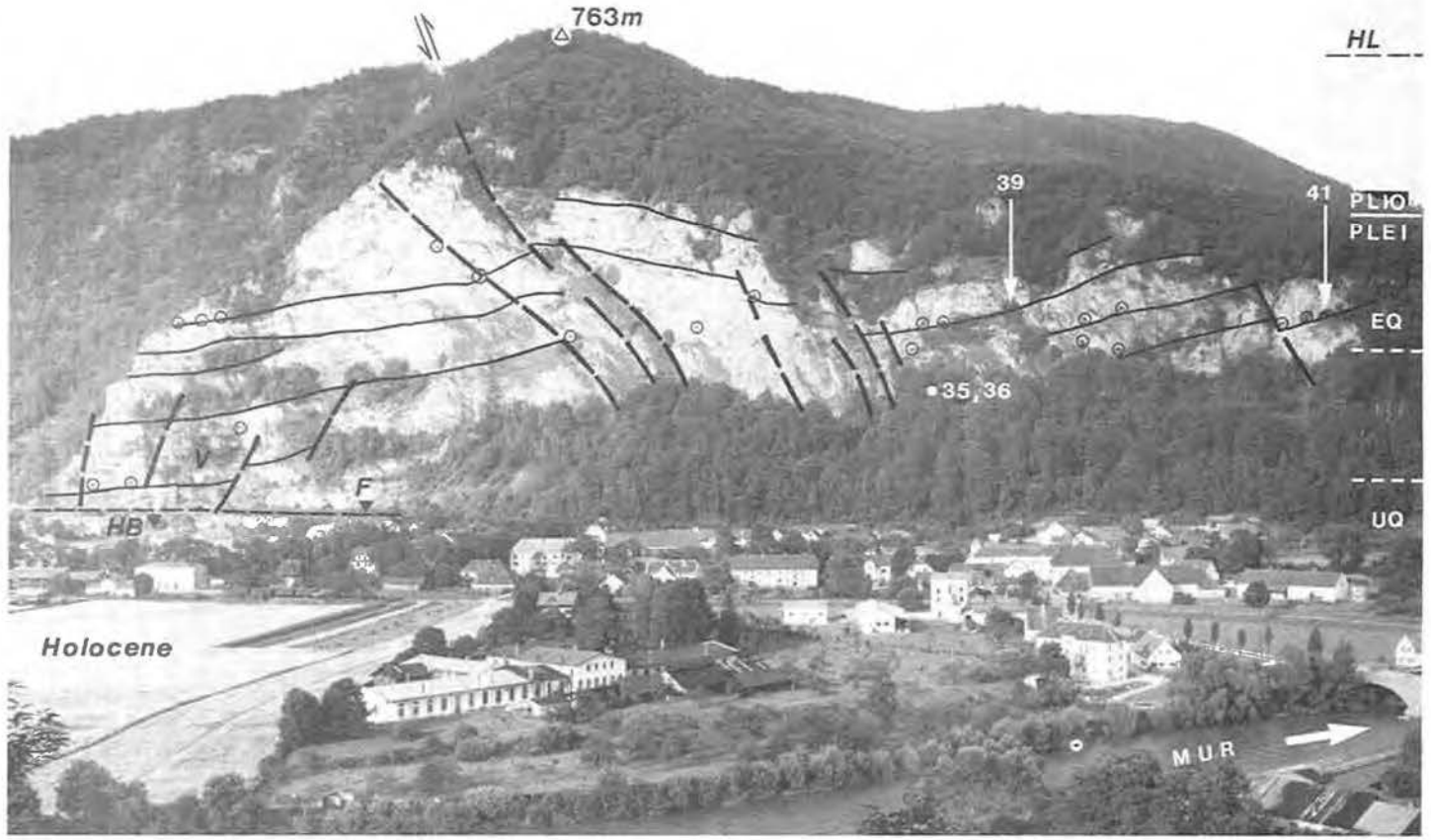

Fig. 2.2: The precipices of the Peggauer Wand with location of caves. View from the church-hill of Deutschfeistritz. Total height between valley floor and Tanneben plateau is approx. 350 m. In the middle of the rock wall a significant upthrust. The southern limb is a gentle syncline, the subjacent northern part dips gently to NW. The Schöckel limestone is partly thick-bedded partly massive. Caves are bound to bedding-planes and faults. HL = Hochstraden level, PLIO/PLEI = approximate level of the Pliocene/Pleistocene boundary, EQ = Early Quaternary, UQ = Upper Quaternary, HB = location of Hammerbach spring, V = ventilation tunnel, F = entrance levels of the tunnel system for "Felshütte Peggau" approximately coincident with the level of the Würm terrace, o = location of registered caves, important with registry numbers. (Photo: H. MAURIN).

This Schöckel nappe is upthrusted on rocks of the Passail Group. Its formerly larger extension is documented by isolated remnants in the eastern part of the basin of Semriach. The tectonically depressed and constricted Schöckel limestone residues in the area of Kesselfall also belong here.

At the western side of the Mur valley the Schöckel nappe extends to the steep-sided precipices of the Feistritzer Felsenwand and of the Kugelstein, and plunges then towards the W under the Parmasegg syncline. As it can be seen at the S-end of the Peggauer Wand there the Schöckel limestone is underlayn by the Arzberg formation which builts up the low saddle between Zitoll and Deutschfeistritz. In the S they are overlayn by the isolated nappe outlier of the church hill of Deutschfeistritz. At the SE-flank of the Kugelstein rocks of the Arzberg formation crop out too. The western borderline of this Schöckel limestone mass is a N–S running fault system, along which Schöckel limestone and Arzberg formation dip steeply to vertically towards the W or E (V. MAURIN, 1954, H. FRITZ, 1986, 1991).

Above the Schöckel nappe there lies the tectonically higher unit of the Rannach nappe. In the area under investigation only the isolated nappe outlier of Krienzerkogel has been preserved. In the region of Hochtrötsch in the N, of the Parmasegg in the W and of the Rannach in the S, however, this unit is being represented to a large extent. The Luegg nappe outlier situated south of Taschen also belongs to the latter.

Besides this nappe tectonics which formed the base structures the younger fracture tectonics is more responsible for the karstification process. Dominant is a fault system with meridional trend. The limestones of the Tanneben massif are relatively settled in comparison with the schists of the Semriach basin in the form of step faults. The karsthydrologically most effective borderline is a fault which delimits the Schöckel limestone of the Eichberg with N 10 E and the basement of the Krienzerkogel which was also built up from these limestones towards the E. There is a second fault zone that can be well recognized approx. 800 m west, here cuts off the Krienzerkogel nappe outlier and trends to the Lurkessel in the N. These meridional faults are also morphologically active in the precipices of the Peggauer Wand and in the Feistritzer Felsenwand. The faults in the lithologically uniform Tanneben plateau which is strewn with terrace sediments and mostly thickly wooded, however, can hardly be mapped. The transition zones between Schöckel limestone and Arzberg formation which crop out in the Badlgraben as well as on the southern margin near the Mitterbach, however, illustrate the internal tectonics of this massif. Equally the same conditions can be found along the accessible underground flood channel of Lurbach which also runs over long distances in this boundary area (V. MAURIN, 1953, 1954). Besides the large N–S faults other fault directions as well as lateral faults can be recognized (s. fig. 2.1, fig. 2.7).

Important for the karstification process is the fact that the limestones have undergone an intensive fracturing besides the dislocations that can be mapped. These joints mostly run vertically on bedding-planes. The joint spacing depends on the type of stress as well as on the thickness of the individual layers. Thin-stratified parts generally show more closeness of fissures. In these generally compact limestones the degree of separation resulting thereof and the character and the position of the bedding-planes are decisive for the primary rock permeability and thereafter for the character and stability of the karst cavities developing.

The age of the fracturing structures of the Tanneben massif is quite varying. A part of it can be attributed to the alpidic compression tectonics, such as lateral faults and steep upthrusts. The large meridionally running step faults are supposed to have

been traced during this time. They received their final formation not before the uplift phases of the basement framework of the "Grazer Bucht" (basin of Graz) during the Younger Tertiary and the Quaternary. This process has been continuing until the latest geological past (V. MAURIN, 1953).

2.2. Morphogeny, Paleohydrography and Karst Development

(V. MAURIN, R. BENISCHKE)

The temporal classification of karst processes, especially that of cave levels can be made either by the analysis of karst phenomena and cave contents (sediments, paleontological and archeological data) or by means of the parallelization with datable surface forms.

A great number of scientists has been exploring the morphological development of the **"Grazer Bergland"** (Highland of Graz). A. WINKLER-HERMADEN (1957) published a summary which is still fundamental today. He is of the opinion that apart from several buried and partly again uncovered older form elements the earliest land surface residues that can still be recognized do not reach back further than to the Late Miocene. The erosion planes in the area of Schöckl and Hochlantsch (18 km north of Schöckl) belong here.

In the course of the Pannonian this hilly landscape was dissected in phases and the mountain edge was partly buried by lowering again. The thick gravel deposits in the schist area southeast of Semriach and in the basin of Passail belong here. Since the equivalent gravel horizons in the basin of Gratkorn (10 km north of Graz) and in the area of Graz lie significantly deeper, it seems that in the Pannonian or soon afterwards enormous flexures and displacements by faults must have occurred. In the Latest Pannonian a system designated as **Trahütten-level** by A. WINKLER-HERMADEN summits about 900 m a.s.l. (Hochglaserer 910 m, Möstlkogel 901 m, Krienzerkogel 906 m, Hausberg 889 m, Eichberg 891 m and corresponding plains in the schist area around Windhofkogel) would have to be classified in the area under investigation. Though the whole area shows a very high degree of speleological exploration – on the whole nearly 300 speleological objects have been registered – we do not know any accessible caves in the region of Peggau–Semriach which could be classified in this system, though it is possible that this fact might be connected with the only fragmentary conservation of plains belonging to this altitude. However, dolines of partly considerable dimensions can be observed on the Hochglaserer (900 m) and on the Möstlkogel (890 m) and also on an intermediate step developed approx. in 820–840 m, like on the saddle on the Eichberg ridge or on the western and eastern side of Hochglaserer.

Depression processes in the Styrian basin in the period between Pannonian/Astian at first caused a strong activation of the erosion in the hinterland (H.W. FLÜGEL, 1975) and in the Upper Astian the formation of a significant plain system which can be well observed along the whole mountain edge (**Kalkleitenmöstl-level** by V. HILBER, 1912, and **Hochstraden-level** by A. WINKLER-HERMADEN, 1957, resp.). Terra rossa and bean ore deposits and partly a deeply decomposed bedrock indicate a subtropical climate of that period.

The Hochstraden-level is also dominant within the study area, and owing to the karst underground it is extremely well preserved (V. MAURIN, 1954, 1960, 1975). Special attention must be drawn to an old valley about half a kilometer wide, on the plateau of the Tanneben massif. On many places it is covered with a strongly

loamified gravel layer partly several meters thick. On the surface mostly quartz, quartzite and compact hornblende schists occur in a loamy-sandy matrix. The grain sizes vary from hazelnut size to head size. A two-meter deep bomb crater found during the middle forties in the forest south of Ertlhube showed that this is not only residual gravel redeposited several times. In the lower part of the crater there were gravels associated with crystalline schists and igneous rocks, but the micaceous and feldspathic rocks were completely "rotten" and immediately became grus under mechanical stress. Carbonate pebbles were not found in this small exposure. This complex gravel accumulation shows, however, that – at least for the western part of this erosion plain belonging to the Hochstraden-level – we must assume a catchment area which reached back into the crystalline frame of the "Grazer Bergland".

The present surface of this Upper Pliocene land is divided by denudation processes into flat basins and cupolas which are only a few meters higher than the surroundings. Numerous dolines of all sizes, extremely small to much more than 100 m diameter, are to be found (F. VORMAIR, 1938, 1940). Many of them are connected with shaft zones through which on account of subterraneous erosion certainly rather great cubages of loose sediments have sagged downward in the course of time into deeper-lying active horizontal subterranean runoff-channels and have been removed by them and are still being removed. There rises the question to which extent the development of such extensive areas with solution dolines depends not only on climate and time but primarily on the existence of water-storing clastic deposits. Part of the Hochstraden-level are moreover quite extensive erosion plains in the Trötsch area, around the Hochbrand, north of the Krienzerkogel, on the Pöllau (area around the village Pöllau) between the Tanneben massif and the Eichberg, on the southern side of the Eichberg and in the schist area of the basin of Semriach.

During that period the basic structure of today's drainage pattern was developed. The erosion plane at the western edge of the Tanneben massif around the Ertlhube possibly already belongs to the primeval Mur river. Presumably the southeast slopes of the Hochtrötsch and the basin of Semriach had a special N–S trended drainage path belonging to the plateau near Pöllau (741 m) and the saddle south of Semriach which has been lowered to 715 m since that time. This old drainage scheme is still documented today by the upper course of the Lurbach orientated towards SW (s. fig. 2.3).

With the Hochstraden-level it is the first time that we can clearly recognize a connection between surface morphology and subterraneous karstification in the area under investigation. Such a pronounced plain system can only develop in a period of longer tectonic stability. With limestone rocks in the groundwater zone it is inevitable that karstification develops below and in the flanks of a valley, in which concomitant karst water circulates under phreatic conditions and forms the basis for the initial development of larger cave galleries.

On the other hand we have already had an accentuated relief at the period of the Hochstraden-level where individual ridges (Hochglaserer, Eichberg etc.) overlook the local outflow horizons (Ertlhube, Pöllau) by 100–150 m. During this relatively long stable period these hills were certainly drained subterraneously. It is well possible that the sinkholes on the NE-side of the Eichberg which are still active have already been developed then (s. fig. 2.4). The large dolines on the Eichberg ridge point to a very intensive karstification of this mountain. Some of them seem to be old collapse dolines.

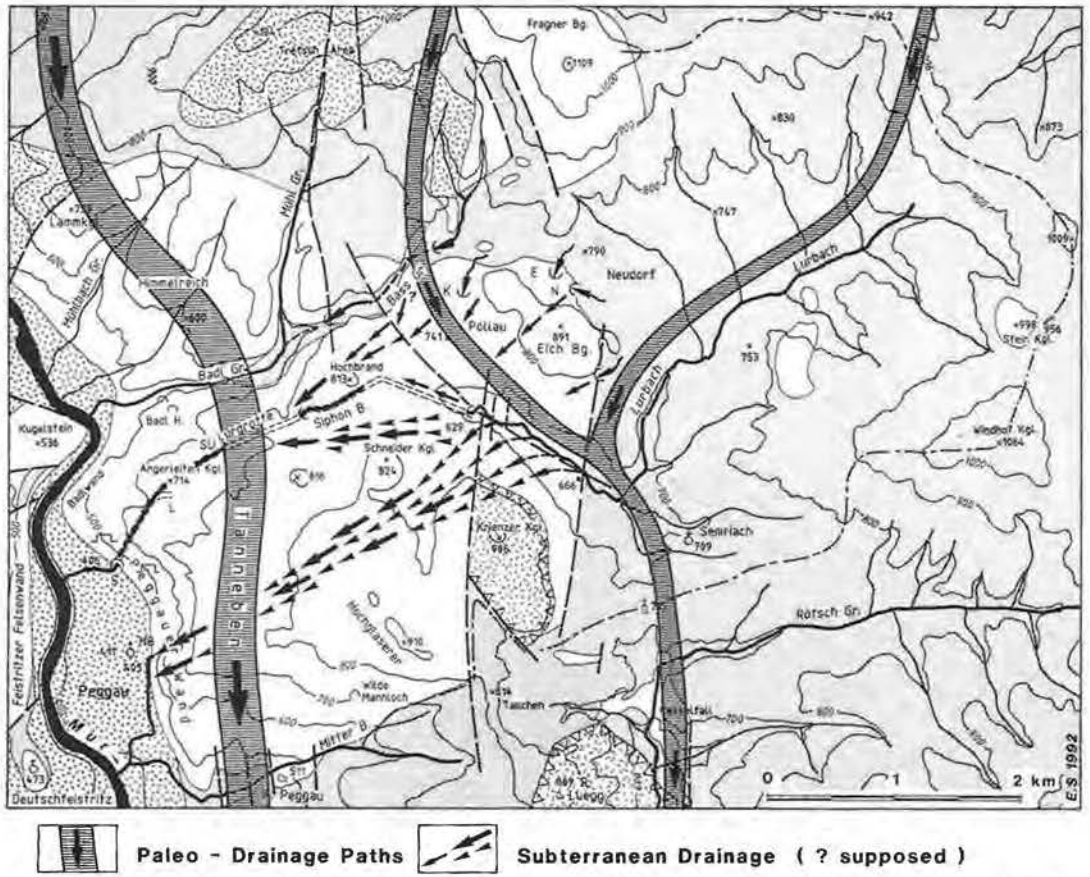

Fig. 2.3: Paleohydrographic features of the study area. Further information see also fig. 2.1. In the W crossing the Tanneben the course of the Paleo-Mur, in the E the Semriach basin is drained completely above ground to the Rötschgraben in the S, arrows indicate schematically the recent underground drainage. The main paleo-drainage paths are given for the uppermost Pliocene.

If in a fluviokarst area the erosion base in the lower course of a surface stream or in the region of an adjoining river is lowered by erosive or tectonic processes, a beheading and diversion of the karst water drainage may occur by regressive subterraneous corrosion and erosion. The surface streams became dry and their channels are being conserved on a karst plateau.

Caves having formerly existed at this level have been eroded during development of the Hochstraden-level. It means that after completion of the Hochstraden-level formerly connected caves became disconnected and represent now isolated objects. As the Hochstraden-level implies also a period of longer stability the before mentioned isolated objects could develop horizontal passages. But as we can see from fig. 2.5 there are no accessible horizontal caves but only shaft openings and a big number of dolines (solutional and collapse structures) as it was pointed out by F. VORMAIR (1938, 1940). This fact leads to the conclusion that horizontal caves had not been preserved or had been developed only to an insignificant extent.

The above mentioned concomitant karst water circulation below the valley floor or in the flanks initialized flow-paths in the underground during the formation of the Hochstraden-level which developed later on (during the formation of the next deeper situated level of the landscape) to larger passages. Funnel-shaped dolines on the surface of the Hochstraden-level with a transition to deeper narrow vertical tubes (karst shafts) show that the dolines are the result of younger speleogenetic processes than the shafts, despite they were traced during the formation of the older level. The shafts therefore enlarged under conditions with stronger drainage of the surface to the underground indicating a rapidly vertical lowering of the adjacent karst water-table as the development of the next deeper level of the landscape

Fig. 2.4: The ponors Eisgrube (E; A.C.R. No. 2836/4) and Bachschwinde (N; A.C.R. No. 2836/64) near Neudorf north of Eichberg (891 m a.s.l.). View from southern slope of Fragnerberg (Photo: R. BENISCHKE).

proceeded. Examples for these processes are possibly the dolines on the Eichberg and dolines near the Ertlhube on the central Tanneben plateau, which were excavated by speleologists at the beginning of this century. The excavation of narrow shafts offered the possibility to access a zone with larger horizontal galleries (e.g. Gessmann-Doline, A.C.R. No. 2836/6) about 50–60 m below the surface of the Hochstraden-level. These passages were developed later probably during the time of the development of a younger level.

As it is pointed out below speleogeny is closely correlated with the morphogeny of the landscape. This fact can be seen in almost all karst regions despite there are deviations depending on lithological and/or tectonic influences. The described processes will be repeated each time the local or regional base level with its corresponding outflow zones is moved to a lower altitude. In any case a rapid lowering (by denudation and/or linear erosion under different climates) will preferably lead to the development of vertical passages (shafts, deeply incised underground canyons etc.), retardation of denudative or erosional processes and long-term tectonic stability will lead to the development of horizontal systems. In both cases and at the same time vadose and phreatic drainage with all its variations exists.

At the transition of Upper Pliocene (Astian) to Early Pleistocene (Calabrian) linear erosion was again activated and consequently a double plain system was developed designated as **Stadelberg-** and **Zahrerberg-level** resp. by A. WINKLER-HERMADEN (1957). Plains strewn with gravel have preserved in the area of Peggau, i.e. in the Himmelreich north of the Badlgraben (640–660 m), on the Feistritzer Felsenwand (660 m), on the NW-side of the Tanneben massif near Angerleitenkogel (660–680 m) as well as on the SW-side in the region of the Brunngraben (660 or 620 m resp.) This significant lowering of the erosion base in the W is due to the erosional force of the Mur river. In the same period, however, the small brooks east of the Tanneben massif deepened only insignificantly. These were the obvious prerequisites for the capture of the old riverlets which had remained and for the deviation of the karst drainage.

The drainage development from the Mur valley towards the E on the Tanneben massif must have proceeded rapidly reaching the eastern border of the Schöckel limestone mass in the Earliest Pleistocene. This eastern border is represented by a significant N–S fault which delimits the Eichberg and the basement of the Krienzerkogel towards the schists of the basin of Semriach. Thus, however, parts of a surface runoff pattern from the southern Trötsch region and the schist region north of Semriach were included in the subterraneous karst water system. Especially in the hooklike course of today's Lurbach the capture and deviation of this earlier upper course of the Rötschbach which had formerly drained towards the S can be easily recognized (Fig. 2.3). For the chronological classification of this process the fact is important that the ridge covered with Pannonian gravels between the basin of Semriach and the Rötschgraben which is deeply incised today has still been preserved in 715 m.

The oldest Lurbach sinkholes that can still be recognized lie at the southern foot of the Eichberg in 720 m. Only a few years ago a larger shaft has opened in this region. The recent lower course of the Lurbach passes the limestone-schist border at Pt. 666 and flows approx. 1 km in a partly gorge-like section to the entrance (629 m) of the cave Lurgrotte (A.C.R. No. 2836/1a). Here it follows a fault zone with NW–SE trend probably having developed only by the collapse of former cave galleries. A magnificent example of this development can be seen in the 60 m high Lurwand

(the big rock wall at the entrance to the cave) rising vertically above the main ponor of today.

From the earliest Quaternary the Mur river is fixed to the narrow transverse valley between the basin of Frohnleiten in the N and the junction of the Übelbach, a tributary from the W. From this time on the karst drainage of the Tanneben massif is totally directed to that strong lowering of this base level with its corresponding outflow zone. The narrow limestone ridge at the W-side of the Mur valley (Feistritzer Felsenwand) is now cut off from these processes and – because of its small catchment – thereafter shows only minor karstification. These conditions change in the lower part of the Schöckel limestone close to the valley floor, particularly at the Badlenge (beginning of the gorge-like part of the Mur transversal valley). There evidences of a significant concomitant subterranean drainage can be found in the flanks and below the former valley floor. Numerous caves with mainly hydrodynamically controlled forms – most of them as phreatic tubes – not only in the Kugelstein and in the region of the Badlwand but also in the lower Badlgraben and in the Peggauer Wand belong here. A temporarily complete subterranean drainage of the basin of Frohnleiten during that time, postulated by H. BOCK (1913), is classified to be doubtful.

The Quaternary erosion in this area by the Mur river is assumed to be about 250 m. But Early Pleistocene erosion plaines and horizons of stronger karstification can be hardly related to the extensively developed terraces of the Styrian basin. In the area of Badl–Peggau erosion planes between 500 and 580 m a.s.l. belong here (for example at the SW-flank of the Lammkogel, in the Himmelreich, in the Badlwand above the present road, on the Kugelstein and at the SW-edge of the Tanneben massif). Most of that erosional levels show gravel deposits with crystalline components. It is significant that for the first time a greater number of well preserved horizontal cave systems with predominantly hydrodynamic controlled features developed in the phreatic zone can be correlated with these levels. An impressive particular example is the cave system with Aragonithöhle (A.C.R. No. 2836/14; 559 m a.s.l.), Naturbrücke (A.C.R. No. 2836/15; 557 m), with Kleine Badlhöhle (A.C.R. No. 2836/16; 536 m) and Große Badlhöhle (A.C.R. No. 2836/17; upper entrance at 547 m, lower entrance at 495 m), the latter developed as a hydraulic controlled, labyrinthic network of passages. The Repolusthöhle (A.C.R. No. 2837/1; 520 m) at the opposite flank of the Badlgraben belongs to the same system. Passage morphology and speleogeny of this system is described thoroughly in V. MAURIN (1951).

The numerous caves in the upper sections of the Peggauer Wand are directed to this early pleistocene outflow level.

To what extent these horizontal passages represent former karst water channels or outlets of the Tanneben massif and therefore of the basin of Semriach or represent possibly a temporarily concomitant groundwater flow of the old Mur river, cannot be decided clearly. Obviously quartz pebbles are abundant in cave sediments.

After A. WINKLER-HERMADEN (1955) these plains and cave-levels belong to his **"Obere Terassengruppe"** (Upper Terrace Group; Calabrian to Günz).

The levels of the **"Mittlere Terassengruppe"** (Middle Terrace Group) after WINKLER-HERMADEN (Günz/Mindel-interglacial to Mindel/Riß-interglacial) are related to corresponding terraces in the region of Frohnleiten. From the morphological point of view they are developed in the region of Peggau–Deutschfeistritz only to a small extent. Only some small planations on the eastern edge of the Kugelstein (at 450 m a.s.l.) and at the churchhill (473 m) of Deutschfeistritz

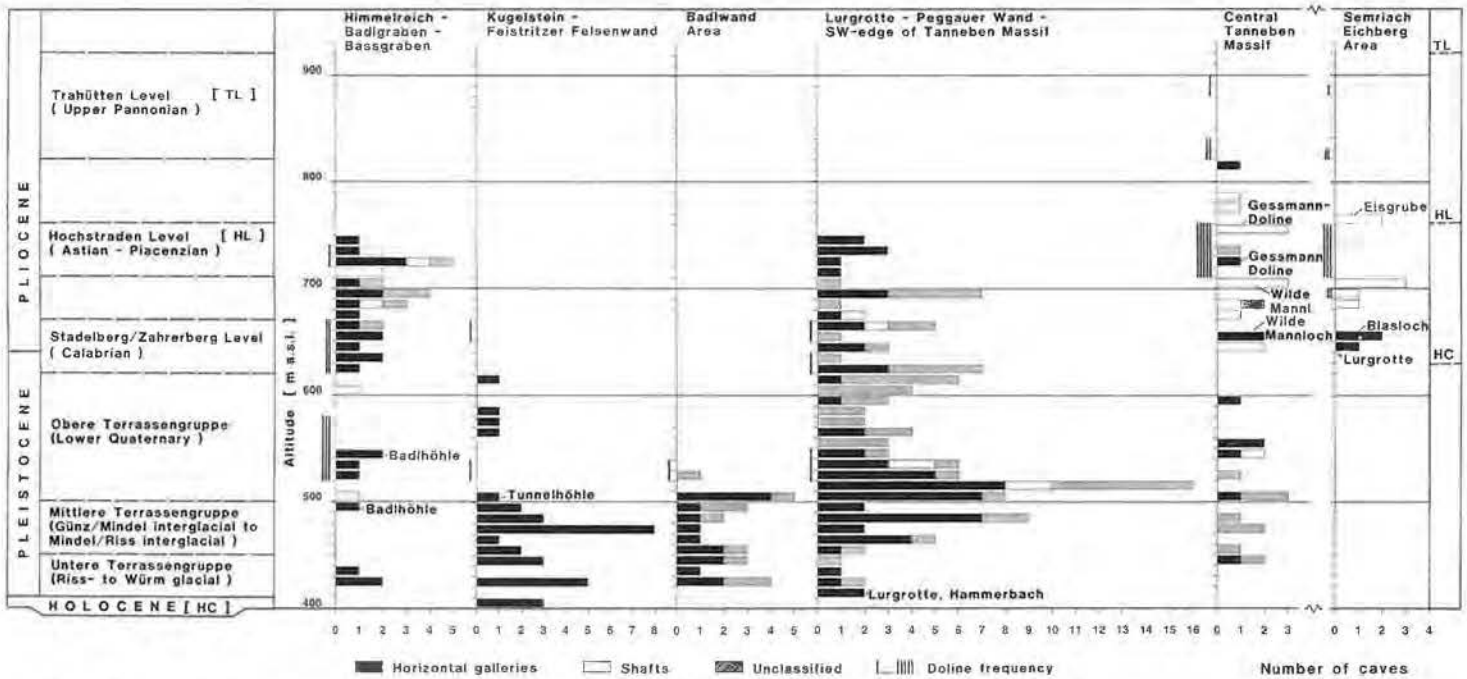

Fig. 2.5: Altitudinal distribution of registered caves of the study area and their relation to morphological levels.

belong here, but numerous caves in the gorge-like part of the Mur valley at Badl (Kugelstein, Badlwand) and in the precipices of the Peggauer Wand (Fig. 2.5). In some of these caves, e.g. in those above the old road, sediment deposits from the ancient Mur can be found. Caves related to this terrace group are for example in the Kugelstein the caves Grabhöhle (A.C.R. No. 2784/5; 450 m) and Stufengrotte (A.C.R. No. 2784/6; 442 m), in the Badlwand the Einsiedlerhöhle (A.C.R. No. 2836/20; 440 m) and Büßergang (A.C.R. No. 2836/88; 460 m) and in the Peggauer Wand the Peggauer-Wand-Höhle I and Ia (A.C.R. No. 2836/35 and 36; 465 m).

The Early Pleistocene **"Untere Terrassengruppe"** (Lower Terrace Group; Riß to Würm glacial) can be linked well to the gravel terraces of the basin of Frohnleiten in the N. Besides the upper Pliocene Hochstraden-level there are in the region of Peggau for the first time extended thick Würm gravel deposits. These glacial terrace plain is preserved along the eastern margin of the valley between Badlenge and Peggauer Wand over a distance of 2 km and a maximum width of 300 m, along the western flank of the valley below the Feistritzer Felsenwand and the church-hill of Deutschfeistritz over a distance of about 1 km. The partly denuded surface of this terrace is situated today in an altitude between 410 and 420 m a.s.l. The wide Holocene plain is incised into there for about 10–15 m.

Based on a number of drillings and geophysical investigations (F. WEBER, 1969) the prewürmian bedrock relief can be reconstructed very well. As it is in the mid section of the Mur valley there also hitherto an underground trough (H.W. FLÜGEL, 1975) which reaches 40 m down below the upper edge of the Würm terrace. In the narrow gorge-like part of the Mur valley between Kugelstein and Badlwand this trough could not be recognized neither by drillings nor by seismic exploration, but doubtless it must extend into the basin of Frohnleiten. The example of this youngest Würm/Holocene development of the valley, which lasted only about 100,000 years, shows very well that each erosional surface and therefore also each level of karstification is correlated with an interval of distinct altitude, whose extent is determined by climatic and for the higher situated Early Pleistocene and Upper Pliocene horizons certainly also by tectonic factors. Such oscillating processes lead to temporary inundation and plugging of older karst channels.

Comparing with the clearly separated older plains of the "Untere Terrassengruppe" of Riß and Würm interglacial there are no significant equivalents in the region of Peggau–Deutschfeistritz, but some caves in the Kugelstein, Badlwand, near the entrance of the Lurgrotte and in the Peggauer Wand. Examples from Kugelstein are the Sinterröhrchenhöhle (A.C.R. No. 2784/9; 420 m) and the Schlüsselloch (A.C.R. No. 2784/19; 425 m), near the entrance of the Lurgrotte the Dirnbachergang (A.C.R. No. 2826/1 c; 447 m) and the Josefinenhöhle (A.C.R. No. 2826/32; 425 m) and the Knochenhöhle (A.C.R. No. 2826/33; 425 m).

In 1944 within the project "Felshütte Peggau" an object of special interest was discovered during blasting operations for the construction of a ventilation tunnel at 436 m a.s.l. for a 2,000 m long tunnel system at the foot of the Peggauer Wand (Fig. 2.2). The object was a sequence of several karst rooms filled almost completely with loam, sand and gravel. A very different association of pebbles of crystalline rocks, partly up to 20 cm diameter, mostly "rotten", proved, that during the Riß glacial or the Riß/Würm interglacial a tributary channel of a flow system belonging to the ancient Mur river inundated or flowed through these caves. These karst rooms are situated behind the today's precipices of the Peggauer Wand directly above the Hammerbach spring (A.C.R. No. 2836/34).

The main tunnel system is at an altitude of 416 m a.s.l., i.e. at the level of the Würm terrace. The tunnels connected about 30 karst objects like shafts and horizontal passages (V. WEISSENSTEINER, 1969). Most of them were plugged by loam. A room at the end of tunnel no. V (170 m east of the entrance) was filled with sandy-silty sediments mixed with coarse gravels. The components were schists from the basin of Semriach. These means that the sediments were deposited in a higher situated genetically older horizon of the active Hammerbach channel flowing out at nowadays about 6 m below.

The Hammerbach – today still ascending from a siphon – has now incised some meters into the accumulation body of the Würm terrace. During the last glacial it was enforced to ascend to the Würm outflow level. This is therefore a significant indication that karst processes had developed during Pre-Würm or Intra-Würm under the present valley floor.

From the morphogenetic point of view and the geological presettings a part (probably only a small amount) of the water from the "Lurbach-Hammerbach-Schmelzbach" karst aquifer could recharge unrecognizably the porous groundwater in the Mur valley along phreatic channels (small conduits, micro-fissures etc.).

Similar conditions can be found at the outlet of the cave Lurgrotte (A.C.R. No. 2836/1 b) about 750 m in the N. This karst channel too was directed to the level of the Würm terrace before the present drainage tunnel was constructed, and the water of the Schmelzbach (S) ascended from deeper lying siphons to the overflow crest preserved in the bedrock at the entrance.

It is more difficult to classify chronologically the morphogeny and therefore the karstification processes in the region of Semriach. For the entire study area a parallel development is assumed in the uppermost Pliocene (Hochstraden-level), but the conditions changed during the earliest Pleistocene because of a very rapid retrogressive underground karst erosion (during this stage erosional processes were probably predominant over corrosive processes) directed from the Mur valley towards E. The oldest Lurbach sinkholes are situated in an altitude of 720 m a.s.l. at the southern slope of the Eichberg, the main present ponor at 629 m (entrance of the Lurgrotte). As on the western side of the Tanneben massif in the Mur valley this development covers an interval of about 250 m in height it is concentrated in the limestone area in Semriach to an interval of about 100 m as long as the Lurbach flows as a surface stream.

Parts of the cave (Tanzboden, Wilde Burg) approx. 5–10 m above the present entrance of Lurgrotte Semriach could be seen as former ponors but are difficult to be classified chronologically.

It is important that in the upper part of the Lurgrotte Semriach near the "Großer Dom" (Big Hall) fragments of older cave levels could be found at 640 m, which can be classified on the basis of speleothems and thick fillings of terra rossa to be of older Quaternary warm period.

The karstification process, however, has significantly advanced in the meantime. From Pt. 666 (at the border between limestones and schists) the Lurbach looses constantly water to the underground and has repeatedly run totally dry in this area. The discovery and exploration of the large approx. 600 m long cave "Blasloch" (A.C.R. No. 2836/229) in the Lurkessel (H. KUSCH, 1991), performed successfully not before 1990, has proved that there are not only narrow aquiferous fissures.

The "Blasloch" cave has a steplike pattern and shows shafts and large horizontal galleries (Fig. 2.6) which lie partly 20 m below today's entrance of the Lurgrotte.

The deepest point hitherto reached in the Blasloch lies approx. 50 m below the level of the present surface stream Lurbach.

Today the Blasloch is not reached under normal to medium water conditions by the waters percolating in the Lurbach bed; in other words the underground drainage of the Tanneben massif reaching back from the Mur valley has advanced so far that the phreatic karst water zone is already lying significantly deeper in the E of the limestone massif too. Only at extreme high-water conditions while the Lurkessel is flooded the Blasloch is inundated too or only if sinkholes in the Lurbach surface channel, which are directly connected with the Blasloch, become occasionally active.

The further course of the percolation waters through sinkholes in the surface channel-bed as well as through the main ponor in the uppermost part of the Lurgrotte is not known in detail. Numerous tracing experiments have shown that during low and medium water conditions the water flows under predominantly phreatic conditions to the Hammerbach spring (HB). Under flood conditions more and more

Fig. 2.6: Fracture controlled dry gallery in the deeper (approx. 40 m below the level of the Lurbach) part of the Blasloch (A.C.R. No. 2836/229). (Photo: R. BENISCHKE).

higher situated and older karst horizons in the vadose region are activated. For both zones an extended complex karst drainage system is assumed, wherein plugging and reactivation and redeposition of sediments happened several times during the course of time.

The most outstanding example of the study area for speleological investigations and therefore to study speleogeny and its relationship to landscape morphogeny is the cave Lurgrotte (A.C.R. No. 2836/1) which runs probably close to the geological basis through the Tanneben massif from Semriach to Peggau.

The vertical projection (Fig. 2.7) shows that the cave represents today a type of vadose drainage system with preserved morphological elements (large flutes and scallops on walls and ceilings) of former phreatic phases. Other indicators are phases of sediment filling particularly in the upper part, and remnants of sediments in higher parts inactive today representing older filling phases.

Breakdown events lead to large ceiling slabs thus forming the so-called "Großer Dom" (Big Hall) and "Blocksberg" (a hall with big boulders). Periods of longer stability only with percolation water from the land surface developed calcite precipitations like stalagmites and stalagtites of considerable size (e.g. the biggest dripstone column which is called "Riese" [The Giant]) and destructing them at some places later on by erosion processes.

From this ramified karst drainage system only the accessible part of the subterranean Lurbach flood channel between Semriach and Peggau is known until now. The results of all these alternating processes can be observed well along these passages. For example, the connective gallery ("Brunellogang") between Lurbach sinkhole inside the cave and the "Großer Dom" (Big Hall) was completely plugged by gravel deposits and thick sinter formations over a long period and was cleared later on and made passable for floods.

The vertical projection of the cave shows also a step-like development with three main stages of forming horizontal passages.

A first stage was the uppermost part in Semriach having developed some substages. A major "event" caused the lowering of the corresponding base level and resulted in the formation of a sequence of shafts and canyons along a big fracture zone (called "Geisterschacht").

The next level reached was about 40–50 m deeper and can be followd through today only episodically active siphon zones down to the "Blocksberg". Below this point after another step of about 30 m the last section of the cave is entered, which represents an active zone with Schmelzbach spring (SU) and Laurins spring (L). This zone is directed to the Quaternary terraces in the Mur valley (evidently all the significant horizontal sections of the cave are directed to such terrace levels) particularly to the Würm terrace remnants of it being visible near the entrance at Peggau.

The last part close to the entrance at Peggau is characterized by several active and nowadays two inactive siphons. The latter had been active until a drainage tunnel had been constructed which lowered the water-table for about 8 m. Today these passages are dry phreatic loops, and show that karstification was at a lower level before the sedimentation of the Würm terrace. The Würm sediments had a tightening effect enforcing the cave to direct its main outlet upwardly again to the surface of that terrace. The same effect can be seen at the Hammerbach spring where also an active siphon goes about 4 m below the present outlet. The level of it coincides with that of the Würm terrace too.

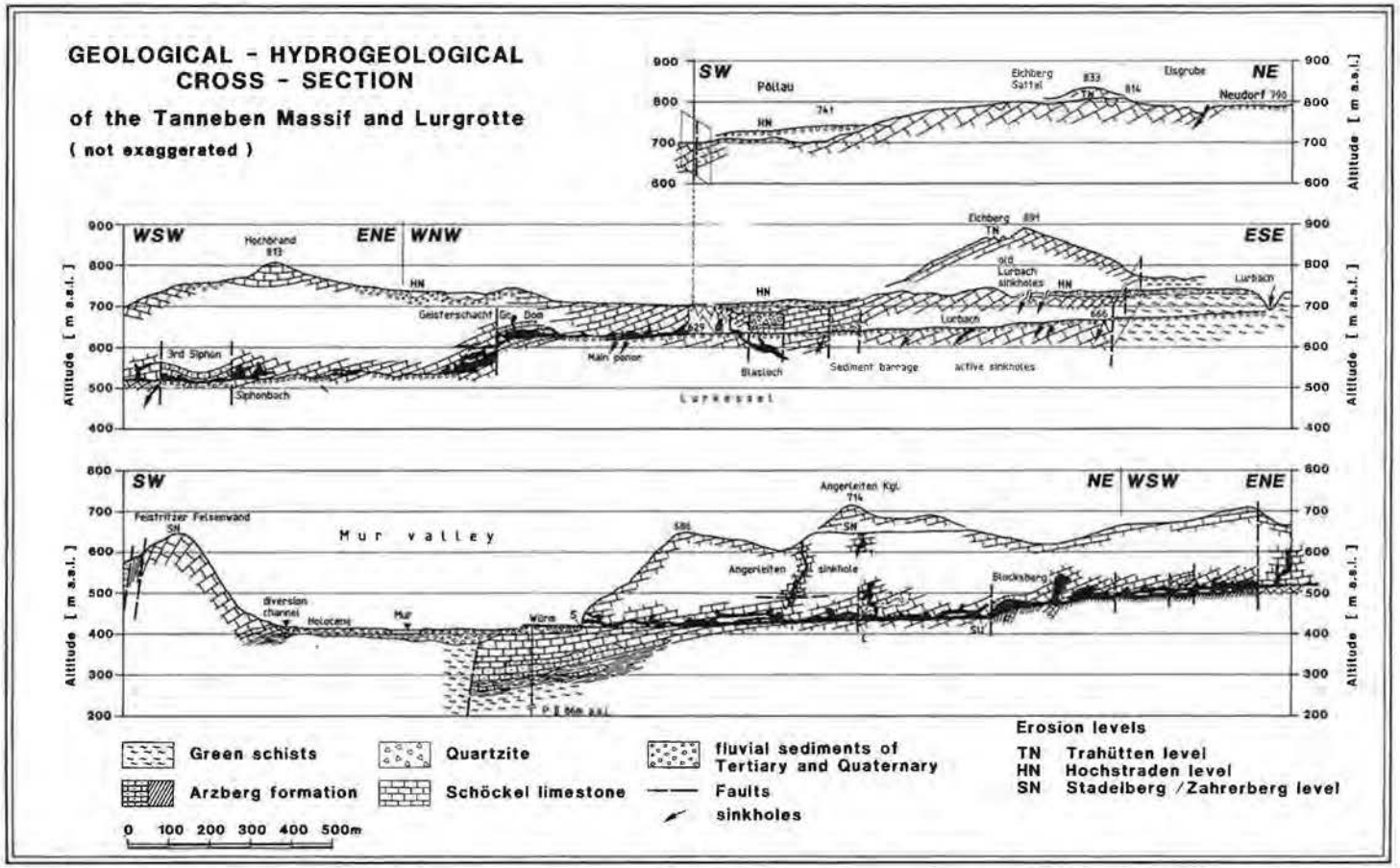

Fig. 2.7: Karsthydrogeological cross-section (W–E) of the Tanneben massif and Eichberg from the Mur valley to the basin of Semriach with Lurgrotte (draft: V. MAURIN, 1992; using cave map of H. BOCK).

2.3. Hydrologic and Climatologic Conditions (T. HARUM, H. STADLER)

2.3.1. General Climatological Review

Because of its position south of the Alps and the prevailing wind direction from N and NW the area of investigation is situated on the leeside relative to precipitation. For this reason the frequent atmospheric conditions with depression zones in the N and NW of the Alps don't bring such high precipitation amounts like in regions north of the Alps. The highest rainfalls are transported to the region in periods with depression zones in the S and SW (over the Mediterranean Sea) and NE and E, but the frequency of such events is not very high. High precipitation amounts with important intensity are measured frequently during local thunderstorm events in summer.

Figure 2.8 shows the seasonal variations of the mean monthly precipitation at the official station of Semriach (alt. 720 m) in comparison with the mean monthly air temperature at the meteorological station Frohnleiten (alt. 440 m) situated in the Mur valley about 20 km north of the investigation area (observation period 1971–1980). The data are published in HYDROGRAPHISCHES ZENTRALBÜRO (1983).

The climate is characterized by relatively low winter precipitation (minimum in December with 27 mm) and a significant maximum in summer (169 mm in July) due to frequent thunderstorm events. The highest daily rainfall height was measured in July 1975 with 93.5 mm. In normal years 262 days are without precipition, 10.5 days have daily sums of more than 20 mm, most of them in summer.

The temperature minimum is reached in January (s. fig. 2.8), maximum in July. In comparison with alpine regions the mean period of total snow cover is short with 54 days (beginning of January until the end of February), only on 2.1 days the snow depth is higher than 50 cm.

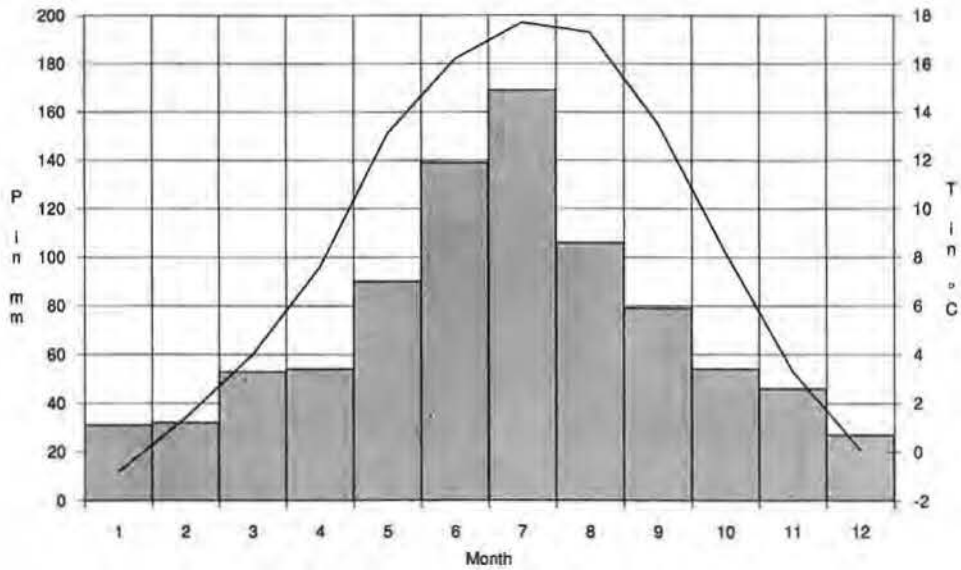

Fig. 2.8: Mean monthly precipitation (in mm) at the raingauge Semriach and mean monthly air temperature at the meteorological station Frohnleiten (°C) for the period 1971–1980.

The mean annual precipitation depth at the raingauge of Semriach is measured with 880 mm with annual variations between 669 and 1,351 mm (period 1971–80). The mean annual air temperature in Frohnleiten is 8.5° C.

2.3.2. Hydrographical Network

The topographic position of the hydrographical network is visible in fig. 2.1. The precipitation is continuously controlled at two raingauges in Semriach (data available since 1965) and on the karst plateau of Tanneben together with the air temperature (since 1986).

The Lurbach creek is draining a catchment area of 14.5 km², which is situated primarily in less permeable schists (s. fig. 2.1). The discharge of the Lurbach as input into the karst system is measured at a gauging station in Semriach upstream of the border between schists and the karstified limestones. Data are available from the period 1965–1973 and – with interruptions due to technical problems with the gage height recorder – since 1987.

The karst massif of Tanneben (surface 8.3 km²) is drained primarily by the two karst springs Hammerbach and Schmelzbach. The discharge of Hammerbach has been continuously measured from 1965–1975 and since 1983, that of Schmelzbach from 1965–1970 and with interruptions since 1983.

The fluctuations of the groundwater level in the porous aquifer of the Mur valley have been measured since 1973 in three observation wells of the hydrographical survey of the Government of Styria.

2.3.3. Hydrological Conditions

The investigation area can be divided into three hydrogeological units with rather different flow and input conditions:

1) The limestone massif of Tanneben (surface 8.3 km²) is intensively karstified and is being drained completely through the underground. There are two principal (Hammerbach and Schmelzbach, s. fig. 2.1) and few small karst springs (Q1–Q6, s. fig. 2.12).
2) The drainage basin of the Lurbach creek (14.5 km²) is situated primarily in less permeable paleozoic schists with low infiltration capacity.
3) The porous aquifer in the Mur valley consists of gravels and sands of the quaternary filling with a total thickness up to 40 m.

The waters from Lurbach and two smaller creeks (Eisgrube and Katzenbachschwinde) disappear into sinkholes. The most important one is the sinkhole of Lurbach at the upper cave entrance of the Lurgrotte in Semriach. The Lurbach creek infiltrates continuously into the karstified limestones and disappears at mean to higher discharges into the cave entrance (at lower discharges some 100 m upstream). After a distance of about 200 m the creek infiltrates in ponors the rest of the following part of the Lurgrotte being dry.

Two springs arise in the lower part of the Lurgrotte: the big spring of Schmelzbach (SU) and the smaller Laurins spring (L). Both form the subterranean stream Schmelzbach (S) which flows through the cave and emerges at the cave entrance in the Mur valley. Higher floods of the Lurbach flow directly through the entire cave system the capacity of the sinkholes in the higher part of the cave not being sufficient.

The discharge data of Lurbach, Hammerbach and Schmelzbach, are listed in tab. 2.1.

*Tab. 2.1: Discharge data in l/s from the input (Lurbach, observation period 1965–1973, 1987–1989) and the karst springs (Hammerbach, 1965–1975, 1983–1989; Schmelzbach, 1965–1970, 1983–1989; Laurins spring 1986–1987). NQ = lowest discharge, MQ = mean annual discharge, HQ = highest flood. * probably influenced.*

	NQ	MQ	HQ	HQ : NQ
Lurbach	*4	141	15,300	3,817
Hammerbach	33	193	2,000	61
Schmelzbach	15	79	11,400	760
Laurins spring	0.4	3.7	12	30

The high flow values of Lurbach and consequently Schmelzbach are only rough approximations, because the short flood crests with extremely quick changing of the water level at the gauging stations provoke high errors concerning the extrapolation of the discharge rating curves. For these reasons and as indicated by

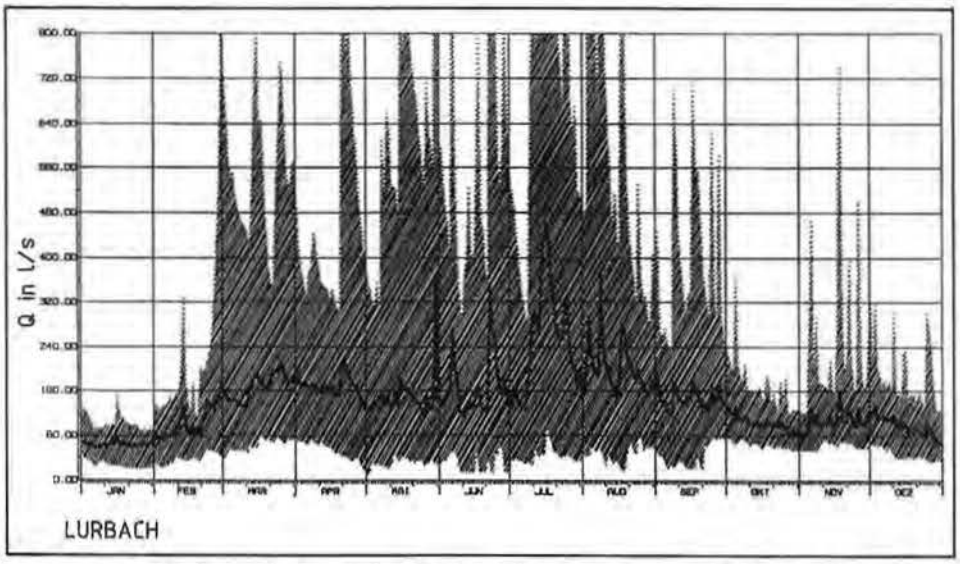

Fig. 2.9: Mean discharge hydrographs of Lurbach (input), Hammerbach and Schmelzbach spring with mean daily extreme values computed from mean daily discharges (l/s). *Continuation p. 37.*

the water balance data it is probable that above all the high runoff data of Lurbach are too low.

In fig. 2.9 the mean discharge hydrographs of Lurbach, Hammerbach and Schmelzbach computed from all mean daily discharges measured are plotted in comparison with the mean daily extreme values. The hydrographs show rather different characteristics.

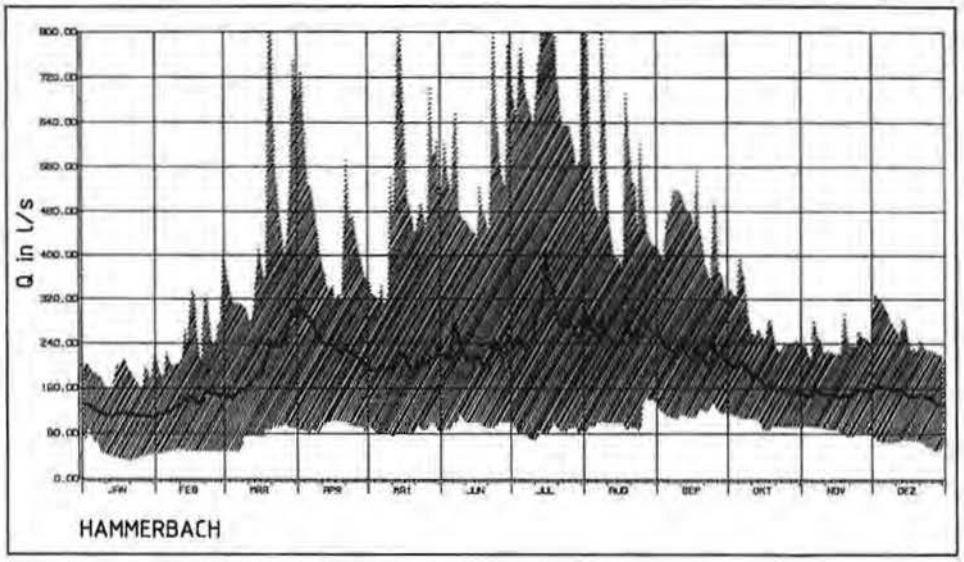

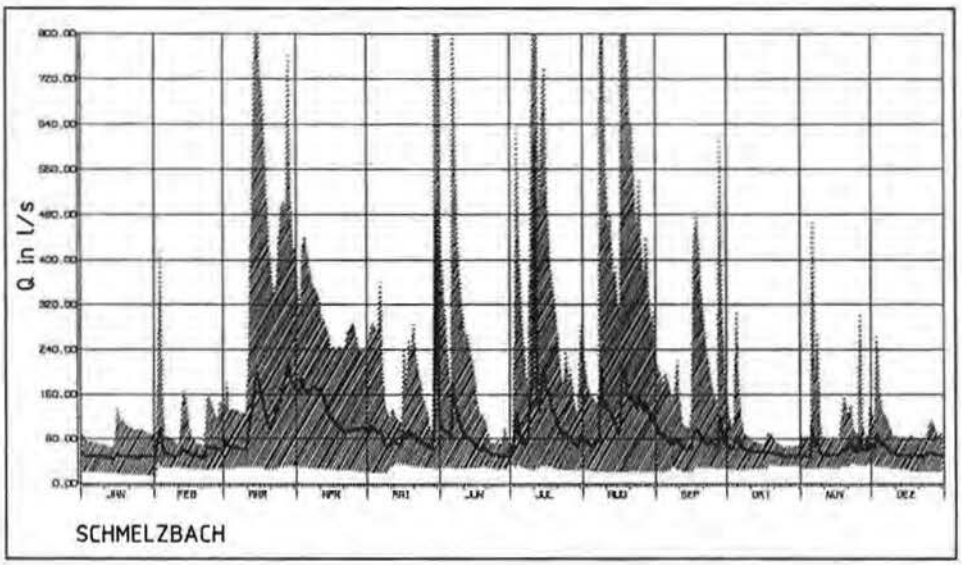

The **Lurbach** hydrograph is typical for a small drainage basin in less permeable rock formations (schists) with low infiltration capacity, a high portion of surface flow and extreme discharge fluctuations (s. tab. 2.1). The hydrograph shows two seasonal maxima due to the climatological conditions (s. also fig. 2.8): a first one in March/April in consequence of the snow melt and a second multipeak maximum due to the high summer precipitation, where the frequent thunderstorms provoke numerous floods which frequently produced destructions in the Lurgrotte. The steep recession limbs of the hydrograph indicate a low storage capacity of the aquifers (porous and fissured) in the catchment area.

Many tracing experiments with tracer injections in the Lurbach sinkhole have shown that **the Hammerbach spring represents the permanent resurgence of Lurbach** the residence time depending on the particular flow conditions during the experiments (s. chap. 5.2.). Only during three experiments at higher flow conditions the tracers injected could be detected in Hammerbach and Schmelzbach spring. These results proved that **at low water conditions both springs drain two isolated aquifer systems which have an episodic connection only at higher discharges.** This overflow from the Hammerbach to the Schmelzbach aquifer is not identical with the direct connection between the Lurbach sinkhole and the Schmelzbach spring due to floods of Lurbach which flow directly through the accessible galleries of Lurgrotte.

The hydrograph of the **Hammerbach spring** as the permanent resurgence of Lurbach is characterized by similar but attenuated discharge fluctuations because in case of extreme floods of Lurbach a high portion of Lurbach water flows through the Lurgrotte and the overflow zone (comp. high flow data in tab. 2.1). For the most part of the year the discharge of the spring is higher than that of Lurbach, which proves that the spring drains not only water from the Lurbach sinkhole but also infiltrated water from the karstified plateau of Tanneben. The low slope of the discharge recessions indicates that the aquifer consists not only of main drainage paths (karst channels, galleries etc.) but also of zones with high storage capacity (microfissured zones, sediment fillings).

The hydrograph of the **Schmelzbach spring** is only episodically influenced by the Lurbach catchment area. At low flow conditions the spring is draining a part of the northern karst plateau and two sinkholes (Eisgrube and Katzenloch) with low discharges as proved by tracing experiments (s. chap. 5.2.). A connection between the Bassgraben (uppermost part of Badlgraben) and the Schmelzbach system seems to be possible but is not yet proved. In times of low flow conditions the flat discharge recessions indicate an aquifer with high storage capacity. The episodically active overflow from the Hammerbach aquifer and furthermore the high floods of Lurbach flowing directly through the cave provoke extreme discharge fluctuations of the Schmelzbach cave stream the water level in the lower part of the Lurgrotte rising sometimes more than 10 m (at some places about 30 m). Contrarily to the Hammerbach spring the Schmelzbach frequently effected inundations near the cave entrance in the village of Peggau the residence time of the flood waves in the cave being extremely short (approx. a half an hour).

In fig. 2.10 the values of discharge exceeding probability of the Hammerbach spring computed from mean daily values as a measure for the filling stage of the karst reservoir are plotted against the corresponding exceedance values of Schmelzbach and Lurbach. It is clearly visible that between low flow and mean flow conditions of the Hammerbach spring there is a strict linear correlation of both parameters due to the permanent connection between Lurbach and Hammerbach on the one hand and to the catchment areas of both springs with partly similar hydrogeological and meteorological conditions on the other hand. Whenever the discharge of the Hammerbach spring exceeds a value of about 200 l/s (which corresponds to the mean annual discharge) usually dry karst channels become active and provoke an overflow of water from the Hammerbach to the Schmelzbach aquifer (T. HARUM et al.,1990; about considerations in the past on the relationship between discharges of Hammerbach and Schmelzbach refer to chap. 5.2.). This discharge value corresponds to a certain level of the karst water table, the "overflow level" being dependent

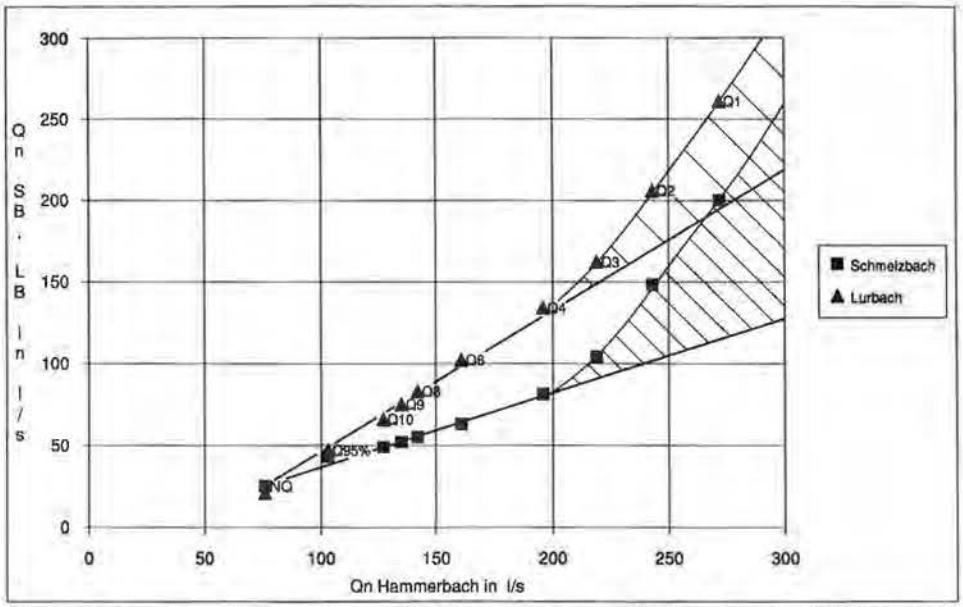

Fig. 2.10: Correlation diagram of mean discharge exceedance probality values (period 1966–1970). Q_n = discharge which is exceeded on n months, $Q_{95\%}$ = discharge which is exceeded on 95% of the year, NQ = discharge minimum.

significantly and first of all on the discharge of Hammerbach. The overflow can also be active at low discharges of Lurbach in times when the Hammerbach aquifer is filled to high extent. Correlations with the Lurbach discharge by H. ZOJER & J. ZÖTL (1974) showed that there is not a constant relationship between Lurbach discharge and the portion of Lurbach water in Schmelzbach.

This overflow level can temporarily change due to changings in sedimentation and erosion of cave sediments in the karst system. But the correlation of the exceedance curves of individual years gave well comparable results, so that it can be deduced that for the most part of the observation period the level of about 200 l/s was valid. Changings seem to be only of temporary character.

Concerning the hydrological conditions in both karst aquifers and their different types of discharge hydrographs three typical hydrological states can be deduced corresponding to three clearly distinguishable flow paths in the karst system not excluding possible minor flow systems (s. chap. 6.1.):

1) At discharges below the overflow level of about 200 l/s of Hammerbach discharge both aquifer systems are completely separated. In this case the Hammerbach spring is draining the total discharge of the Lurbach sinkhole and the southern part of the karstified plateau of Tanneben. The isolated Schmelzbach aquifer drains the northern part of the plateau and two sinkholes with small discharges. **Under these conditions there exists no connection between the sinkhole of Lurbach and the two springs in the lower part of the Lurgrotte (Schmelzbach and Laurins spring).**
2) The overflow from the Hammerbach to the Schmelzbach aquifer becomes active at flow rates of the Hammerbach spring higher than the mean annual discharge.

Under these conditions the Schmelzbach spring is draining a portion of water from the Lurbach catchment area (basin of Semriach). This portion increases with the increasing Hammerbach discharge.

3) **Extreme floods take three different flow paths in the underground.** The greatest portion of Lurbach water flows direc:ly through the presently accessible cave (length 5 km), resurges in the Schmelzbach spring and causes its extreme discharge fluctuations. A second portion flows through the sinkholes in the higher part of the cave to the Hammerbach aquifer where it is once more separated into two components, one flowing to the outlet of the Hammerbach spring and the other through the overflow zone to the Schmelzbach spring.

2.3.4. Characterization of Discharge Recessions

2.3.4.1. Methodology

After longer dry weather periods the decrease of discharge can be characterized by the exponential function (E. MAILLET, 1905)

$$Q_t = Q_0 e^{-\alpha t}, \qquad (2.1)$$

where

Q_t = discharge after the time t of the recession period (l/s),
Q_0 = discharge at time t = 0 (intersection with the ordinate),
α = recession coefficient (d^{-1}),
e = base of the natural logarithm.

The slope α is characteristic for the depletion of the groundwater reservoirs in the catchment area and gives informations about the storage capacity of the aquifer.

Plotting log Q versus t the hydrograph recessions which follow this exponentional function will be a straight line. Not straightlined sections in the first part of the recession limb with greater slopes represent the sum of several exponential functions corresponding to flow components with shorter retention.

For the separation of the flow components of the discharge hydrograph it is necessary to split the curve in separate exponential functions, starting at the point with the lowest discharge (end of recession). For the last recession limb of the hydrograph which follows the above mentioned equation after E. MAILLET (1905) a curve is fitted using the method of the least squares.

This function which corresponds to the **base flow component** is extrapolated back under the hydrograph (usually for karst regions until the theoretical base flow peak under the discharge maximum). Then the difference between total hydrograph and computed base flow is plotted again giving the sum of **direct and interflow component** (for springs usually only the direct flow component).

Then the same procedure is repeated – if possible – for the separation of direct flow and interflow (B.S. BARNES, 1939).

The two or three α-values computed in this way correspond to the flow components with different storage conditions and – as function of α – depletion times.

This method is used by a recently developed computer program (F. GRAF, 1991), which analyses the recession limbs of mean daily discharges. Periods with continuous runoff recessions are chosen automatically and compared with times without precipitation or with probably no groundwater recharge. Recession limbs with the

best fit (high correlation coefficient and random distribution of the residuals) are selected for further calculations. In a next step the α-value and the intersection with the ordinate of each recession and its components and the depletion time of the different storage components are calculated, ditto the mean values, standard deviation and variance of α and Q_0. The volumes of quasi mobile water (water which can be discharged without hydraulic stimulation) are computed by the equation

$$V = Q_0 \cdot 86.4/\alpha \ (m^3) . \qquad (2.2)$$

2.3.4.2. Results

For the evaluation hydrological data are available as mean daily discharges between the years 1965 and 1975. Twenty-six significant recession periods were chosen from the gauging stations Lurbach (input, catchment area in less permeable schists) and the karst springs Hammerbach and Schmelzbach (output). The results are shown in tab. 2.2 and 2.3. The mean depletion functions calculated from the 26 recession limbs are plotted in fig. 2.11.

Tab. 2.2: Mean values of the recession function parameters for Lurbach (input), Hammerbach and Schmelzbach (output).

	VOLUME (m^3)			DEPLETION TIME (d)		αdirect (d^{-1})	Q_0 (l/s)	αbase (d^{-1})	STD. ERR. αbase	Q_0 (l/s)
	total	direct	base	direct	base					
Lurbach	387,000	14,200	373,000	12.5	180	0.5114	56	0.0422	0.0009	181
Hammerbach	1.109,000	6,000	1.103,000	19.0	505	0.2690	16	0.0149	0.0002	190
Hammerb.-Lurb.	722,000							0.0146		173
Schmelzbach	508,000	9,000	499,000	22.0	555	0.2493	23	0.0118	0.0002	68
Karst total	1.230,000									

Tab. 2.3: Total water volumes related to MQ and $MoMNQ_T$ (mean monthly NQ).

	MQ (l/s)	V_{MQ} (m^3)	$MoMNQ_T$ (l/s)	V_{MoMNQT} (m^3)	Depl. time (d from MQ)	Depl. time (d from $MoMNQ_T$)
Lurbach	129	264,000	72	147,000	187	172
Hammerbach	180	1.044,000	135	783,000	547	529
Schmelzbach	97	710,000	57	417,000	612	596
Total Tanneben	148	1.490,000	120	1.053,000		

It is clearly visible that the Lurbach hydrograph is characterized by a mean depletion curve with a significantly greater slope for direct and base flow (higher α-values) and a shorter depletion time (after 187 d the groundwater reservoir is empty, i.e. Q < 0.1 l/s) than both karst springs.

It proves that parts of the karst aquifer have a higher storage capacity than the drainage basin of the Lurbach, situated in noncarbonatic rocks. The karst aquifer can be characterized by two rather different drainage systems, one with low retention is formed by greater conduits (direct flow) and the other one (base flow) by zones with high storage capacity (micro fissured zones, sediment fillings). The water volumes calculated in tab. 2.2 show the significant difference between direct flow

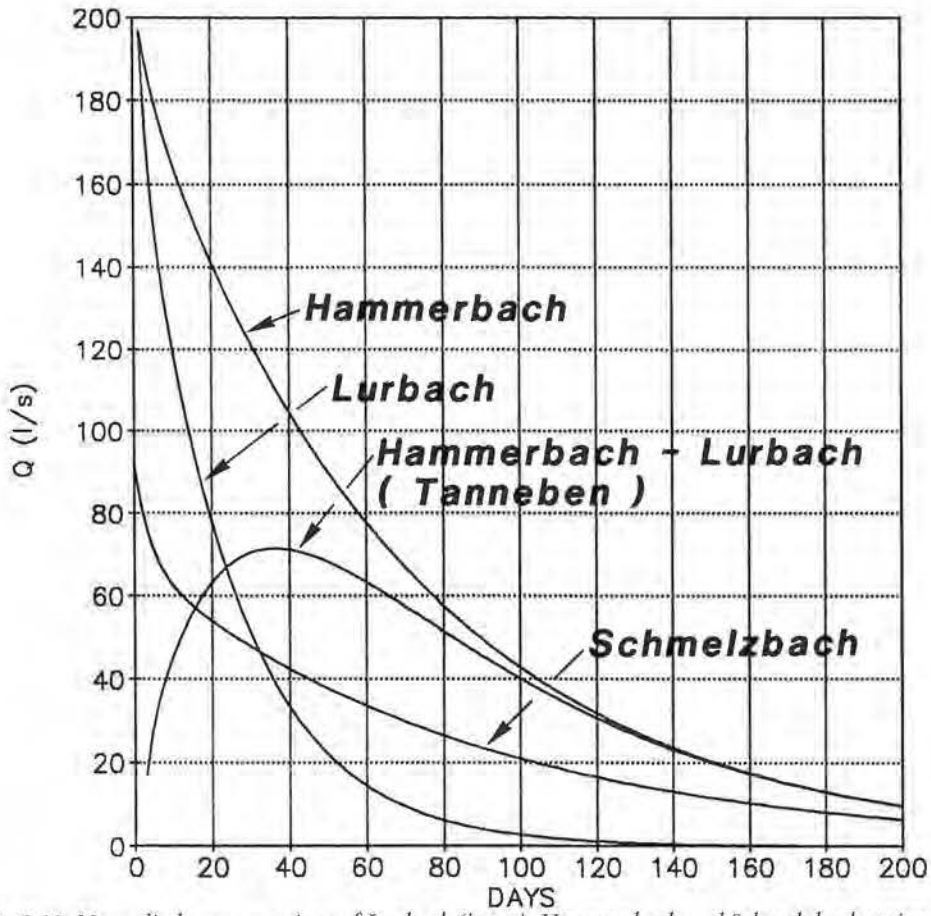

Fig. 2.11: Mean discharge recessions of Lurbach (input), Hammerbach and Schmelzbach spring and karst water from Tanneben (= difference between Hammerbach and Lurbach recession).

and base flow, the base flow volumes being between 55 (Schmelzbach) and 186 (Hammerbach) times greater than the direct flow volumes.

At discharges of the Hammerbach spring below 200 l/s (no active overflow to the Schmelzbach system) the Hammerbach aquifer is completely recharged by the Lurbach drainage basin and from the precipitation on the karst plateau of Tanneben. The difference of Hammerbach and Lurbach depletion curves, plotted in fig. 2.11, gives informations about the hydrodynamic features of the portion of karst water from Tanneben and represents the main output portion of water from the karst aquifer stored over a longer time.

The depletion curves in fig. 2.11 are computed from recession periods with a maximum length of 35 days and extrapolated to 200 days assuming a corresponding period without groundwater recharge and validity of the α-values calculated for the complete depletion of the reservoirs. These assumptions can only be theoretical (not so long dry weather periods in the investigation area, the short recession periods

without precipitation give no informations about the depletion function of the aquifer parts with the highest storage capacity).

It is visible in fig. 2.11 that at a Hammerbach discharge of about 200 l/s the input from Lurbach and the total Hammerbach output are equal. At higher discharges the overflow to the Schmelzbach aquifer is active, input from Lurbach is higher than Hammerbach output.

In the first part of the recession curves the difference of input and output is increasing, reaching its maximum about 36 days after the starting point (t = 0) of the recession curves with 71 l/s. This peak retardation of the difference curve can be explained by the hydrodynamic processes during and after a flood of the Lurbach. At high discharges the elevated karst water level provokes a positive hydraulic gradient between the main conduits and the zones with lower permeability, i.e. "older" reservoir water is retarded and event water flows f.e. from the karst channels into the micro fissures and is stored there over a longer time. Subsequently the falling water level in the channels provokes a change of the hydraulic gradient to the opposite direction. Therefore the inflow of "older" reservoir water from the less permeable zones increases with decreasing spring discharge and reaches its maximum with high retardation compared to the discharge peak at the karst spring. The assumptions mentioned above are confirmed by the fact, that the recession curves of singular events have nearly the same shape. Deviations from the mean values are dependent on the maximum discharge values and the hydrological conditions before the runoff event.

The portion of older reservoir water in the spring discharge increases continuously and reaches 100% when the Lurbach reservoir (input) is theoretically empty approx. 180 days after recession start.

The volume of this water stored over a longer time is 65% of the total Hammerbach volume (s. tab. 2.2), which proves the high storage capacity of the retardation zones.

2.3.5. Interactions between the Karst and Porous Aquifer in the Mur Valley

Most of the tracing experiments with injections into the sinkhole of Lurbach gave as results recovery rates in the range of 60–70% at the Hammerbach spring (s. chap. 5.2.). Due to the fact that there exist no other important springs which could drain the remaining 30% of the tracers injected, it was assumed in literature (e.g. V. MAURIN, 1952, H. BATSCHE et al.,1967) that the porous aquifer in the Mur valley is recharged directly by karst water from the Tanneben massif. This assumption seems to be possible because the karstification base (paleozoic schists) is deeper than the substratum of the quaternary gravels and sands which is formed by the same paleozoic limestones as the Tanneben massif.

All karst springs are situated at the altitude of the Würm terrace. In the Lurgrotte there are no indications that the karstification goes deeper than the present outlet. As to Hammerbach spring it is known that a siphon some meters behind is 4 m deeper than the outlet. Therefore a groundwater recharge by karst water from the saturated zone of the Hammerbach aquifer seems possible.

The investigations by G. SCHICKOR (1983) show that the porous aquifer consists of quaternary gravel and sands with relatively high permeability (coefficient of permeability $2–3 \times 10^{-3}$ m/s) and an aquifer thickness up to 16 m in a N–S directed erosion channel near the eastern valley border with the outcropping paleozoic limestones. The groundwater is used for the water supply of the village Peggau and for some private water supplies.

The question of possible interactions between karst and porous aquifer was one of the main points of the investigations of the ATH-group. Additionally to the existing monitoring network installed by the governmental hydrographical survey and by G. SCHICKOR (1983) the piezometric head was measured in all existing wells of the groundwater field at two different hydrological situations (higher and lower groundwater level). The water table contours for the example of a high groundwater level in spring 1991 are represented in fig. 2.12. The situation is characterized by a

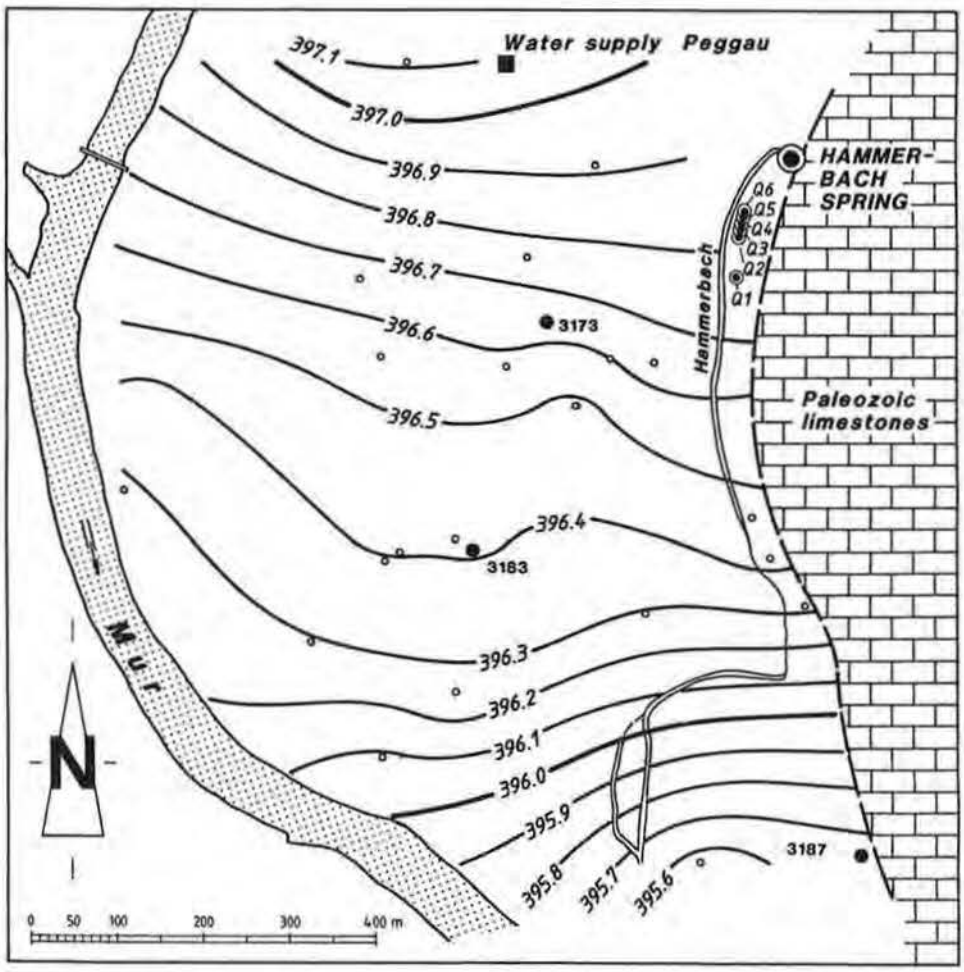

Fig. 2.12: Groundwater contours at higher groundwater level (910607) in the porous aquifer near the Hammerbach spring.

general N–S direction of the groundwater flow parallel to the river Mur and the eastern valley border formed by the outcropping limestones. The gradient of the groundwater table is low with a mean value of 1.1×10^{-3}. Even in the zone near the outlet of the Hammerbach spring no groundwater mound is visible which could indicate a significant groundwater recharge by karst water. South of the spring near the Hammerbach creek the groundwater table is elevated a little (about 10 cm). This elevation can be effected by water losses from the Hammerbach creek (the bed of the stream is some meters higher than the groundwater level) or by a recharge by small amounts of karst water. The water table contours at low groundwater level (March 1991) give the same flow directions and therefore are not represented.

The seasonal fluctuations of the groundwater level in three observation wells of the hydrographical survey of the years 1973–1975 are represented in fig. 2.13 in comparison to the discharge hydrographs of the river Mur (gauging station Graz) and the Hammerbach spring as main outlet of the karst aquifer. Both hydrographs are characterized by rather different seasonal fluctuations of the discharge due to the different hydrological conditions in their drainage basins. The river Mur drains a catchment area of 6,989 km², an important part being situated in regions with high altitudes (mean altitude of the drainage basin c. 1,250 m, highest regions more than 3,000 m). The late snow melt in the higher alpine regions effects a large runoff peak in spring and summer followed by the floods due to the summer precipitation. On the contrary the snow melt in the small Hammerbach catchment area (surface 19.4 km², mean altitude 800 m) is finished earlier giving only a shorter discharge peak in March/April. The comparison of the significantly distinct hydrographs of the Mur river and the Hammerbach spring with the seasonal fluctuations of the groundwater level enables us to draw conclusions on the origin of the groundwater. The three observation wells are situated in different distances from the Mur (s. fig. 2.12) and are characterized by very similar fluctuations of the groundwater level. It is clearly visible that they depend in a significant way on the runoff fluctuations of the river Mur the reactions of the groundwater level on floods of the river showing a retardation of about two weeks. The groundwater table reaches the same large maximum in spring and summer as the river due to the late snow melt in the higher regions of the great drainage basin. Therefore it can be deduced that the river infiltrates in the groundwater field downstream of its entrance from the narrow part of the valley north of Peggau into the larger basin.

The comparison of the normalized seasonal fluctuations of Mur and Hammerbach with those of the groundwater level of the year 1974, their correlation analysis and double-mass curves (Fig. 2.14) confirm that the groundwater field is mainly influenced by the flow regime of the river Mur both parameters showing a significant statistical correlation (correlation coefficient $r = 0.79$) in comparison with the correlation analysis of the discharge of Hammerbach and groundwater level which only gives a correlation coefficient of $r = 0.05$.

Summarizing the results of the recharge conditions of the groundwater field one can deduce that there are no indications that the porous aquifer in the Mur valley could be recharged by greater amounts of karst water from the Tanneben massif. The fluctuations of the groundwater level and the flow direction in the field indicate that the aquifer is primarily recharged by water from the river Mur infiltrated in the northern part of the basin. A small amount of karst water exfiltration through the fissured limestones in the deeper zone of the Hammerbach aquifer in the range of some l/s cannot be excluded due to the small elevation of the groundwater level

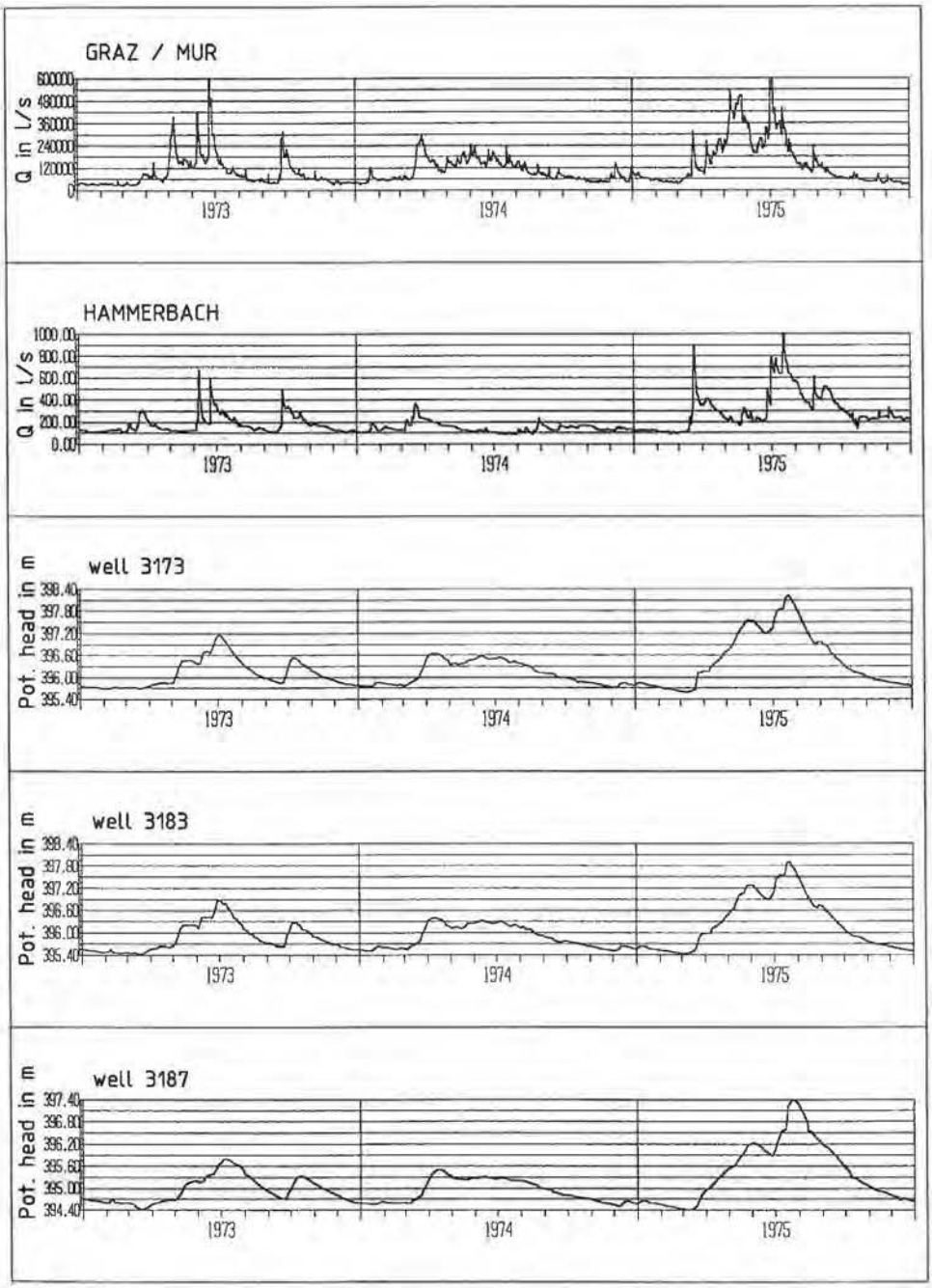

Fig. 2.13: Mean daily discharges of the Mur river (gauging station Graz) and the Hammerbach spring compared with the fluctuations of the groundwater level in three observation wells (period 1973–1975).

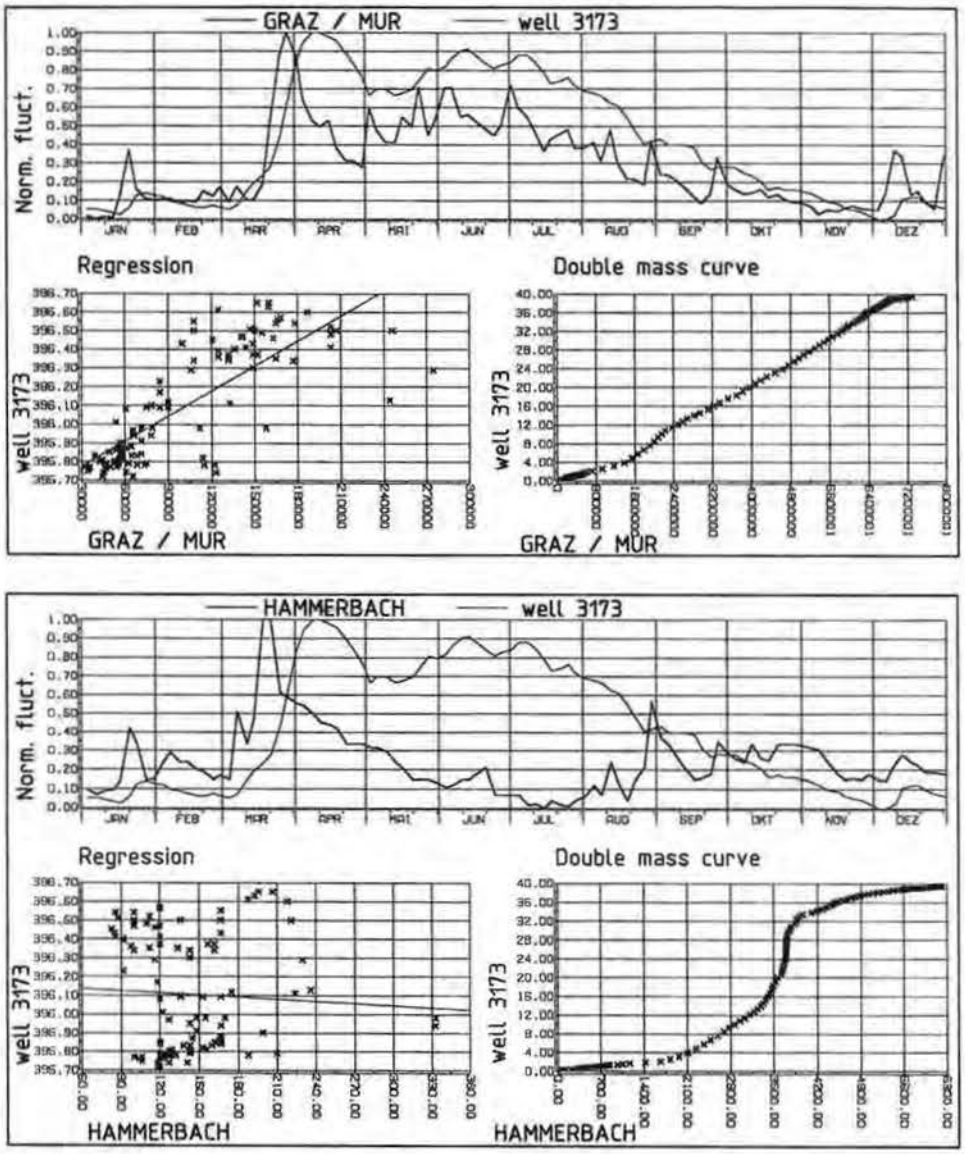

Fig. 2.14: Correlation analysis of the discharges of the Mur river and the Hammerbach spring with the corresponding piezometric heads in the porous aquifer (observation well 3173). Data are used from the year 1974.

south of the Hammerbach spring, but it could also be explained by small losses of water from the bed of the Hammerbach watercourse.

2.3.6. Water Balance

For the estimation of the mean water balance the hydrological data from the observation period 1966–70 were used where complete measuring series for all

parameters exist. The water balance equation for the total catchment area (22.8 km²) including the input from the Lurbach drainage basin can be written as

$$Q_T = P - ET_r, \tag{2.3}$$

where

$Q_T = Q_{HB} + Q_S + Q_{SO}$ = sum of mean annual discharges of the karst springs Hammerbach (HB) and Schmelzbach (S, both are measured) and a possible subterranean outflow (SO) into the porous aquifer (not measured).
P = mean annual areal precipitation,
ET_r = mean annual real evapotranspiration.

The discharge of the springs Q1–Q6 (only a few l/s) is included in Q_T the gauging measurements being always executed downstream of their inflow in the Hammerbach, the discharge of Schmelzbach spring and Laurins spring is included in Q_S.

The entire catchment area of the karst springs (s. fig. 2.1) is well delimitable in the N by the southern border of the small valley of Badlgraben, in the S by the outcropping karstification basis formed by schists (s. chap. 2.1.) and in the E by the orographic watershed of the Lurbach drainage basin (less permeable schists). From the entire surface of 22.8 km² 14.5 km² are the portion of the Lurbach drainage basin, the remaining 8.3 km² represent the forested karst plateau of Tanneben which is completely drained through the underground (no surface flow). An exact delimitation of the catchment areas of Hammerbach and Schmelzbach on the karst plateau is not possible, but it can be assumed that the Hammerbach spring drains the southern part of the plateau (c. 4.9 km²), the Schmelzbach and Laurins spring the northern part (c. 3.4 km²).

As mean areal precipitation the measured values of the raingauge in Semriach are assumed to be representative for the catchment area the station being situated in the Lurbach basin (alt. 720 m). The real evapotranspiration was calculated by means of the equation of TURC (cit. in D.M. GRAY, 1970):

$$ET_r = P/\{0.9 + [P/(300 + 25\,T + 0.05\,T^3)]^2\}^{0.5} = 441 \text{ mm}, \tag{2.4}$$

where

P = 897 mm = mean annual precipitation depth,
T = 7.4° C = mean annual air temperature.

T was calculated by linear correlation of the measured temperatures and corresponding altitudes of the neighbouring meteorological stations in Graz-Andritz, Frohnleiten (both in the Mur valley) and Teichalpe (in the N of the investigation area, alt. 1,180 m).

The results of the water balance calculations represented in fig. 2.15 can only be considered as a rough approximation of the reality taking into account all possible errors first of all concerning the measurement of rainfall and snow and extrapolation to areal precipitation, calculation of the real evapotranspiration only with the parameters precipitation and air temperature (no complete meteorological station in the investigation area), discharge measurement, delimitation of the catchment area etc. Therefore one can say that the results of the water balance agree well. The relatively high evapotranspiration seems to be realistic taking into account that an important part of the catchment is forested.

The interpretation of the remaining term from the water balance equation (7.5% of the mean annual precipitation resp. 49 l/s) is difficult. There are three possibilities:

1) The measured output (discharge of both springs) does not represent the total outflow from the karst aquifer. In this case this deficit can be considered completely or partially as a subterranean flow component of karst water into the porous groundwater field. Comparing with the tracer recovery rates of 60–70% at the Hammerbach spring (s. chap. 5.2.), this explanatation is possible the deficit being 27% of the mean discharge of Hammerbach. Taking into account the flow conditions in the porous aquifer (s. fig. 2.12) only a not punctual diffuse groundwater recharge by karst water through fine fractured fissures in deeper zones of the limestones seems to be possible but could not be proved on the basis of the existing measurement network.
2) The period for a water balance is too short, the deficit in the water balance represents a retention component in this case.
3) The deficit is effected by errors in calculation of mainly the evapotranspiration and/or the mean areal precipitation.

Summarizing the results of the hydrological investigations one can deduce that a certain amount of groundwater recharge by karst water from the Tanneben massif cannot be excluded. If a subterranean outflow of karst water exists it probably happens in the area near the outlet of the Hammerbach spring (saturated zone of the karst aquifer) and can only be in the range of about max. 50 l/s which flow in a diffuse way through fine-fractured fissures (not punctual through karst channels) into the porous aquifer. A groundwater recharge near the Schmelzbach outlet seems to be improbable the subterranean cave stream having no losses in the entire lower part of the Lurgrotte which shows no indications of a deeper karstification.

On the other hand the numerous tracer experiments never gave indications of a groundwater recharge by karst water the injected tracers never being detected at the wells sampled in the groundwater field (comp. chap. 5.2.).

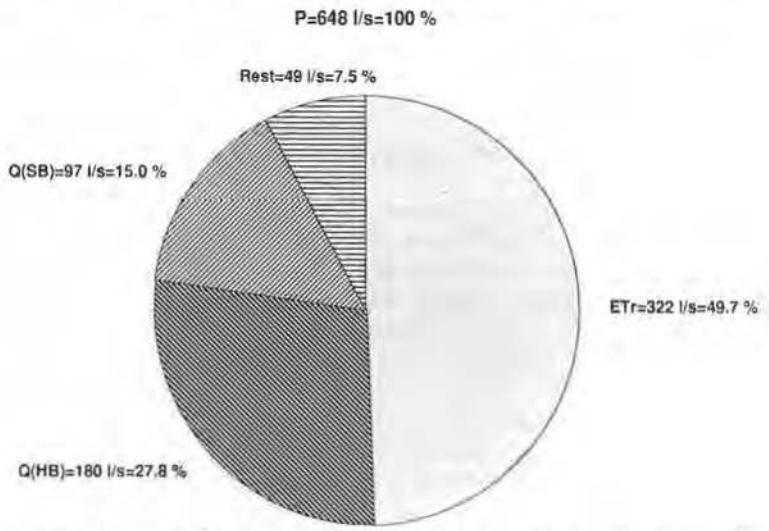

Fig. 2.15: Water balance data of the karst aquifer (period 1966–1970). P = mean annual precipitation, ET, = mean annual real evapotranspiration after TURC.

3. Long-Term Investigations with Natural Tracers

(T. HARUM, H. ZOJER, H.P. LEDITZKY, R. BENISCHKE, W. STICHLER, P. TRIMBORN, D. RANK, V. RAJNER)

3.1. Introduction, Sampling Sites and Analyzed Parameters

Additionally to the short-term investigations, which give informations about the hydrodynamic processes during one hydrologic event (s. chap. 4.), the long-term observation of the fluctuations of the contents of natural tracers leads to results about the seasonal variations of aquifer storage and recharge. Unfortunately, on account of financial problems the sampling intervals are usually too long in aquifers with a high portion of water with short residence times in the underground such as the Lursystem.

In the period from February 1986 to July 1987 samples were taken from representative waters in intervals of 14 days and analyzed on the major ions and contents of the environmental stable isotope Oxygene-18.

As representative input into the karst system waters from three sinkholes **Lurbach (LB), Katzenloch (K) and Eisgrube (E)** were sampled. The sampling program included the main karst springs in the Mur valley **Hammerbach spring** (HB), **Q1, Schmelzbach spring (SU), Laurins spring** (L) – both last-named outlets are situated in the lower part of the Lurgrotte – and the **Schmelzbach** (S) at the entrance of the Lurgrotte in Peggau, which principally drains the Schmelzbach spring and Laurins spring. Furthermore the waters from **two wells in the porous aquifer of the Mur valley** were sampled (one well for a private water supply called Mild and the well for the water supply of the village of Peggau). The position of the sampling sites has been represented in the hydrogeological map in fig. 2.1, for the porous aquifer in fig. 2.12.

The samples were analyzed on the major ions calcium, magnesium, sodium, potassium, chloride, nitrate, sulphate and bicarbonate in the laboratory of the IGH Graz. The parameters electrical conductivity, water temperature and pH were measured together with the discharge directly in the field. The stable isotope oxygene-18 was measured in the laboratory of the Institute for Hydrology (GSF Munich).

3.2. Hydrological Conditions During the Observation Period

The mean annual precipitation of the years 1986 and 1987 in the investigation area corresponds with values of 825 mm and 950 mm resp. at the station in Semriach to a normal year. Also the mean annual discharge of the Hammerbach with 180 l/s corresponds to the mean discharge of the period 1966–1975.

The daily precipitation amounts in Semriach are plotted in fig. 3.1 in comparison with the discharge hydrographs of the principal karst springs Hammerbach and Schmelzbach (mean daily discharges, in periods with breaks due to technical problems with the water level recorders the values of single discharge measurements are plotted), Laurins spring (only single measurements) and the fluctuations of the groundwater level at the water supply well of Peggau).

Both winters were relatively cold with high amounts of snow (more than 1 m in February 1986) and low flows of the springs. The discharge hydrographs of the karst springs are characterized by two periods with high discharges: a first one in

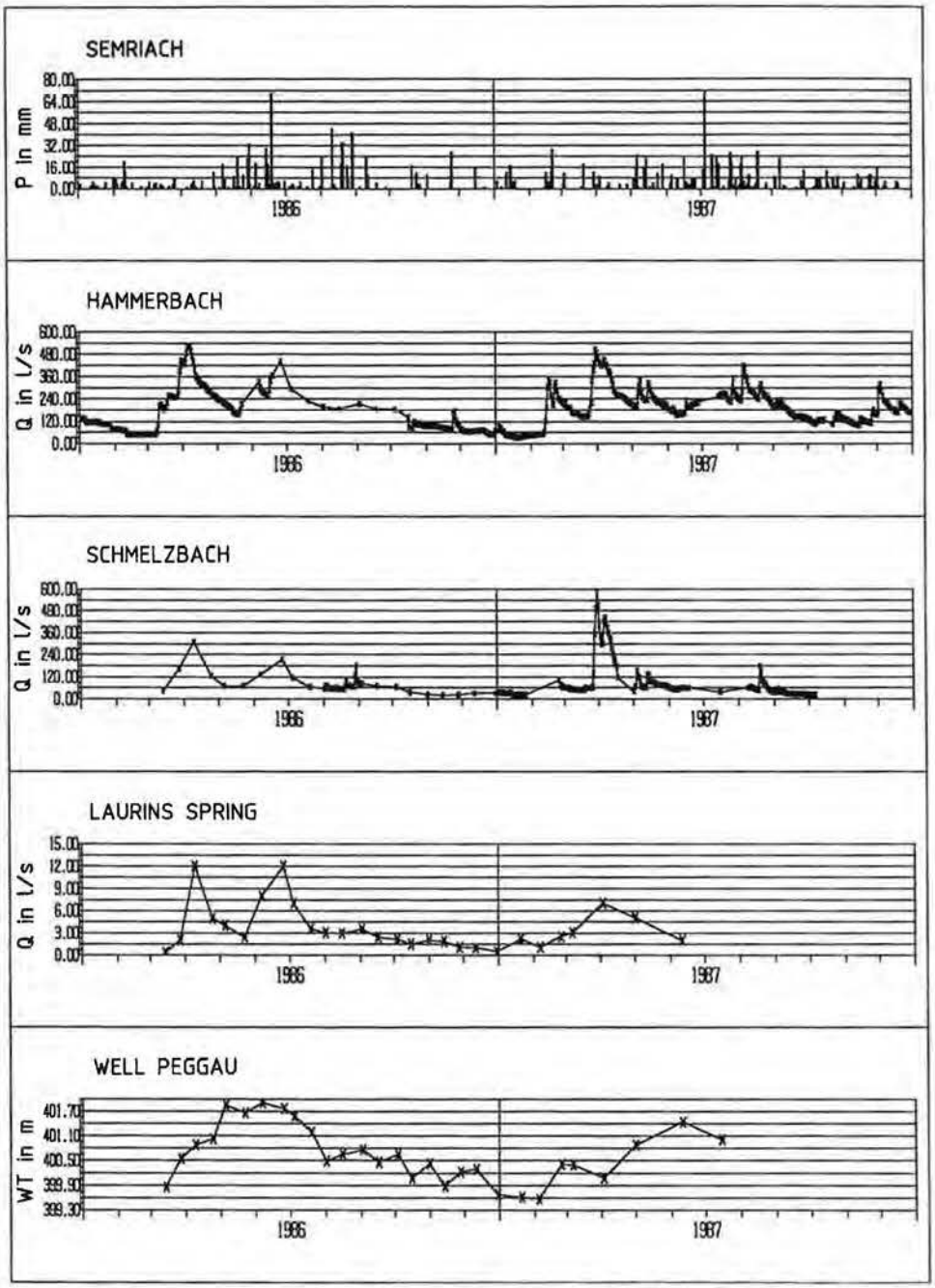

Fig. 3.1: Hydrometeorological conditions during the period of the hydrochemical and isotopcal investigations (1986–1987). Daily precipitation at the raingauge Semriach, mean daily discharges (partially only single discharge measurements) of Hammerbach and Schmelzbach spring, discharge of the Laurins spring and fluctuations of the groundwater level at the water supply well in Peggau (pos. of all measuring sites s. fig. 2.1).

February/March due to the snow melt and a second one in summer due to storm events with high precipitation intensity.

The fluctuations of the groundwater level, represented in fig. 3.1, show a minimum in February/March and a significant maximum in June due to the later snow melt in the higher regions of the catchment area of the river Mur (c. chap. 2.3.).

3.3. Hydrochemical Investigations

3.3.1. Hydrochemical Characterization of the Flow Conditions by Means of Computed Calcite Saturation Indices and CO_2-Partial Pressures

The CO_2-partial pressure depends primarily on the vegetation and the soil types in the catchment area. In literature values are mentioned in the range of $10^{-1.8}$–$10^{-2.5}$ at (T.C. ATKINSON, 1977), whereas the p_{CO2} of the atmosphere is in the range of $10^{-3.5}$ at. Due to the direct contact with the atmosphere surface waters are usually in equilibrium with the p_{CO2} of the air. Groundwaters with an important vertical infiltration component usually reach an equilibrium status with the p_{CO2} of the soil air (J. FANK et al., 1989).

The solution capacity of calcite and dolomite in water is normally small, it increases with the CO_2-content. Due to the carbonate solution CO_2 is consumed (decrease of CO_2-partial pressure), in closed systems without input of CO_2 the p_{CO2} can decrease under the atmospheric CO_2-partial pressure. In open systems like shallow groundwaters and karst aquifers higher solution rates are possible due to the supplement of CO_2 consumed by the solution processes.

For these reasons the calculated saturation indices and CO_2-partial pressures represent a good natural tracer enabling us to draw conclusions on the origin of different water types in dependance on the different infiltration conditions in their catchment areas. Water types with the same origin (comparable infiltration conditions referring to vegetation, lithology, soil types and altitude of the catchment area) are characterized by a linear correlation between the parameters calcite saturation index ($Si_{Calcite}$) and the logarithm of the CO_2-partial pressure ($\log p_{CO2}$). In fig. 3.2 the values of calcite saturation indices ($Si_{Calcite}$) are plotted against the corresponding CO_2-partial pressures (p_{CO2}). Both parameters are calculated with the program WATEQ (A. BATH,1980, J. FANK, 1988).

Such linear relations between both parameters are clearly visible for the waters of the Katzenloch sinkhole, the Laurins spring and at low water conditions for the Schmelzbach spring.

The **Laurins spring** (L) draining only waters of the unsaturated zone infiltrated on the forested karst plateau of Tanneben which are rich in CO_2 is characterized by a supersaturation and high calcium concentrations. The strong linear correlation during the whole observation period proves that there is no mixture with water from the saturated zone (Hammerbach system). The low seasonal fluctuations of the values in fig. 3.2 indicate that the spring is draining primarily zones with fine fissures and sediment fillings with high storage capacity and relatively long residence times. These results are in accordance with those of the isotopical investigations (s. chap. 3.4. and 6.2.) and the results of the tracing experiments (s. chap. 5.2).

The values of the **Lurbach** (LB) show higher deviations of the parameters from the straight saturation line in fig. 3.2. This effect is typical for water from a catchment

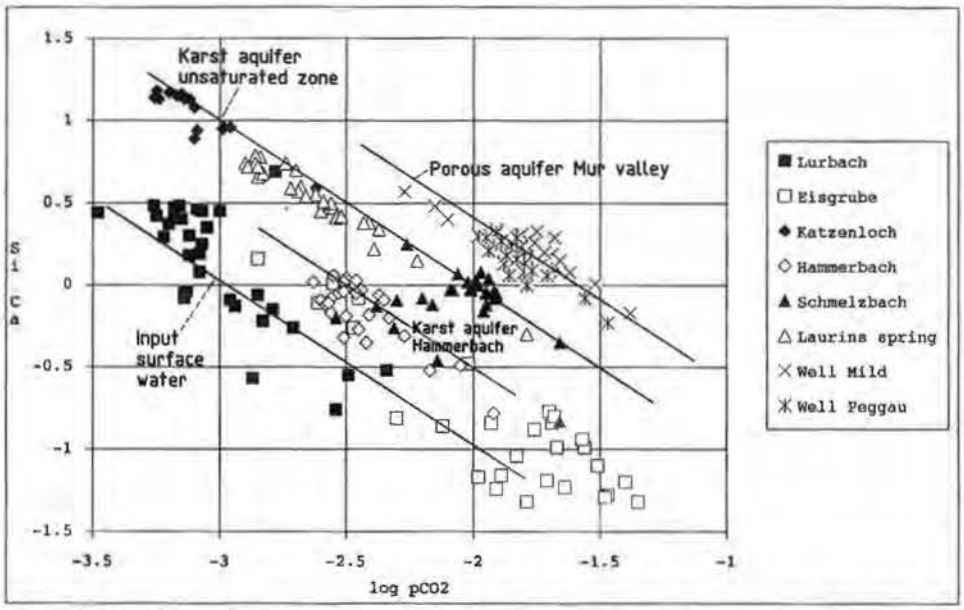

Fig. 3.2: Correlation diagram of CO_2-partial pressure (log p_{CO2} and the corresponding calcite saturation indices (Si_{Ca}) of the sampled waters (data from the observation period 1986–1987).

area with low infiltration capacity (less permeable schists), high discharge fluctuations and a high portion of surface flow on the total discharge hydrograph (s. chap. 2.3.).

The values of the **Hammerbach spring** (HB and also spring Q1, which belongs to the same aquifer and is not plotted in fig. 3.2) are placed between those of Lurbach (permanent connection) and infiltration waters from the karst plateau (represented by the Laurins spring). The fluctuations being lower than those of Lurbach reflect the temporarily and quantitatively changing mixture of both water components.

The **Schmelzbach spring** (SU) at low water conditions in autumn and winter shows the same relation of the parameters $Si_{Calcite}$ and p_{CO2} as the Laurins spring, both springs being without connection in these periods with the Hammerbach resp. Lurbach system. During low water seasons the Schmelzbach spring drains only the northern part of the Tanneben plateau (same infiltration conditions as the waters of the Laurins spring) and the sinkholes Katzenloch and Eisgrube. Their connection with both sinkholes is proved by tracing experiments (s. chap. 5.2). The waters of the sinkhole Katzenloch draining a local karst aquifer are situated on the same saturation line as the Schmelzbach spring, those of the sinkhole Eisgrube being on the same line as the Lurbach catchment area (both in less permeable schists).

The snow melt in spring and the higher summer precipitation provoke the filling of the Hammerbach aquifer and the temporary overflow of Hammerbach water into the Schmelzbach aquifer. The mixture effects a strong dilution of the Schmelzbach water by lower mineralized Hammerbach water and a move in the direction of the $Si_{Calcite}$-p_{CO2}-relation of the Hammerbach spring (Fig. 3.2). This overflow can only be observed when the discharge of the Hammerbach spring exceeds an "overflow mark" of about 200 l/s.

Extreme floods of the Lurbach take their way directly through the Lurgrotte and reach the Schmelzbach spring with only short retardation. In this case the portion of Lurbach water in the total discharge of the spring is so dominant that the water reaches nearly the $Si_{Calcite}$-p_{CO2}-relation of the Lurbach. Naturally it is not possible to determine the hydrodynamic processes of such short events with a sampling interval of 14 days, but some indications in fig. 3.2 show that the flow through the cave was sometimes active.

Contrary to the Schmelzbach spring the Laurins spring never shows an episodic or permanent connection with the Hammerbach system.

The waters sampled from two wells in the porous aquifer in the Mur valley, which are situated near the outcropping limestones at the valley border, are characterized by the highest p_{CO2}-values due to the higher CO_2-input through the unsaturated zone with low thickness and high permeability (gravel, sand). All plotted points in fig. 3.2 are situated on the same straight line in such a manner that no indication of a mixture with karst water of the Hammerbach or Schmelzbach type can be deduced. Comparing with the results of the hydrological investigations (s. chap. 2.3.) it seems improbable that the aquifer in the Mur valley is recharged by greater amounts of karst water from the investigation area.

3.3.2. Calcium-Magnesium-Ratio

A simple correlation of the calcium-magnesium concentrations (Fig. 3.3) allows a differentiation of the geological catchment areas of the different water types. The **input waters** of the sinkholes Lurbach and Eisgrube having their catchment areas primarily in schists are characterized by comparatively low calcium and higher magnesium concentrations.

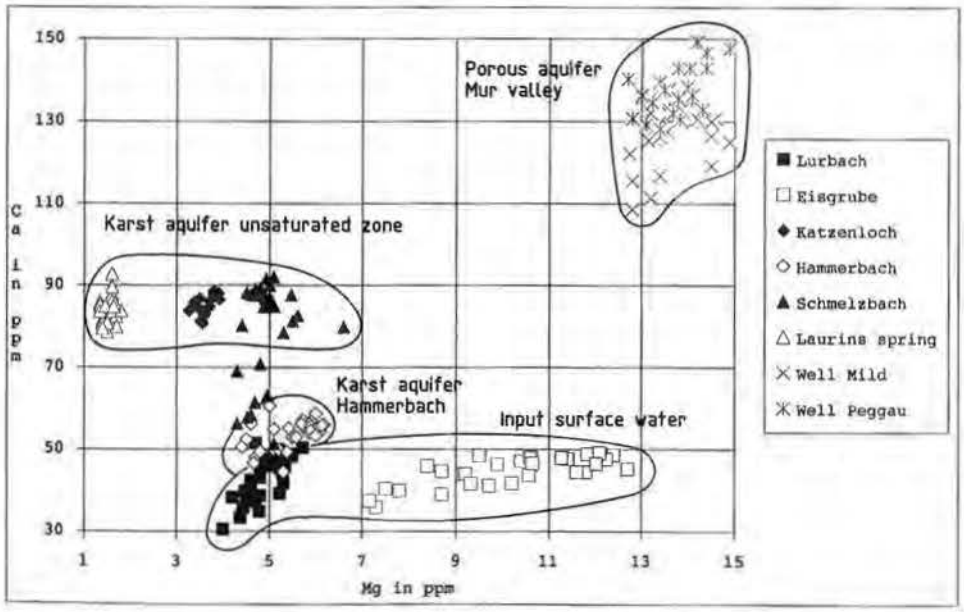

Fig. 3.3: Calcium-magnesium correlation of the sampled waters (data from the observation period 1986–1987).

The **Laurins spring** being recharged only by the unsaturated zone of the central and northern part of the karstic plateau shows low magnesium values due to the catchment area in non-dolomitic paleozoic limestones and high calcium concentrations due to the high contents of CO_2 of the input water. The low seasonal fluctuations indicate a long residence time in the unsaturated zone.

The **Schmelzbach spring** having a similar catchment area at low water conditions in the northern part of the karstic plateau is characterized by a water type similar to that of Laurins spring with a little higher magnesium contents due to a permanent small component of water from the sinkholes Eisgrube and Katzenloch.

The **Hammerbach spring** represents the mixture of two components (water from Lurbach and the karstic plateau of the Laurins type).

It is clearly visible in fig. 3.3 that the Schmelzbach water sometimes shows a mixture with water of the Hammerbach aquifer due to the periodically active overflow of Hammerbach water into the Schmelzbach aquifer in times of higher discharges of the Hammerbach spring.

3.3.3. Seasonal Variations of Selected Chemical Parameters

The seasonal variations of the **electrical conductivity** as a measure of the total mineralization are represented in fig. 3.4, in fig. 3.5 the discharges are plotted against the corresponding conductivities.

Due to the permanent connection between the Lurbach sinkhole and the Hammerbach spring (and the spring Q1 respectively which belongs to the Hammerbach aquifer as proved by tracing experiments, s. chap. 5.) both graphs show similar seasonal fluctuations with distinct dilution effects in periods of higher discharge (s. also fig. 3.1).

The conductivity curve of the **Hammerbach spring** (and spring Q1 resp.) is characterized by higher values and is attenuated in comparison with Lurbach due to a certain residence time of the Lurbach water in the aquifer, solution processes in the karst aquifer and the mixture with higher mineralized water from the unsaturated zone of the Laurins spring type with low and inverse seasonal fluctuations of the electrical conductivity.

The graph of the **Laurins spring** can be assumed as representative for this type of water. Contrary to the karst springs draining the saturated zone the mineralization is increasing with increasing discharge (s. fig. 3.5) due to the high enrichment with CO_2 transported by the infiltrated waters which leads consequently to high solution rates.

The **Schmelzbach spring** being isolated from the Hammerbach aquifer in periods of low Hammerbach discharge (below the overflow mark of about 200 l/s, s. chap. 2.3.) consequently shows similar fluctuations as the Laurins spring in these times. The snow melt in spring and the higher summer precipitation provoke the rising of the karst water level in the Hammerbach system and consequently the sudden activation of karst channels and an overflow of Hammerbach water into the Schmelzbach aquifer. The episodical mixture with lower mineralized Hammerbach water is clearly visible by strong dilution effects concerning the total mineralization (conductivity) in fig. 3.4 and 3.5 (events in March/April and June 1986 and February and May 1987).

The seasonal variations of the conductivity of two wells in the **porous aquifer** in the Mur valley (not plotted in fig. 3.4) indicate a quite higher mineralization of

the porous aquifer (conductivity 700–840 µS · cm⁻¹/25° C). This effect and also the fluctuations seem to depend on local anthropogenic influences. There are no indications on temporary dilution processes due to recharging by karst water. From the major ions chloride was selected as a conventional mobile tracer. The graphs

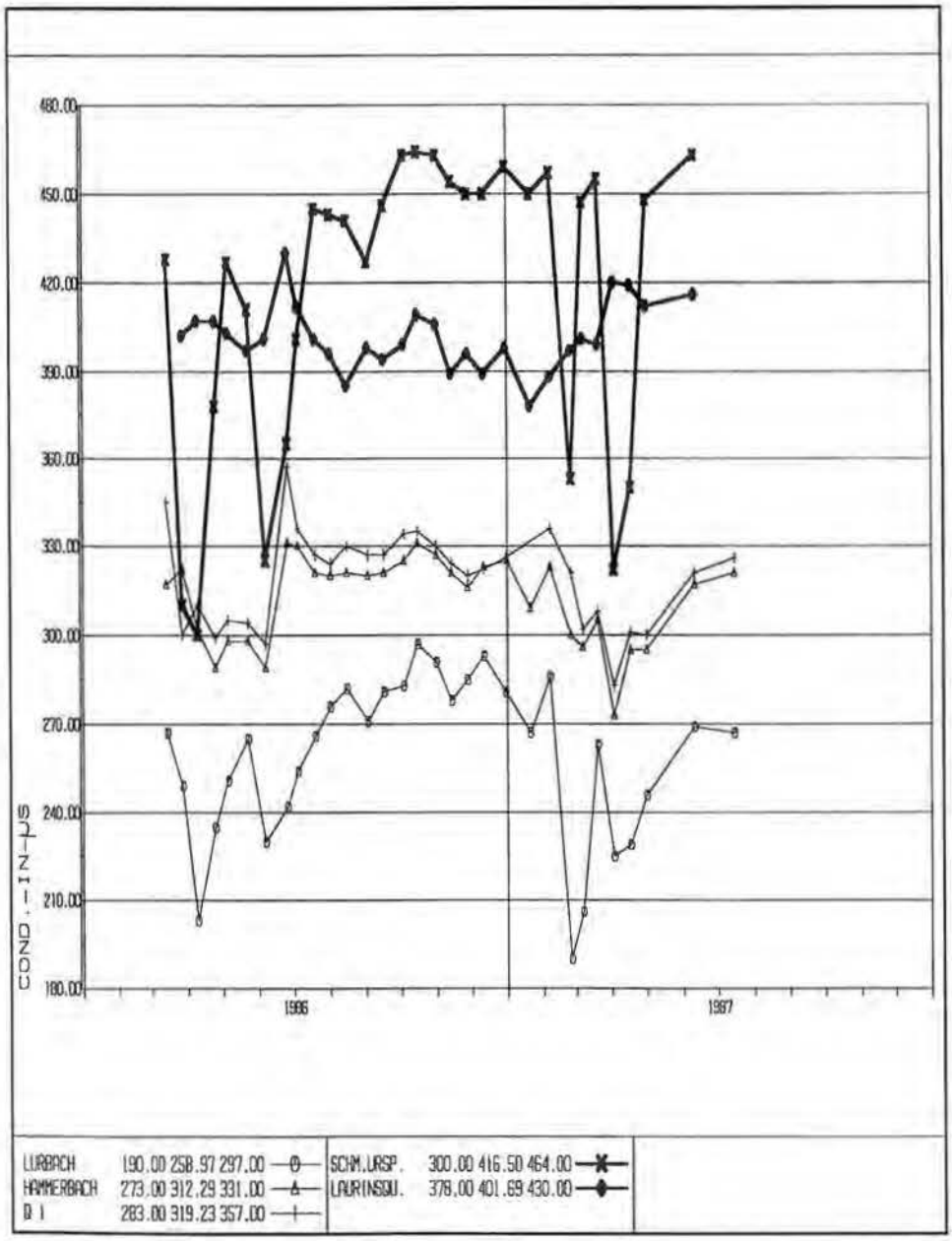

Fig. 3.4: Seasonal variations of the electric conductivity (µS · cm⁻¹/25° C).

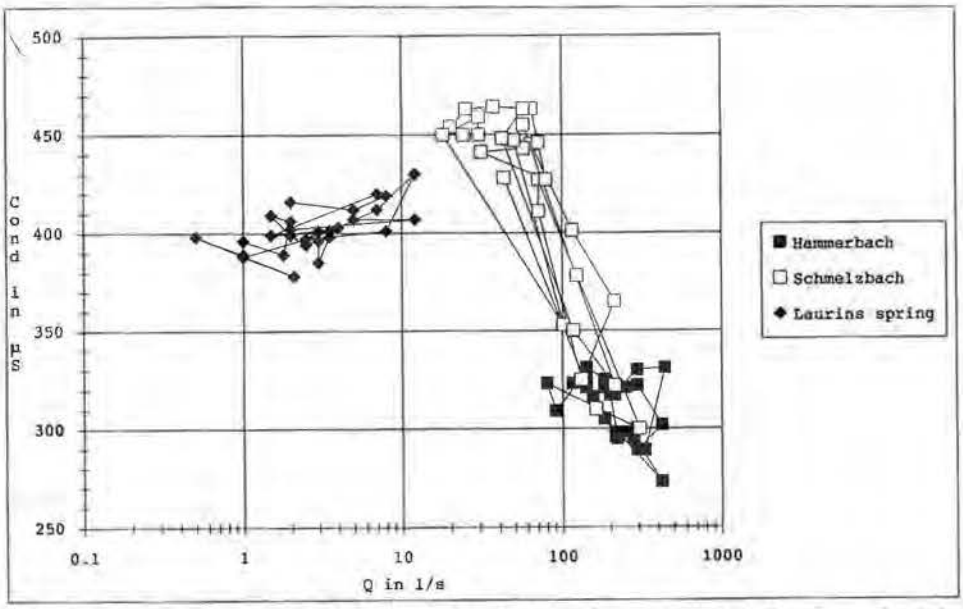

Fig. 3.5: Correlation diagram of discharge (Q in l/s) and corresponding electric conductivity ($\mu S \cdot cm^{-1}/25°$ C, data from the observation period 1986–1987).

are plotted in fig. 3.6. The water from the unsaturated zone is characterized by low chloride contents with small seasonal variations. The highest contents with the highest fluctuations were measured for the input water at the Lurbach sinkhole. Floods of the Lur river provoke strong dilution effects.

Due to the low background concentrations of the waters in the karst massif, the significant differences between karst waters and input waters and its high chemical stability and mobility chloride represents a good natural tracer for the determination of the processes of karst water recharge and hydrodynamics. The chloride response curves at the output (Hammerbach and Schmelzbach) confirm the above mentioned results concerning the electric conductivity (and also of other ions their graphs not being presented in this study).

3.3.4. Separation of Flow Components

On the base of the chemical parameters it is possible to separate the portion of infiltration water from the Tanneben plateau from the discharge hydrographs of both main springs (Hammerbach and Schmelzbach) applying the mixing equation (comp. chap. 4.)

$$Q_B = Q_T (C_T - C_I)/(C_B - C_I)\,, \qquad (2.5)$$

where

Q_T = total discharge at the spring (Hammerbach, Schmelzbach) in l/s,
Q_B = "base flow component", discharge from the karstic plateau in l/s,
C_T, C_B = corresponding tracer concentrations in ppm,
C_I = tracer concentration of the input from Lurbach in ppm.

As parameters the electrical conductivity and the chloride contents were selected due to the significant differences between karst water and input water. Concerning

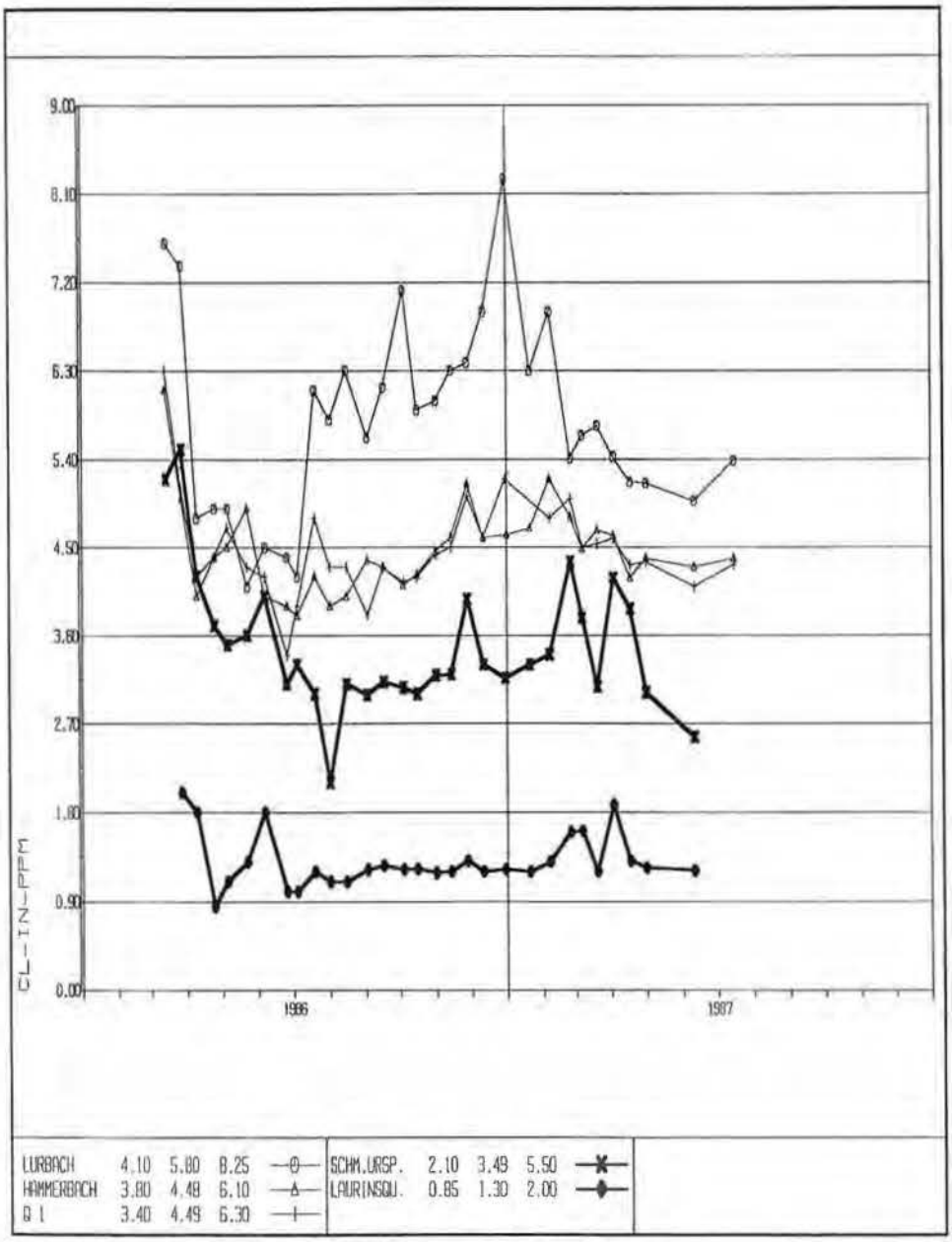

Fig. 3.6: Seasonal variations of the chloride contents (in ppm).

the electrical conductivity it has to be taken into account that solution and adsorption processes can influence the results. Chloride is a conventional tracer with high chemical stability and mobility in the aquifer, therefore physicochemical reactions can be neglected.

Due to the long observation intervals (14 days) and the well-known quick changing of the hydrodynamic conditions in the aquifer the results can only represent a rough approximation of the reality, but they agree well with the results of the hydrograph separation during a flood event (comp. chap. 4.) and also give an idea of the seasonal variations of aquifer recharge and storage.

In fig. 3.7 the discharge hydrograph of the **Hammerbach spring** is plotted in comparison with the discharges coming from the karst plateau computed by means of the conductivity and the chloride contents. As input concentrations of both parameters the seasonal variations of their contents in the Laurins spring were used assuming them to be representative for the flow component from the karstic plateau (input through the unsaturated zone). Both curves agree well at low water conditions, at higher discharges the curve computed from the conductivity gives higher values probably due to quick solution effects in the karst aquifer during floods.

Both curves indicate the permanent connection between Lurbach and Hammerbach the percentage of Lurbach water in the Hammerbach discharge being high during all seasons.

For the **Schmelzbach spring** the discharge component from the karst plateau computed with the same two parameters gives a better comparability of both curves (Fig. 3.8) probably due to the shorter flow time of Lurbach water to the Schmelzbach spring so that processes of solution cannot occur. It is clearly visible that there is no connection with the Hammerbach system resp. Lurbach in periods of low discharges the flow component from the karst massive being 100% during these times. At higher flow conditions (especially in periods of snow melt and floods in summer) an important percentage of the total discharge of the Schmelzbach spring consists of water from the Hammerbach aquifer.

In tab. 3.1 the mean discharges and percentages of the calculated flow components are listed.

Tab. 3.1: Flow components in the discharge of Hammerbach and Schmelzbach spring computed by means of chemical tracers.

	HAMMER-BACH		SCHMELZ-BACH		Total discharge HB + S	
	l/s	%	l/s	%	l/s	%
Mean Q	207	100	86	100	293	100
Karst water comp. from Tanneben (Cl^-)	56	31	58	67	114	39
Karst water comp. from Tanneben (Cond.)	77	37	57	66	134	46
Comp. Lurbach water (Cl^-)	151	69	28	33	179	61
Comp. Lurbach water (Cond.)	130	63	29	34	159	54

Comparing these results with the mean discharge of Lurbach (s. chap. 2.3.3.) one can deduce that more than 80% of the mean Lurbach discharge drains to the Hammerbach spring having a permanent connection with the Lurbach sinkhole and only about 20% to the Schmelzbach spring through an episodically active overflow zone.

Only during short-termed floods of the Lurbach which take their way directly through the Lurgrotte greater amounts of Lurbach water drain to the Schmelzbach spring.

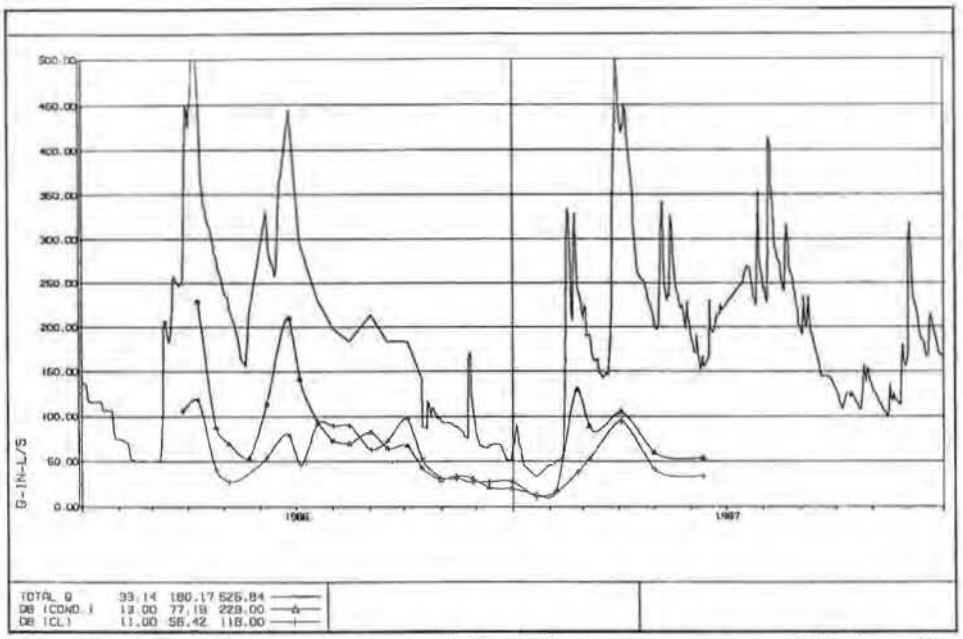

Fig. 3.7: Hammerbach spring: total mean daily discharges and separation of the karst flow component from Tanneben (QB) by means of chemical natural tracers (conductivity and chloride contents).

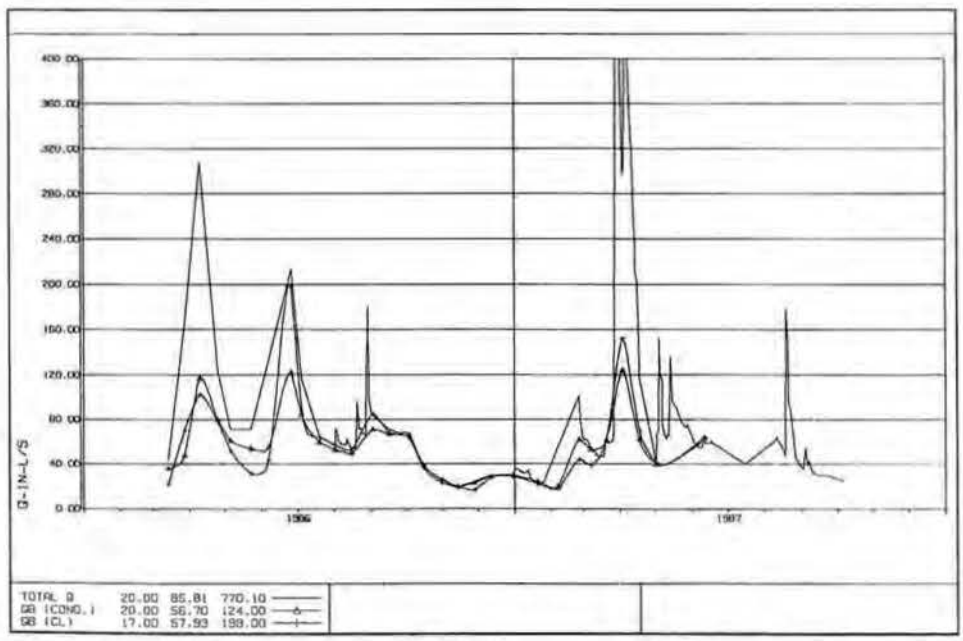

Fig. 3.8: Schmelzbach spring: total mean daily discharges (partially only single measurements) and separation of the karst flow component from Tanneben (QB) by means of chemical natural tracers (conductivity and chloride contents).

3.4. Investigations by Means of Environmental Isotopes

As described above oxygen-18 data from various sites are available for the years 1986 and 1987, the sampling periods for tritium are more scattered during the seventies.

3.4.1. Oxygen-18 Measurements

The sampling intervals of two weeks between March 1986 and July 1987 offer a reasonable number of analyses for the interpretation related to each site.

Considering the mean values, four drainage systems can be recognized. The Semriach basin is represented by the Lurbach as well as by the Eisgrube (mean oxygen-18 –10.6 δ‰). Most complex is the catchment area of Hammerbach as well as of Schmelzbach. Both are influenced by the Lurbach, effecting a slightly lower oxygen-18 content. The Laurins spring however represents exclusively the infiltration in the northwestern Tanneben plateau. The average ^{18}O-value indicates with some 0.4 δ‰ lower than that of Lurbach somehow the existence of an altitude effect. The last system can be defined as the Quaternary porous aquifer of the Mur valley. The mean ^{18}O-content is placed in the magnitude of –10.1 δ‰. The groundwater is isotopically mixed showing the fact that groundwater regeneration originates from the Mur river and direct precipitation in the valley floor. The alimentation from the Tanneben karst seems to be rather negligible.

The calculation of representative mean values of the stable isotope usually permits the application of the **altitude effect**. In the particular case a clear identification of the mean altitudes is hardly possible since the depletion of data does not exceed 0.6 δ‰. Additionally to this fact instead of two sites only Eisgrube can be used as a standard, its drainage area can be delimited easily by geological, morphological and hydrological criteria. For a rough classification of recharge areas a decrease of some 0.2–0.3 δ‰/100 m is suggested according to other studies in the Eastern Alps (W. STICHLER & H. ZOJER, 1986).

Deriving from these considerations Laurins spring would correspond to a mean altitude of 650–700 m, thus not representing the recharge of the whole plateau but only of the northwestern part. The average values of Hammerbach and Lurbach are not significantly different, which shows that their systems are interconnected, and Hammerbach drains the main upper part of Tanneben plateau. Referring to the Semriach basin the water of Eisgrube indicates a subsurface drainage from a higher located (800–850 m) but local recharge area. On the other hand the content of Lurbach is composed of a various mixture of surface and subsurface water from the whole basin, corresponding a mean elevation of about 870 m. Slightly lower located is the recharge area of Schmelzbach, due to the fact, that its drainage is influenced by Lurbach only temporarily.

Knowing the meteorological and hydrological conditions the **seasonal fluctuations** of the ^{18}O-content can gain some hints at the storage characteristics of the investigated waters (Fig. 3.9). For the recharge of the schist rocks within the Semriach basin the curves of Eisgrube and Lurbach are highly significant. The melting period of April 1986 is expressed by a clear drop down of the concentration at both sites, followed by a rather parallel course of the curves till October 1986. The late autumn and the winter 1986/87, a time of low runoff, show a good coincidence of the two graphs. It can be concluded, that Lurbach drains at such conditions almost

only subsurface water, which is stored mostly in the weathered zone. Therefore at low water conditions Lurbach represents the same drainage dynamics as Eisgrube.

The concentration curve of Laurins spring reflects the drainage system in the unsaturated zone of the karst massif. It does not respond to snow melting in April

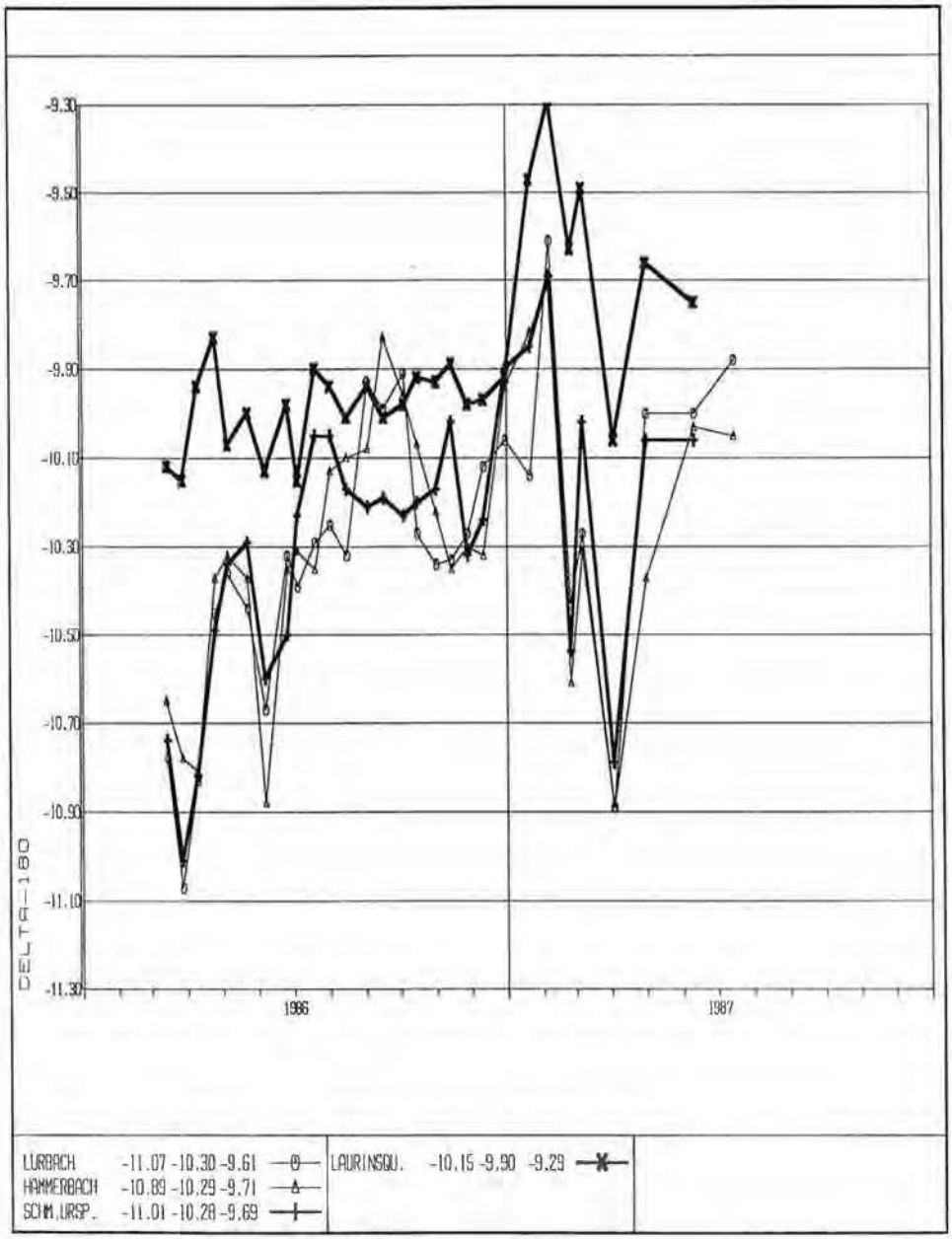

Fig. 3.9: Seasonal fluctuations of ^{18}O (δ‰) 1986–1987.

1986 and to intensive rainfalls during the summer as well as to the following dry period. The fluctuations are limited within the measurement accuracy, they illustrate a high storage capacity in the micro fissures of the carbonate rock and cave sediment fillings. During the winter 1987 the isotope content increased about 0.5 δ‰. This could be considered as an activation of water movement within the fissured and fractured carbonate rocks. This effect shows, that the classical application of the exponential models is not valid for the drainage in the unsaturated zone of solid rocks. Such processes can be correlated to events happened even a longer time ago.

The seasonal variations of the isotope content in the shallow aquifer of the Mur valley are relatively damped. The snow melting is only suggested and delayed till to the early summer, the heavy rainfalls in the summer can be recognized just in the autumn. Thus the fine clastic sediment cover of the Quaternary gravels prevent a quick penetration through the unsaturated zone within the unconsolidated accumulations.

The isotope fluctuations of both springs, Hammerbach and Schmelzbach, indicate the complex drainage and storage conditions of the karst massif. The fact of a continuous connection between Lurbach and Hammerbach and an alimentation of the Schmelzbach system only in a time of high inflow has been confirmed by the isotope investigations. During periods of rather high inflow of Lurbach (March and August 1986) both curves are similar, however, in the time when the discharge of Hammerbach remains below 200 l/s, both curves show a significant nonconformity. Whereas in this time the isotopic composition of Hammerbach is getting closer to Lurbach, Schmelzbach is representing the discharge of the karst water originating from precipitation on the Tanneben plateau and the area northeast of it (Eichberg and surrounding region with sinkholes). For such particular time periods Schmelzbach is more representative than Laurins spring which seems to have a more local recharge area without active sinkholes.

3.4.2. Tritium Data

Figure 3.10 illustrates the curves of the monthly tritium values beginning with February 1971 till June 1973. The curve of the precipitation need not be explained, as a typical yearly course can be read from it. Somewhat more difficult is the interpretation of surface waters (Lurbach) or else spring waters (Schmelzbach, Hammerbach and Laurins spring).

A generally declining trend of tritium content is to be observed in Lurbach, indicating that even schist areas are subject to some kind of underground storage. The snowmelt in February 1972 pronounces most clearly that it complies fully with the properties of a surface runoff. The Schmelzbach reflects a nonsynchronous, gently fluctuating discharge pattern.

The annual curve of the tritium content of Hammerbach suggests a relationship as well with Lurbach as with Schmelzbach. This statement becomes obvious in a frequency distribution (H. ZOJER & J. ZÖTL, 1974) which indicates that Hammerbach carries Lurbach water, and additionally it is alimentated from the karst water body.

Comparing with the other data a significant declining trend at Laurins spring cannot be observed. A reasonable portion of old water is suggested, thus agreeing with the interpretation of stable isotopes. The quantitative assessment with regard to turnover times of the particular waters is discussed in chap. 6.2.

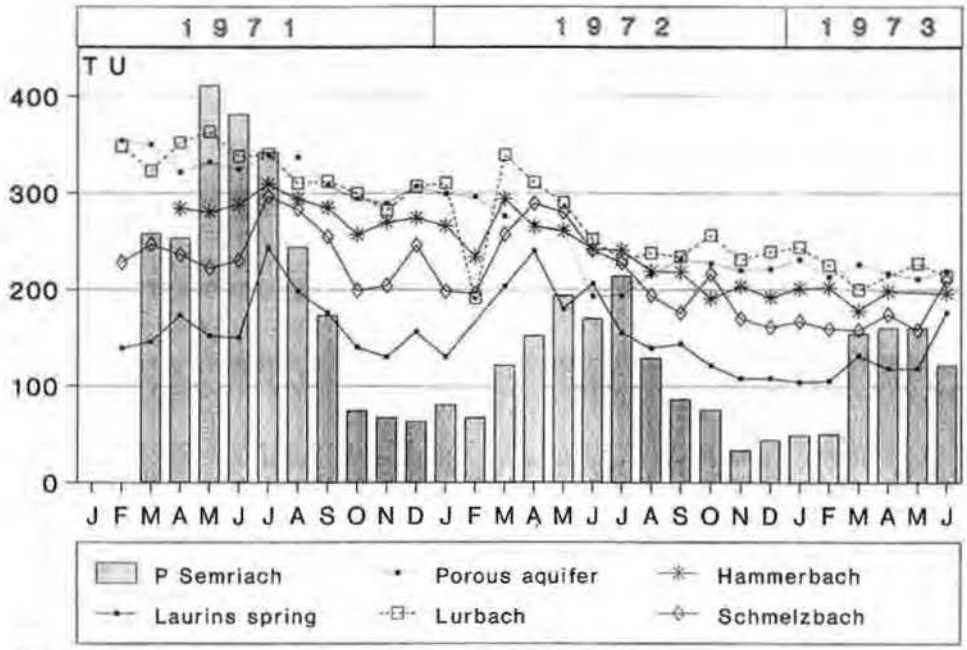

Fig. 3.10: Tritium concentration curves 1971–1973.

4. Short-Term Investigations by Means of Natural Tracers

(T. HARUM, H. ZOJER, W. STICHLER, P. TRIMBORN)

4.1. Purpose of the Investigations

Long-term investigations with natural tracers (chemical parameters and environmental isotopes can only give approximative ideas about the fluctuations of the parameters and the hydrodynamic processes in karstic aquifers. Usually the sampling intervals are too long (in the case of the Lur system 14 days, s. chap. 3.) to determine the hydrodynamic features in aquifers with a high percentage of young flow components with quick changings in time of the input-output conditions.

From other investigations (e.g. P. FRITZ et al., 1976, H. MOSER & W. RAUERT, 1980, I. MÜLLER & J.G. ZÖTL, 1980, V.C. KENNEDY et al., 1986) it is known, that the measurement of natural tracers in short intervals during flood events can provide important additional informations about the mixing processes in karst aquifers and gives the possibility of separating the discharge of karstic springs into flow components with different transit times.

4.2. Input Conditions

In the summer of 1988 during the combined multitracing experiment of the ATH-group with injections in the sinkhole of the Lurbach (s. chap. 5.1.) water samples were taken of the Lurbach (input), the two springs in the lower part of the Lurgrotte (Schmelzbach spring and Laurins spring) and the main outlets Hammerbach spring

and Schmelzbach in intervals of 1.5 h. The water samples were analysed on the ions calcium, magnesium, sodium, potassium, chloride, nitrate and sulphate in the laboratory of the IGH Graz and for their contents in the stable isotope oxygene-18 in the laboratory of GSF Munich.

One day after the injection on June 28th, 1988 a local thunderstorm in the higher part of the basin provoked a flood event of the Lurbach creek (peak flood 1.6 m^3/s). The two rain gauges one in the lower part of the Semriach basin and the other on the Tanneben plateau measured only 2 mm/d. It can be assumed, therefore, that the input from this meteorological event in the karst system came only from the upper Lurbach catchment area, whereas the input of precipitation on the Tanneben plateau through the unsaturated zone can be neglected.

Figure 4.1 shows the time-concentration curves of the chemical parameters calcium, potassium and nitrate and the stable isotope ^{18}O measured at the Lurbach sinkhole (input) during the flood event in comparison with the discharge hydrograph. The high portion of surface water in the Lurbach discharge provokes a dilution effect for most of the chemical parameters measured (Ca^{2+}, Mg^{2+}, Cl^-, SO_4^{2-}). After a short time of hydraulic stimulation of groundwater from the catchment area (piston effect) dilution begins at the same time as the flood peak (s. fig. 4.1).

On the other hand the concentrations of the pollution parameters potassium and nitrate increase in a significant way with the discharge with the same retardation as the dilution processes of the other ions. This effect can be explained by the outwashing of manure from the fields and grasslands in the catchment area (T. HARUM et al., 1990), which is mainly used by agriculture (farming).

Due to the isotopically light precipitation event (summer thunderstorm) the contents of the stable isotope ^{18}O rise with the discharge the maximum concentration being about 1 δ‰ higher than the background (s. fig. 4.1).

The significant fluctuations of some of the hydrochemical and isotopical parameters at the Lurbach sinkhole (input) during the flood event represent good natural tracers for the characterization of the hydrodynamic processes in the karst aquifer, above all, because there was practically no precipitation on the karst plateau of Tanneben. For this reason the input from the plateau during this event could be neglected for the hydrograph separation procedure of the discharges of the two karstic springs, Hammerbach and Schmelzbach.

The following natural tracers were used:

Ca^{2+}: It shows a strong dilution effect at the input (s. fig. 4.1). Disadvantages are quick solution effects in the aquifer and processes of ion exchange (W. KOLLMANN, 1979, H.P. LEDITZKY, 1978, J. GOLDBRUNNER & H.P. LEDITZKY, 1979, H.P. LEDITZKY, 1981), where calcium is replaced by potassium in clay minerals of the cave sediments. This reversible effect is known by tracer experiments with salts in the Lurbach system.

Mg^{2+}: It is a conventional natural tracer, which gives good results in karst aquifers in comparison with stable isotopes (I. MÜLLER & J. ZÖTL, 1980), but during the flood event the dilution was not as significant as for calcium.

NO_3^-: In this case it seems to be an applicable tracer, on the one hand because of the significant concentration peak at the input (s. fig. 4.1), on the other hand because the nitrate input from the forested karstic plateau is lower (low background concentration). In this case physico-chemical reactions in the karst aquifer seem to be neglectable.

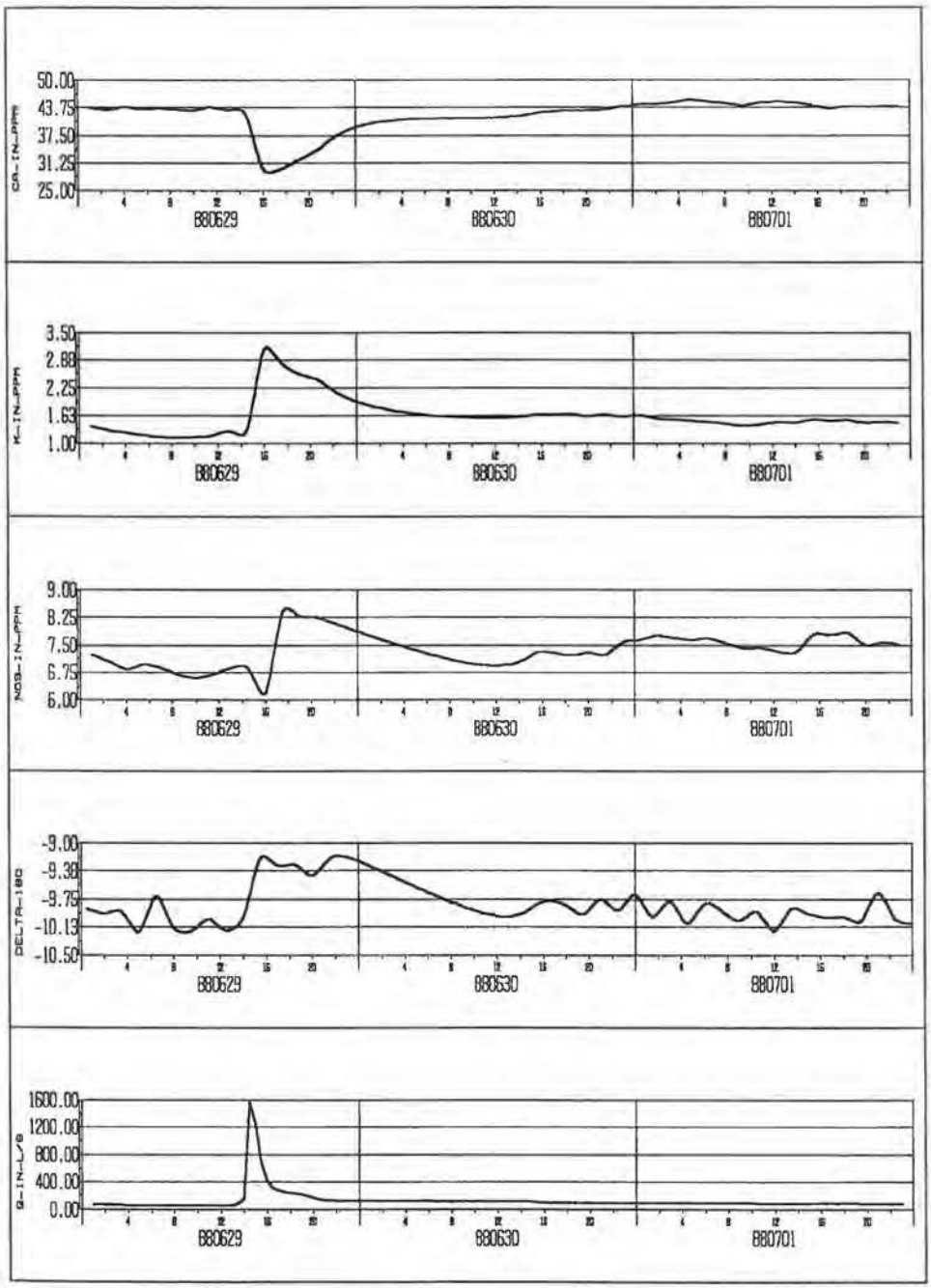

Fig. 4.1: Lurbach sinkhole (input), flood event 880629–880701. Discharge at the gauging station Lurbach in l/s, time-concentration curves of the ions calcium, potassium and nitrate (conc. in ppm) and the stable isotope ^{18}O (δ‰).

^{18}O: The stable isotope represents a conventional "ideal" natural tracer. The peak during the flood event was significant enough. Errors can be provoked by the relatively high background fluctuations (measurement error ± 0.15 δ‰). For this reason the time-concentration curves of the two karstic springs were partially smoothed by using a running mean.

Potassium, which shows like nitrate a significant peak at the input during the flood event, was not used, because it is usually characterized by retardation effects in the aquifer due to adsorption and ion exchange (H.P. LEDITZKY, 1978). The ions sodium and chloride were not applicable, because their time-concentration curves for the Hammerbach spring were influenced by the passage of the salt tracers injected in the Lurbach sinkhole (s. chap. 5.1.).

4.3. Output

Before the flood event the discharge of the **Hammerbach** spring was in the range of 188–190 l/s the overflow to the Schmelzbach system not being active. For this reason all the dissolved artificial tracers, injected one day before the flood event in the Lurbach sinkhole reappeared only in the Hammerbach spring and in some small springs (Q1–Q6) belonging to the Hammerbach system at the same time as the discharge of Hammerbach began to rise (s. chap. 5.1.).

In fig. 4.2 the time-concentration curves of the ions Ca^{2+}, Cl^-, NO_3^- and the stable isotope ^{18}O are plotted in comparison with the discharge of the Hammerbach spring. Like magnesium also calcium shows – with a certain retardation – a continuous dilution, which is not so significant compared with the input due to processes of solution and cation exchange (H.P. LEDITZKY, 1978) and of mixing with higher mineralized water coming from the Tanneben plateau.

The ions sodium, potassium and chloride were influenced by the salt tracers injected (s. chap. 5.1.).

Nitrate shows a light dilution until the peak discharge due to the discharging of "older" reservoir water, hydraulically stimulated by the flood, with lower nitrate contents. The passage of the manure, outwashed from fields in the Lurbach catchment area by the thunderstorm event begins after the discharge peak. It is characterized by the increase of nitrate concentrations in fig. 4.2 and is representative for event water outflowing from the aquifer.

The artificial tracers injected into the Lurbach sinkhole one day before the flood are represented by the chloride concentrations shown in fig. 4.2. They arrived in the Hammerbach spring at the same time, when the spring discharge began to rise. So they are representing – in comparison with the event water component from the flood of Lurbach – an "older" flow component.

The fluctuations of the stable isotope ^{18}O show the same effect as the chemical parameters. At first "older" reservoir water with the same background concentrations as the input (Lurbach water and water from the Tanneben plateau have nearly the same contents in ^{18}O due to the similar mean altitude of both catchment areas) is discharged hydraulically stimulated (piston effect). The outflow of isotopically lighter event water is characterized by increasing concentrations (peak 0.6 δ‰ above the background).

The discharge hydrograph of the **Schmelzbach spring** is characterized by a quicker hydraulic reaction. The circumstance that there was no connection with

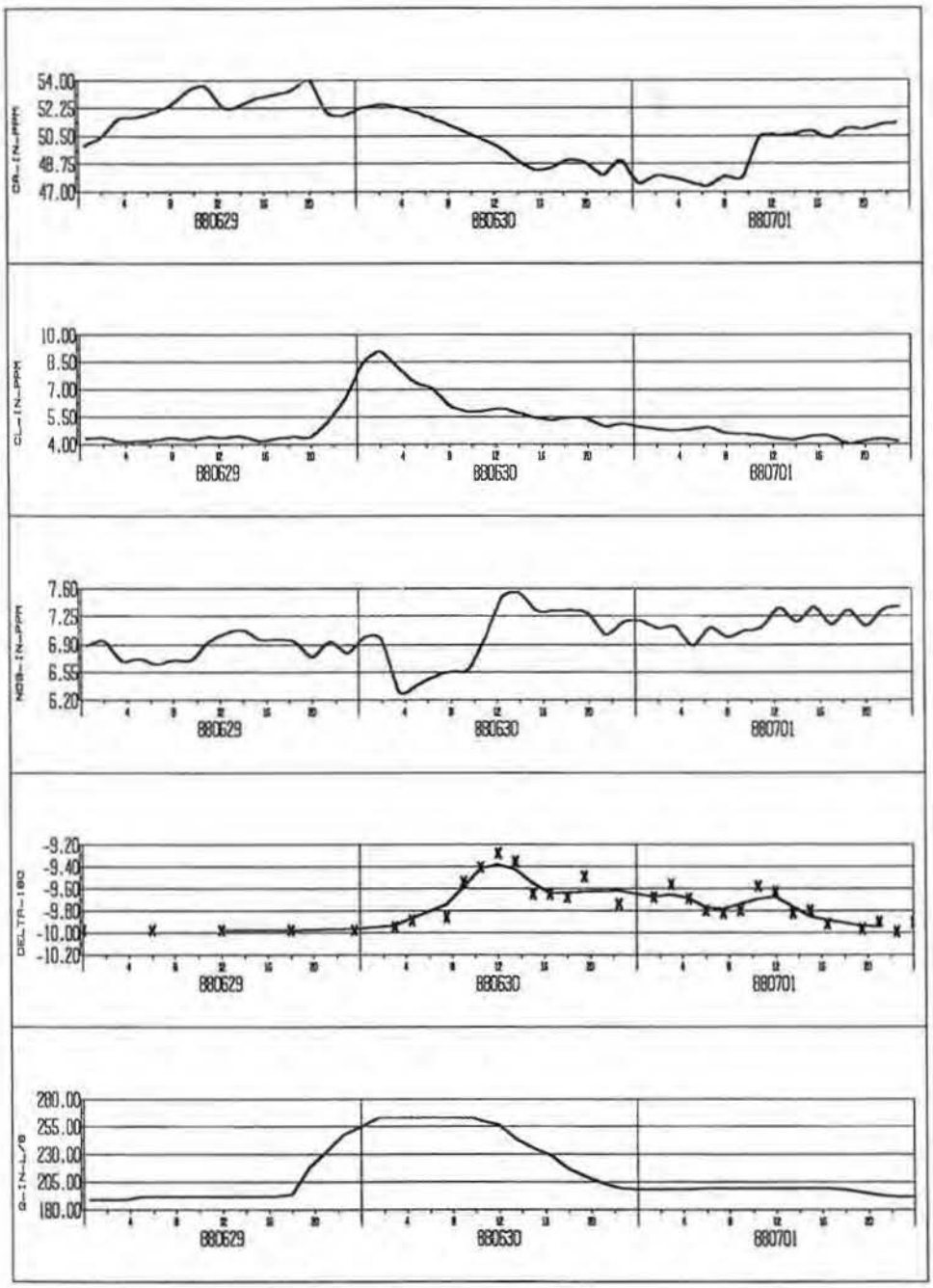

Fig. 4.2: Hammerbach spring, flood event 880629–880701. Discharge in l/s, time-concentration curves of the ions calcium, chloride and nitrate (conc. in ppm) and the stable isotope ^{18}O (δ‰).

the Lurbach sinkhole and the Hammerbach system before the flood provokes more significant fluctuations of the chemical and isotopical parameters. The sudden inflow of Lurbach water effects at first, that "older" reservoir water from the Schmelzbach aquifer with higher mineralization than Hammerbach water is discharged hydraulically stimulated by the flood. The dilution represented by the calcium contents in fig. 4.3 begins about 6 h later and reaches its maximum 17 h after the discharge peak. The high dilution process continues during 1.5 days and represents the period with active overflow of water with lower mineralization from the Hammerbach aquifer ($Q > 200$ l/s, s. fig. 4.2). The calcium contents begin to increase, when the discharge of the Hammerbach spring decreases under the overflow mark (s. chap. 2.3.).

The nitrate concentrations of the Schmelzbach show the inverse effect. They begin to increase at the same time when the dilution of calcium and also magnesium starts and reach their maximum 22 h after the discharge peak. Due to their origin by outwashing of manure in the Lurbach catchment area by the thunderstorm precipitation, they prove the short-termed connection with the Hammerbach system as well as the appearence of the undissolved artificial tracers microspheres and phages (s. chap. 5.1.), which were probably retarded by cave sediments and fine fissures in the upper part of the Hammerbach system. The dissolved tracers being transported with lower retardation could only be detected in the Hammerbach spring. For this reason it can be assumed that the periodical overflow from Hammerbach to Schmelzbach system takes place in the upper part of the Hammerbach aquifer.

The fluctuations of the stable isotope ^{18}O (Fig. 4.3) confirm the results with the chemical parameters. The peak of ^{18}O-concentration cannot be determined due to the lack of some water samples in the period of higher discharges.

The **Laurins spring** shows no significant fluctuations of discharge and the chemical and isotopical parameters measured (Fig. 4.4). It proves the results of the long-term investigations and tracer experiments (s. chap. 3. and 5.), that the spring is draining an isolated aquifer system (catchment area in the central and northern part of the Tanneben plateau) with long mean transit time of the infiltrated water and has no connection with the Hammerbach and Schmelzbach aquifer.

The fluctuations of calcium of the Laurins spring are not corresponding to hydrodynamic processes, they are probably related to precipitation effects of calcite from the supersaturated water.

4.4. Hydrograph Separation by Means of Natural Tracers and Runoff Depletion Curves

The discharge of karstic spring consists of different components with different residence times in the aquifer. For karstic aquifers the discharge of springs can often be separated into two components, which are usually termed **baseflow** and **direct flow** corresponding to their different residence time. The direct flow component represents the portion of water infiltrated from precipitation, which flows directly with short retardation through the main channels in the karst system to the spring. The base flow component consists of water stored in the aquifer over a longer time.

The conventional hydrograph separation procedures using the exponential function after E. MAILLET (1905, s. chap. 2.3.) and extrapolating this depletion function back under the peak of the total hydrograph allow an approximative separation of the two components base flow and direct flow (for surface drainage

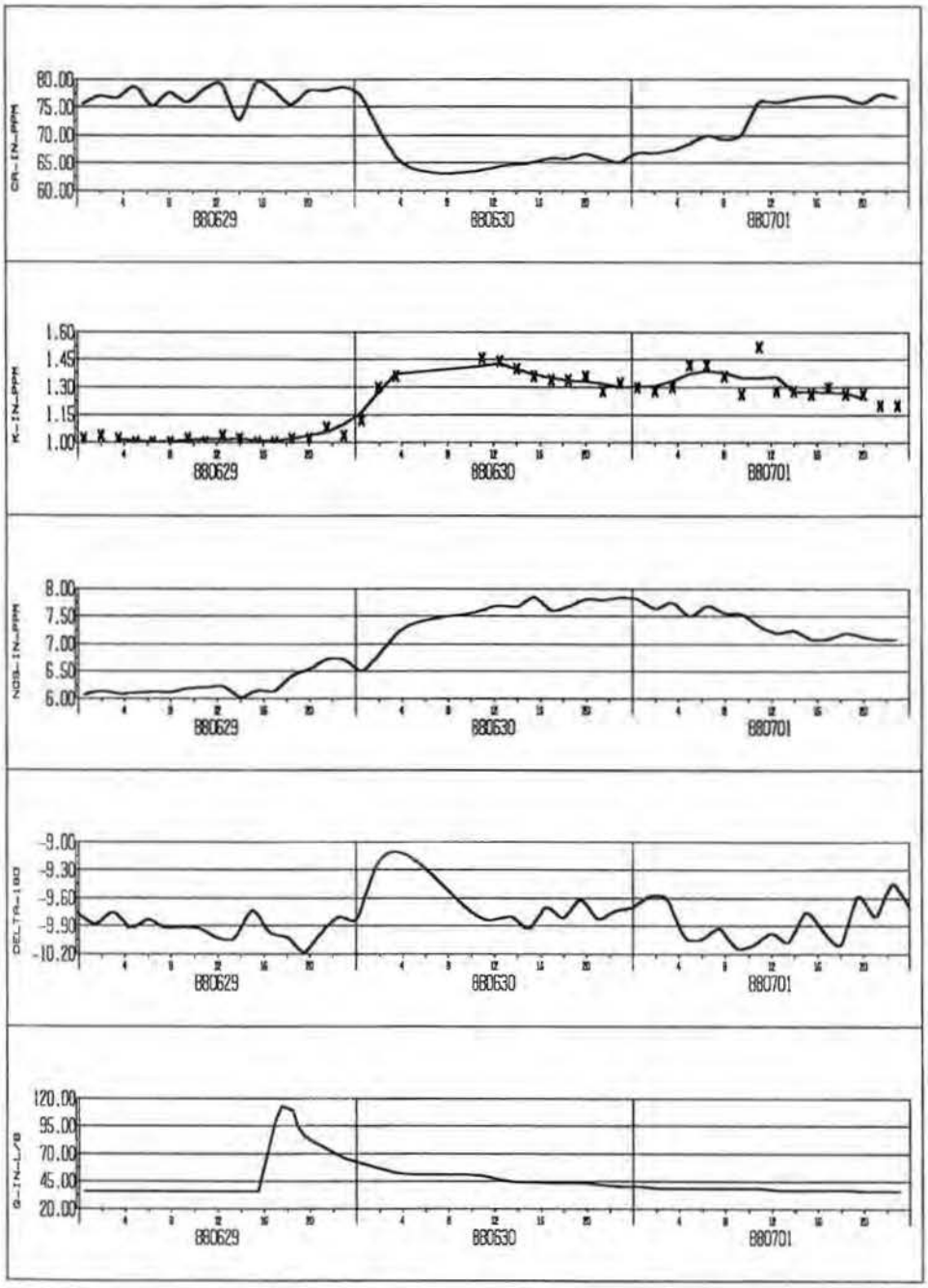

Fig. 4.3: Schmelzbach spring, flood event 880629–880701. Discharge in l/s at the gauging station (cave entrance), time-concentration curves of the ions calcium, potassium and nitrate (conc. in ppm) and the stable isotope ^{18}O (δ‰).

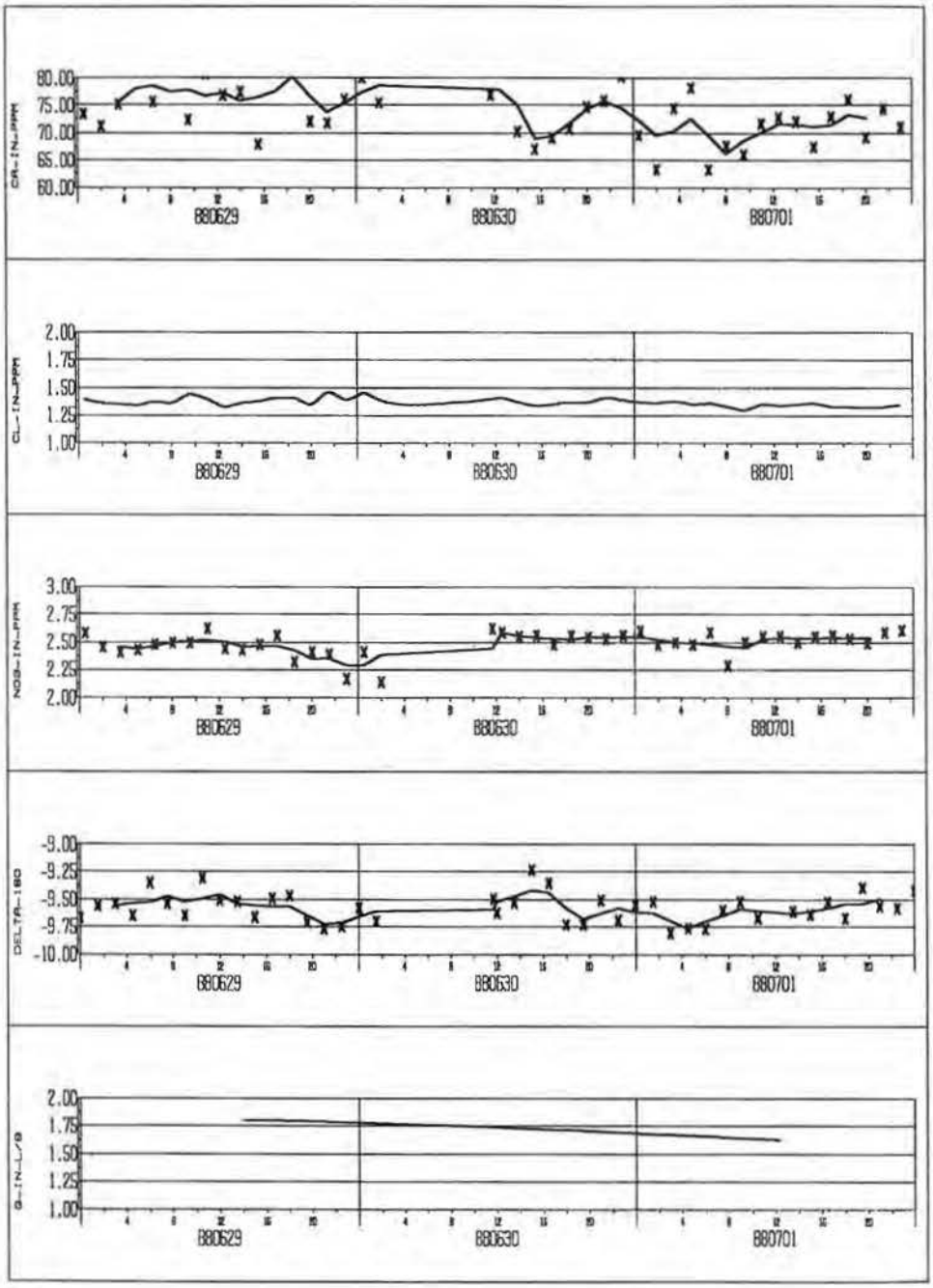

Fig. 4.4: Laurins spring, flood event 880629–880701. Discharge in l/s, time-concentration curves of the ions calcium, chloride and nitrate (conc. in ppm) and the stable isotope ^{18}O (δ‰).

basins surface flow). This method gives only informations about the hydraulic behaviour of the aquifer (I. MÜLLER & J. ZÖTL, 1980). The water volumes calculated are corresponding to the volume of mobile water, not including quasistagnant water, i.e. water, which can only be discharged by hydraulic stimulation.

Contrary the measurement of natural tracers (stable isotopes, chemical parameters) of input and output gives the possibility of estimating the portions of **older reservoir water** and **event water** discharged at the spring and provides informations about the mixing processes and piston effects in the aquifer. The water volumes calculated by means of natural tracers include the volume of quasistagnant water in the system and are not directly comparable with the volumes of direct and base flow components computed by the classical hydraulic separation method. For hydrogeological investigations it seems to be important to include both methods, because they give complementary informations about the aquifer characteristics.

The discharge components can be separated combining the simple mixing equations

$$Q_T = Q_D + Q_B \tag{4.1}$$

and

$$Q_T C_T = Q_D C_D + Q_B C_B \tag{4.2}$$

to

$$Q_B = Q_T (C_T - C_D)/(C_B - C_D), \tag{4.3}$$

where

Q_T = total discharge at the spring (Hammerbach, Schmelzbach) in l/s,
Q_B = base flow component, "older" reservoir water in l/s,
Q_D = direct flow component, event water input from Lurbach in l/s,
C_T, C_B, C_D = corresponding tracer concentrations.

Assumption of this method are significant differences in the contents of the natural tracers in input and output. In the case of the flood event in the Lurbach system in the summer of 1988 the input was performed only by the flood of the Lurbach, precipitation input from the karstic plateau of Tanneben could be neglected.

For both springs different assumptions have to be considered. The **Hammerbach spring** has a permanent connection with the Lurbach sinkhole. For this reason even before the flood runoff event a part of the spring discharge has to be taken into account as direct flow component in the main flow channels. For the separation procedure using nitrate as tracer it was possible to determine this portion by the mixing equation assuming the same NO_3^--background of the water from the karst plateau as for Schmelzbach at low water conditions before the flood. This was not possible with the stable isotope ^{18}O due to the similar background concentrations of karst water and Lurbach water (similar mean altitude of both catchment areas). For this reason the discharge of Hammerbach before the flood event cannot be separated using the stable isotope.

The results are demonstrated in fig. 4.5, where the total discharge hydrograph and baseflow component calculated by the classical hydraulic method are compared with the event water and baseflow components, using NO_3^- and ^{18}O as tracer. In spite of the fact, that different assumptions for both tracers were used, the results

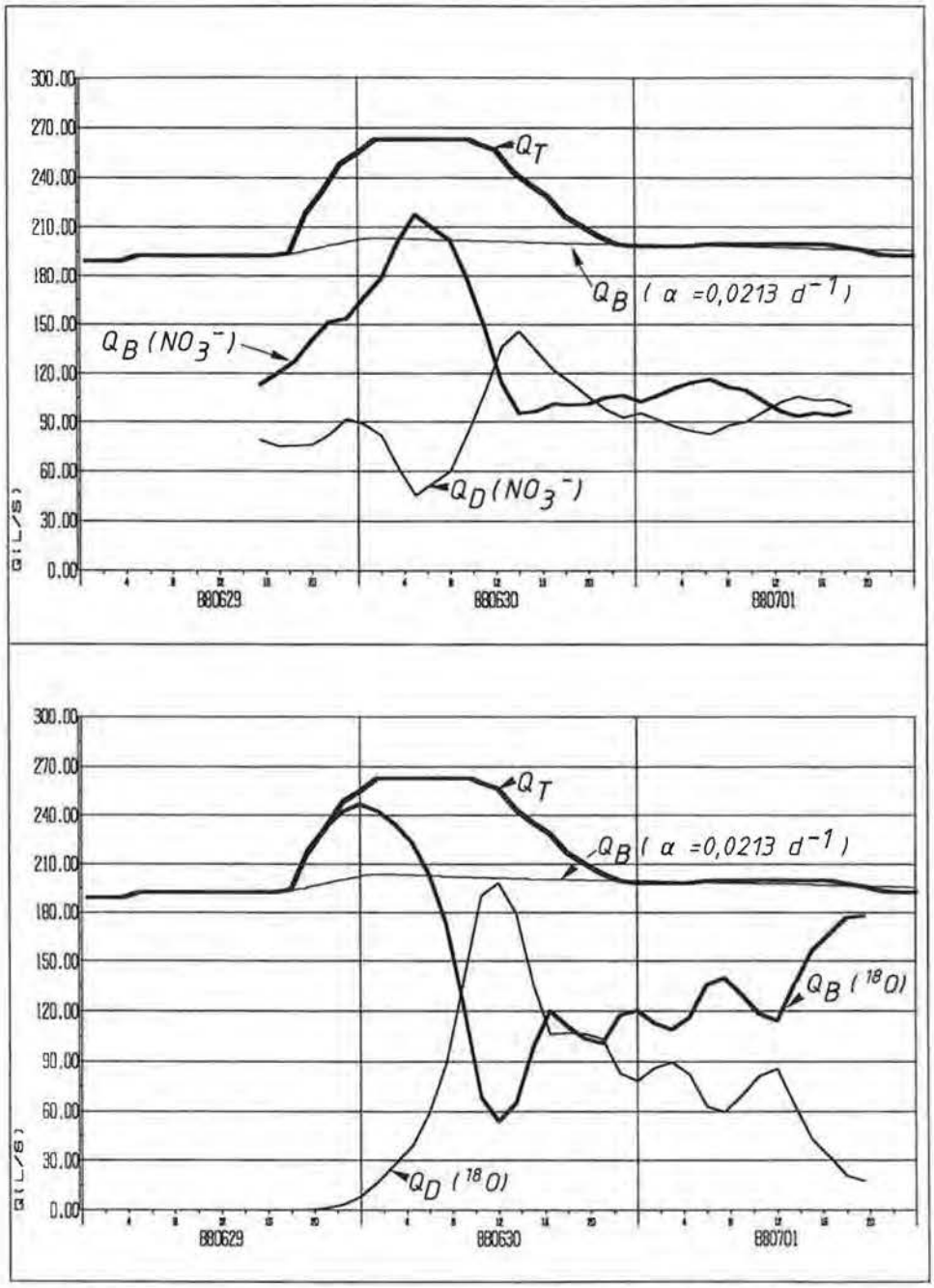

Fig. 4.5: Hammerbach spring, flood event 880629–880701. Hydrograph separation by means of the natural tracers nitrate (upper diagram) and oxygene-18 (lower diagram) compared with the base flow component computed from the equation after E. MAILLET (1905). Q_T = total spring discharge in l/s, Q_D = direct flow (event water) component, Q_B = base flow (older reservoir water) component, α = recession coefficient (eq. 2.1).

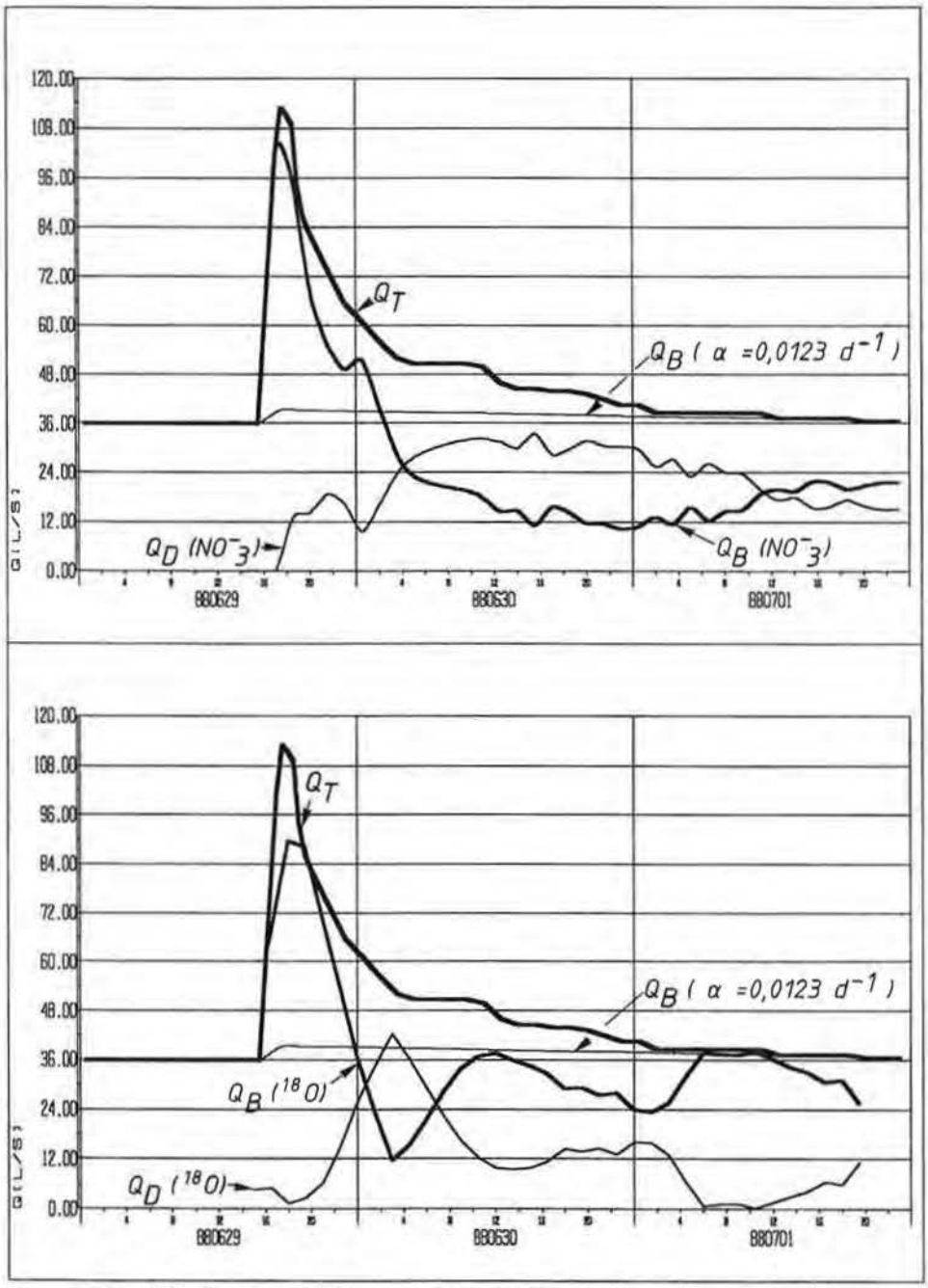

Fig. 4.6: Schmelzbach spring, flood event 880629–880701. Hydrograph separation by means of the natural tracers nitrate (upper diagram) and oxygene-18 (lower diagram) compared with the base flow component computed from the equation after E. MAILLET (1905). Q_T = total spring discharge in l/s, Q_D = direct flow (event water) component, Q_B = base flow (older reservoir water) component, α = recession coefficient (eq. 2.1).

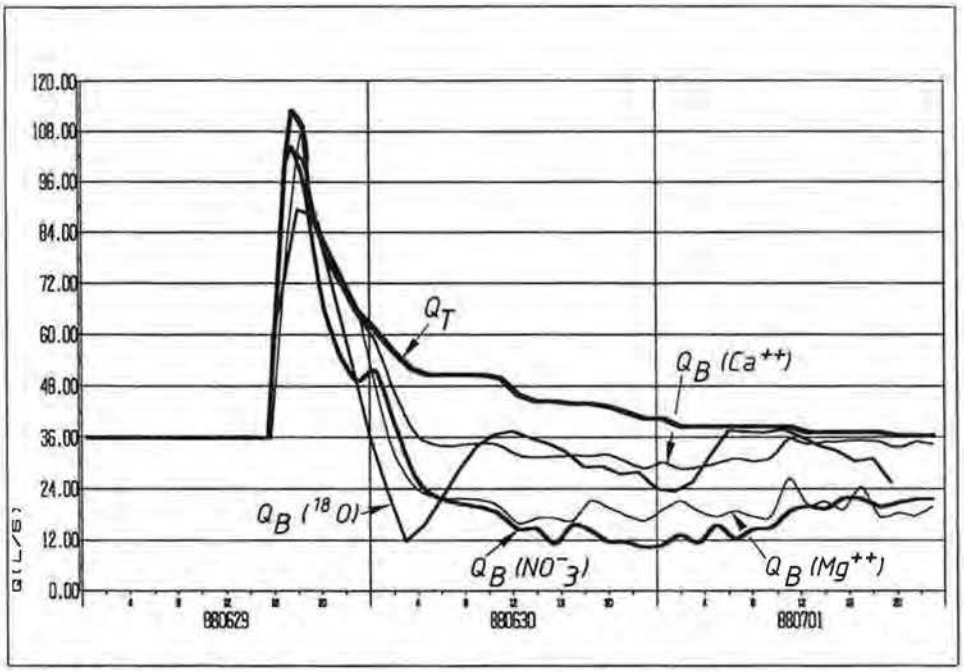

Fig. 4.7: Schmelzbach spring, flood event 880629–880701. Hydrograph separation by means of natural tracers. Older reservoir water components (QB) computed from the concentrations of calcium, magnesium, nitrate and oxygene-18.

are well comparable. It is clearly visible, that at the beginning of the flood event a high portion of the discharge consists of the base flow component, i.e. that "older" reservoir water is discharged hydraulically stimulated by the rising karst water level in the system. The event water component begins to increase with retardation, the maximum of direct flow being reached some hours after the peak of the total discharge.

The hydraulic hydrograph separation extrapolating back the exponential function after E. MAILLET (1905) provides quite different results with a much lower portion of the base flow component under the peak of the discharge hydrograph in comparison with the event water component computed by means of natural tracers (s. fig. 4.5). The reason can be explained by the above mentioned methodological differences and assumptions of both methods.

The hydrograph separation procedure for the **Schmelzbach spring** was performed using the ions calcium, magnesium and nitrate and the stable isotope oxygene-18. The flow components computed are plotted in fig. 4.6 and 4.7 in comparison with the total hydrograph. It is clearly visible, that a strong piston flow effect is provoked by the sudden inflow of Lurbach water in the Schmelzbach system, the overflow zone being activated due to the rising karst water level in the Hammerbach system. The percentage of older reservoir water under the discharge peak is in the range of 90%. The dilution with water inflowing from the Hammerbach system begins with high retardation, whereas the event water component reaches its maximum 16 h after the peak of the total discharge.

Both flow components are characterized by a significant secondary peak. In accordance with the results of the artificial tracing experiments (s. chap. 5.2.) and modelling of the tracer breakthrough curves (s. chap. 6.1.) it can be assumed, that these secondary peaks are probably associated with different flow systems (flow paths) with different transit times of the natural tracers in the Schmelzbach aquifer.

Like for the Hammerbach spring the base flow curve computed from the MAILLET-equation gives quite lower values under the peak.

Figure 4.7 gives a comparison of the baseflow curves computed from calcium, magnesium, nitrate and ^{18}O. Calcium gives for the tailing part too high values due to processes of solution and ion exchange in the aquifer. The curves computed by the tracer concentrations of nitrate and magnesium have nearly the same shape. The ^{18}O-base flow curve is influenced by the background fluctuations the difference between peak and background fluctuations not being very high.

The water volumes of the discharge components of both springs Hammerbach and Schmelzbach computed by means of the tracers NO_3^- and ^{18}O and by hydraulic hydrograph separation are compared in tab. 4.1.

Tab. 4.1: Water volumes computed from hydrograph separation by means of the natural tracers nitrate and oxygene-18 and extrapolation of the runoff depletion curves (discharge data from the gauging stations Hammerbach and Schmelzbach). Water volumes in m³ during the runoff event 880629–880701 (input from the Lurbach sinkhole 28,736 m³).

	HAMMER-BACH		SCHMELZ-BACH		Total volume output	
	m³	%	m³	%	m³	%
Total volume	42,778	100.0	9,763	100.0	52,541	100.0
"Older" reservoir water (NO_3^-)	24,888	58.2	5,315	54.4	30,203	57.5
"Older" reservoir water (^{18}O)	29,444	68.8	7,341	75.2	36,785	70.0
Base flow (rec. curve)	38,714	90.5	7,594	77.8	46,308	88.1
Event water (NO_3^-)	17,890	41.8	4,448	45.6	22,338	42.5
Event water (^{18}O)	13,334	31.2	2,422	24.8	15,756	30.0
Direct flow (rec. curve)	4,064	9.5	2,169	22.2	6,233	11.9

The results show that the event water components computed with the stable isotope ^{18}O are generally lower in comparison with the volumes computed by nitrate. The reason is that the fluctuations of the stable isotope were not significant enough in comparison with the background fluctuations due to analytical errors (error ± 0.15 δ‰). For this reason in the case of the flood event in summer 1988 the chemical parameters, particularly nitrate, can be assumed as better natural tracer.

Comparing the event water volumes (computed from the nitrate and ^{18}O-contents) from tab. 4.1 with the input volume from Lurbach of 28,736 m³, we receive the tracer outputs in % for both springs listed in tab. 4.2.

The results show that part of the event water input from Lurbach was not yet discharged at both springs. Assuming, that there are no losses of the natural tracers in the aquifer due to adsorption or recharge of the porous groundwater field, it can be supposed that part of the event water input is stored over a longer time in the karst system and is discharged later. This assumption seems to be realistic, if we compare with the results from the artificial tracing experiments with similar

Tab. 4.2: Event water output volumes in % of input Lurbach (28,736 m³).

	NO_3^-	^{18}O
Hammerbach	62.3	46.4
Schmelzbach	15.5	8.4
Total output	77.7	54.8

breakthrough rates of "ideal" tracers (s. chap. 5.2.). The mathematical characterization of the discharge recession curves of input and output (s. chap. 2.3.) confirm also, that a high amount of water percolating the karst system at the Lurbach sinkhole is stored over a longer time in fine fissures and cave sediments in both aquifers. This high storage capacity of less permeable zones in the karst massif is also verified by the isotopical investigations (s. chap. 3.4. and 6.2.).

5. Tracing Experiments

5.1. Combined Tracing Experiment 1988

5.1.1. Organization, Injection and Sampling (R. BENISCHKE)

5.1.1.1. Injection Site

The injection of all the tracers used for this experiment was in the cave LURGROTTE (A.C.R. No. 2836/1a) in Semriach in a section called "Halle der Eingeschlossenen".

The possibilities to inject tracers vary with the inflow characteristics of the Lurbach. During low water conditions the channel bed is dry and the Lurbach disappears some 100 m upstream at a sediment barrage in a sinkhole at the southern bank. During medium to high water conditions the Lurbach while it looses continuously water flows also into the cave and disappears after 100–150 m behind the entrance into unaccessible sinkholes, and only at extreme water conditions the entire cave system from Semriach to Peggau (in the Mur valley at the W-end of the Tanneben massif) becomes active (s. chap. 2.3.).

During the experiment 1988 the main amount of the Lurbach flowed into the cave and disappeared into the sinkholes inside, therefore the injection was carried out at that site.

5.1.1.2. Hydrometeorologic Conditions During the Experiment

The discharge of the Lurbach measured at the entrance of the Lurgrotte (s. fig. 2.1) on June 28th, 1988 was 47 l/s.

Tab. 5.1: Discharge rates (l/s) at gauging stations during the experiment 1988.

Station	Period	Max.	Min.	Var.	Mean
Lurbach (LB)	880628–880706	1,568	64	1,504	141
Schmelzbach (S)	880628–880715	113	31	82	36
Hammerbach (HB)	880628–880715	263	168	95	194

Tab. 5.2: Precipitation in mm (calc. from daily rainfall at Tanneben [00.00–00.00] and Semriach [07.00–07.00]).

Station	Altitude	Period	Sum	Max.	Mean
Semriach	670	880626–880715	61.5	25.2 (880713)	2.05
Tanneben	750	880626–880715	90.6	27.1 (880714)	4.53

Most of the measured runoff data can be classified as lower mean water conditions. On the day of the tracer injection there was no precipitation. One day after the injection on June 28th, 1988 a local thunderstorm in the higher part of the drainage basin of Lurbach caused a flood event (peak flood 1.6 m^3/s at the gauging station, Lurbach hydrograph s. fig. 4.1). The two rain gauges in Semriach (in the lower part of the basin) and on the Tanneben plateau measured only 2 mm/d. A more detailed explanation of this event is given in chap. 4.

The general hydrometeorologic conditions are presented in chap. 2.3.

5.1.1.3. Used Tracers

Fluorescent tracers

Naphthionate	Naphthionsäure Na-salz	FLUKA A.G., CH	
Pyranine	Pyranin 108%	C.I. No. 59040 BAYER A.G., Germany	C.I. Solvent Green 7
Uranine	Uranin AP konz.	C.I. No. 45350 MERCK, Germany	C.I. Acid Yellow 73
Eosin	Basacid-Rot 316	C.I. No. 45380 BASF A.G., Germany	C.I. Acid Red 87
Sulphorhodamine G	Orcoacid Sulpho-Rhodamine G ex.	C.I. No. 45220 ORGANIC DYESTUFFS Corp., USA	C.I. Acid Red 50
Rhodamine B	Basonyl-Rot 540	C.I. No. 45170 BASF A.G., Germany	C.I. Basic Violet 10

Anorganic tracers

Lithium chloride	LiCl (min. 99.3%)	CHEMETALL GmbH, Germany
Sodium bromide	NaBr (min. 99%)	
Indium-114	^{114m}In-EDTA	Activation by GSF

Particle tracers

Microspheres, YO, 0.89 µ	Fluoresbrite™ Carboxylate Microspheres (2.5% Solid-Latex), 0.89 µ diameter, yellowish-orange, POLYSCIENCES LTD.
Microspheres, YG, 0.95 µ	Polybead™ fluorescent Noncarboxylate Microspheres (2.5% Solid-Latex), 0.95 µ diameter, yellowish-green POLYSCIENCES LTD.
Microspheres, BB, 1.00 µ	Fluoresbrite™ Carboxylate Microspheres (2.5% Solid-Latex), 1.00 µ, bright blue, POLYSCIENCES LTD.
Salmonella phages P22H5	Prepared by INST. OF BIOLOGY, UNIV. LJUBLJANA, SLOVENIA.

5.1.1.4. Injection

All the tracers (13 total) have been injected on June 28th, 1988. Table 5.3 gives an overview.

5.1.1.5. Sampling (Sites, Organization)

During the experiment the main springs at the western side of the Tanneben massif have been examined. This sampling sites are named Schmelzbach (S), Schmelzbach spring (SU), Laurins spring (L), Hammerbach spring (HB), Q2, Q3, Q4, Q5, Q6

Tab. 5.3: Tested tracers (type, amount, date and time of injection, responsibilities for injection) listed in chronological order. The names for the individual tracers are given in a short form (commercial name). Abbreviations of laboratories responsible for the injection s. tab.5.5.

Tracer	Amount	Time	Responsibility
Pyranine	5 kg	09.00–09.02	IGH
Microspheres, YO, 0.89 µ	1 ml (6.5×10^{10})	09.15	KÄSS
Microspheres, YG, 0.95 µ	1 ml (5.3×10^{10})	09.15	KÄSS
Microspheres, BB, 1.00 µ	1 ml (4.5×10^{10})	09.15	KÄSS
Salmonella-phages P22H5	8×10^{14} pfu	09.28	BIO
Rhodamine B	4 kg	09.34–09.36	AGK
Sodium bromide	50 kg	09.55–09.57	GSF
Lithium chloride	100 kg	10.10–10.12	KÄSS
Indium-114	60 mCi	10.22	GSF
Sulphorhodamine G	3 kg	10.25–10.29	IGH
Eosin	5 kg	10.35–10.38	IGH
Naphthionate	25 kg	10.45–10.48	GEOFRB, GSF
Uranine	2 kg	10.50–10.54	IGH

Tab. 5.4: Basic data of the sampling sites, altitude (m a.s.l.) of injection place is 629 m. The altitudes are taken from the official topographic map or from geodetic measurements, distances from the injection point are approximate values taken from the map, the "Diff.Alt."-value is therefore calculated under the previous assumptions.

Name	Abbrev.	Altitude (m a.s.l.)	Distance from injection (m)	Diff. alt. inj.-sampl.	Characteristics
Schmelzbach	S	406	3,000	233	Cave stream outlet (Lurgrotte Peggau)
Schmelzbach spring	SU	424	2,130	215	Cave spring (Lurgrotte Peggau)
Laurins spring	L	416	2,420	223	Cave spring (Lurgrotte Peggau)
Hammerbach spring	HB	405	3,080	234	Outlet of siphon
Q 2-spring	Q 2	405	3,080	234	Resurgence in adjacent detritus
Q 3-spring	Q 3	405	3,080	234	Resurgence in adjacent detritus
Q 4-spring	Q 4	405	3,080	234	Resurgence in adjacent detritus
Q 5-spring	Q 5	405	3,080	234	Resurgence in adjacent detritus
Q 6-spring	Q 6	405	3,080	234	Resurgence in adjacent detritus
Lurbach	LB	640	–	–	Surface stream (input)

and for input-control the hydrochemistry of the Lurbach (LB). For location refer to fig. 2.1 and 2.12. For basic data s. tab. 5.4.

The samples have been taken by automatic samplers in intervals of 1.5 h.

Generally the tracers have been detected only in Hammerbach spring (HB) and the adjacent outlets (Q1–Q6) but not in Schmelzbach (S) except the detection of microspheres and phages (s. resp. chap. 5.1.5. and 5.1.6.). Samples of the tracers in Q1–Q6 were analyzed only by IGH.

5.1.1.6. Analytical Procedures

After sampling the original samples have been divided into working samples as necessary and then distributed by IGH to the individual analytical laboratories

Tab. 5.5: Analytical laboratories and methods. Abbreviations of the laboratories: AGK = Dept. of Applied Geology, Techn. Univ. Karlsruhe, Germany; BIO = Inst. of Biology, Univ. Ljubljana, Slovenia; GEOFRB = Dept. f. Hydrology, Inst. f. Geography, Univ. Freiburg, Germany; GSF = GSF-Inst. f. Hydrology, Munich, Germany; HMZ = Hydrometeorological Inst., Ljubljana, Slovenia; IGH = Inst. f. Geothermics and Hydrogeology, Joanneum Research, Graz, Austria; KÄSS = W. KÄSS, Umkirch, Germany. Annotations see p. 81.

Tracer	Laboratory	Method	Instrument
Naphthionate	GEOFRB	SFL (synchro-scan, pH-treatm.)	PERKIN ELMER 500
	GSF	SFL (synchro-scan, pH-treatm.)	AMINCO SPF 500 Ratio
Pyranine	AGK	SFL (synchro-scan, pH-treatm., MCD)	PERKIN ELMER LS 3
	GSF	SFL (synchro-scan, pH-treatm., MCD)	AMINCO SPF 500 Ratio
	IGH	SFL (synchro-scan, pH-treatm., MCD)	AMINCO SPF 500 Ratio
	HMZ	SFL (synchro-scan, pH-treatm.)	PERKIN ELMER 204
Uranine	AGK	SFL (synchro-scan, pH-treatm., MCD)	PERKIN ELMER LS 3
	GSF	SFL (synchro-scan, pH-treatm., MCD)	AMINCO SPF 500 Ratio
	IGH	SFL (synchro-scan, pH-treatm., MCD)	AMINCO SPF 500 Ratio
	HMZ	SFL (synchro-scan, pH-treatm., MCD)	PERKIN ELMER 204
Eosin	GSF	CC-sep., SFL (synchro-scan, pH-treatm.)	AMINCO SPF 500 Ratio
	IGH	SFL (synchro-scan, pH-treatm.)	AMINCO SPF 500 Ratio
	HMZ	SFL (synchro-scan, pH-treatm., MCD)	PERKIN ELMER 204
Sulphorhodamine G	AGK	SFL (synchro-scan, pH-treatm.)	PERKIN ELMER LS 3
	GSF	SFL (synchro-scan, pH-treatm.)	AMINCO SPF 500 Ratio
	IGH	SFL (synchro-scan, pH-treatm., MCD)	AMINCO SPF 500 Ratio
	HMZ	CC-sep., SFL (synchro-scan, pH-treatm.)	PERKIN ELMER 204
Rhodamine B	AGK	SFL (synchro-scan, pH-treatm.)	PERKIN ELMER LS 3
	GSF	SFL (synchro-scan, pH-treatment), MCD	AMINCO SPF 500 Ratio
	IGH	SFL (synchro-scan, pH-treatment), MCD	AMINCO SPF 500 Ratio
	HMZ	CC-sep., SFL (synchro-scan, pH-treatm.)	PERKIN ELMER 204
Lithium	KÄSS	FLAES	ZEISS FMP 4
	GSF	FLAES, DCP-AES	VARIAN Spectra A-40, BECKMANN Spectraspan VI
Bromide	GSF	IC (Electrochemical Detection)	DIONEX
Chloride	IGH	IC (Conductivity Detection)	DIONEX 2010i
Indium-114m	GSF	Gamma-Spectrometry	Multi-Channel Analyzer , (Harshaw, Canberra)
Microspheres	KÄSS	Fluorescence Microscope Counting	ZEISS Axioscope
Phages	BIO	Agar Layer Method	

(Tab. 5.5). From the originally injected tracers also a small quantity to prepare standards has been provided for each laboratory.

Annotations:

SFL: Spectrofluorimetry.

Synchro-scan: Simultaneous scanning of excitation and emission monochromators with a constant wavelength difference (the appropriate value depends on the analyzed dye tracer and the selected pH-conditions of the working solution), for more information s. chap. 5.1.2.1.

pH-treatment: For the used organic dye tracers defined pH-conditions in the working solution are necessary either to achieve a maximum fluorescence and/or to separate the individual tracer from each other; for more information s. chap. 5.1.2.1.

IC: Ion Chromatography
IGH: DIONEX-Conductivity Detector; eluent: 1.7/1.8 mmol $NaHCO_3/Na_2CO_3$; regenerant: 1.4 ml H_2SO_4-conc./2 l H_2O-dest.; injection volume: 50 µl; flow rate: 2.0 ml/min; samples are filtrated with 0.45 µ prior to injection; separation column: DIONEX IonPac AS4A; suppressor: DIONEX AMMS-1; guard column: DIONEX IonPac AG4A (same type as separator but shorter).
GSF: Electrochemical Detector: DIONEX (with Ag/AgCl-electrode); eluent: 0.011 m $NaNO_3$; regenerant: none; injection volume: 0.5 ml; flow rate: 2 ml/min; samples were not treated; separation column: DIONEX HPIC AS-5; guard column: DIONEX NG1; potential: 0.1 mV.

FLAES: Flame Atomic Emission Spectrometry
KÄSS: Lithium was measured in emission mode at $\lambda = 670.8$ nm. Both standards and samples were treated with ammonium oxalate to overcome Ca-interference on the lithium signal.
GSF: Lithium was measured in the laboratory of Technical University (Munich), Inst. f. Wassergütewirtschaft, with a detection limit of about 30 ppb, with air/acetylene flame at $\lambda = 670.8$ nm, without any treatment.

DCP-AES: Direct Current Plasma Atomic Emission Spectrometry
GSF: Lithium was measured at GSF-Institute of Ecological Chemistry. The detection limit was reported as 5 ppb, without any treatment.

MCD: Mathematical multi-component discrimination of spectra based on the solution of n linear equations.

5.1.2. Results with Fluorescent Tracers

5.1.2.1. General Remarks (R. BENISCHKE)

The presentation of the tracer transit curves in diagrams follows a suggestion of H. BEHRENS, i.e. that the results of the different laboratories are related to the same time period and the concentrations are normalized as fractions of the injected amount of tracer (as $10^{-5} \cdot M$; in mg).

$$\text{Normalized value } (m^{-3}) = \text{Conc } (mg/m^3) \cdot 10^5/M \text{ (mg)}.$$

This presentation has some advantages for comparison of different tracers with different injected amounts. For a presentation of the different results of the same tracer from individual laboratories it is equivalent to give concentrations or fractions or normalized values. But it is easier to compare the different tracers in the same or different diagrams.

All fluorescent tracers have been analyzed by two or even four laboratories. **It was not the aim of the experiment to carry out interlaboratory tests to standardize the analytical methods and to evaluate under defined statistical assumptions. Nevertheless the results show the necessity of a standardization**

of tracer analytics particularly for separation procedures, if two or more tracers are present in the same sample.

Problems for the evaluation and comparison originated from the time lag between sampling and analysis, from transport and different storage conditions. The samples were brought to the IGH-laboratory and there divided into working samples and then sent by mail to the cooperating laboratories. All laboratories had different capacity to analyze the samples. So it was reported for the GSF-samples, that because of shortness of laboratory labour capacity, samples of the Lurbach experiment could only be processed about 10 months after sampling. By comparing GSF-results on fluorescent tracers with the very stable tracer bromide and with previous fluorimetric measurements of other laboratories, in the stored samples partial decay of pyranine, naphthionate and uranine was evident which was probably caused by microbial degradation.

This decay took place in a very irregular manner which can be seen in fig. 5.1.

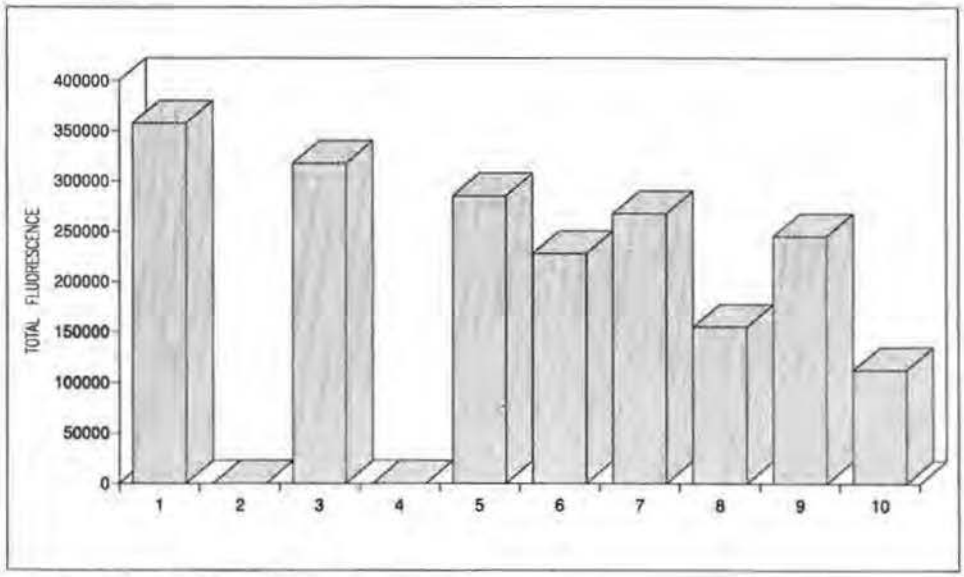

Fig. 5.1: Samples of Hammerbach from 880630/10.30 (1, 2), 12.00 (3, 4), 13.30 (5, 6), 15.00 (7, 8) and 16.30 (9, 10). Evaluated are only total fluorescence intensities under synchro-scan (25 nm with EDTA). Samples 1, 3, 5, 7, 9 measured on 880706, corresponding measurements of the same samples as 2, 4, 6, 8, 10 on 890502. Storage conditions: dark, under room temperature (18–25° C).

Storage conditions and time of analysis:

GEOFRB: Storage dark and at c. 16° C,
Samples of 880628–880715 (each selected) in 8807.

AGK: Storage dark and at room temperature,
Samples of 880628–880715 (each selected) in 8809.

GSF: Storage dark and at room temperature without further treatment,
Samples of 880629–880701 (each selected) in 8904.

IGH: Storage dark and at 18–25° C without further treatment,
Samples of 880628–880701 (each selected) on 880706,
Samples of 880701–880703 (each selected) on 880711,

Samples of 880703–880704 (each selected) on 880714,
Samples of 880704–880705 (each selected) on 880719,
Samples of 880705–880707 (each selected) on 880722,
Samples of 880707–880710 (each selected) on 880727,
Samples of 880710–880712 (each selected) on 880801,
Samples of 880712–880715 (each selected) on 880802.

HMZ: Storage dark and at 18–24° C,
Samples of 880627–880702 (four samples/day selected) on 881018–881021,
Samples of 880703–880715 (two samples/day selected) on 881018–881021 and 881207–881231.

Annotation:

In the following subsections for each laboratory and each dye tracer the specific measurement conditions are given in a table:

λ_{max}(nm) = fluorescence emission peak
$\Delta\lambda$ (nm) = specific wavelength difference between excitation and emission monochromator
pH = pH-value set to achieve the best result
Reagent = substance to set the pH-value
EDTA = Tetranatriumethylendiamintetraacetate
AGK (10 g/10 ml; 20 µl to 3.5 ml cuvette)
GSF (10 g/10 ml; 20 µl to 3.5 ml cuvette)
IGH (22.61 g/100 ml; 2 drops to 3.5 ml cuvette)
AMM = ammonia-buffer
samples were exposed to NH_3-vapour for c. 6 h
CARB = sodium-carbonate-buffer
HMZ (11 ml 10% [w/v] Na_2CO_3 : 9.5 ml 10% [w/v] $NaHCO_3$; 300 µl to 10 ml sample)
ACET = acetate-buffer
AGK (1 : 1 mixture of 4.5 M K-acetate with 5.5 M acetic acid; 20 µl to 3.5 ml cuvette)
GSF (1 : 1 mixture of 4.5 M K-acetate with 5.5 M acetic acid; 20 µl to 3.5 ml cuvette)
GSF (acetic acid conc., 10 µl to 3.5 ml cuvette for pH 3)
IGH (1 : 1 mixture of 4.5 M K-acetate with 5.5 M acetic acid; 2 drops to 3.5 ml cuvette)
HMZ (1 : 1 mixture of 4.5 M K-acetate with 5.5 M acetic acid; 50–60 µl to 10 ml sample)
H_2SO_4 = sulfuric acid 95–97%
AGK (1 drop to 3.5 ml cuvette)
IGH (1 drop to 3.5 ml cuvette)
HMZ (20 µl H_2SO_4 (1 : 3) to 10 ml sample)
C.C. = column chromatography to separate tracers
MCD = mathematical multi-component discrimination, in this column the spectrally interfering tracers are listed, which were eliminated by MCD
D.L. = detection limit (ppb) if reported by the laboratory
Std. Matrix = D is distilled water or equivalent, SW is dye-free supply water
Treatm. = F is sample filtration prior to analysis
n.a. = not applied

5.1.2.2. Results with Naphthionate (H. BEHRENS, Ch. LEIBUNDGUT)

The GEOFRB-samples between 880628 and 880715 were analyzed very quickly and were completely evaluated.

In the GSF-samples naphthionate showed strong decay effects (related to a probable biological degradation), as well as in comparison to the bromide tracer and in comparison to earlier measurements made by GEOFRB (ref. to fig. 5.2).

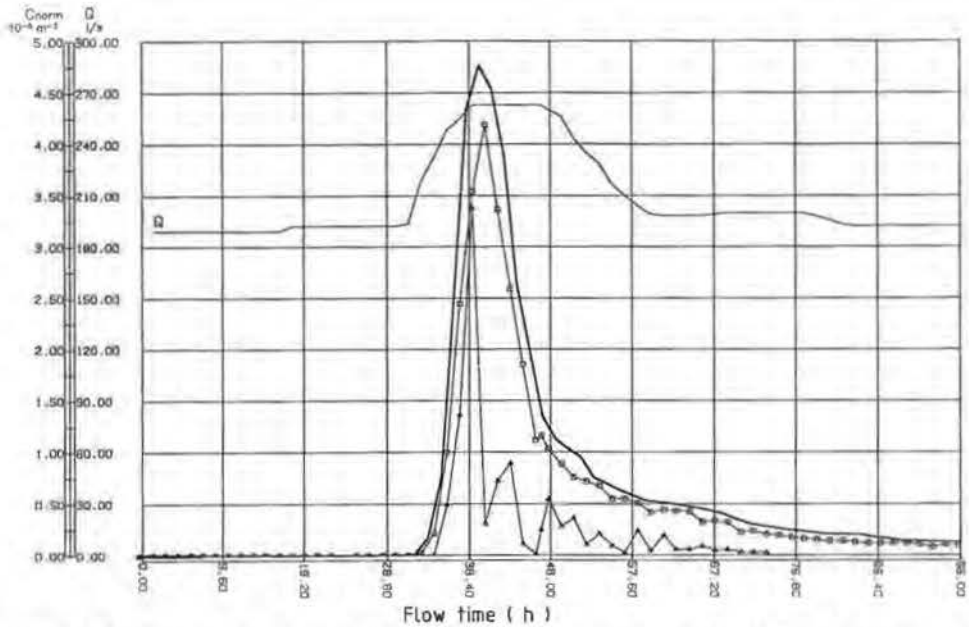

Fig. 5.2: Tracing experiment 1988: breakthrough curves at Hammerbach spring of the tracer naphthionate measured by different laboratories compared with bromide as reference tracer (measured by GSF, bold-faced line). Abbreviations of laboratories s. tab. 5.5. C_{norm} = normalized concentration, Q = discharge in l/s, flow time in h since injection, squares = measured by GEOFRB, triangles = measured by GSF.

Tab. 5.6: Comparison of analytical and instrumental settings for naphthionate. Abbrev. of laboratory names see annotations in previous subsection and tab. 5.5.

Lab.-Name	λ_{max} (nm)	Synchro-scan $\Delta\lambda$ (nm)	pH	Reagent	CC	MCD	D.L. (ppb)	Std. matrix	Treatm.
GEOFRB	420 ± 5	95	7.5	AMM	n.a.	n.a.	0.5	SW	sedimentation, siphoning
GSF	419	104	4.8	ACET	n.a.	n.a.	0.08	SW	n.a.

5.1.2.3. Results with Pyranine (H. BEHRENS, R. BENISCHKE, B. REICHERT, M. ZUPAN)

Pyranine was analyzed by four different laboratories (AGK, GSF, IGH, HMZ). Ref. to fig. 5.3.

Because of a technical problem with an automatic sampler the series for AGK and HMZ are incomplete between 880630/03.00 and 880630/09.00. The missing values for the tracer concentrations were added by linear interpolation, therefore the tracer transit curve looks in that region like a straight line.

In GSF-samples pyranine was almost completely destroyed. Only in two samples from the breakthrough maximum distinguishable but dramatically reduced amounts of the tracer were found while in the rest of the samples only traces were still detectable. The evaluation of GSF-samples covered only the period between 880629 and 880701.

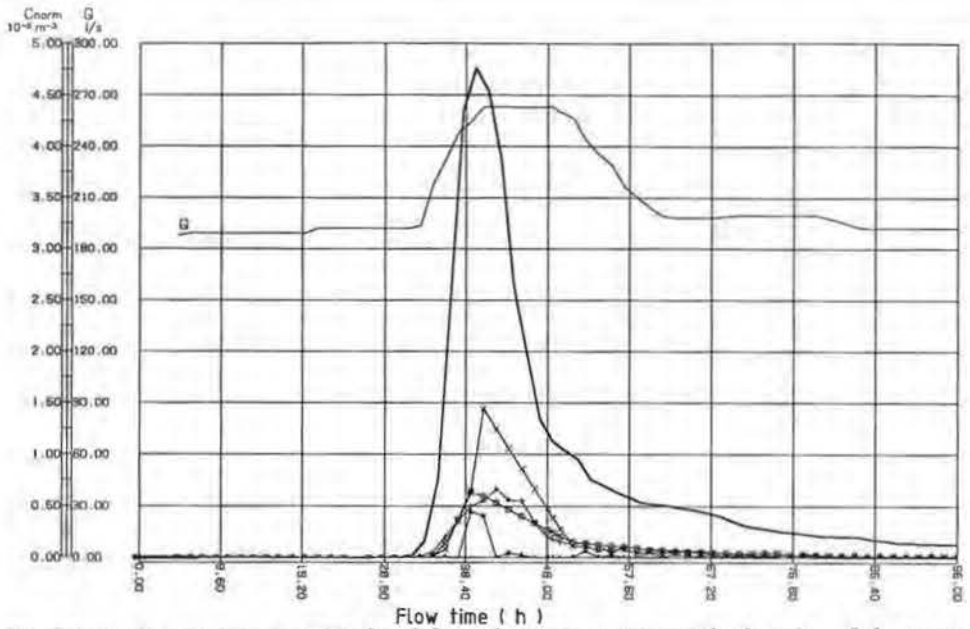

Fig. 5.3: Tracing experiment 1988: breakthrough curves at Hammerbach spring of the tracer pyranine measured by different laboratories compared with bromide as reference tracer (measured by GSF, bold-faced line). Abbreviations of laboratories s. tab. 5.5. C_{norm} = normalized concentration, Q = discharge in l/s, flow time in h since injection, squares = measured by AGK, triangles = measured by GSF, + = measured by IGH, x = measured by HMZ.

Tab. 5.7: Comparison of analytical and instrumental settings for pyranine. Abbrev. of laboratory names see annotations in previous subsection and tab 5.5. ° means lower limit of working range.

Lab.-Name	λ_{max} (nm)	Synchro-scan $\Delta\lambda$ (nm)	pH	Reagent	CC	MCD	D.L. (ppb)	Std. matrix	Treatm.
AGK	512	103	4.8	ACET	n.a.	UR	0.06	SW	F (if necessary)
GSF	511	104	4.8	ACET	n.a.	UR	0.01	SW	n.a.
IGH	511	108	2	H_2SO_4	n.a.	UR	0.025°	D	n.a.
HMZ	510	108	2	H_2SO_4	n.a.	UR	0.08	SW	n.a.

With respect to the interpolated values the results of AGK and IGH gave a fairly good correspondence. The results from GSF are significantly lower and showed a more fluctuating behaviour. This can be explained from photochemical and/or biological degradation (from chemical analyses of the Hammerbach it was known that a very high bacteriological contamination from a waste water inflow from the Semriach basin via Lurbach might cause degradation effects). Degradation of the GSF-samples occured probably due to a longer storage time under room temperature before the analysis. In comparison with the AGK and IGH samples the results from HMZ brought too high values for the rising part of the transit curve. After 880630/12.00 the values correspond with those of the others.

5.1.2.4. Results with Uranine (H. BEHRENS, R. BENISCHKE, B. REICHERT, M. ZUPAN)

In GSF-samples uranine showed a moderate decay in some samples after the breakthrough maximum, while in the rest of the samples the tracer appeared to be still unchanged showing a representative tracer behaviour in comparison of the reference bromide (ref. to fig. 5.4).

The IGH-samples are in good correspondence with the AGK-, GSF- and HMZ-samples. Differences can be seen in the time of the peak. MCD-correction was performed by a system of four to five linear equations established by measurement of pure standards.

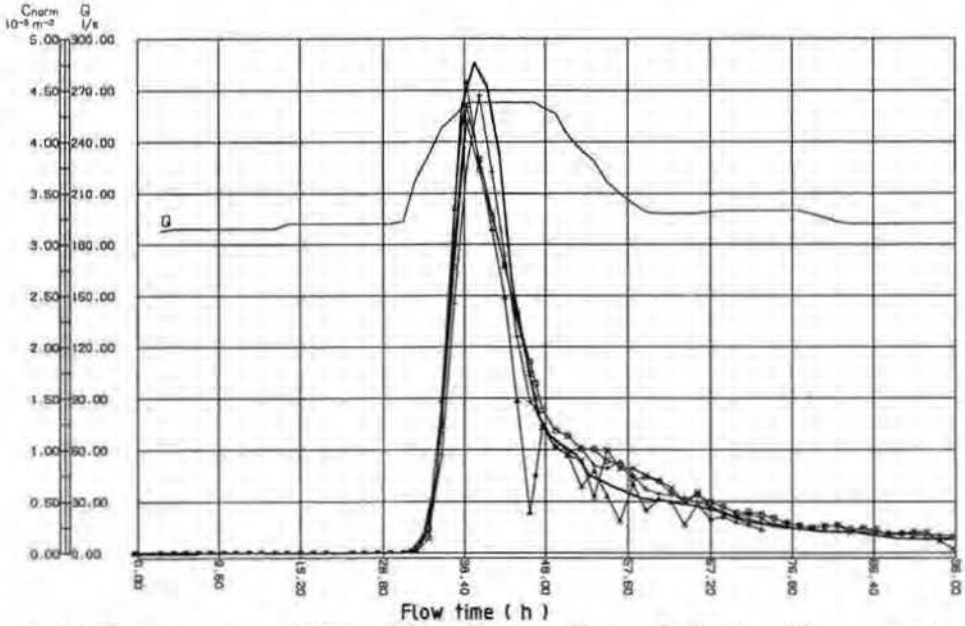

Fig. 5.4: Tracing experiment 1988: breakthrough curves at Hammerbach spring of the tracer uranine measured by different laboratories compared with bromide as reference tracer (measured by GSF, bold-faced line). Abbreviations of laboratories s. tab. 5.5. C_{norm} = normalized concentration, Q = discharge in l/s, flow time in h since injection, squares = measured by AGK, triangles = measured by GSF, + = measured by IGH, x = measured by HMZ.

Tab. 5.8: Comparison of analytical and instrumental settings for uranine. Abbrev. of laboratory names see annotations in previous subsection and tab. 5.5.

Lab.-Name	λ_{max} (nm)	Synchro-scan $\Delta\lambda$ (nm)	pH	Reagent	CC	MCD	D.L. (ppb)	Std. matrix	Treatm.
AGK	514	25	> 10	EDTA	n.a.	PYR, EO	0.002	SW	F (if necessary)
GSF	512	25	~ 10	EDTA	n.a.	PYR, EO	0.002	SW	n.a.
IGH	516	25	~ 10	EDTA	n.a.	PYR, EO, SRG	0.002	D	n.a.
HMZ	513	25	~ 10	CARB	n.a.	PYR	0.02	SW	n.a.

The MCD-correction in HMZ-samples was performed after H. BEHRENS (1988).

All samples are well comparable in the rising part of the breakthrough, later only GSF-samples (see above) showed stronger fluctuation (probably due to the late analysis time).

As mentioned in chap. 5.1.1.5. samples of the springs Q1–Q6 were analyzed only by IGH. They have for all tracers a similar or even the same shape of transit curves as the Hammerbach spring (HB).

5.1.2.5. Results with Eosin (H. BEHRENS, R. BENISCHKE, M. ZUPAN)

For breakthrough curves in comparison with bromide refer to fig. 5.5.

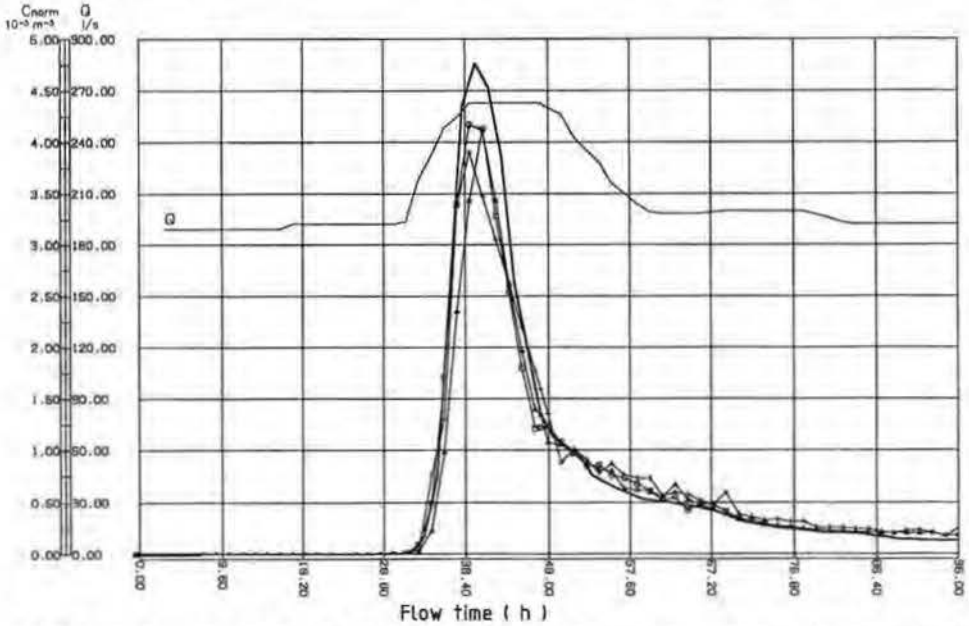

Fig. 5.5: Tracing experiment 1988: breakthrough curves at Hammerbach spring of the tracer eosin measured by different laboratories compared with bromide as reference tracer (measured by GSF, bold-faced line). Abbreviations of laboratories s. tab. 5.5. C_{norm} = normalized concentration, Q = discharge in l/s, flow time in h since injection, squares = measured by GSF, triangles = measured by IGH, + = measured by HMZ.

*Tab. 5.9: Comparison of analytical and instrumental settings for eosin. Abbrev. of laboratory names see annotations in previous subsection and tab. 5.5. * means the lower limit of working range.*

Lab.-Name	λ_{max} (nm)	Synchro-scan $\Delta\lambda$ (nm)	pH	Reagent	CC	MCD	D.L. (ppb)	Std. matrix	Treatm.
GSF	535	25	5.1	ACET	appl.	PYR, UR	0.08	SW	n.a.
IGH	540	25		EDTA	n.a.	PYR, UR, SRG, RHB	0.025*	D	n.a.
	541	25	~ 5	ACET	n.a.	UR, SRG, RHB	0.025*	D	n.a.
HMZ	538	25	4.6	ACET	n.a.	n.a.	0.10	SW	n.a.

GSF-samples were obviously not effected by decay and showed a representative tracer behaviour.

IGH-samples showed differences in the rising part of the breakthrough comparing them with GSF-analyses, also a time lag is possible. Both attempts from measurements made in alkaline or slightly acid solution brought comparable results when applying MCD as given in tab. 5.9. The discrimination from sulphorhodamine G was performed by MCD, which has its limit if high concentration differences lead to complete spectral overlapping by the interfering substance. Therefore a CC-procedure (H. BEHRENS, 1988) is recommended.

HMZ-samples are in good correspondence with GSF-analyses with respect to the interpolated values during and after the peak.

5.1.2.6. Results with Sulphorhodamine G (H. BEHRENS, R. BENISCHKE, B. REICHERT, M. ZUPAN)

GSF-samples showed a more or less representative tracer behaviour with exception of some small reduction of concentration in the breakthrough maximum. This could have been caused by small losses due to sorption processes.

IGH-samples are significantly lower than AGK- and GSF-samples which may be caused by sorption effects during storage prior to analysis but not by a degraded series of the used standards.

HMZ-samples were analyzed by synchro-scan ($\Delta\lambda$ = 25 nm) after adsorption on silica sand (0.2–0.5 mm) and desorption by water at pH 7 after H. BEHRENS (1982).

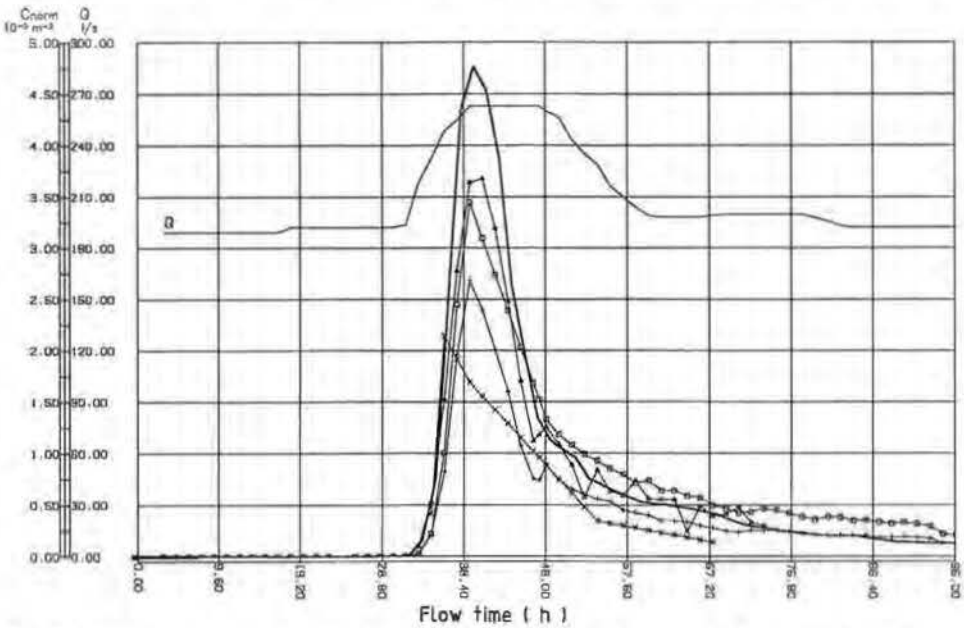

Fig. 5.6: Tracing experiment 1988: breakthrough curves at Hammerbach spring of the tracer sulforhodamine measured by different laboratories compared with bromide as reference tracer (measured by GSF, bold-faced line). Abbreviations of laboratories s. tab. 5.5. C_{norm} = normalized concentration, Q = discharge in l/s, flow time in h since injection, squares = measured by AGK, triangles = measured by GSF, + = measured by IGH, x = measured by HMZ.

*Tab. 5.10: Comparison of analytical and instrumental settings for sulphorhodamine G. Abbrev. of laboratory names see annotations in previous subsection and tab. 5.5. * means lower limit of the working range.*

Lab.-Name	λ_{max} (nm)	Synchro-scan $\Delta\lambda$ (nm)	pH	Reagent	CC	MCD	D.L. (ppb)	Std. matrix	Treatm.
AGK	555	25	< 4	H_2SO_4	n.a.	n.a.	0.003	SW	F (if necessary)
GSF	555	25	~ 3	ACET	n.a.	RHB	0.007	SW	n.a.
IGH	557	25	~ 5	ACET	n.a.	UR, EO, RHB	0.025*	D	n.a.
HMZ	555	25	~ 7	n.a.	appl.	n.a.	1.00	SW	n.a. (but C.C.)

The separation with this method from rhodamine B was problematic, another attempt (after H. BEHRENS et al., 1976) showed bad results too. Therefore the results differ significantly from the other (s. fig. 5.6).

5.1.2.7. Results with Rhodamine B (H. BEHRENS, R. BENISCHKE, M. ZUPAN)

Breakthrough curves are shown in fig. 5.7.

Results from AGK-samples are given only for the period 880701/10.30 to 880702/10.30. Due to the lack of an appropriate separation method these values are not representative for the rhodamine B breakthrough.

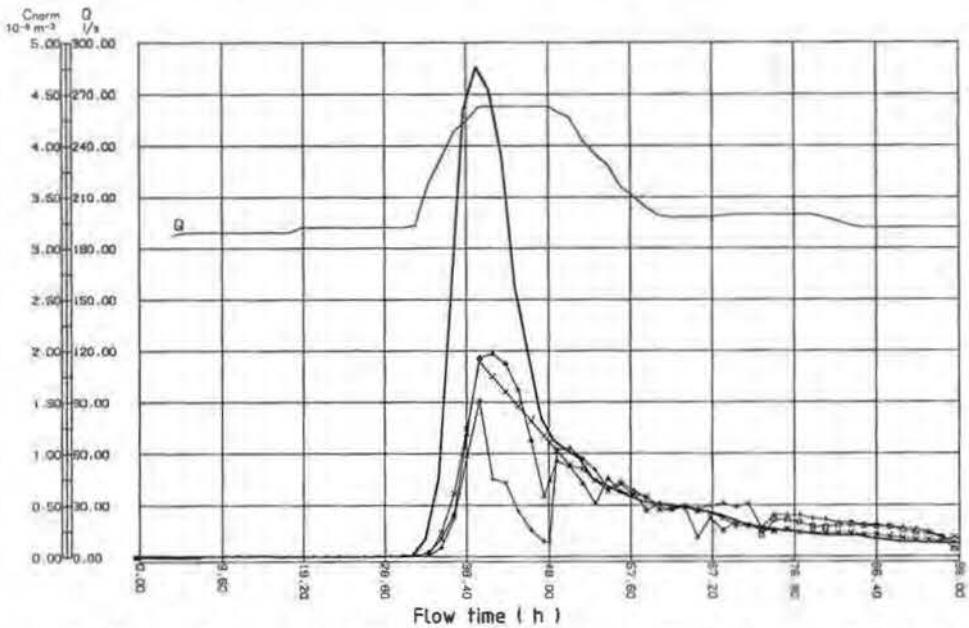

Fig. 5.7: Tracing experiment 1988: breakthrough curves at Hammerbach spring of the tracer rhodamine B measured by different laboratories compared with bromide as reference tracer (measured by GSF, bold-faced line). Abbreviations of laboratories s. tab. 5.5. C_{norm} = normalized concentration, Q = discharge in l/s, flow time in h since injection, squares = measured by AGK, triangles = measured by GSF, + = measured by IGH, x = measured by HMZ.

*Tab. 5.11: Comparison of analytical and instrumental settings for rhodamine B. Abbrev. of laboratory names see annotations in previous subsection and tab. 5.5. * means lower limit of the working range*

Lab.-Name	λ_{max} (nm)	Synchro-scan $\Delta\lambda$ (nm)	pH	Reagent	CC	MCD	D.L. (ppb)	Std. matrix	Treatm.
AGK	576	25	< 4	H_2SO_4	n.a.	n.a.	0.005	SW	F (if necessary)
GSF	582	25	~ 3	ACET	n.a.	SRG	0.008	SW	n.a.
IGH	579	25	~ 5	ACET	n.a.	UR, EO, SRG	0.025*	D	n.a.
HMZ	575	25	~ 7	n.a.	appl.	n.a.	0.05	SW	n.a. (but C.C.)

GSF-samples showed a representative behaviour with respect to the time response of the tracer breakthrough. In quantitative respect, however, the measured concentrations were clearly reduced in relation to expected values for a representative tracer behaviour.

IGH-samples showed a dramatic reduction during the time of the peak but good correspondence in the tailing part of the breakthrough after 880630/10.00 with the results of the other. For the reduction of fluorescence the same is possible as for sulphorhodamine G.

The separation of rhodamine B from sulphorhodamine G in HMZ-samples showed the same difficulties in analysis as obtained with sulphorhodamine G.

5.1.3. Results with Salt Tracers

5.1.3.1. Results with Lithium (W. KÄSS)

The lithium-kation was investigated at three different laboratories (ref. to chap. 5.1.1.6.):

- Umkirch (W. KÄSS) with FLAES,
- Neuherberg (GSF-Ecology with DCP-AES,
- Munich (Technical University) with FLAES.

A significant increase of lithium was only detectable in the Hammerbachquelle. The results were in fairly good correspondence with each other (Fig. 5.8). The natural background was found with 0.4 ppb in the Schmelzbach, with 0.5 ppb in the Hammerbach.

5.1.3.2. Results with Bromide (H. BEHRENS)

Bromide is assumed as chemical stable and as an extremely conservative tracer. Because of this behaviour and of the fact that bromide occurs only at very low background concentrations (often negligible) it was selected for comparison purposes as a reference tracer (Fig. 5.9).

5.1.3.3. Results with Chloride (R. BENISCHKE)

Chloride is assumed to be a chemical stable and conservative tracer like bromide and with comparable geochemical mobility. The only disadvantage is that the natural background of chloride is much higher than that of bromide, thus initiating problems how to take into consideration natural fluctuations during the tracer transit. Conventionally the background to be taken is either an average value prior to the

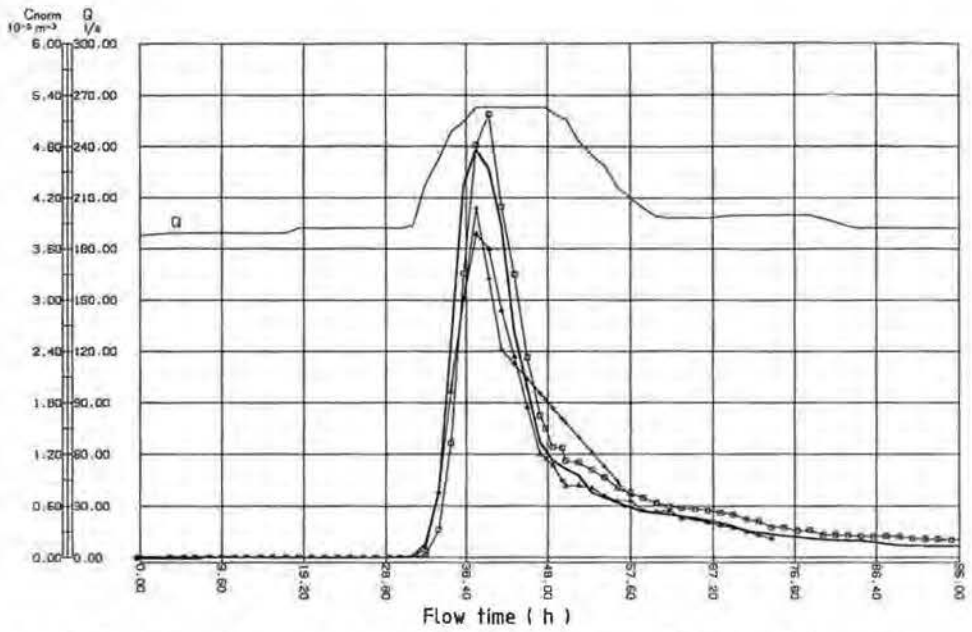

Fig. 5.8: Tracing experiment 1988: breakthrough curves at Hammerbach spring of the tracer lithium measured by different laboratories compared with bromide as reference tracer (measured by GSF, bold-faced line). Abbreviations of laboratories s. tab. 5.5. C_{norm} = normalized concentration, Q = discharge in l/s, flow time in h since injection, squares = measured by W. KÄSS, triangles = measured by GSF (Institute of Ecology), + = measured by TU Munich.

first arrival of the tracer or the highest value analyzed before that time. This background value must be subtracted from all sample values to achieve the net concentration. In most cases the natural background will be stable under more or less constant runoff conditions. When the period of the tracer transit is one with fluctuating discharge strong dilution or concentration effects may occur, which cannot be taken into account during the transit. Then a bigger error in the calculations particularly for recovery rates will arise. In this experiment chloride as an artificial tracer comes from the injected lithium chloride (Fig. 5.9). It can be seen from the breakthrough curves that chloride has reached the background much quicker than the other ionic tracers indicating that the natural chloride background which is significantly higher than that of the others has been diluted during the flood event having occurred during the experiment.

5.1.4. Results with Indium-114 (H. BEHRENS)

5.1.4.1. Introduction

^{114m}Indium is a γ-emitting radionuclide with a halflife-period of 49.5 d, emitting γ-energies of 190, 558 and 725 MeV. To be suitable as a water tracer it has to be used in the proper chemical form for which the EDTA-complex has proven to be a good choice.

5.1.4.2. Production of the Radionuclide and Tracer Preparation

For the production of ^{114m}indium about 2.6 g of indium metal-powder sealed in

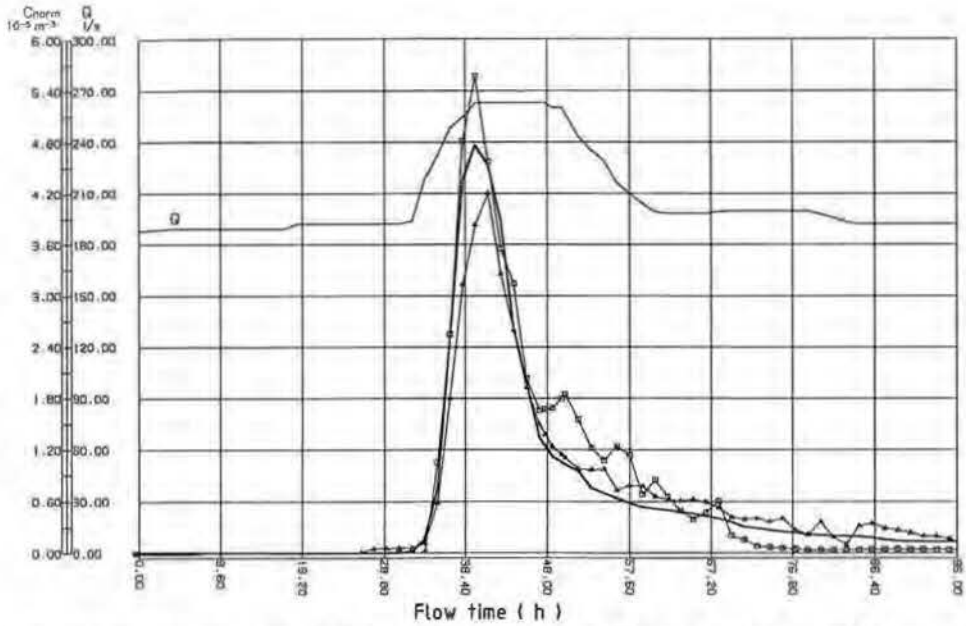

Fig. 5.9: Tracing experiment 1988: breakthrough curves at Hammerbach spring of the tracers chloride and indium-114 compared with bromide as reference tracer (measured by GSF, bold-faced line). Abbreviations of laboratories s. tab. 5.5. C_{norm} = normalized concentration, Q = discharge in l/s, flow time in h since injection, squares = measured by IGH, triangles = measured by GSF.

a quartz ampoule were irradiated with neutrons in the research reactor of the Technical University of Munich for a period of three days during the week preceding the tracing experiment. The produced activity was about 60 mCi.

To avoid transportation in liquid form wich would afford large shielded container, the untouched ampoule was transported to the test site postponing the preparation of the tracer directly to the injection site. The irradiated indium powder was brought into a 1 l-glass bottle and dissolved with dilute hydrochloric acid under gentle heating in a water bath. Escaping of radioactive aerosols was prevented by venting the bottle through a raschig tube. After dissolution and dilution the complexing agent EDTA was added in a 10-fold excess and the solution was neutralized with ammonia. The solution was made up to 1 l and a reference of 10 ml was separated. The remaining tracer solution was used as injection volume (990 ml) and instantaneously injected in the Lurbach sinkhole in the Lurgrotte (s. time schedule chap. 5.1.1.4.).

5.1.4.3. Tracer Analysis

Measurement of the radioactivity for the ^{114m}indium determination was made as soon as possible to avoid attenuation of the signal as a consequence of radioactive decay. This could be carried out until the end of July, 1988.

To achieve maximum counting efficiency it was attempted to concentrate the radiotracer from the available samples (500 ml) for effecting an optimal counting geometry. For this purpose the anionic indium complex was separated from the solutions by sorption on an anion exchanger (DOWEX 2×8, 200–400 mesh), in small columns of 3.5 ml bed volume. After air drying, the resin samples were counted

with a GeLi semiconductor setup using high resolution γ-spectrometry of the 725 MeV line. To obtain better counting statistics for samples of the tailing part of the tracer transit curve, concentrates of three succeeding samples were combined.

5.1.4.4. Results

^{114m}Indium was detected in samples of Hammerbach, but not in those of Schmelzbach. If the radiotracer appeared in the latter, the concentration should have been below the detection limit of about 10^{-6} of the injected amount of tracer per unit volume of water (m^3). The tracer breakthrough curve for the Hammerbach is documented in fig. 5.9.

5.1.5. Results with Microspheres (W. KÄSS, R. BENISCHKE)

The experiment 1988 at Lurbach system was the first attempt to use a special type of microspheres in a karst drainage system. Earlier experiments with spores (uncoloured, coloured or fluorescent) and solid matter (wood, cork etc.) suffered from a limitation because of their size. So a lot of developmental work had to be done to optimize for example the behaviour of spores in flow processes (A. MAYR, 1953, M. DECHANT, 1959, 1967, J. DREYER, 1987). Therefore in search of additional particle tracers microspheres were found to be applicable not only for tracing successfully karst water drainage but also porous groundwater.

Microspheres have been developed for investigations of blood circulation. For example they are applied in human medicine intravenously.

From tab. 5.3 it can be seen that the microspheres have a considerable smaller diameter (about 1 µm) than Lycopodium spores (reported to be about 35 µm). The material is a carboxylate (polycarboxylate, YO, BB) or noncarboxylate (polystyrene, YG), which is coloured with different fluorescent dyes.

In the Lurbach experiment the microspheres were suspended in dilute detergent. Sampling was carried out with automatic samples. Sample volume was 250 ml. The analyte was concentrated on black membrane filters (provided with a counting grid), and the evaluation was carried out by counting under a fluorescence microscope.

The results are seen in fig. 5.10 and tab. 5.12 and 5.13. The microspheres mainly reappeared in the Hammerbach spring and sporadically in the Schmelzbach due to the hydrologic conditions (decreasing discharge rates after a runoff event). From the individual types of microspheres only the noncarboxylate (polystyrene) microspheres reappeared and none of the others. This can be explained by different charged surfaces of the spheres and polarity, i.e. that polystyrene had probably low affinity to clay minerals (in cave sediments). The other two types of microspheres probably had been adsorbed strongly to clay sediments.

5.1.6. Results with Salmonella Phage P22H5 (M. BRICELJ, G. KOSI)

As sinking waters as well as springs in rural areas are often polluted with coliform bacteria, coliphages can occur in considerable background numbers, thus making their use inconvenient in cases of possible high dilution. Consequently the P22H5 phage of Salmonella typhimurium LT2 strain (H.O. SMITH & M. LEVINE, 1967) was introduced in tracing experiments by the researchers of the Institute of Biology, Ljubljana (M. BRICELJ et al., 1986). It is well known that the bacteriophages of mouse typhoid fever producing bacteria rarely occur in natural waters (N.D. SEELY & S.B. PRIMROSE, 1982). The injection of phage tracer was carried out on June 28th, 1988 at 9.28 a.m. just after the injection of microspheres and before the

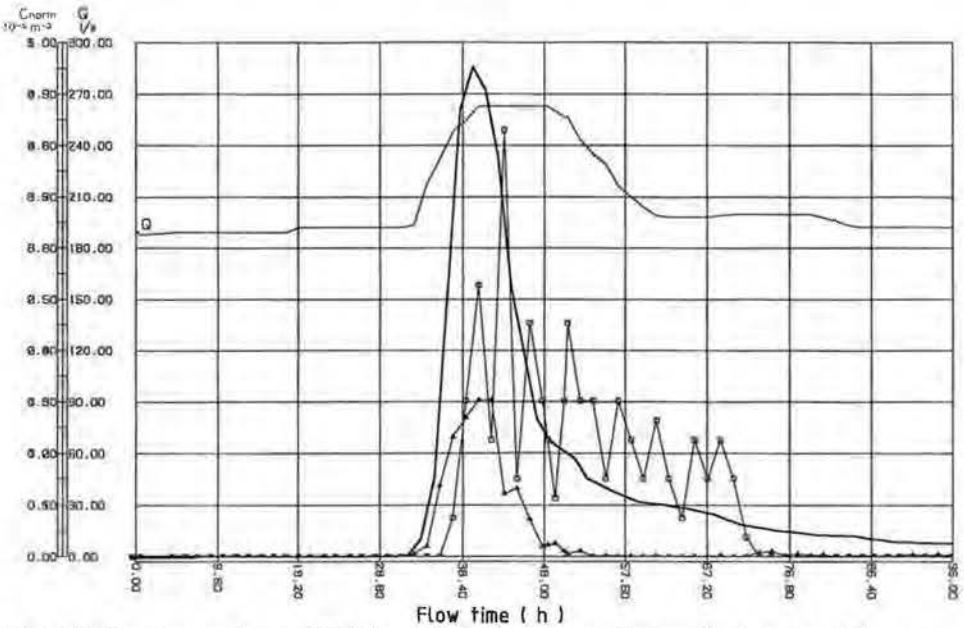

Fig. 5.10: Tracing experiment 1988: breakthrough curves at Hammerbach spring of the tracers noncarboxylate (polystyrene) microspheres and Salmonella phage P22H5 compared with bromide as reference tracer (measured by GSF, bold-faced line). Abbreviations of laboratories s. tab. 5.5. C_{norm} = normalized concentration, Q = discharge in l/s, flow time in h since injection, squares = measured by W. KASS, triangles = measured by BIO.

rhodamine B. The total quantity of phage tracer was 8×10^{14} p.f.u. (plaque forming units) and the phage pulp was poured instantaneously (within c. 2 sec) into the Lurbach. Nalidixic acid resistant strain of Salmonella typhimurium LT2 strain was used as the host bacterium for the clear plaque mutant P22H5 phage.

The samples were examined in screening tests applying the Most Probable Number method (MPN-method) and the positive results in Hammerbach spring were completed by agar layer method.

The agar layer method consists of mixing the suspension of host bacteria in a stage of active multiplication with the watersample and melted soft agar in the tube at 45° C. Without delay the contents of the tube are plated on the top of petri dish and the dishes are incubated at 37° C between four and 18 hours. If the sample contains infective phages, clear circles or plaques appear on the medium clouded by the bacterial growth. Each plaque is considered to be formed by one phage. The number of phages in water samples is expressed as the number of plaque forming units (abbrev. p.f.u.) in 1 ml of water sample.

The MPN-method for the determination of phages in water samples was developed from the MPN-method for the evaluation of the coliform bacteria in water samples (Y. KOTT et al., 1986)

The limit of detection of phage particles by agar layer methods was 0.2 p.f.u./ml of sample and 6 p.f.u. in 100 ml sample for the MPN-method.

The phage tracer reappeared in Hammerbach spring (HB) and Schmelzbach (S). The zero samples and all the collected samples before the first positive sample were

negative, so we could conclude that there was no background of salmonella phage in the Lurbach system. The first positive sample in Hammerbach spring was obtained after 31 h and maximum velocity was calculated as 2,430 m/d. The maximum concentration of phage tracer, 2,440 p.f.u. appearred after 41.5 h. The centre of gravity of the tracer curve expressed as t_g was evaluated as 53.4 h and v_{med} was calculated as 1,411 m/d. The calculated recovery rate of the phage tracer was 2.5%. The position of the peak of all tracers curves was very similar but the recovery rates were very different. Particularly the values for particle tracers such as microspheres and phages were very low (Fig. 5.10).

The particle tracers were the only tracers recovered from Schmelzbach (S). The recovery of microspheres was 0.07% and that of the phages was not calculated, because phages were found in numbers that could be assessed only semiquantitatively by the MPN-method (Tab. 5.12). But nevertheless the reappearance of particle tracers in the underground system of the Schmelzbach (S) indicates that these tracers have been adsorbed to underground water bed surfaces in Lurbach system and pushed by high waters to Schmelzbach system after the storm that followed the injection. We believe that the main reason for such low recovery of particle tracers originates from their ability to adsorb continuously to charged surfaces. Therefore a part of the tracer gets lost resulting in low recovery values.

5.1.7. Summary and Characteristic Data (R. BENISCHKE)

The reference tracer

The breakthrough curves (Fig. 5.2–5.10) of the tracers can be found in the chapters above. All of them are compared with bromide as a reference tracer. Bromide is taken as a very stable, conservative tracer with low natural background concentrations and high analytical sensitivity. Its mobility can be compared with that of chloride but the latter has the disadvantage of a relatively high natural background concentration.

Background and matrix effects

The natural background of fluorescent tracers, microspheres and phages was zero, that for anorganic salts measured before the first arrival of each of them was low for lithium and bromide and slightly higher for chloride. For the evaluation the greatest problem is to define for anorganic salts a background level which is valid during the observation period because it is not possible to measure the fluctuations of the natural background during the experiment. When varying background concentrations it is possible to calculate any recovery rate, which means that the background level has to be established carefully. Difficulties may arise if the natural background e.g. for chloride will be diluted during a flood event which interferes the tracer transit. So it may happen that the natural background before the experiment is higher than at the end of the experiment, which leads to the question whether a linear or non-linear interpolation or an average value for the background is allowed or not.

Another more artificially produced background is that of sample bottles or resulting from inproper establishment of calibration standards. Glass bottles release from their inner walls very often anorganic ions particularly alkali elements that contribute to the background. A check before using such bottles will overcome this source of error. On the other hand plastic bottles are often very adsorptive to cations depending on the material. So a good compromise should be found taking into

account what ions are to be measured when purchasing sample bottles. It is recommended for calibration standards particularly when analyzing contaminated waters to match the sample matrix as far it is possible and practicable.

Physico-chemical behaviour and analytical methods

The analytical methods applied are given in chap. 5.1.1.6. and for all used tracers in chap. 5.1.2.1.–5.1.2.6.

For the fluorescent tracers and anorganic salts a number of very similar analytical methods is available. The most sensitive are fluorimetric and radiochemical followed by normal photometric or flame photometric methods and wet chemistry. The results documented show that in the future it is very necessary to develop standardized methods which are tested in interlaboratory comparisons. From the fluorescent tracers the best agreement of the results were achieved with uranine also in comparison with bromide, slightly less with eosin. These two dyestuffs are predominantly anionic tracers under natural pH-conditions, i.e. that a part of them may react as cations which are sorptive to clay minerals occurring in cave sediments. Whereas sulphorhodamine G and rhodamine B are very sensitive fluorescent tracers with low detection limits they suffer on adsorption because of their cationic structure. This can be seen in fig. 5.6 and 5.7 comparing them with bromide. Naphthionate as a UV-sensitive tracer showed good results but with reduced sensitivity (excitation and emission wavelengths are influenced by a natural high UV-background of the water and by effects originating from Raman-scatter of water molecules). But it is possible to overcome these disadvantages applying a greater amount of tracer. The worst results of the fluorescent tracers brought pyranine. The reason is not an analytical one. It seems that it was highly affected by biological degradation. Hammerbach spring water has coli and coliforme bacteria up to excessive amounts originating from untreated waste-water from the basin of Semriach.

The lithium tracer showed a smaller response comparing it with the bromide reference. Differences in the results of the different laboratories are explained in chap. 5.1.3.1.

Indium and chloride correlate well with bromide, but chloride seems to have to high concentrations due to background effects (which influence the evaluation), whereas the indium concentrations are lower due to possible sorption on sediments despite it was injected as EDTA-complex.

The analytics of the particle tracers is based on microscopic counting techniques or biological methods. The microspheres applied for the first time in this area showed a very fluctuating response in the spring with differences from one sampling time to the next of up to more than 100%. As it was pointed out in the related chap. 5.1.5. only the polystyrene spheres could be detected probably due their low affinity to charged surfaces of clayey sediment particles. There was no extended experience on the necessary amount to inject, on improved sampling and evaluation techniques but nevertheless the results proved the applicability of such a tracer. The same can be said about the phages whose breakthrough graph of the normalized values is lower than that of the microspheres but had a smoother shape.

Time of analysis and storage conditions of samples

It is obvious for the fluorescent tracers that with respect to the contaminated waters the time lag between sampling and analysis and therefore the storage conditions (s. chap. 5.1.2.1.) have been very decisive for the results. As it was reported for GSF-samples about naphthionate and pyranine a strong decay took place, because samples

Tab. 5.12: Recovery rates of injected tracers obtained during the tracing experiment 1988 at Hammerbach spring (HB). The first value of each line represents the recovery rate (%) at the end of the observation period of each laboratory, the second for a comparable observation period (for anorganic and particles it is 880704/00.00) valid for each tracer. The calculated recovery rates are rounded values. For abbrev. of laboratories refer to tab. 5.5.

Tracer	AGK	GEOFRB	GSF	IGH	HMZ	KÄSS	BIO
Lithium	– –	– –	– –	– –	– –	68.6 (880715) 60.6 (880704)	– –
Bromide	– –	– –	56.4 (880704) 56.4 (880704)	– –	– –	– –	– –
Chloride	– –	– –	– –	74.7 (880708) 72.5 (880704)	– –	– –	– –
Indium	– –	– –	56.3 (880706) 54.1 (880704)	– –	– –	– –	– –
Phages	– –	– –	– –	– –	– –	– –	2.6 (880715) 2.5 (880704)
Microspheres	– –	– –	– –	– –	– –	7.9 (880701) 7.9 (880704)	– –
Naphthionate	– –	46.1 (880715) 39.4 (880701)	13.4 (880701) 13.4 (880701)	– –	– –	– –	– –
Pyranine	7.5 (880715) 7.1 (880701)	– –	1.7 (880701) 1.7 (880701)	7.9 (880715) 7.2 (880715)	12.2 (880714) 11.2 (880714)	– –	– –
Uranine	59.6 (880715) 47.3 (880701)	– –	41.2 (880701) 41.2 (880701)	56.2 (880715) 45.4 (880701)	57.8 (880715) 46.3 (880701)	– –	– –
Eosin	– –	– –	45.7 (880701) 45.7 (880701)	58.5 (880715) 42.5 (880701)	58.2 (880715) 46.2 (880701)	– –	– –
Sulphorhod. G	60.2 (880715) 42.5 (880701)	– –	42.0 (880701) 42.0 (880701)	40.9 (880715) 28.2 (880701)	23.9 (880701) 23.9 (880701)	– –	– –
Rhodam. B	4.6 (880702) 0.4 (880701)	– –	25.9 (880701) 25.9 (880701)	33.0 (880715) 20.1 (880701)	35.8 (880709) 27.5 (880701)	– –	– –

Tab. 5.13: Flow times and flow velocities are based on the time of 1st appearance (t_{max}), time of concentration peak (t_{Peak}) as well as time of centroid ($t_{Centr.}$) since the time of injection and on the distance between injection point and Hammerbach spring (HB). The calculated flow times and flow velocities are rounded values. v(t) means that the first value for each tracer is always velocity the second in brackets the flow time. GSF-values for lithium are from GSF-Institute f. Ecological Chemistry. Rhodamine B values of AGK differ significantly due to the small data set available and the difficulties in selective analytical separation from sulphorhodamine G. For abbrev. of laboratories refer to tab. 5.5. *Continuation p. 99.*

Tracer	v(t)	AGK	GEOFRB	GSF	IGH	HMZ	KÄSS	BIO
Lithium	Max.	–	–	92.4 (33.3)	–	–	101.5 (30.3)	–
	Peak	–	–	78.3 (39.3)	–	–	75.4 (40.8)	–
	Centr.	–	–	66.8 (46.1)	–	–	36.8 (83.7)	–
Bromide	Max.	–	–	100.7 (30.6)	–	–	–	–
	Peak	–	–	77.8 (39.6)	–	–	–	–
	Centr.	–	–	58.3 (52.9)	–	–	–	–
Chloride	Max.	–	–	–	101.5 (30.3)	–	–	–
	Peak	–	–	–	78.3 (39.3)	–	–	–
	Centr.	–	–	–	53.0 (58.1)	–	–	–
Indium	Max.	–	–	102.2 (30.1)	–	–	–	–
	Peak	–	–	75.8 (40.6)	–	–	–	–
	Centr.	–	–	51.8 (59.5)	–	–	–	–
Phages	Max.	–	–	–	–	–	–	99.2 (31.0)
	Peak	–	–	–	–	–	–	74.2 (41.5)
	Centr.	–	–	–	–	–	–	54.5 (56.5)

Micro-spheres	Max.	–	–	–	–	–	82.7 (37.3)	–
	Peak	–	–	–	–	–	71.2 (43.3)	–
	Centr.	–	–	–	–	–	60.0 (51.4)	–
Naph-thionate	Max.	–	94.1 (32.8)	89.9 (34.3)	–	–	–	–
	Peak	–	76.5 (40.3)	79.5 (38.8)	–	–	–	–
	Centr.	–	46.0 (66.9)	71.2 (43.2)	–	–	–	–
Pyranine	Max.	89.3 (34.5)	–	93.3 (33.0)	93.3 (33.0)	93.3 (33.0)	–	–
	Peak	79.0 (39.0)	–	79.0 (39.0)	73.3 (42.0)	76.1 (40.5)	–	–
	Centr.	61.5 (50.1)	–	67.5 (45.6)	51.3 (60.1)	55.7 (55.3)	–	–
Uranine	Max.	94.3 (32.7)	–	98.8 (31.2)	98.8 (31.2)	98.8 (31.2)	–	–
	Peak	79.7 (38.7)	–	79.7 (38.7)	76.7 (40.2)	79.7 (38.7)	–	–
	Centr.	40.4 (76.3)	–	68.1 (45.2)	43.8 (70.3)	40.7 (75.6)	–	–
Eosin	Max.	–	–	98.0 (31.4)	98.0 (31.4)	98.0 (31.4)	–	–
	Peak	–	–	79.1 (38.9)	76.2 (40.4)	79.1 (38.9)	–	–
	Centr.	–	–	66.8 (46.1)	33.6 (91.8)	46.1 (76.8)	–	–
Sulpho-rhod. G	Max.	93.1 (33.1)	–	97.5 (31.6)	97.5 (31.6)	89.1 (34.6)	–	–
	Peak	78.8 (39.1)	–	75.9 (40.6)	78.8 (39.1)	85.4 (36.1)	–	–
	Centr.	34.6 (89.1)	–	66.2 (46.5)	32.2 (95.8)	69.4 (44.4)	–	–
Rhodam.B	Max.	42.2 (72.9)	–	95.0 (32.4)	95.0 (32.4)	95.0 (32.4)	–	–
	Peak	41.4 (74.4)	–	74.3 (41.4)	77.1 (39.9)	77.2 (39.9)	–	–
	Centr.	37.1 (83.1)	–	62.5 (49.3)	31.6 (97.5)	43.9 (70.2)	–	–

were analyzed some months later. All samples were stored in the dark under room temperature which means that the storage conditions promoted bacterial growth and therefore tracer degradation. For the future it means that analysis of fluorescent tracers a long time after sampling is senseless.

Recovery rates of the experiment 1988

The calculated recovery rates as percentage of the absolute amount of tracer injected can only be compared on the basis of defined observation periods, and if there was a considerable natural background on the proper value defined before. In tab. 5.12 two recovery rates are given, one for the total observation period for each tracer and one value for a observation period which was the same for all tracers.

It is clear that all the calculations are influenced not only by analytical errors but also by errors in the discharge measurements. The final statistical error of the recovery rate was not determined quantitatively but is estimated to be fairly high with respect to the reported non-standardized evaluation methods and the actual time of analysis and all other influences actually happened until and during analysis.

Flow times and flow velocities

The flow times and the flow velocities have to be seen under the same aspects reported before and represent therefore only calculated values. As the determination of the time of first arrival of a tracer depends essentially on the sensitivity of the analytical method the peak of concentration or load is more representative. Centroid values of the breakthrough curves (for concentration or load) would characterize the tracer transport much better but unfortunately it is not always possible to extend the observation period to get reliable results. Thus centroid values given in tab. 5.13 depend on the observation period and have more informal character. Particle tracers show in many cases a slightly higher flow velocity calculated from the first appearance than dissolved tracers which can be explained that particles are transported mainly in the mid-current of a stream and can only be "diluted" to their individual size. During the experiment 1988 the time differences between particle tracers and dissolved tracers were not significant.

5.2. Results of all Tracing Experiments from 1927–1991

(R. BENISCHKE, T. HARUM)

5.2.1. Historical Notes

This chapter gives information on all experiments carried out under scientifically controlled conditions. It will start with some historic notes on attempts in the last century to investigate the course of the Lurbach disappearing into underground at Semriach and is more or less also a documentation for important stages of development in tracer hydrology.

The probably oldest information about the Lurbach sinkhole and a mutual connection to Schmelzbach at the W-end of the Tanneben massif as a curiosity of nature was given by Joseph Carl KINDERMANN (1779):

> "Semriach, ein Markt von 60 Häusern. Bei dem Markte verliert sich ein Bach in einem Berge und kömmt, nachdem er gegen 2000 Klafter unter demselben fortgeflossen, endlich unweit Peckau wieder zum Vorschein"
> (Semriach a village with 60 houses. There a stream got lost in a mountain and reappears lastly near Peggau after flowing about 2,000 spans beneath it).

This description was obviously the idea of the local people, who "knew" with a horse-sense, that the Lurbach recharges the Hammerbach or the Schmelzbach in Peggau.

Also in the last century there starts the detailed geological exploration of the study area. A geological cross-section from W to E through the Tanneben massif with respect to the Lurbach system and the idea of a connection between Lurbach at Semriach and outlets in Peggau was given by G. WURMBRAND (1871). Considerations about this connection and a thorough observation of flood events in the basin of Semriach and their effect on inundations in Peggau lead to results, which are close to present day ideas of the hydrogeological characteristics of the Lurbach system. These ideas at first expressed in the last century in a local newspaper by F. THINNFELD (1873) – a countess interested in natural history – are still fundamental for ideas about the dynamic connection between Hammerbach spring and Schmelzbach. Therefore they are given here in an original full-text citation:

„Am Fuße des Felsens – im Orte Peggau selbst – entströmt dem Berge ein rascher klarer Bach, welcher nach kurzem Laufe, während dessen er zwei Mühlen und eine Drahtstiftenfabrik in Gang bringt, unterhalb Peggau in die Mur fällt.

Ein zweiter, weit schwächerer Bach fließt etwa zehn Minuten Weges nördlich von Peggau ebenfalls aus der Tanneben, und das Felsenportal, aus dem er zu Tage tritt, sieht imposanter aus, als der Ausfluß des Peggauer Baches.... Das mindestens der Peggauer Bach identisch mit dem bei Semriach in die Tanneben einfließenden Bache sei, darüber dürfte wohl kein Zweifel obwalten; ein anderes ist es mit dem nördlicheren dem sogenannten Schmelzbach. Während, nach jedem Regengusse der Peggauer Bach sich trübt und etwas anschwillt, hat ein solcher auf den Schmölzbach keinen Einfluß und derselbe bleibt beinahe immer klar. Das Wasser des Peggauer Baches trübt sich jedoch erst 16–17 Stunden nach Beginn des Regens im Semriacher Thale und bleibt manchmal einen Tag, bei anhaltenderem oder stärkerem Regen aber auch zwei oder drei Tage trüb.

Doch wächst der Bach nie stark an, während der Schmölzbach, so klein er gewöhnlich ist und bleibt, bei s e h r heftigen Gewittergüssen starke Ueberschwemmungen verursacht. So zerstörte er am 30. August 1865 nach einem furchtbaren Gewitter und Wolkenbruch, der auch die Bezirksstraße durch den Badelgraben gänzlich verwüstete, die damals neugebaute Sägemühle und war noch am nächsten Tage ein tosender Wildbach, während der Peggauer Bach zwar sehr trübe und größer als gewöhnlich war, doch nirgends seine Ufer überfluthete. Nur im Jahre 1827, zur Zeit der größten Ueberschwemmung, die es im ganzen Lande seit Menschengedenken gab, soll auch der Peggauer Bach nach vierzehntägigem Regen übergegangen und in manche tiefliegende Häuser geflossen sein. .... Das ist aber auch das einzigemal, daß man von einem Uebergehen des Peggauerbaches weiß, während beim Schmelzbache nach jedem stärkeren, länger heftig andauernden Regengusse verderbenbringende Ueberschwemmungen zu befürchten sind. Diese sonderbaren Erscheinungen, welche sich zu widersprechen scheinen, dürften wohl nur damit zu erklären sein, daß man annehmen muß, der Lauf des Baches durch den Berg sei eine geraume Strecke so verengt, daß nicht mehr als eine bestimmte Wassermasse durchfließen kann, während bei großer Wasseranstauung ein anderes höheres Rinnsal, das in Verbindung mit dem Schmölzbache ist, erreicht wird, durch welches dann die größere Wassermasse schnell abläuft."

(At the foot of the rock – in the village of Peggau – a rapid flowing stream emerges from the mountain [Ann.: i.e. the Peggauer Wand] which falls after a short course at the lower end of Peggau into the Mur set going two mills and a stud factory.

A second much smaller stream emerges from the Tanneben too in a distance of about 10 minutes north of Peggau, but the outlet in the rocks, from which it emerges, looks more impressive than the outlet of the Peggauer Bach [Ann. i.e. Hammerbach spring].... That the Peggauer Bach is identical at least with the stream flowing near Semriach into the Tanneben would be beyond all doubts. Differently it is the case with the northern stream the so-called Schmelzbach. Since the Peggauer Bach becomes turbid and rises a little after every rainfall there is no influence on the Schmelzbach which remains clear almost anytime. The water of the Peggauer Bach, however, becomes turbid 16–17 hours after the beginning of the rain in the basin of Semriach and remains turbid sometimes a period of one day, during persistent or stronger rainfall also two or three days.

But never the stream rises very strongly, since the Schmelzbach – as it is usually very small – causes during very intense thunderstorms strong inundations. So it destroyed on 30th August 1865 after terrible thunderstorms, that devastated totally also the road through the Badlgraben, the saw-mill newly built at that time, and was also during the next day a roaring mountain torrent, whereat the Peggauer Bach was very turbid and larger than normal but did not inundate anywhere its banks. Only in the year 1827 during the time of the biggest inundation which happened in the country within the memory of man, it is said that the Peggauer Bach flowed over after a fortnight lasting rain and having flooded several deeper situated houses .... But this was the only time, that an overflow of the Peggauer Bach was reported, whereas for the Schmelzbach after any stronger or longer heavy rainfall destructive inundations are suspected. These peculiar events, which seem to contradict each other, could be explained only under the assumption, that the course of the stream through the mountain is narrowed along a considerable distance, that not more than a distinct amount of water can flow through, while for a greater damming up of the water, an other higher situated watercourse is reached, which is connected with the Schmelzbach and through which a greater amount of water can be drained.)

These precise observations – at that time without any possibility to access the subterranean parts of the Tanneben karst – could be confirmed quantitatively (T. HARUM et al., 1990) based on thorough evaluations of hydrological data about Hammerbach and Schmelzbach (comp. chap. 2.3.3.).

About 170 years after J.C. KINDERMANN the connection between the Lurbach in Semriach and the Hammerbach spring in Peggau could be proved by a scientifically planned, performed and well documented tracing experiment (V. MAURIN, 1952).

The idea to trace the course of the Lurbach by an appropriate substance is reported in a topographic description of the last century (STEIR. GEBIRGSVEREIN, 1882):

„Das Lugloch liegt 650 m hoch. Aus demselben ergiesst sich der sogenannte Hammer- oder Schmelzbach, identisch mit dem Semriacher Bach, welcher auf der anderen Seite im Boden verschwindet. Man hat, um die Identität festzustellen, Sägespäne in den Semriacher Bach geworfen, welche im Hammerbach wieder zum Vorschein kamen".

(The Lugloch is in an altitude of 650 m. It discharges as Hammer- or Schmelzbach and is identical with the Semriacher Bach, which disappears at the other side into underground. To determine the identity sawdust had been thrown into the Semriacher Bach which reappeared in the Hammerbach).

The interest in the hydrologic and karsthydrogeologic phenomena concerning the Lurbach originated from excessive rainfall events, which caused a flooding of the Semriach basin. It is reported in the chronicle of the church in Semriach that the most outstanding flood was at the end of the 18th century, where the water was dammed up to an altitude of approx. 700 m a. s. l., which means that the water reached close to the church. This damming-up occurred each time the Lurbach sinkhole had been blocked by spilled-in trees, bushes, blocks and other material.

Another evidence of a connection between Lurbach and Hammerbach brought an event on March 24th, 1900, when so-called "Lederer Lohe" (tan liquor) from a tannery at the Lurbach near Semriach could be found (A. MAYER sen., 1900).

In 1927 the first scientifically planned experiment was carried out (G. KYRLE, 1928), but a scientific planning and accurate preparation is not necessarily successful, if the available or applied methods for the investigation are not adequate. The experiment was planned to prove a connection between Lurbach and Schmelzbach resp. Hammerbach for low water conditions. The experiment carried out with salt (injection of 250 kg salt on 270218/21.00 and on 270219, fuchsine and particles) failed because of wrong assumptions, inproper analytical methods and a too short observation time. The conclusion was that no connection exists between the points under investigation.

The first proof of a connection between Lurbach and Hammerbach succeeded 1952 (V. MAURIN, 1952), when a larger amount of salt (800 kg) had been injected and the observation time (82 h) was long enough.

Repeated experiments in 1959 and 1966 showed that some other sinkholes (Eisgrube [E] and Katzenbachschwinde [K] north of the Eichberg; s. fig. 2.1) have connections with the Schmelzbach (V. MAURIN & J. ZÖTL, 1959, H. BATSCHE et al., 1967). The years 1959 and 1966 had been the beginning of an intense investigation of tracer properties. A lot of different substances had been examined to be appropriate for experiments.

1959 blue Lycopodium spores had been injected into the Eisgrube in the NW of Neudorf, uncoloured Lycopodium spores, blue coloured sawdust, Diatomea and plastic spheres (Vestyron N) into the Lurbach sinkhole and red coloured sawdust inside the Lurgrotte at the 3rd siphon. This experiment proved again the connection between Lurbach and Hammerbach. The detection of two blue spores in the 3rd siphon was taken as evidence for a connection with the Eisgrube. The examination of the Schmelzbach spring remained negative.

1966 was an experiment to check a number of tracers for their applicability (H. BATSCHE et al., 1967). Iodine-131, tritium, manganese, brown-coloured Lycopodium spores and uranine had been injected into Lurbach sinkhole, blue coloured Lycopodium spores into the Eisgrube, ammonium bromide and green coloured Lycopodium spores into the Katzenbach sinkhole. It was described that a connection between Katzenbach sinkhole and Schmelzbach spring, Cascade stream and the Laurins spring exists. A connection between Lurbach and Schmelzbach was not proved clearly and was possibly a contamination. The same can be concluded for the detection of green spores in the Laurins spring, because all experiments later under very different hydrologic conditions never showed any evidence for a connection with Lurbach. This can also be derived from the results obtained from environmental isotopes and hydrochemistry (s. chap. 3. and 4.).

1970 two experiments have been carried out to investigate the behaviour of indium (injected as EDTA-complex) for neutron activation analysis (J. ZÖTL, 1971). The experiments succeeded in so far that the connection between Lurbach and Hammerbach could be proved again and that indium was recognized as a suitable tracer (see also the experiment 1988). In the same year two experiments with uranine and sulphorhodamine G and B have been carried out to check the possibility to apply two different fluorescent tracers at the same time and to separate them from each other. At that time only filter fluorimeter were available (F. BAUER, 1972).

From 1971–1983 experiments in a two years interval had been carried out during Postgraduate Training Courses on Groundwater Tracing Techniques (J. ZÖTL, 1971–1979, H. ZOJER, 1981–1983) with a more or less constant amount of tracer substances. The experiments had not been carried out to prove new connections or to test tracers. As sampling points only Hammerbach and Schmelzbach had been taken. Because the experiments had been carried out always in autumn (with exception of an additional experiment in summer 1975) in most cases under medium to low water conditions only a detection in the Hammerbach spring was possible (s. tab. 5.14 and 5.15).

1985 was again a combined experiment which was prepared to verify connections between sinkholes in the Neudorf area, to get information on transit times and connections between the surface of the karst massif of Tanneben, and to investigate more thoroughly the Schmelzbach spring (SU) and Laurins spring (L) inside the

cave. The experiment was successful, because it showed that all tracers injected at the surface could be detected in the Hammerbach as well as in the Schmelzbach and Laurins spring but with small recovery rates (2–3%) compared to the rates of tracers injected in the Lurbach sinkhole. The low recovery rates resulted from the injection on the top of the unsaturated zone.

Tracers injected into the Lurbach ponor (amidorhodamine B 200 and potassium chloride) first arrived 28–32 h after the injection and had their peak about 42 h after injection with a recovery rate of about 50–70%. The tracer injected into the Eisgrube (sodium chloride) arrived about 55 h after injection in the Schmelzbach (S), with a peak approx. 120 h after injection and a recovery rate of 9% for sodium and 34% for chloride. Eosin injected on the surface at Ertlhube arrived 67 h and had its peak 157 h after the injection. Uranine injected into the Schneiderkogelhöhle (A.C.R. No. 2836/61) reappeared 183 h and had its peak (only an irregular and very isolated one) about 332 h after the injection. This shows that there was and still is a considerable retardation of the tracers in the unsaturated zone which covers an altitudinal interval of about 350–400 m. Furthermore the experiment verified the connection between the Eisgrube (A.C.R. No. 2836/64) and the Schmelzbach spring but gave no evidence for a connection with the Laurins spring (comp. with the experiment of 1966). Tracers injected in the Lurbach sinkhole reappeared as expected in the Hammerbach. Also samples from some groundwater wells along the margin of the limestone massif in Peggau had been analyzed but did not give any evidence of a tracer (R. BENISCHKE et al., 1988, H. ZOJER, 1985).

The subsequent sampling over a period of about 1.5 years showed that the tracer uranine could be detected until spring 1987 (but at that time only by enrichment on activated carbon and not directly in water samples). These results indicated long mean residence times of waters and are in good correspondence with the results of hydrological, hydrochemical, isotopic analyses and mathematical modelling (ref. to chap. 3. and 6.).

1987 was another experiment during a training course which simply brought the same results obtained during earlier experiments (R. BENISCHKE et al., 1987). The 1988 experiment is described in chap. 5.1. Also the groundwater wells as mentioned above had been observed, but again no tracer could be detected.

1989 high water conditions brought new insights into the karst system and it was the first time that calculated recovery rates gave approximately 100% (within the range of analytical and hydrologic measurement errors). The tracer transit curves clearly showed a superposition of different hydraulic systems derived from the time shift in the composite transit curves (R. BENISCHKE & T. HARUM, 1990). This phenomenon will be discussed in more detail in chap. 6.1. on tracer models.

The last experiment was carried out in 1991 at the last Postgraduate Training Course during low water conditions (R. BENISCHKE & P. HACKER, 1991). The only response on the injected tracers was at Hammerbach as expected.

In the following subsections the results of all experiments are summarized.

5.2.2. Types of Tracers Injected

From the different types of tracers listed below only a few were applied during almost all tracing experiments and only a few gave representative results, let compare the experiments with each other and lead to interpretable hydrogeological results. Most of the tracers are used only to test the substance for its suitability.

Anorganic salts

Sodium chloride (as cooking salt or for animals)
Potassium chloride (as fertilizer)
Lithium chloride (techn. quality)
Ammonium bromide
Potassium bromide
Sodium bromide

Fluorescent dyes

Uranine AP (MERCK), Uranine Sicomet (SIMON & WERNER), Uranine conc (SIMPSON)
Sulphorhodamine B
Sulphorhodamine G (HOECHST, ORGANIC DYESTUFFS CORP.)
Amidorhodamine B 200 (HOECHST)
Eosin Y (MERCK), BASACID-Rot 316 (BASF)
Pyranine 108% (BAYER)
Sodium-Naphthionate (FLUKA)
Tinopal CBS-X (CIBA-GIGY)
Hostalux PN (CIBA-GEIGY)

Particles

Uncoloured, blue, red, brown, green, yellow, orange spores
Cork
Wood
Sawdust blue and red
Plastic spheres (Vestyron N)
Diatomea
Polystyrene microspheres (0.89 µ, 0.95 µ, 1 µ)
Salmonella phages

Radioactive and other tracers

Tritium
Iodine-131
Indium-114m-EDTA
Mn-EDTA

We selected for the calculation of flow transit times and velocities of the older experiments only the tracers uranine and chloride because they were applied in almost all cases.

5.2.3. Transit Times and Flow Velocities

The flow velocities derived from the numerous tracing experiments show the relation between discharge rates and transit times of tracers.

Tables 5.14 and 5.15 summarize the data from all evaluable experiments carried out since 1927. Because of the nature of the used tracer substances and the different observation periods it can give only an approximation of real flow velocities and transit times. The table gives only data for the main sampling sites Hammerbach spring (HB) and Schmelzbach (S) and for the applied quasi-ideal tracers uranine and chloride. Other tracers as mentioned in the previous section are not compared because of lack of evaluable data. There are only few data for high water conditions because most of the experiments were carried out in autumn during low to medium runoff conditions.

The normalized breakthrough curves of the tracer experiments summarized in tab. 5.14 and 5.15 are plotted for the example of the fluorescent dye uranine in fig. 5.11 for the Hammerbach spring. It is clearly visible that the numerous tracing

Tab. 5.14: Summary of all evaluable tracing experiments since 1927 for uranine. Results for Hammerbach spring and Schmelzbach. Injection places E = main ponor at entrance of Lurgrotte in Semriach, SF = ponor at sediment barrage upstream of E, I = ponor in the cave Lurgrotte about 100 m downstream of E. n = not evaluated because lack of data, n.m. = not measured, n.d. = measured but not detected. Continuation p. 108-109.

SAMPLING PLACE	HAMMERBACH SPRING											
Tracer:	URANINE	URANINE	URANINE	URANINE	URANINE	URANINE	URANINE	URANINE	URANINE	URANINE	URANINE	URANINE
Amount (kg):	5.000	3.000	3.000	0.500	3.000	3.000	3.000	3.000	3.000	2.000	2.000	3.000	1.000
Injection Place:	E	E	E	E	E	E	E	E	SF	SF	I	E	SF
Distance (m):	3,080	3,080	3,080	3,080	3,080	3,080	3,080	3,080	3,340	3,340	3,080	3,080	3,340
Injection Date/Time:	660326/11.25	710912/13.50	730908/15.00	750626/19.07	750906/13.15	770910/13.30	790908/14.00	810905/14.45	830910/13.25	870829/16.20	880628/10.50	890902/14.17	910907/14.38
Integration Start:	660326/11.25	710912/13.50	730908/15.00	750626/19.07	750906/13.15	770910/13.30	790908/14.00	810905/14.45	830910/13.25	870829/16.20	880629/16.30	890902/14.17	910907/14.38
Integration Period (h):	108.58	80.17	119.00	172.88	104.75	114.50	114.00	116.50	118.75	303.67	382.50	186.72	172.37
Q-Range (l/s):	128–142	120–146	88–95	343–939	385–428	63–116	136–146	179–201	113–119	208–288	168–263	338–543	163–185
Recovery Rate (%)	65.0	24.6	15.6	n.e.	60.2	9.6	43.2	34.6	72.1	81.9	57.8	76.2	70.4
First Appearance:	660328/00.00	710913/18.00	730910/22.00	750627/13.00	750907/04.00	770912/18.10	790910/00.30	810906/18.15	830912/12.40	870830/20.00	880629/19.30	890903/06.00	910908/18.20
h after Injection:	36.50	28.17	55.00	17.29	14.75	52.67	34.50	27.50	47.25	27.67	32.67	15.72	27.70
CONCENTRATION PEAK													
Conc. (mg/m³):	470.000	83.400	43.860	7.100	68.900	32.000	141.000	64.600	188.010	99.406	83.940	107.088	38.563
h after Injection:	47.00	38.17	75.00	30.02	18.75	74.50	46.25	37.25	68.58	35.67	38.67	19.97	46.37
Date/Time:	660328/10.30	710914/04.00	730911/18.00	750628/02.00	750907/08.00	770913/16.00	790910/12.15	810907/04.00	830913/10.00	870831/04.00	880630/01.30	890903/10.15	910909/13.00
CONCENTRATION CENTRE OF GRAVITY													
Conc. (mg/m³):	n.e.	23.061	14.351	n.e.	18.237	10.180	36.561	18.390	60.634	23.620	16.225	25.310	9.108
h after Injection:	n.e.	48.94	86.17	n.e.	34.64	82.64	58.51	51.29	75.72	58.79	77.20	38.26	73.16
Date/Time:	n.e.	710914/14.46	730912/05.10	n.e.	750907/23.54	770914/00.09	790911/00.31	810907/18.02	830913/17.08	870901/03.07	880701/16.02	890904/04.33	910910/15.48
LOAD MAXIMUM													
C*Q (mg/s):	n.e.	10.508	4.167	n.e.	26.527	3.016	19.176	11.939	21.809	21.472	22.068	39.624	7.146
h after Injection:	n.e.	38.17	75.00	n.e.	18.75	80.50	46.25	39.50	68.58	35.67	38.67	19.97	46.37
Date/Time:	n.e.	710914/04.00	730911/18.00	n.e.	750907/08.00	770913/22.00	790910/12.15	810907/06.15	830913/10.00	870831/04.00	880630/01.30	890903/10.15	910909/13.00
LOAD CENTRE OF GRAVITY													
C*Q (mg/s):	n.e.	2.895	1.362	n.e.	6.921	0.899	4.943	3.432	7.032	5.053	4.569	9.378	1.686
h after Injection:	n.e.	48.79	86.21	n.e.	35.38	84.61	58.86	51.77	75.63	59.63	70.80	37.80	71.33
Date/Time:	n.e.	710914/14.37	730912/05.13	n.e.	750908/00.38	770914/02.07	790911/00.52	810907/18.31	830913/17.03	870901/03.58	880701/09.38	890904/04.05	910910/13.58
FLOW VELOCITIES (m/h)													
First Appearance:	84.38	109.34	56.00	178.14	208.81	58.48	89.28	112.00	70.69	120.71	94.28	195.93	120.58
Conc. Peak:	65.53	80.69	41.07	102.60	164.27	41.34	66.59	82.68	48.70	93.64	79.65	154.23	72.03
Conc. Centre of Gravity:	n.e.	62.93	35.75	n.e.	88.91	37.27	52.64	60.05	44.11	56.81	39.90	80.50	45.65
Load Maximum:	n.e.	80.69	41.07	n.e.	164.27	38.26	66.59	77.97	48.70	93.64	79.65	154.23	72.03
Load Centre of Gravity:	n.e.	63.13	35.73	n.e.	87.05	36.40	52.33	59.49	44.16	56.01	43.50	81.48	46.83
TIME RATIOS													
$T_{Conc\text{-}Peak}/T_1$:	1.28	1.35	1.37	1.72	1.27	1.41	1.33	1.35	1.45	1.28	1.18	1.27	1.67
$T_{Load\text{-}Peak}/T_{Conc\text{-}Peak}$:	n.e.	1.00	1.00	n.e.	1.00	1.08	1.00	1.06	1.00	1.00	1.00	1.00	1.00

SAMPLING PLACE	SCHMELZBACH							
Tracer:	URANINE	URANINE	URANINE	URANINE	URANINE	URANINE	URANINE	URANINE	URANINE
Amount (kg):	5.000	3.000	3.000	0.500	3.000	3.000	3.000	3.000	2.000	2.000	3.000	1.000
Injection Place:	E	E	E	E	E	E	E	SF	SF	I	E	SF
Distance (m):	3,000	3,000	3,000	3,000	3,000	3,000	3,000	3,325	3,325	3,000	3,000	3,325
Injection Date/Time	660326/11.25	710912/13.50	730908/15.00	750626/19.07	750906/13.15	770910/13.30	790908/14.00	810905/14.45	830910/13.25	870829/16.20	880628/10.50	890902/14.17	910907/14.38
Integration Start:	–	–	–	n.m.	750906/13.15	–	–	810905/14.45	–	–	–	890902/14.17	–
Integration Period (h):	–	–	–	–	104.75	–	–	116.50	–	–	–	186.47	–
Q-Range (l/s):	–	–	–	–	230–5,500	–		109–128	–	–	–	79–537	–
Recovery Rate (%):	0.0	0.0	0.0	–	20.0	0.0	0.0	35.6	0.0	0.0	0.0	27.3	0.0
First Appearance:	n.d.	n.d.	n.d.	n.m.	750907 0800	n.d.	n.d.	810906/16.10	n.d.	n.d.	n.d.	890903/03.00	n.d.
h after Injection:	–	–	–	–	18.75	–	–	25.42	–	–	–	12.72	–
CONCENTRATION PEAK													
Conc. (mg/m³):	n.d.	n.d.	n.d.	n.m.	39.400	n.d.	n.d.	55.200	n.d.	n.d.	n.d.	67.930	n.d.
h after Injection:	–	–	–	–	22.75	–	–	41.25	–	–	–	21.72	–
Date/Time:	–	–	–	–	750907/12.00	–	–	810907/08.00	–	–	–	890903/12.00	–
CONCENTRATION CENTRE OF GRAVITY													
Conc. (mg/m³):	n.d.	n.d.	n.d.	n.m.	9.169	n.d.	n.d.	17.624	n.d.	n.d.	n.d.	14.408	n.d.
h after Injection:	–	–	–	–	36.86	–	–	64.92	–	–	–	43.16	–
Date/Time:	–	–	–	–	750908/02.07	–	–	810908/07.40	–	–	–	890904/09.27	–
LOAD MAXIMUM													
C*Q (mg/s):	n.d.	n.d.	n.d.	n.m.	14.617	n.d.	n.d.	7.066	n.d.	n.d.	n.d.	12.660	n.d.
h after Injection:	–	–	–	–	22.75	–	–	41.25	–	–	–	21.72	–
Date/Time:	–	–	–	–	750907/12.00	–	–	810907/08.00	–	–	–	890903/12.00	–
LOAD CENTRE OF GRAVITY													
C*Q (mg/s):	n.d.	n.d.	n.d.	n.m.	3.708	n.d.	n.d.	2.059	n.d.	n.d.	n.d.	2.874	n.d.
h after Injection:	–	–	–	–	34.48	–	–	63.90	–	–	–	38.07	–
Date/Time:	–	–	–	–	750907/23.44	–	–	810908/06.39	–	–	–	90904/04.21	–
FLOW VELOCITIES (m/h)													
First Appearance:	–	–	–	–	160.00	–	–	118.02	–	–	–	235.85	–
Conc. Peak:	–	–	–	–	131.87	–	–	72.73	–	–	–	138.12	–
Conc. Centre of Gravity:	–	–	–	–	81.39	–	–	46.21	–	–	–	69.51	–
Load Maximum:	–	–	–	–	131.87	–	–	72.73	–	–	–	138.12	–
Load Centre of Gravity:	–	–	–	–	87.01	–	–	46.95	–	–	–	78.80	–
TIME RATIOS													
$T_{Conc.Peak}/T_1$:	–	–	–	–	1.22	–	–	1.61	–	–	–	1.70	–
$T_{Load.Peak}/T_{Conc.Peak}$:	–	–	–	–	1.00	–	–	1.00	–	–	–	1.00	–

SAMPLING PLACES	HAMMERBACH + SCHMELZBACH							
RECOVERY RATES (%)								
Hammerbach Spring:	65.0	24.6	15.6	n.e.	60.2	9.6	43.2	34.6	72.1	81.9	57.8	76.2	70.4
Schmelzbach:	0.0	0.0	0.0	n.m.	20.0	0.0	0.0	0.0	0.0	0.0	0.0	27.3	0.0
Sum Total:	65.0	24.6	15.6	n.e.	80.2	9.6	43.2	35.6	72.1	81.9	57.8	103.5	70.4

Tab. 5.15: Summary of all evaluable tracing experiments since 1927 for chloride. Results for Hammerbach spring and Schmelzbach. Injection places E = main ponor at entrance of Lurgrotte in Semriach, SF = ponor at sediment barrage upstream of E, I = ponor in the cave Lurgrotte about 100 m downstream of E. n.d. = measured but not detected. Continuation p. 112–113.

SAMPLING PLACE	HAMMERBACH SPRING												
Tracer:	CHLORIDE	CHLORIDE	CHLORIDE	CHLORIDE	CHLORIDE	CHLORIDE	CHLORIDE	CHLORIDE	CHLORIDE	CHLORIDE	CHLORIDE	CHLORIDE	CHLORIDE
Amount (kg):	489.990	562.810	562.810	545.600	554.000	541.220	534.200	640.770	301.445	525.091	83.627	300.340	503.195
Injection Place:	E	E	E	E	E	E	E	SF	E	SF	I	E	SF
Distance (m):	3,080	3,080	3,080	3,080	3,080	3,080	3,080	3,340	3,080	3,340	3,080	3,080	3,340
Injection Date/Time:	520510/06.20	710912/13.50	730908/15.00	750906/13.15	770910/13.30	790908/13.40	810905/13.30	830910/13.50	850831/13.45	870829/12.30	880628/10.50	890902/14.00	910907/13.15
Integration Start:	520510/06.20	710912/13.50	730908/15.00	750906/13.15	770910/13.30	790908/13.40	810905/13.30	830912/11.00	850831/13.45	870829/12.30	880629/16.30	890902/14.00	910907/13.15
Integration Period (h):	98.67	54.00	119.00	60.75	114.50	114.33	117.75	73.25	106.25	200.00	379.50	55.00	188.75
Q-Range (l/s):	150–185	120–146	88–95	385–428	63–116	136–146	179–201	113–119	185–189	208–288	168–263	363–370	163–203
Recovery Rate (%):	60.8	36.9	23.6	51.9	14.6	45.5	41.7	64.4	80.9	86.3	74.7	60.1	68.3
First Appearance:	520511/18.00	710913/20.00	730911/04.00	750907/04.00	770912/22.00	790910/02.30	810906/08.05	830912/15.10	850901/20.15	870830/18.30	880629/16.30	890903/01.30	910908/22.00
h after Injection:	35.67	30.17	61.00	14.75	56.50	36.83	18.58	49.33	30.50	30.00	30.33	11.50	32.75
CONCENTRATION PEAK													
Conc. (mg/l):	28.500	22.000	11.100	10.200	7.950	23.500	11.250	35.300	14.200	31.140	4.880	9.560	25.250
h after Injection:	47.17	40.17	79.00	16.75	74.50	46.58	36.75	66.17	42.50	37.78	39.33	20.50	41.75
Date/Time:	520512/05.30	710914/06.00	730911/22.00	750907/06.00	770913/16.00	790910/12.15	810907/02.15	830913/08.00	850902/08.15	870831/02.17	880630/01.30	890903/10.30	910909/07.00
CONCENTRATION CENTRE OF GRAVITY													
Conc. (mg/l):	8.931	6.470	3.880	3.318	2.613	6.083	3.139	11.235	3.627	8.278	1.127	2.664	5.501
h after Injection:	51.52	49.75	89.390	25.72	85.08	60.36	55.48	76.63	59.54	51.54	58.14	27.84	65.44
Date/Time:	520512/09.51	710914/15.35	730912/08.23	750907/14.58	770914/02.35	790911/02.02	810907/20.59	830913/18.28	850903/01.17	870831/16.02	880630/20.18	890903/17.50	910910/06.41
LOAD MAXIMUM													
C*Q (mg/s):	4,639.000	2.772	1.055	3.927	0.748	3.196	2.020	4.095	2.670	6.726	1.283	3.537	4.679
h after Injection:	44.67	40.17	79.00	16.75	80.50	46.58	40.75	66.17	42.50	37.78	39.33	20.50	41.75
Date/Time:	520512/03.00	710914/06.00	730911/22.00	750907/06.00	770913/22.00	790910/12.15	810907/06.15	830913/08.00	850902/08.15	870831/02.17	880630/01.30	890903/10.30	910909/07.00
LOAD CENTRE OF GRAVITY													
C*Q (mg/s):	1,482.000	0.808	0.368	1.272	0.239	0.822	0.586	1.303	0.681	1.779	0.306	0.981	1.031
h after Injection:	51.38	49.62	89.42	25.94	86.86	60.74	56.04	76.53	59.54	52.03	55.27	27.78	64.76
Date/Time:	520512/09.43	710914/15.27	730912/08.25	750907/15.11	770914/04.22	790911/02.24	810907/21.32	830913/18.22	850908/01.17	870831/16.32	880701/17.26	890903/17.47	910910/06.01
FLOW VELOCITIES (m/h)													
First Appearance:	86.35	102.09	50.49	208.81	54.51	83.63	165.77	67.71	100.98	111.33	101.55	267.83	101.98
Conc. Peak:	65.30	76.67	38.99	183.88	41.34	66.12	83.81	50.48	72.47	81.41	78.31	154.24	80.00
Conc. Centre of Gravity:	59.78	61.91	34.46	119.75	36.20	51.03	55.52	43.59	51.73	64.80	52.98	110.63	51.04
Load Maximum:	68.95	76.67	38.99	183.88	38.26	66.12	75.58	50.48	72.47	81.41	78.31	154.24	80.00
Load Centre of Gravity:	59.95	62.07	34.44	118.74	35.46	50.71	54.96	43.64	51.73	64.19	55.73	110.87	51.57
TIME RATIOS													
$T_{Conc\text{-}Peak}/T_t$:	1.32	1.33	1.30	1.14	1.32	1.27	1.98	1.34	1.39	1.26	1.30	1.78	1.28
$T_{Load\text{-}Peak}/T_{Conc\text{-}Peak}$:	0.95	1.00	1.00	1.00	1.08	1.00	1.11	1.00	1.00	1.00	1.00	1.00	1.00

SAMPLING PLACE SCHMELZBACH												
Tracer:	CHLORIDE	CHLORIDE	CHLORIDE	CHLORIDE	CHLORIDE	CHLORIDE	CHLORIDE	CHLORIDE	CHLORIDE	CHLORIDE	CHLORIDE	CHLORIDE
Amount (kg):	489.990	562.810	562.810	545.600	554.000	541.220	534.200	640.770	301.445	525.091	83.627	300.340	503.195
Injection Place:	E	E	E	E	E	E	E	SF	E	SF	I	E	SF
Distance (m):	3,000	3,000	3,000	3,000	3,000	3,000	3,000	3,325	3,000	3,325	3,000	3,000	3,325
Injection Date/Time:	520510/06.20	710912/13.50	730908/15.00	750906/13.15	770910/13.30	790908/14.00	810905/13.30	830910/13.25	850831/14.10	870829/16.20	880628/10.50	890902/14.00	910907/14.38
Integration Start:	–	–	–	750906/13.15	–	–	810905/13.30	–	–	–	–	890902/14.00	–
Integration Period (h):	–	–	–	62.75	–	–	117.75	–	–	–	–	559.00	–
Q-Range (l/s):				371–5,500			109–128					53–226	
Recovery Rate (%):	0.0	0.0	0.0	27.7	0.0	0.0	36.2	0.0	0.0	0.0	0.0	23.3	0.0
First Appearance:	n.d.	n.d.	n.d.	750907/06.00	n.d.	n.d.	810906/18.00	n.d.	n.d.	n.d.	n.d.	890903/03.00	n.d.
h after Injection:	–	–	–	16.75	–	–	28.50	–	–	–	–	13.00	–
CONCENTRATION PEAK													
Conc. (mg/l):	n.d.	n.d.	n.d.	6.000	n.d.	n.d.	8.900	n.d.	n.d.	n.d.	n.d.	6.200	n.d.
h after Injection:	–	–	–	22.75	–	–	42.50	–	–	–	–	22.50	–
Date/Time:	–	–	–	750907/12.00	–	–	810907/08.00	–	–	–	–	890903/12.30	–
CONCENTRATION CENTRE OF GRAVITY													
Conc. (mg/l):	n.d.	n.d.	n.d.	1.582	n.d.	n.d.	2.968	n.d.	n.d.	n.d.	n.d.	1.524	n.d.
h after Injection:	–	–	–	31.30	–	–	66.47	–	–	–	–	33.05	–
Date/Time:	–	–	–	750907/20.33	–	–	810907/07.58	–	–	–	–	890903/23.03	–
LOAD MAXIMUM													
C*Q (mg/s):	n.d.	n.d.	n.d.	3.330	n.d.	n.d.	1.139	n.d.	n.d.	n.d.	n.d.	1.155	n.d.
h after Injection:	–	–	–	30.75	–	–	42.50	–	–	–	–	22.50	–
Date/Time:	–	–	–	750907/20.00	–	–	810907/08.00	–	–	–	–	890903/12.30	–
LOAD CENTRE OF GRAVITY													
C*Q (mg/s):	n.d.	n.d.	n.d.	0.936	n.d.	n.d.	0.348	n.d.	n.d.	n.d.	n.d.	0.291	n.d.
h after Injection:	–	–	–	31.12	–	–	65.30	–	–	–	–	31.81	–
Date/Time:	–	–	–	750907/20.22	–	–	810908/06.48	–	–	–	–	890903/21.48	–
FLOW VELOCITIES (m/h)													
First Appearance:	–	–	–	179.10	–	–	105.26	–	–	–	–	230.77	–
Conc. Peak:	–	–	–	131.87	–	–	70.59	–	–	–	–	133.33	–
Conc. Centre of Gravity:	–	–	–	95.85	–	–	45.13	–	–	–	–	90.78	–
Load Maximum:	–	–	–	97.56	–	–	70.59	–	–	–	–	133.33	–
Load Centre of Gravity:	–	–	–	96.40	–	–	45.94	–	–	–	–	94.32	–
TIME RATIOS													
$T_{Conc\text{-}Peak}/T_1$:	–	–	–	1.36	–	–	1.49	–	–	–	–	1.73	–
$T_{Load\text{-}Peak}/T_{Conc\text{-}Peak}$:	–	–	–	1.35	–	–	1.00	–	–	–	–	1.00	–
SAMPLING PLACES HAMMERBACH + SCHMELZBACH													
RECOVERY RATES (%)													
Hammerbach Spring:	60.8	36.9	23.6	51.9	14,6	14.6	45.5	41.7	64.4	80.9	86.3	74.7	60.1	68.3
Schmelzbach:	0.0	0.0	0.0	27.7		0.0	0.0	36.2	0.0	0.0	0.0	0.0	23.3	0.0
Sum Total:	60.8	36.9	23.6	79.6	14,6	14.6	45.5	77.9	64.4	80.9	86.3	74.7	83.4	68.3

experiments give rather different tracer responses at the spring the measured concentrations and calculated transit times (s. tab. 5.14 and 5.15) depending on the hydrological conditions during the experiments. All time-concentration curves are characterized by a long tailing part and often by secondary peaks. Due to the fact that the curves obtained for the quasi-ideal tracer chloride (not plotted in fig. 5.11) show the same shape as those for uranine one can deduce that this long tailing part is not a result of tracer retardation by sorption and/or diffusion. Therefore the assumption seems to be realistic that the tracer responses reflect the superposition of different time-concentration curves corresponding to different flow systems (or flow paths) with different transit times in the Hammerbach aquifer. This assumption was the basis for the mathematical modelling of the tracer concentration curves (s. chap. 6.1.).

Only during three tracing experiments with higher flow conditions (1975, 1981, 1989) the tracers injected into the Lurbach sinkhole could also be detected in Schmelzbach spring. The normalized response curves for uranine are plotted in fig. 5.12. Like for the Hammerbach spring the tracer responses reflect the superposition of different curves corresponding to different flow systems. For the two experiments with the highest discharges of both karst springs in 1975 and more clearely because of the shorter observation intervals in 1989 the first superposed parts of the curve with two peaks can be associated with two known flow paths: the first one with the shortest transit time represents the flow of Lurbach water through the accessible and during these experiments active part of the Lurgrotte, the second one the overflow from the Hammerbach to the Schmelzbach aquifer (R. BENISCHKE & T. HARUM, 1990). In 1981 (experiment at higher medium water conditions) the flow path through the accessible part of the cave was probably inactive.

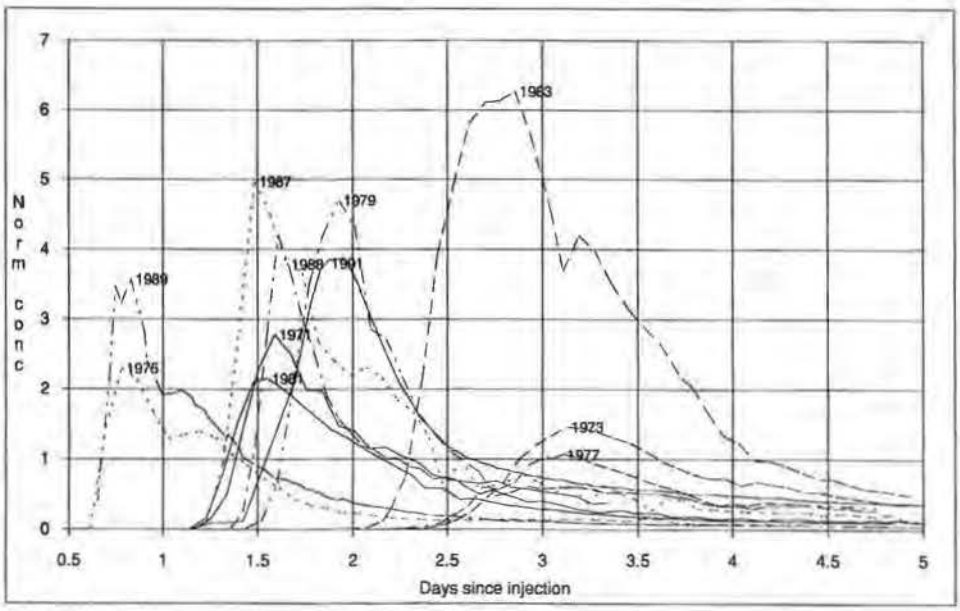

Fig. 5.11: Hammerbach spring: normalized breakthrough curves for uranine of all tracing experiments with injections into the Lurbach sinkhole.

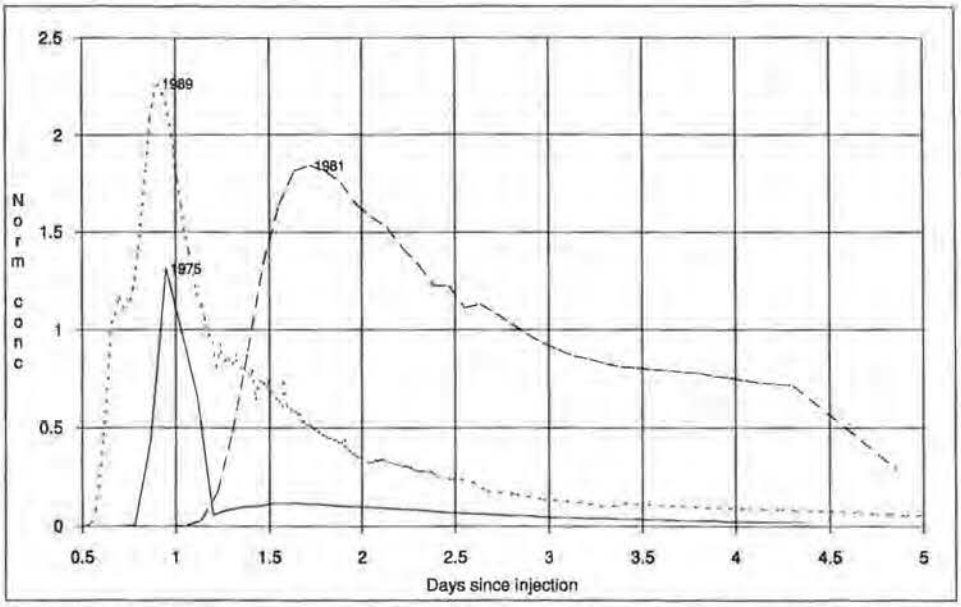

Fig. 5.12: Schmelzbach spring: normalized breakthrough curves for uranine of all tracing experiments with injections into the Lurbach sinkhole.

In fig. 5.13 the mean discharges (computed as arithmetic mean of maximum and minimum discharge) of the Hammerbach spring (HB) are plotted against the corresponding tracer recoveries (in % of injected tracer) for uranine and chloride. Taking into account all possible errors which can influence the value of recovery (discharge measurement, tracer analyses, background fluctuations of the chloride contents) the recovery rates of both tracers are well comparable. This indicates that tracer losses for uranine due to retardation or diffusion effects are negligible or due to an accidental error both tracers show nearly the same losses for different reasons (e.g. losses for uranine due to adsorption and for chloride due to a longer residence time of the high concentrated heavy salt solution near the injection site).

Figure 5.13 shows that the recovery rates for both tracers increase significantly with the discharge of the Hammerbach spring giving variations of the recovery rates between 10% (1977) and 100% (1989, total recovery HB + SB).

On the recent stage of the investigations two possibilities of explanation of this phenomenon or their combination are possible if we neglect tracer losses by adsorption or diffusion:

1) An important portion of the injected tracers is stored at low water conditions over a longer time in microfissured zones, cave sediments and in inactive karst channels. This explanation seems to be realistic comparing with the results of evaluation of the discharge depletion curves of input and output which indicate that an important portion of Lurbach water is stored over a longer time (s. chap. 2.3.4.).
2) A relatively constant portion of water from the Hammerbach aquifer flows through microfissured zones in a diffuse way into the porous aquifer of the

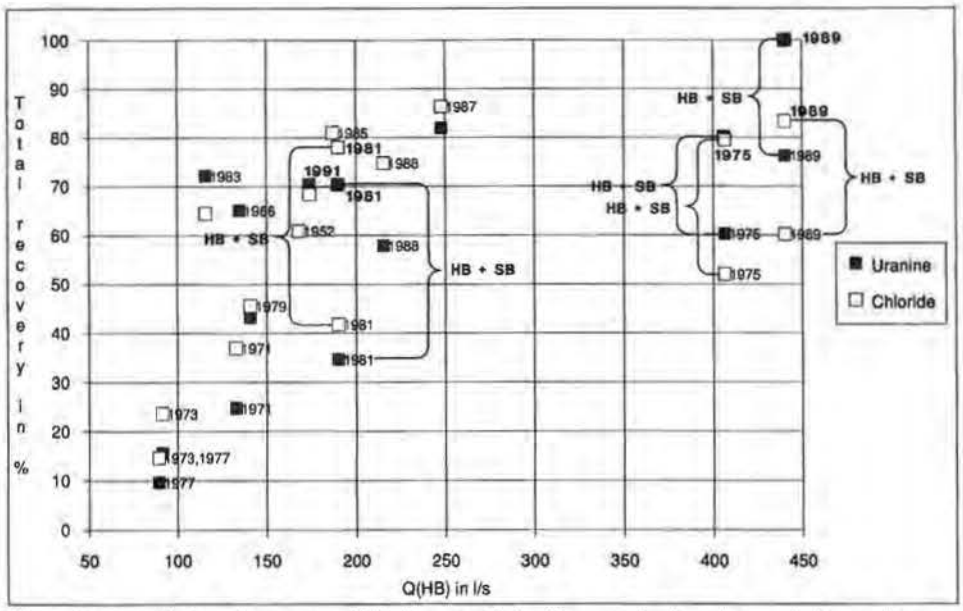

Fig. 5.13: Correlation diagramm of discharges of the Hammerbach spring and the total tracer recoveries for uranine and chloride at Hammerbach and Schmelzbach spring of all tracing experiments with injections into the Lurbach sinkhole.

quaternary filling in the Mur valley (cf. chap. 2.3.5. and 2.3.6.). Therefore the percentage of tracer losses is higher at low water conditions.

The transit times of the tracer uranine (expressed by the concentration peak in h after injection) between the Lurbach sinkhole and the Hammerbach spring as function of the mean discharge of the spring (and discharge extreme values during the experiments) are plotted in fig. 5.14. The exponential function indicates that the residence time in the karst aquifer depends significantly on the spring discharge and varies between 19 h (experiment 1975 at high water conditions) and 75 h (experiment 1973 with the lowest discharges). The experiments with tracer detection also in Schmelzbach are marked separately in fig. 5.14. It is clearly visible that the overflow from Hammerbach to Schmelzbach aquifer is only active at higher discharges.

6. Application of Tracer Models

6.1. Mathematical Modelling of Tracer Experiments in the Karst of Lurbach System (P. MALOSZEWSKI, T. HARUM, R. BENISCHKE)

6.1.1. Introduction

Water storage and water flow in karstic groundwater systems focus a lot of attention, especially in the countries where drinking water is mainly obtained from the karst. The estimation of the water volume in the karstic catchment areas and the prediction of protection zones against contamination in the surrounding of those

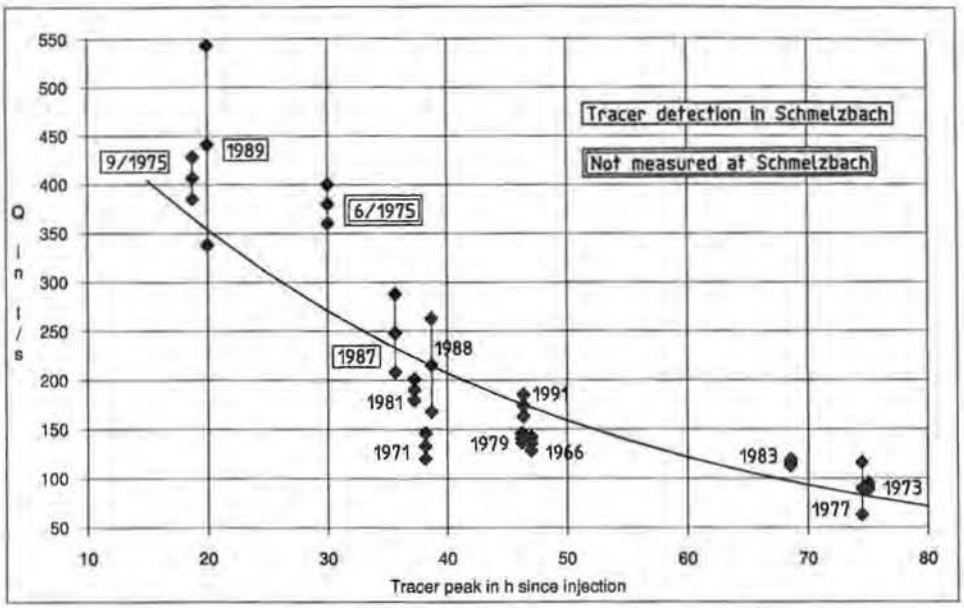

Fig. 5.14: Correlation diagramm of discharges of the Hammerbach spring and the transit time (tracer concentration peak in h since injection) for uranine at Hammerbach spring of calculated from all tracing experiments with injections into the Lurbach sinkhole.

areas play then a very important role. Experimental works in the karst are mainly based on classical hydraulic methods in which the parameters are obtained from analysing the recharge-discharge relations (S. DREISS, 1989, Th. PFAFF, 1987).

For several years the applicability of environmental and artificial tracer methods has been permanently increasing (R. BENISCHKE et al, 1988, D. RANK et al, 1991, J.-F. QUINLAN et al, 1987). Especially artificial tracer experiments have been already widely applied. Several well described tracer experiments performed in karst of different types can be found in the literature (W. KÄSS, 1972, R. GOSPODARIC & P. HABIČ, 1976, R. GOSPODARIČ et al., 1976, H. BEHRENS et al., 1981, A. MORFIS & H. ZOJER, 1986). In most cases the purpose of these experiments was the determination of flow directions and/or hydraulic connections between injection and detection sites. Unfortunately only some of these experiments have been interpreted quantitatively. The interpretation is usually mostly based on the method of moments (A. KREFT & A. ZUBER, 1978) applied directly to the tracer concentration curve or on a simple one dimensional dispersion model developed for porous aquifers by A. LENDA & A. ZUBER (1970).

It means that in most cases the transport parameters such as water velocity (mean transit time of tracer) and dispersivity are being determined without model calibration or by calibration of an unadequate model, because the tracer concentration curves in karst are characterized by strong tailing effect and often by several peaks.

As shown by P. MALOSZEWSKI & A. ZUBER (1990, 1992) the method of moments applied to the tracer breakthrough curves characterized by tailing effect provides a strong overestimation of longitudinal dispersivity and underestimation of water velocity. The dispersivities obtained in this way range from hundred of meters to

kilometers (I. STOBER, 1988). Additionally these parameters used in one dimensional dispersion model yield the tracer breakthrough curve far from the concentrations measured. Even by applying the fitting procedure, the simple one dimensional model cannot fit the tracer concentration curve correctly. This means that the model is not calibrated properly and, consequently, not validated (s. P. MALOSZEWSKI & A. ZUBER, 1992, for the definition of these terms).

Three approaches have been proposed so far to deal with the tailing effect. The first consists of coupling of the dispersion equation for mobile water in conduit fractures with the diffusion equation for stagnant water in the microporous matrix (P. MALOSZEWSKI & A. ZUBER, 1985). The second consists of considering the tracer curve as a result of superposition of several flow paths (A. ZUBER, 1974, A. KREFT et al., 1974) and also different flow paths in series (R. ROGALSKI, 1988). The third is the combination of both above approaches (P. MALOSZEWSKI & A. ZUBER, 1985, K.-P. SEILER et al., 1989). In the present work the second approach is employed and further developed for modelling tracer transport in the karstic system of Lurbach.

6.1.2. Mathematical Concept

Most tracer experiments were performed in the karst of Lurbach system under quasi steady state conditions, i.e., the discharge of the Hammerbach spring was nearly constant during the tracer passage. The tracers were injected directly into the Lurbach creek entering the karstic system in a sinkhole and observed in two karstic outflows: Hammerbach and Schmelzbach springs (s. chap. 5.). All the tracer curves observed were characterized by strong tailing effects or even by additional peaks. Such effects cannot be described only by single one dimensional dispersion model. The determination of transport parameters using any simple estimation method without model calibrations cannot yield acceptable results. The shape of the tracer curves suggested that the tracer is transported in several parallel flow paths (subsystems). The idea of the tracer transport is shown in fig. 6.1. R. ROGALSKI (1988) employed a model consisting of two parallel flow paths, whereas here up to five were possible.

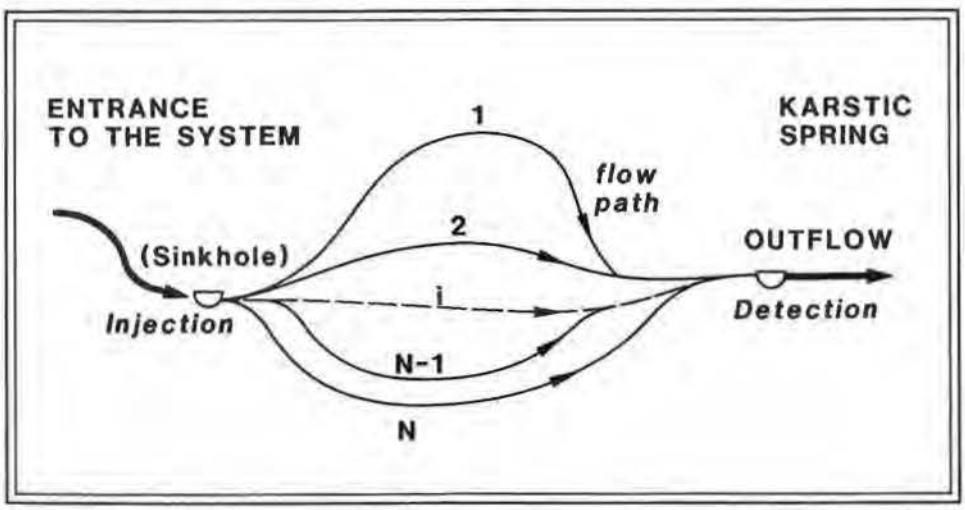

Fig. 6.1: Hydrological model of the water flow through drainage channels in the karstic system.

A similar multiflow model was presented by A. ZUBER (1974) and used by A. KREFT et al. (1974) for interpreting tracer experiments in fractured karstified rocks. In the present work this approach is employed to karstic conduits. It is assumed that the tracer transport can be considered separately for each flow path and that there are no interactions between the flow paths. Possible diffusion of tracer from the mobile water into the stagnant water in the microporous matrix and/or in temporarily nonactive parts of the karstic system is neglected. Under these assumptions on each parallel flow path the transport of an "ideal" (nonreactive) tracer is governed by a one dimensional dispersion model:

$$D_i \frac{\partial^2 C_i}{\partial x^2} + v_i \frac{\partial C_i}{\partial x} = \frac{\partial C_i}{\partial t}, \qquad (6.1)$$

where $C_i(x,t)$is the concentration of tracer in water, v_i is the mean water velocity, and D_i is the dispersion coefficient for the i-th flow path. The molecular diffusion in water in the comparison to the hydrodynamic dispersion is negligible due to high water velocities. The dispersion coefficient is then

$$D_i = \alpha_i v_i, \qquad (6.2)$$

where α_i is defined as the dispersivity on the i-th flow path.

The model assumes that the whole mass of tracer, M, instantaneously injected in time t = 0 at the entrance to the system, is there well mixed and divided into N portions which immediately enter the N flow subsystems. This means that the tracer mass M_i entering each subsystem is proportional to the volumetric flow rate Q_i through that subsystem. All the flow paths meet again in the outflow from the system (spring) where instantaneous good mixing of the tracer takes place. The conceptual flow model is shown in fig. 6.2. It is clear that in nature some flow paths may originate and end somewhere in the system (s. fig. 6.1), but not like shown in fig. 6.2. Independently from that, the model parameters are always related to flow paths which begin in the sinkhole (injection site) and end in the outflow from the system

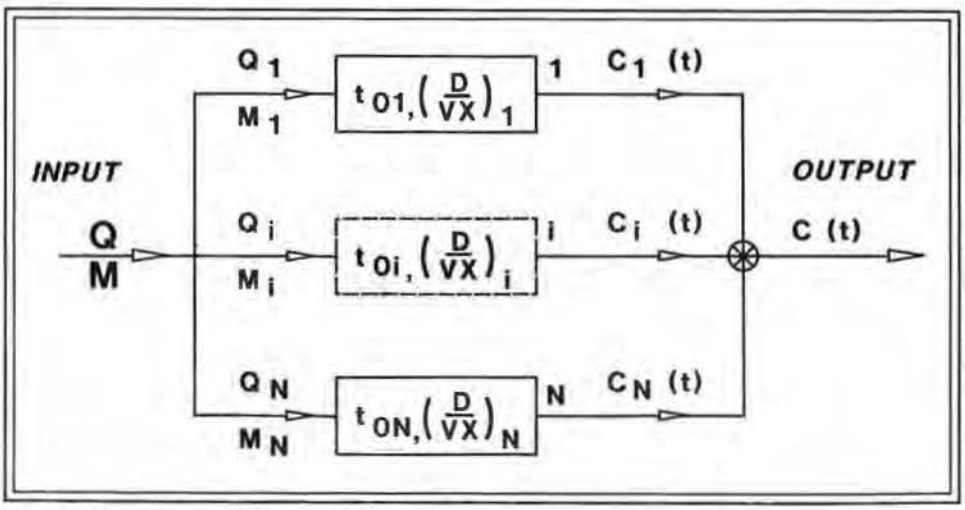

Fig. 6.2: The conceptual flow model.

(spring). **Due to this fact, the model has to be considered as a rough approximation of the reality.** The number of possible flow subsystems N is one of the parameters of the model and has to be determined during its calibration (fitting). The parameters of the model found from the tracer data strongly depend on the tailing part of the tracer concentration curve and the accuracy of its measurement. The flow distances, x_i, measured between the injection and detection site (sinkhole and spring, respectively) can be different for different flow paths and is not exactly known. Due to this fact it is always convenient to use as transport parameters: the mean transit time of water $t_0 = x/v$ and the dispersion parameter $D/vx = \alpha/x$. Assuming steady state flow conditions the mean transit time of water for the i-th flow path, t_{0i}, is simultaneously equal to the ratio of the volume of water V_i to the volumetric flow rate of water Q_i through the flow subsystem:

$$t_{0i} = x_i/v_i = V_i/Q_i \,. \tag{6.3}$$

For an instantaneous injection described by the Dirac function

$$C_i(0,t) = M_i/Q_i \cdot \delta(t) \tag{6.4}$$

the solution of eq. (6.1) has the following form:

$$C_i(t) = \frac{M_i}{V_i} \frac{1}{\sqrt{4\pi (D/vx)_i (t/t_{0i})^3}} \cdot \exp\left[-\frac{(1 - t/t_{0i})^2}{4 (D/vx)_i (t/t_{0i})}\right], \tag{6.5}$$

where

$$(D/vx)_i = \alpha_i/x_i \tag{6.6}$$

is the dispersion parameter on the i-th flow path.

The tracer concentration measured in the outflow from the system is the weighted mean concentration from all flow paths

$$C(t) = \sum_{i=1}^{N} [Q_i C_i(t)]/Q \,, \tag{6.7}$$

where $C_i(t)$ is the tracer output concentration at the end of the i-th flow path and Q is the total discharge measured in the karstic spring equal simultaneously to the sum of partial flow rates:

$$Q = \sum_{i=1}^{N} Q_i \,. \tag{6.8}$$

It can be deduced from eq. (6.7) that the tracer concentration $C_i(t)$ at the end of i-th flow path is diluted by other flow paths

$$C_{mi}(t) = Q_i C_i(t)/Q \,. \tag{6.9}$$

$C_{mi}(t)$ is now the tracer concentration from the i-th flow subsystem observed in the outflow from the whole system. Combining eq. (6.5) and (6.9) one obtains:

$$C_{mi}(t) = \frac{M_i}{Q} \frac{1}{t_{0i}\sqrt{4\pi (D/vx)_i (t/t_{0i})^3}} \cdot \exp\left[-\frac{(1 - t/t_{0i})^2}{4 (D/vx)_i (t/t_{0i})}\right]. \tag{6.10}$$

The total output concentration (eq. 6.7) is the superposition of the partial concentrations, $C_{mi}(t)$

$$C(t) = \sum_{i=1}^{N} C_{mi}(t) \,. \tag{6.11}$$

The theoretical tracer recovery R obtained in the outflow from the system is

$$R = Q \cdot \int_0^\infty C(t)\,dt\,, \tag{6.12}$$

whereas the partial tracer recoveries R_i observed at the end of each i-th flow path are calculated using the same equation but instead of Q and C(t) one has to use Q_i and $C_i(t)$. By introducing eq. (6.9) into (6.12) one obtains

$$R_i = Q \cdot \int_0^\infty C_{mi}(t) = M_i\,. \tag{6.13}$$

The mass of tracer injected into i-th flow path, M_i, can be then found using eq. (6.13) to the i-th tracer concentration curve measured in the outflow from the whole system. Theoretically the sum of all partial recoveries is equal to the total recovery and to the mass of tracer injected

$$R = \sum_{i=1}^{N} R_i = M\,. \tag{6.14}$$

The mathematical flow model for the Lurbach system is described by eq. (6.10) and (6.11).

The parameters of the model are the number of flow subsystems (N) and the parameters for each of the N flow paths. Each i-th flow path has its own mean transit time of water, t_{0i}, dispersion parameter, $(D/vx)_i$ and the flow rate, Q_i, represented by the mass of tracer, M_i.

6.1.3. Determination of the Parameters

The solution of the inverse problem, i.e. the determination of all parameters from the tracer curve cannot be done automatically due to the high number of unknowns. The solution can be obtained by dividing step by step the experimental curve into partial curves, starting by the first peak of the experimental curve and looking for the best fit of the theoretical solution (eq. 6.10) to the concentrations measured at the initial part of the curve. In the next step this theoretical curve is substracted from the whole tracer concentration curve and the procedure repeated until the background concentration is reached. The number of flow subsystems N will then be automatically found. As a result of fitting the parameters t_{0i} and $(D/vx)_i$ are determined step by step for all flow paths. The parameter M_i is estimated next, by applying eq. (6.13) to the partial theoretical curves calculated with known values of t_{0i} and $(D/vx)_i$. Finally, the whole theoretical curve can be calculated (eq. 6.11) and compared with the experimental curve.

In practice, the total recovery of tracer (eq. 6.12) is very often smaller than the mass injected (M). In such a case the real recoveries R_i have to be used instead of M_i in eq. (6.11) and (6.10).

Similarly, when the tracer curves are observed in several outflows from the karstic system, each single outflow must be separately considered and R used instead of M. The ratio of i-th recovery R_i to the total recovery R observed in the outflow produces the portion of tracer r_i transported through the i-th flow subsystem. According to the model assumption this quantity is equal to the ratio of volumetric flow rate in i-th flow path Q_i to the whole discharge Q of the outflow

$$r_i = R_i/R = Q_i/Q\,. \tag{6.15}$$

From the above equation it is clear that the estimation of the r_i parameter from the recoveries ratio enables to calculate the flow rates Q_i on each flow path (for known discharge Q) and then from eq. (6.3) the volumes of water V_i in different flow subsystems

$$V_i = Q_i \cdot t_{0i} = r_i \cdot Q \cdot t_{0i}. \tag{6.16}$$

The sum of V_i is equal to the whole water volume V in the drainage channels of the karstic system between the sinkhole of creek and its outflow

$$V = \sum_{i=1}^{N} V_i, \tag{6.17}$$

6.1.4. Results of Modelling and Discussion

It was mentioned earlier that the tracers were injected into the Lurbach creek (input) and observed in the outflows: Hammerbach and Schmelzbach springs (outputs). Twenty tracer experiments have been performed since 1927 – three experiments were not completed but 17 tracer concentration curves were sufficiently well recorded to be modelled. The tracer passage was detected mainly in Hammerbach spring (15 curves). Only at discharges of the Hammerbach spring higher than about 200 l/s, the tracer passage was also detected in Schmelzbach spring. This phenomen was observed in 1970, 1975, 1981, 1987 to 1989 experiments (s. chap. 5.2.) but only two of them (1981 and 1989) could be modelled. In 1988 a multitracer experiment with three "ideal" tracers uranine, bromide and eosin injected simultaneously was performed by the ATH-group. The tracer curves obtained for uranine and eosin have nearly the same shape as that for bromide. It shows that the strong tailing effect observed in the experiments was not a result of possible sorption or diffusion, but can well be explained by the flow conditions. In some experiments the water samples were collected not long enough to obtain the whole tracer curve and it was necessary to extrapolate the tailing parts. The discharge of Hammerbach spring was nearly constant during most of experiments (steady state conditions). However, the mean discharge was different from year to year (80–360 l/s). The results of modelling for Hammerbach and Schmelzbach drainage systems are summarized in tab. 6.1–6.9. The velocities and dispersivities on different flow paths were calculated assuming the same lenghts of the N flow paths x_i in each system separately (x = 3.1 km for Hammerbach and x = 3.0 km for Schmelzbach).

The model proposed in this study yields a good fit in all experiments. It means that the model was in all cases properly calibrated and that the idea of multiflow seems to be applicable for this system. The examples of model calculations for tracer experiments performed in 1952, 1979 and 1988 are shown in fig. 6.3–6.6. The final results of modelling can only be discussed for Hammerbach system. There are not sufficient data for the Schmelzbach system to make any general conclusions.

6.1.4.1. Flow Paths

In the Hammerbach system between three and five flow paths (flow subsystems) were found. It is questionable if five flow paths really exist because it is difficult to model the end parts of tracer curve due to low concentration, close to background. On the other hand, some experiments, particulary for low discharges, were ended too early and consequently the determination of all flow paths was not possible. However, the experiment with bromide and uranine in 1988 showed that up to five flow subsystems probably exist.

*Tab. 6.1: Results of calculations for Hammerbach system (tracers, mean transit times, dispersivities on different flow paths). FP1, FP2, FP3, FP4 and FP5 = mean flow path 1, 2, 3, 4 and 5; *) = tracer experiment was ended to early and the whole tracer curve was not available.*

Year	Tracer	Mean transit times t_{0i} (days)					Dispersivity α_i (m)				
		FP1	FP2	FP3	FP4	FP5	FP1	FP2	FP3	FP4	FP5
1952	Chloride	2.0	2.6	3.3			23.0	6.3	12.9	–	–
1971	Uranine	1.7	2.4	3.1	*)		25.0	16.5	16.5	–	–
1973	Uranine	3.3	4.5	*)			24.3	13.9	–	–	–
1977	Uranine	3.2	4.5	*)			20.5	28.3	–	–	–
1979	Uranine	2.0	2.6	3.4	4.6	–	20.6	6.6	23.2	13.6	–
1981	Uranine	1.5	2.0	2.9	4.4	–	15.5	32.0	37.0	39.3	–
1983	Uranine	2.8	3.6	5.0	*)		18.7	15.8	9.2	–	–
1985	Amidor.	1.8	2.5	3.2	4.1	5.4	12.7	19.0	7.5	20.0	15.0
1987	Uranine	1.6	2.2	3.0	4.4		20.1	13.3	31.2	37.8	
1988	Bromide	1.7	2.2	2.8	3.6	5.0	11.3	9.8	16.5	8.5	27.0
	Uranine	1.7	2.2	2.9	3.6	4.3	11.6	16.5	14.3	7.5	6.5
	Eosin	1.7	2.2	2.8	*)		12.0	12.8	11.0	–	–
1989	Uranine	0.9	1.3	1.8	2.4	3.5	27.0	27.5	26.0	30.0	40.0
1991	Uranine	1.9	2.5	3.3	4.3	6.6	18.0	22.0	20.0	22.0	30.0
	Chloride	1.8	2.4	3.2	4.3	6.0	15.5	17.5	19.5	22.0	30.0

*Tab. 6.2: Results of calculations for Hammerbach system (mean discharge during experiment, portion of tracer and mean partial volumetric flow rates for different flow subsystems). FP1, FP2, FP3, FP4 and FP5 = mean flow path 1, 2, 3, 4 and 5; *) = tracer experiment was ended to early and the whole tracercurve was not available; [b] = bromide; [c] = chloride; [u] = uranine; [e] = eosin.*

Year	Mean Q (l/s)	Portion of tracer r_i					Mean partial flow rates Q_i (l/s)				
		FP1	FP2	FP3	FP4	FP5	FP1	FP2	FP3	FP4	FP5
1952	170.0	0.82	0.09	0.09			139.4	15.3	15.3	–	–
1971	133.0	0.63	0.21	0.16	*)		83.8	27.9	21.3	–	–
1973	91.5	0.75	0.25	*)			68.6	22.9	–	–	–
1977	81.3	0.64	0.36	*)			52.0	29.3	–	–	–
1979	141.0	0.69	0.09	0.15	0.07	–	97.3	12.7	21.2	9.9	–
1981	195.0	0.43	0.35	0.15	0.07		83.9	68.3	29.3	13.7	–
1983	116.0	0.65	0.28	0.07	*)		75.4	32.5	8.1	–	–
1985	186.0	0.55	0.18	0.09	0.11	0.07	102.3	33.5	16.7	20.5	13.0
1987	200.0	0.53	0.23	0.17	0.07		106.0	46.0	34.0	14.0	
1988	182.0[b]	0.69	0.13	0.09	0.03	0.06	125.6	23.7	16.4	5.5	11.1
	182.0[u]	0.64	0.21	0.09	0.03	0.02	116.5	38.2	16.4	5.5	3.6
	182.0[e]	0.74	0.18	0.08	*)		134.7	32.8	14.6	–	–
1989	360.0	0.44	0.30	0.15	0.07	0.03	158.4	108.0	54.0	25.2	10.8
1991	185.0[u]	0.47	0.19	0.12	0.12	0.09	87.0	35.2	22.2	22.2	16.7
	185.0[e]	0.51	0.17	0.15	0.11	0.06	94.4	31.5	27.8	20.4	11.1

Tab. 6.3: Results of calculations for Hammerbach system (total volume of water in the system, mean partial volumes of water in different flow subsystems and mean water velocities of water). FP1, FP2, FP3, FP4 and FP5 = mean flow path 1, 2, 3, 4 and 5.

Year	Total V (10^3 m^3)	Mean partial water volumes V_i (10^3 m^3)					Mean water velocity v_i (m/h)				
		FP1	FP2	FP3	FP4	FP5	FP1	FP2	FP3	FP4	FP5
1952	31.3	23.3	3.5	4.4	–	–	65.8	49.6	39.4		
1971	23.7	12.4	5.8	5.5	–	–	75.0	54.2	41.7		
1973	28.7	19.7	9.0	–	–	–	38.5	28.4			
1977	24.3	12.9	11.4	–	–	–	40.3	28.5			
1979	29.6	16.8	2.7	6.1	4.0	–	64.6	49.8	38.0	28.1	
1981	35.9	14.3	9.2	7.5	4.9	–	83.3	64.6	44.4	29.2	
1983	32.1	18.3	10.4	3.4	–	–	45.4	35.4	27.5		
1985	39.6	15.9	7.2	4.6	7.4	5.8	71.1	52.1	39.9	31.3	23.9
1987	39.0	14.8	8.8	9.0	6.0		80.3	59.2	42.5	29.0	
1988	35.6	20.2	4.8	4.2	1.7	4.7	75.4	58.6	45.8	36.1	25.8
	33.9	18.4	8.1	4.3	1.8	1.4	76.3	57.5	44.5	35.5	30.0
	32.1	21.5	6.8	3.7	–	–	76.0	57.4	45.4		
1989	39.0	11.5	11.7	7.6	5.0	3.0	150.0	103.2	72.9	54.2	36.7
1991	43.7	14.3	7.8	6.6	8.3	6.7	64.6	50.0	37.5	28.8	20.8
	42.1	14.6	6.5	7.7	7.9	5.4	69.6	52.5	39.6	29.2	20.8

*Tab. 6.4: Results of calculations for Schmelzbach system (tracers, mean transit times, dispersivities on different flow paths). FP1, FP2, FP3, FP4 and FP5 = mean flow path 1, 2, 3, 4 and 5; *) = tracer experiment was ended to early and the whole tracercurve was not available.*

Year	Tracer	Mean transit times (days)					Dispersivity (m)				
		FP1	FP2	FP3	FP4	FP5	FP1	FP2	FP3	FP4	FP5
1981	Uranine	1.8	2.8	4.3	*)		50.0	55.0	42.0	–	–
1989	Uranine	1.0	1.6	2.4	4.2	0.7	49.4	39.5	42.0	60.0	3.7

*Tab. 6.5: Results of calculations for Schmelzbach system (mean discharge during experiment, portion of tracer and mean partial volumetric flow rates for different flow paths). FP1, FP2, FP3, FP4 and FP5 = mean flow path 1, 2, 3, 4 and 5; *) = tracer experiment was ended to early and the whole tracercurve was not available.*

Year	Mean Q (l/s)	Portion of tracer					Mean partial flow rates (l/s)				
		FP1	FP2	FP3	FP4	FP5	FP1	FP2	FP3	FP4	FP5
1981	112.0	0.39	0.32	0.29	*)		43.7	35.8	32.5	–	–
1989	152.0	0.52	0.23	0.13	0.11	0.02	79.0	35.0	19.8	15.2	3.0

Tab. 6.6: Results of calculations for Schmelzbach system (total volume of water in the system, mean partial volumes of water in different flow subsystems and mean water velocities of water). FP1, FP2, FP3, FP4 and FP5 = mean flow path 1, 2, 3, 4 and 5.

Year	Total V (10^3 m^3)	Mean partial water volumes V_i (10^3 m^3)					Mean water velocity V_i (m/h)				
		FP1	FP2	FP3	FP4	FP5	FP1	FP2	FP3	FP4	FP5
1981	28.0	7.0	8.6	12.4	–	–	70.8	45.8	28.9		
1989	23.2	7.6	5.4	4.2	5.8	0.3	131.8	80.6	52.7	29.7	189.2

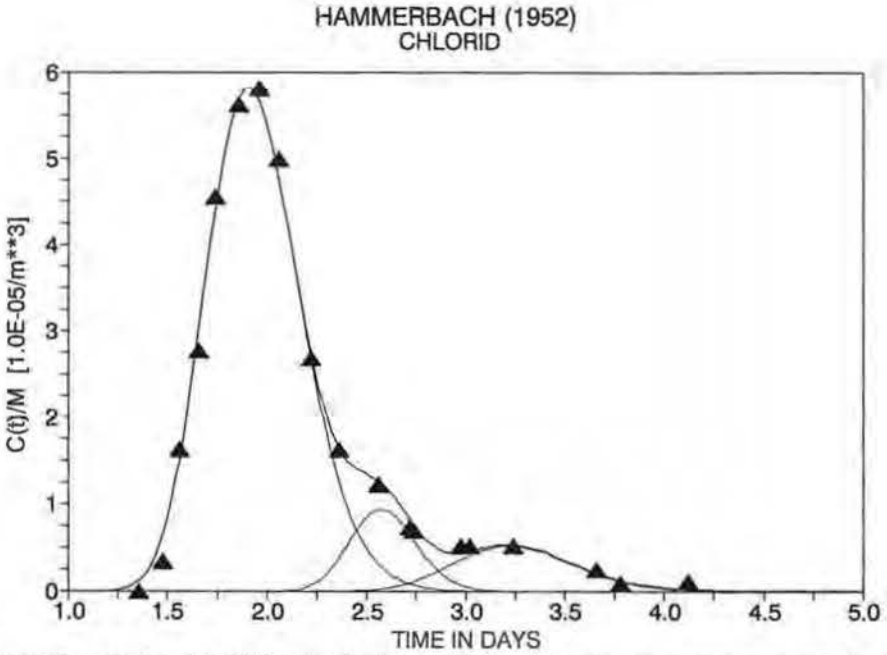

Fig. 6.3: The calculated (solid line) and observed (triangle) tracer concentration curves for the experiment performed in 1952 with chloride (dashed lines correspond to the partial curves).

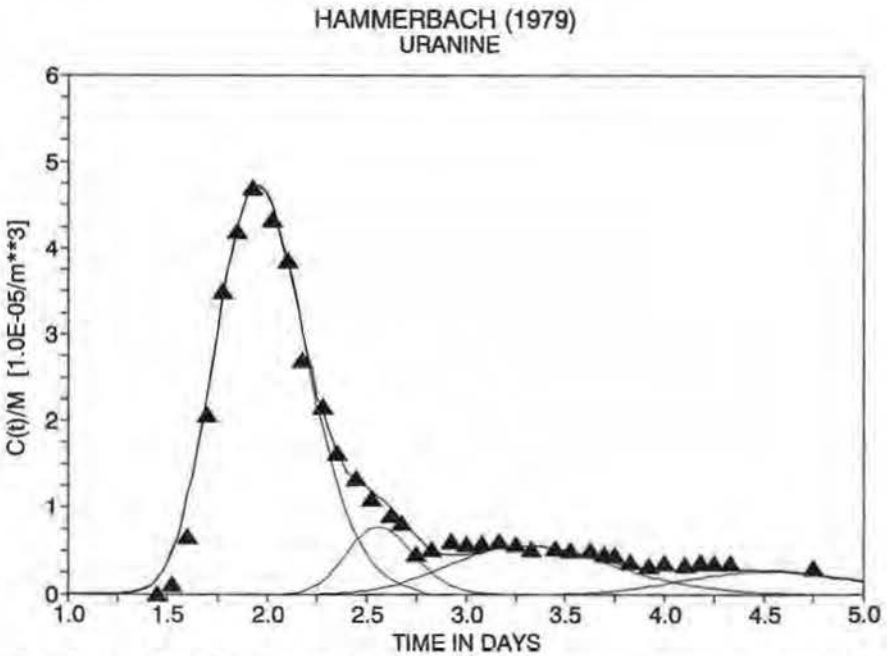

Fig. 6.4: The calculated (solid line) and observed (triangle) tracer concentration curves for the experiment performed in 1979 with uranine (dashed lines correspond to the partial curves).

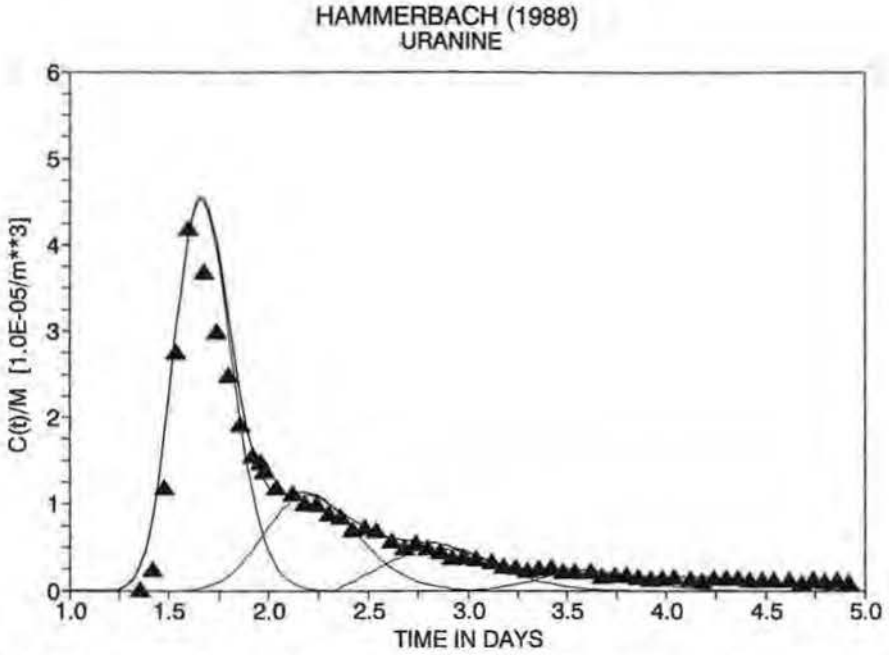

Fig. 6.5: The calculated (solid line) and observed (triangle) tracer concentration curves for the experiment performed in 1988 with uranine (dashed lines correspond to the partial curves).

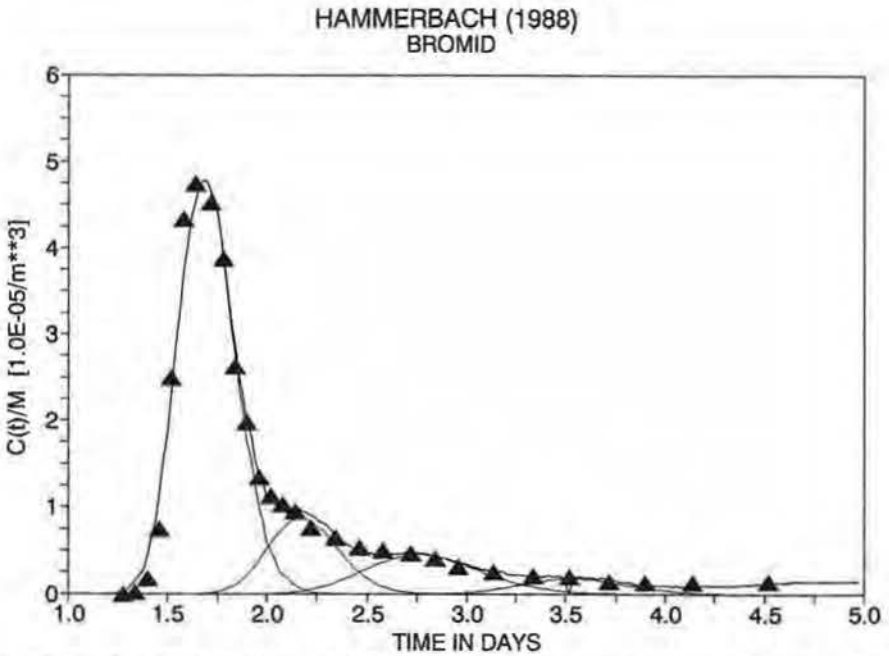

Fig. 6.6: The calculated (solid line) and observed (triangle) tracer concentration curves for the experiment performed in 1988 with bromide (dashed lines correspond to the partial curves).

6.1.4.2. Dispersivities

The dispersivities obtained for different flow paths are summarized in tab. 6.1. Table 6.7 includes their mean values. Figures 6.7–6.10 show a relatively low scatter of dispersivity values for different flow paths. This scatter increases from 10–25 m for the 1st flow path to 8–40 m for the 4th flow path. The mean values calculated separately for each flow path differ not so much (19.9–24.7 m). The dispersivities are generally independent from the discharge (s. fig. 6.7–6.10). The average value of all dispersivities is about 20 m.

Tab. 6.7: Mean dispersivities on the different flow paths and the average dispersivity for the Hammerbach and Schmelzbach systems. FP1, FP2, FP3, FP4 and FP5 = mean flow path 1, 2, 3, 4 and 5.

System	Dispersivity (m)					
	Total	FP1	FP2	FP3	FP4	FP5
Hammerbach	19.4	18.4	17.2	18.8	22.3	24.8
Schmelzbach	49.0	49.7	47.3	42.0		

6.1.4.3. Mean Transit Times

The mean transit times and water velocities vary very strongly but the general trend is that t_{0i} decreases (v_i increases) with increasing discharge Q (s. fig. 6.11). The mean transit time for the whole system is calculated as

$$t_0 = V/Q = \sum_{i=1}^{N} V_i/Q = \sum_{i=1}^{N} (r_i \cdot t_{0i}). \qquad (6.18)$$

6.1.4.4. Flow Rates and Volumes of Water

The portions of the tracer transported in each flow path, r_i, found from the tracer recoveries, were used to calculate the partial flow rates Q_i (s. tab. 6.2) and then, taking t_{0i}, to estimate the partial volumes of water V_i and the whole volume of water V in the system (s. tab. 6.3). Figures 6.12–6.14 show that V_i are nearly independent from the discharge Q. Figure 6.15 suggests that the total volume of water V may depend on the discharge Q for lower Q values. However all experiments with low discharges were finished too early and the additional flow paths could not be found. The rough approximation of the missing parts of the tracer breakthrough curves and reinterpretation of those experiments showed that the whole water volume V should be also considered as constant with rising discharge (s. fig. 6.15).

It seems that for the discharge variation between 80 and 400 l/s the whole drainage system is always saturated and has the total capacity for water limited to the volume of about 40×10^3 m³. The arithmetic means of V_i calculated for different flow paths and their sums (understood as the maximum water volume in the system) are summarized in tab. 6.8.

The water volume in Schmelzbach system is estimated to be about 26×10^3 m³. The whole drainage part of the karstic system between the Lurbach-sinkhole and the Hammerbach and Schmelzbach springs has about 65×10^3 m³. The water volumes in the Hammerbach and Schmelzbach drainage systems are shown in fig. 6.16 and 6.17.

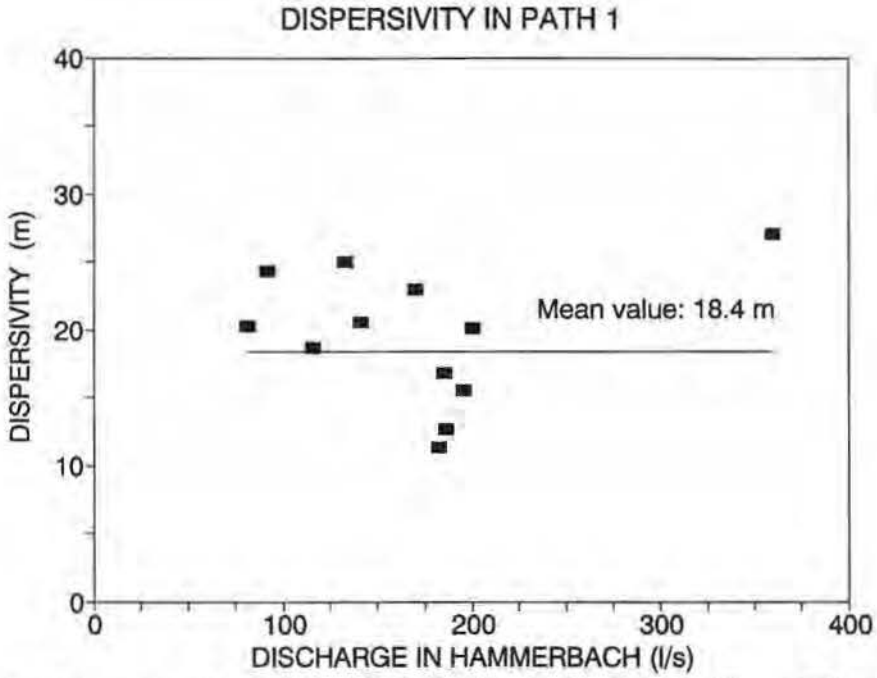

Fig. 6.7: Dispersivities α obtained for the 1st flow path in experiments with different discharge Q.

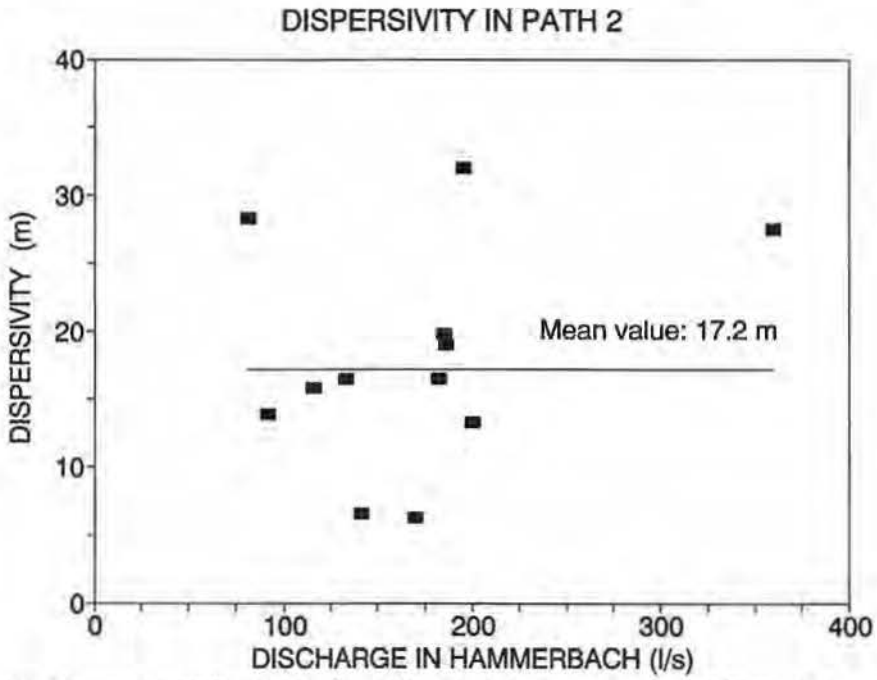

Fig. 6.8: Dispersivities α obtained for the 2nd flow path in experiments with different discharge Q.

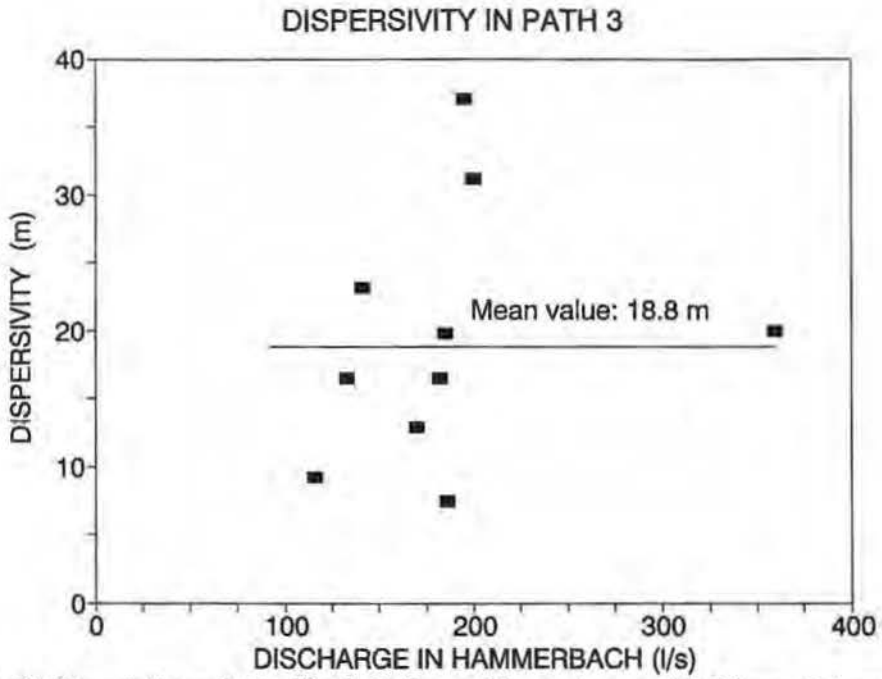

Fig. 6.9: Dispersivities α obtained for the 3th flow path in experiments with different discharge Q.

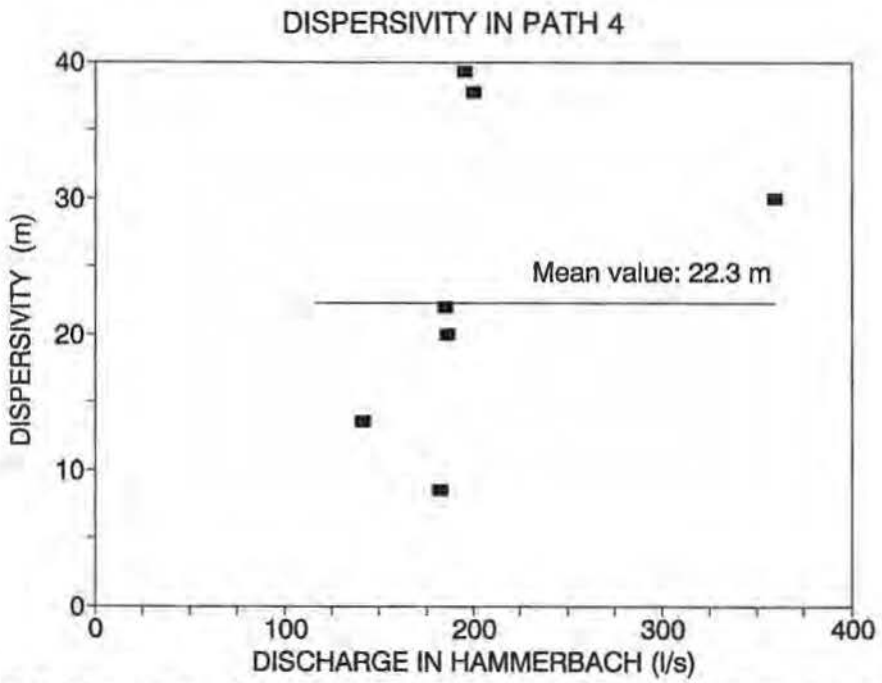

Fig. 6.10: Dispersivities α obtained for the 4th flow path in experiments with different discharge Q.

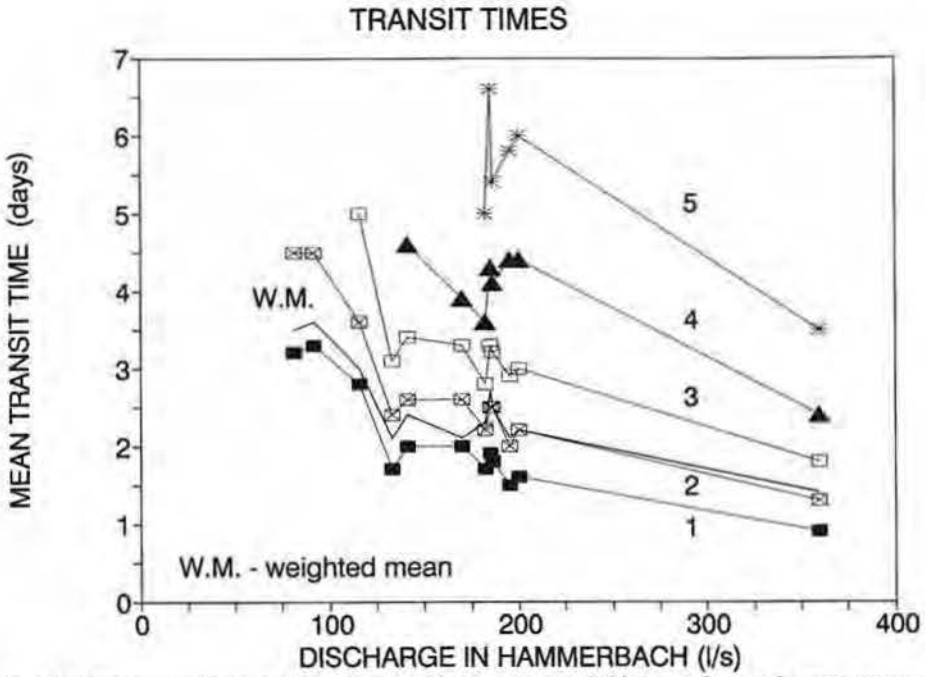

Fig. 6.11: Mean transit time of the Hammerbach system (solid line) and partial transit times on different flow paths as a function of discharge Q.

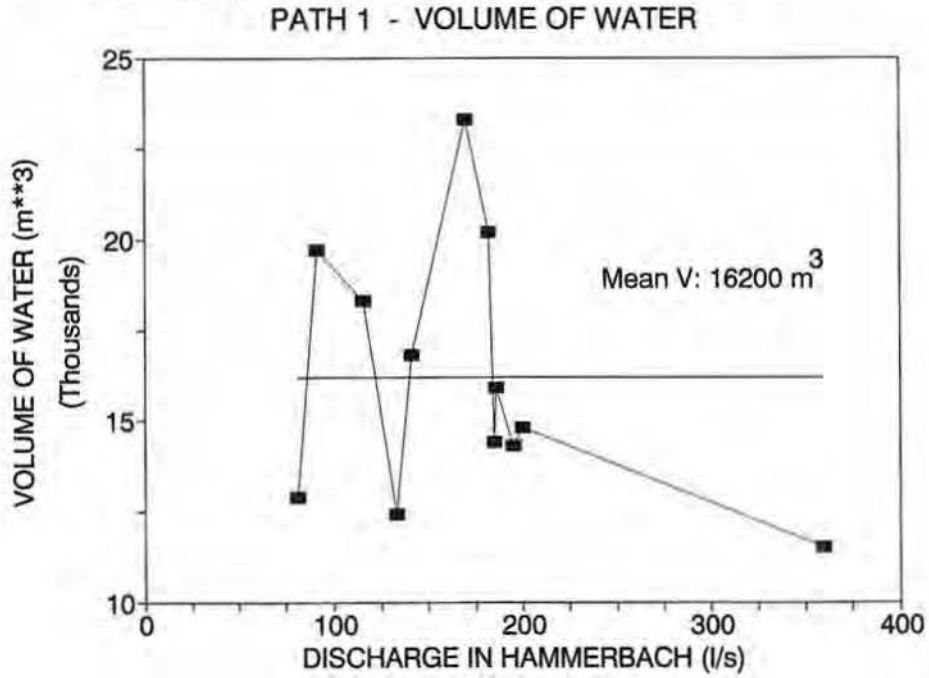

Fig. 6.12: Volume of water found in the 1st flow path of Hammerbach system as a function of discharge Q.

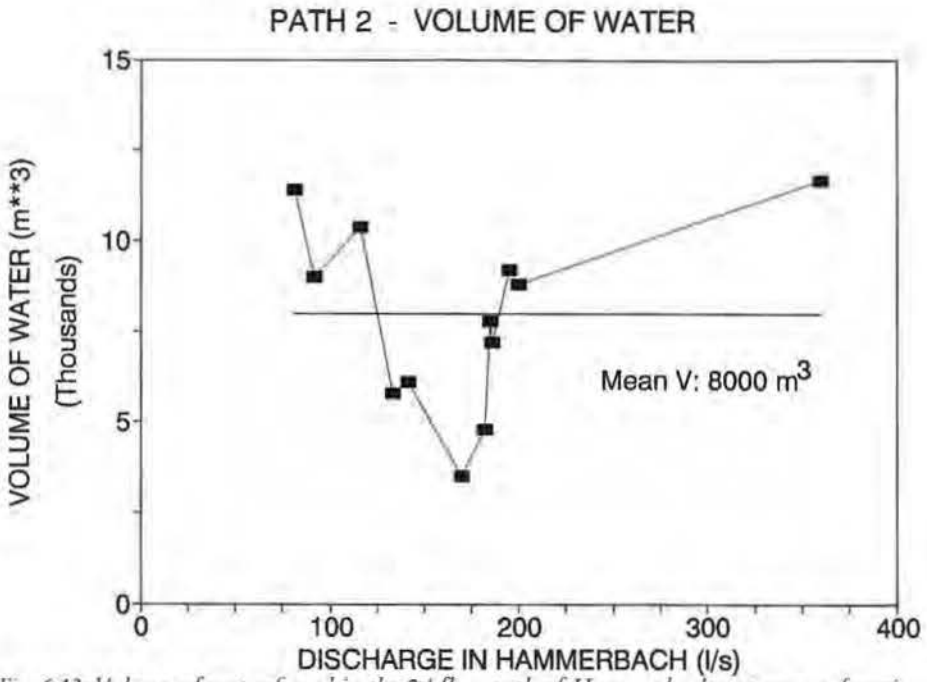

Fig. 6.13: Volume of water found in the 2nd flow path of Hammerbach system as a function of discharge Q.

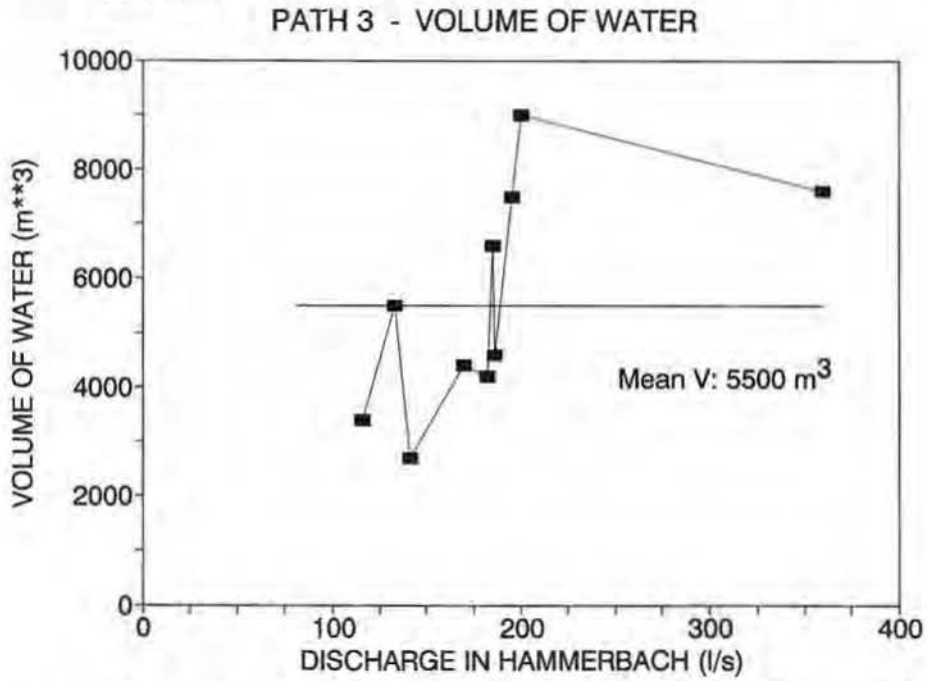

Fig. 6.14: Volume of water found in the 3th flow path of Hammerbach system as a function of discharge Q.

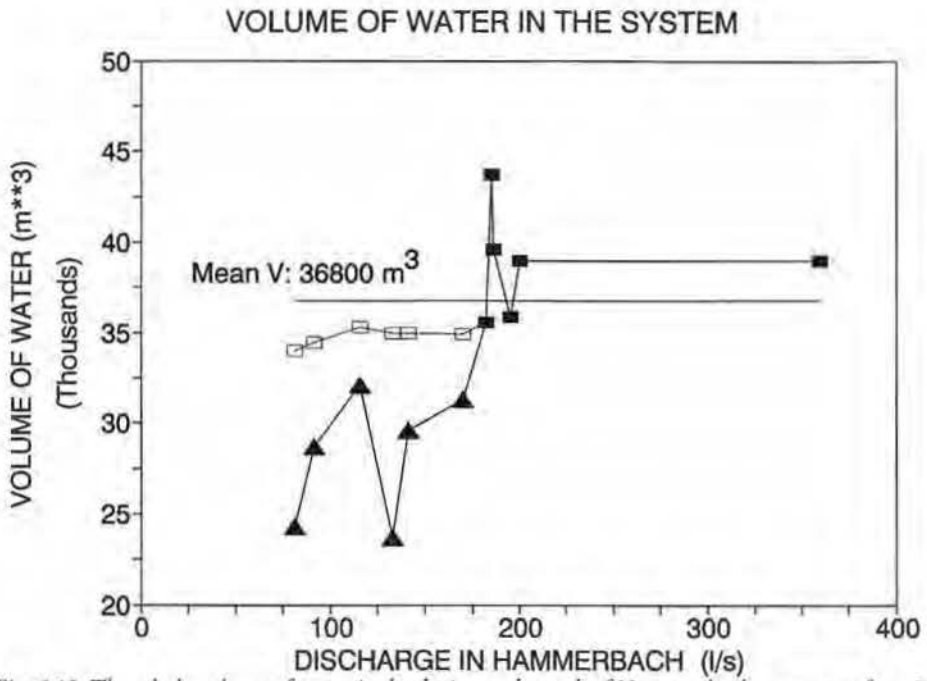

Fig. 6.15: The whole volume of water in the drainage channels of Hammerbach system as a function of discharge Q (triangles represent results from experiments which were finished to early; empty squares are estimated water volumes in those experiments).

Tab. 6.8: Maximum total and mean partial water volumes in drainage systems of Hammerbach and Schmelzbach. FP1, FP2, FP3, FP4 and FP5 = mean flow path 1, 2, 3, 4 and 5.

System	Volume of water in 10^3 m^3					
	Total(max)	FP1	FP2	FP3	FP4	FP5
Hammerbach	40.0	16.2	8.0	5.5	5.3	5.0
Schmelzbach	25.5	7.3	7.0	8.3	2.9	–

6.1.4.5. Prediction of Tracer Transport

The linear regression analysis applied to the Hammerbach system showed that the partial flow rates Q_i can with a satisfactory accuracy be estimated as a linear function of the total discharge Q:

$$Q_i = f(Q) = \beta_i \cdot Q \,. \qquad (6.19)$$

Results of the calculation of β_i for the four flow subsystems are shown in fig. 6.18–6.21 and agree well with the mean values of r_i found from individual experiments (Tab. 6.9).

As the system was found to be always saturated, eq. (6.19) gives the possibility to predict the mean transit time of water for single flow paths for different steady state flow conditions. Taking additionally into account nearly constant dispersivities for different flow paths, the model proposed in this study can be used to predict

HAMMERBACH

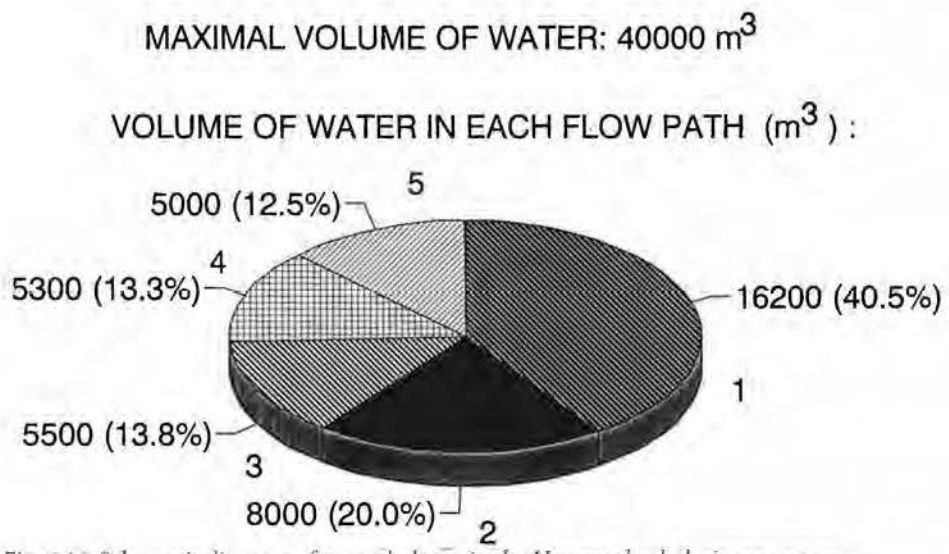

Fig. 6.16: Schematic diagram of water balance in the Hammerbach drainage system.

SCHMELZBACH

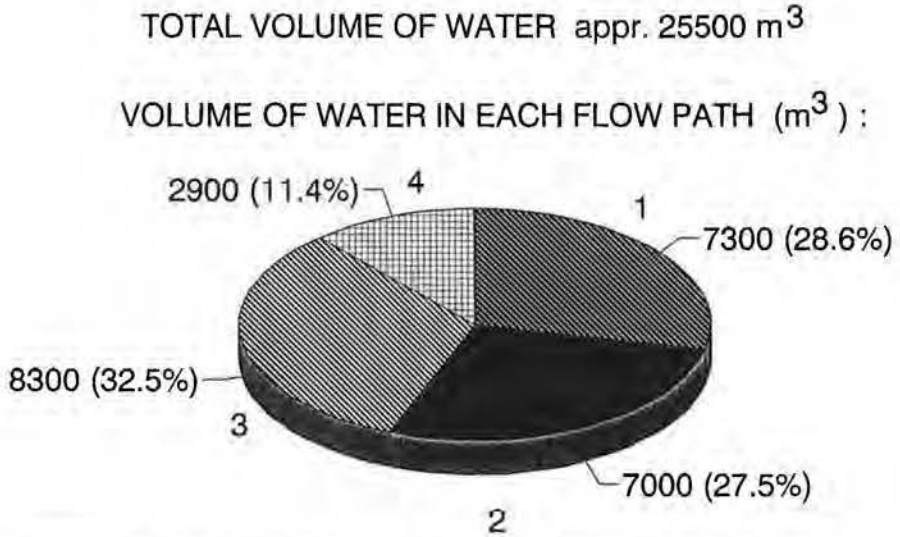

Fig. 6.17: Schematic diagram of water balance in the Schmelzbach drainage system.

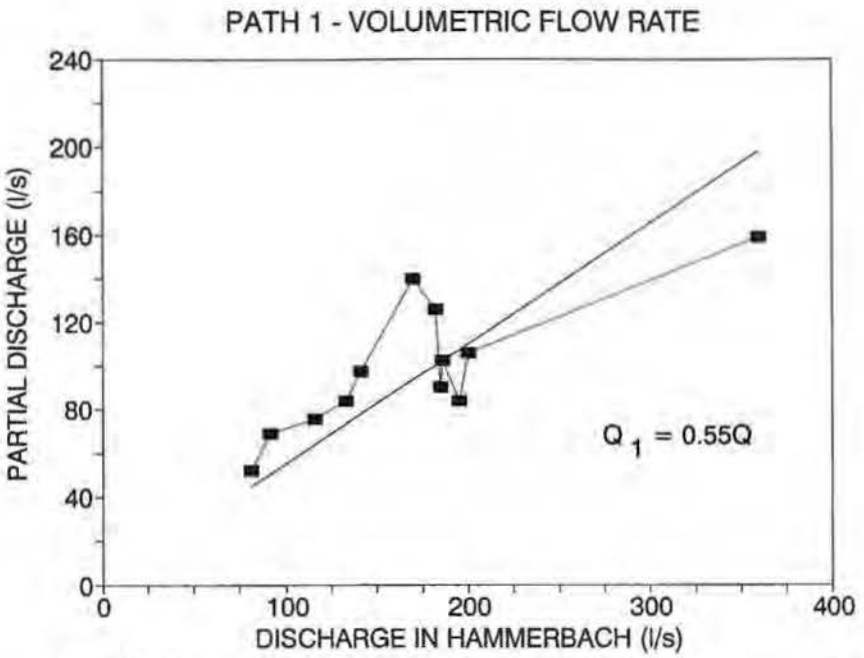

Fig. 6.18: Partial discharges in the 1st flow path as a function of the whole discharge $Q_1 = f(Q)$ approximated using linear regression.

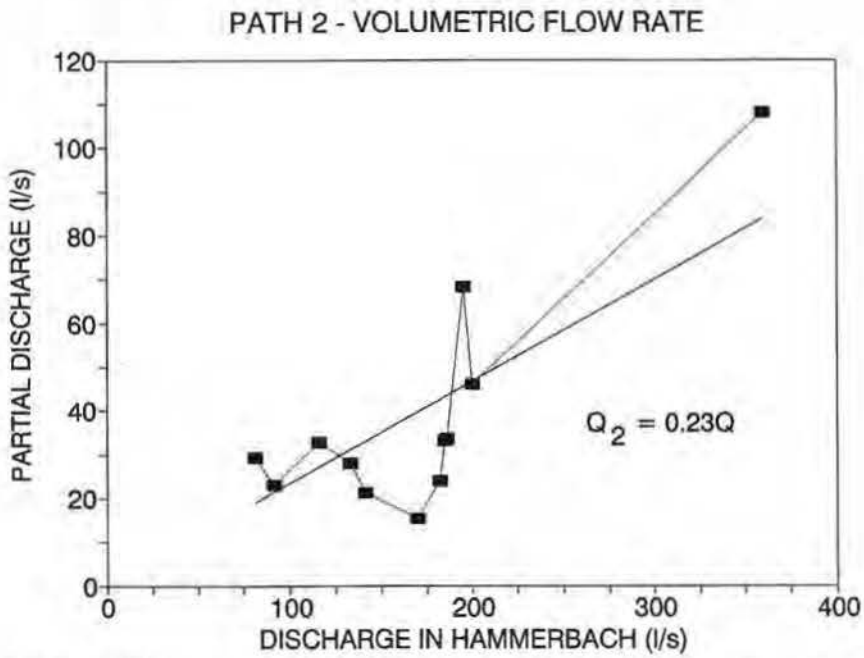

Fig. 6.19: Partial discharges in the 2nd flow path as a function of the whole discharge $Q_2 = f(Q)$ approximated using linear regression.

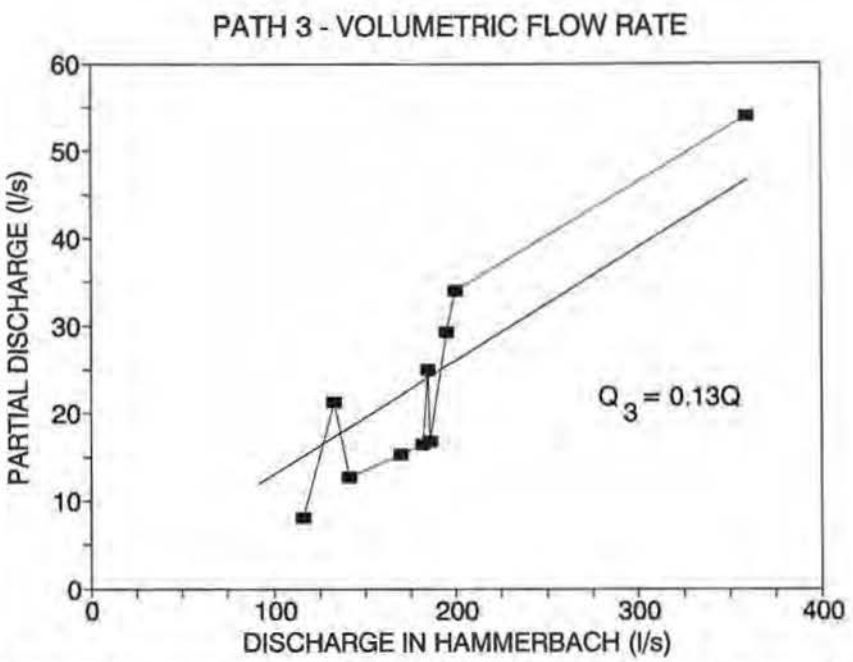

Fig. 6.20: Partial discharges in the 3th flow path as a function of the whole discharge $Q_3 = f(Q)$ approximated using linear regression.

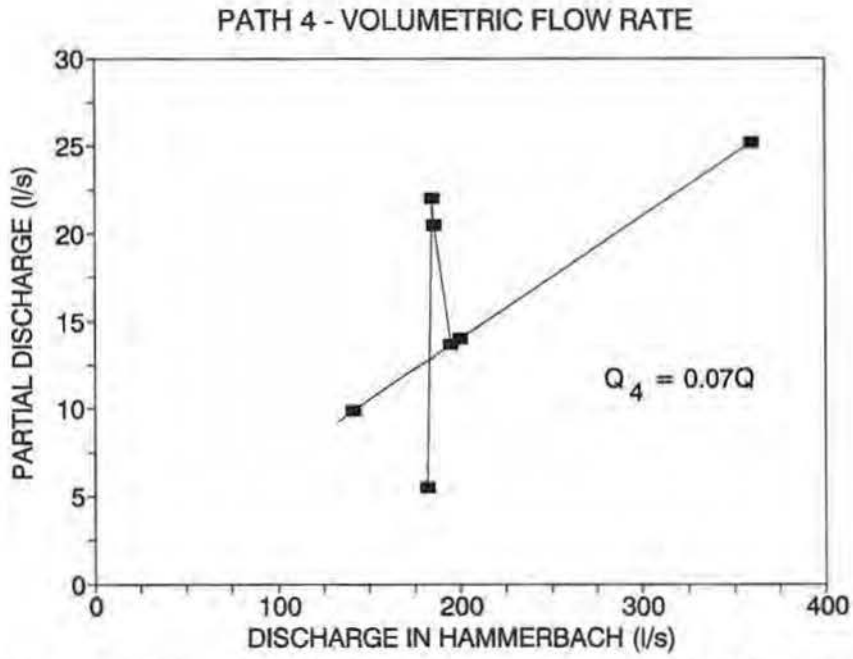

Fig. 6.21: Partial discharges in the 4th flow path as a function of the whole discharge $Q_4 = f(Q)$ approximated using linear regression.

Tab. 6.9: Mean portions of volumetric flow rates Q (discharge) flowing through different flow subsystems in drainage systems of Hammerbach and Schmelzbach. FP1, FP2, FP3, FP4 and FP5 = mean flow path 1, 2, 3, 4 and 5.

System	Portion of discharge in flow paths					
	Total	FP1	FP2	FP3	FP4	FP5
Hammerbach	1.0	0.55	0.22	0.12	0.07	0.04
Schmelzbach	1.0	0.45	0.27	0.21	0.06	0.01

the travel time of conservative solute (tracer or pollutant) in the Lurbach system for any state of steady flow, i.e. for any Q if this Q can be assumed as constant during the solute travel.

6.2. Modelling of Environmental Tracer Data

(P. MALOSZEWSKI, T. HARUM, H. ZOJER)

6.2.1. Introduction

The idea of the groundwater flow through a karstic catchment system was presented by R. BENISCHKE et al. (1988), K.-P. SEILER et al. (1989) and D. RANK et al. (1992) and is shown here in fig. 6.22. Generally, a karstic reservoir is approximated by two different flow systems.

The first system consists of a fissured-porous aquifer and has to be considered as a double porosity medium including mobile water flowing through the fissures and quasi stagnant water, or stagnant, in the microporous matrix. The surface of

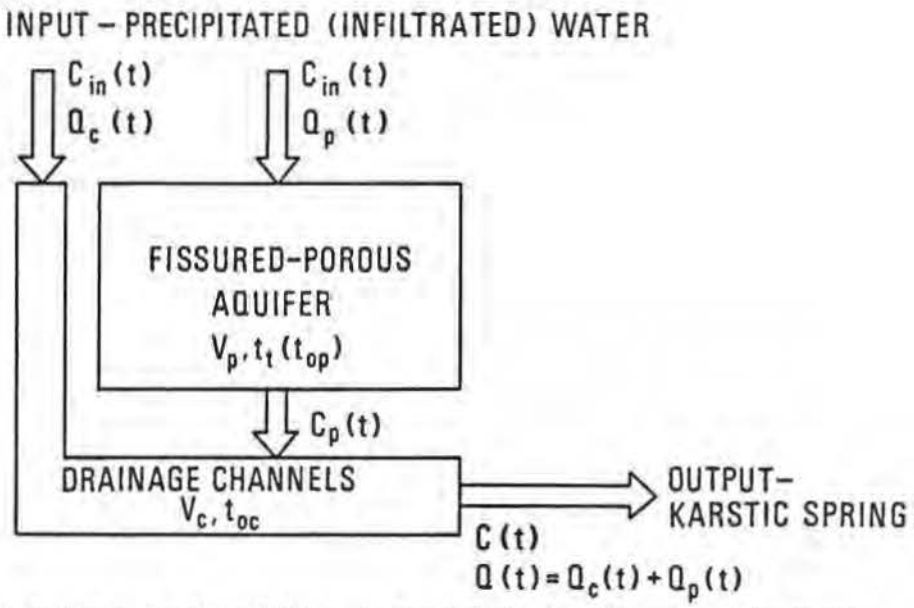

Fig. 6.22: Conceptual model of the water flow in the karstic catchment area (after D. RANK et al., 1992).

the system is in most cases the recharge zone of the catchment area. This system may be partially unsaturated and have a much greater storage volume than the second one. The tracer flow through this system is described by the dispersion-convection transport equation coupled with the diffusion term describing diffusive exchange of tracer between mobile and stagnant water (P. MALOSZEWSKI & A. ZUBER, 1984, 1991). The second system consists of the drainage channels. They can be connected directly with the surface of the catchment area through the sinkholes. The storage volume of this system is relatively small and the water flow very rapid. The tracer transport can be approximated by the piston flow model (taking into consideration the environmental tracer data) or by the dispersion model (for artificial tracer experiments).

The environmental tracer data were collected in the area under investigation mainly for a better understanding of the circulation of water in the system and for a quantitative estimation of the water storage volumes in different parts of the system. The mathematical modelling of the water flow through the drainage part of the system was performed on the basis of information obtained from the artificial tracer experiments described in detail in the previous chapter. This means that the drainage part of the system was considered as known for the modelling of environmental tracer data.

6.2.2. Basic Hydrologic Information

According to information given in chap. 2.3. the whole catchment area of Tanneben ($S_T = 22.8$ km^2) consists of schists of low permeability in the Lurbach catchment area ($S_{LB} = 14.5$ km^2) and of the karst massif of the Tanneben Plateau ($S_{PL} = 8.3$ km^2). The whole catchment area of Tanneben is drained by two karstic springs Hammerbach and Schmelzbach with the mean discharge $Q_{HB} = 192$ l/s and $Q_S = 97$ l/s, respectively.

Assuming that the whole groundwater system is closed (there is no underground water inflow or outflow) the mean yearly infiltration rate of $I = 400$ mm/a can be easily calculated from the sum of both discharges and the surface of the catchment area. For the mean annual precipitation equal to 900 mm/a it yields the mean evapotranspiration of about 500 mm/a which agrees reasonably with calculated 440 mm/a based on the classical method after TURC (s. chap. 2.3.6.).

Assuming the mean infiltration rate as constant on the whole surface of Tanneben, the volumetric flow rate of water infiltrating in the Tanneben Plateau and flowing through the karst massif into both springs is estimated to be $Q_{PL} = I \cdot S_{PL} = 105$ l/s. The water infiltrating through the surface of the Lurbach catchment area is collected by the Lurbach creek and inflows with $Q_{LB} = 184$ l/s (computed from the water balance equation, s. chap. 2.3.) directly through the sinkhole into the drainage channel systems of Hammerbach and Schmelzbach springs.

The mean discharge of each spring consists of two water components: first – Lurbach creek water, and second – water infiltrating in the Tanneben plateau and flowing through the karst massif.

6.2.3. Environmental Tracer Data

The measurements of the environmental tracer tritium were used to estimate water volumes in the karst massif of the Tanneben plateau and in the porous-fissured aquifer of the Lurbach catchment area. The tritium input function $C_{inp}(t)$ was calculated

for each year as a yearly weighted mean based on the simple infiltration model given by G.H. DAVIS et al. (1967):

$$C_{inp}(t) = \sum_{i=1}^{12} (P_i C_i \alpha_i) / \sum_{i=1}^{12} (P_i \alpha_i), \qquad (6.20)$$

where P_i is the mean monthly precipitation amount, C_i the tritium content in precipitation and α_i the infiltration coefficient for the i-th month, respectively. It is assumed that the infiltration coefficients have the constant values α_S and α_W in two periods: summer (from April to September i = 4,9) and winter (from October to March i = 10,3), respectively, and that these values do not change from year to year. For the hydrological situation in the Tanneben catchment area the summer to winter infiltration coefficient was assumed $\alpha = \alpha_S/\alpha_W = 0.5$. J. GRABCZAK et al. (1984) have shown that if $\alpha \geq 0.4$, the result of modelling is nearly independent of the assumed value of α. The input function was calculated for the period 1950–1990 taking monthly precipitation amounts from the meteorological station of Frohnleiten (about 20 km to N in the Mur valley) and the tritium contents in precipitation for the Vienna station.

The output functions, $C_{out}(t)$ were the tritium concentrations in the water outflowing from different parts of the system: in the Lurbach creek at the sinkhole, in the Hammerbach and Schmelzbach springs and in a small spring (Laurins spring) in the vicinity of the Schmelzbach spring.

6.2.4. Mathematical Modelling

For the groundwater system being in a steady state (constant volumetric flow rate Q through the system and constant volume of water V in the system) the relation between input and output environmental tracer concentrations is given by the well known convolution integral (P. MALOSZEWSKI & A. ZUBER, 1982)

$$C_{out}(t) = \int_0^\infty C_{inp}(t-\tau)\, g(\tau) \exp(-\lambda\tau) d\tau, \qquad (6.21)$$

where λ is the radioactive decay constant (0.0564 a^{-1} for tritium) and $g(\tau)$ is the so-called weighting function or transit time distribution function which for the dispersion model is (P. MALOSZEWSKI & A. ZUBER, 1984):

$$g(\tau) = \frac{1}{\tau} \frac{1}{[4\pi (P_D)^* (\tau/t_t)]^{1/2}} \exp\left[-\frac{(1-\tau/t_t)^2}{4 (P_D)^* (\tau/t_t)}\right], \qquad (6.22)$$

where t_t is the mean transit time of tracer and $(P_D)^*$ is the artificial dispersion parameter describing the variance of the distribution of the transit times. Both parameters are the fitting parameters of the model. Their values are found by fitting the theoretical output concentrations calculated using eq. (6.21) with (6.22) to the tritium concentrations measured in the output.

In the saturated porous media, the mean transit time of tracer t_t is equal to the mean transit time of water:

$$t_0 = V_m/Q, \qquad (6.23)$$

where V_m is the volume of the mobile water in the system. In a karst massif considered as a double-porosity medium the mean transit time of tracer t_t can be used to estimate the total volume of water in the system (V_{tot}), i.e. the sum of the mobile

water in karstified fissures (V_m) and the stagnant water in the microporous rock matrix (V_{im})

$$t_r = V_{tot}/Q = (V_m + V_{im})/Q \,. \tag{6.24}$$

The above equation is valid only when the mean transit time of water is long enough (t_0 greater than about one year), see P. MALOSZEWSKI & A. ZUBER (1984). After determining the mean transit time of tracer (or water) from the environmental tracer data it is easy to find the volume of water in the system by applying eq. (6.23) or (6.24) for the known volumetric flow rate through the system Q. The surface of the catchment area (S), the mean total porosity (n), and the mean thickness of the aquifer (H) are related by:

$$H = Qt_r(Sn) \,. \tag{6.25}$$

6.2.5. Results of Modelling

The best fit of the theoretical tritium output curve to the concentrations measured in **Lurbach creek,** shown in fig. 6.23, was obtained with $(t_r)_{LB} = 4$ a and $(P_D)^* = 0.15$. By applying eq. (6.24) to the mean discharge of Lurbach creek $Q_{LB} = 184$ l/s it yields the mean total volume of water (stagnant and mobile) in this porous-fissured catchment area of about $V_{LB} = 23.2 \times 10^6$ m^3. For the aquifer thickness of 4–6 m and the catchment area of 14.5 km^2, the mean total porosity of weathered zone of schists calculated from eq. (6.25) is n = 0.3 which agrees well with the estimated from the geological data.

In both karstic springs the interpretation of tritium data is more complicated because the output concentrations result from mixing of two different flow components. The **Laurins spring** which collects water only from the karst massif (free of additional components) has shown the mean transit time of tracer of about 40 a (s. fig. 6.24). Unfortunately this spring is not representative for the whole karst massif. The total mean volumetric flow rate of water through the karst massif was estimated to be $Q_{PL} = 105$ l/s but this water flux is divided into two components $(Q_{PL})_{HB}$ and $(Q_{PL})_S$ of the Hammerbach and Schmelzbach springs, respectively. The artificial tracer experiments have shown that Schmelzbach water is free of the Lurbach creek water as long as the discharge of Hammerbach spring was lower than 200 l/s. This finding allows to calculate the mean discharge of Schmelzbach spring resulting from the infiltration of water into the Tanneben plateau $(Q_{PL})_S$ as equal to about 35 l/s. Consequently, the rest of water flux given as

$$(Q_{PL})_{HB} = Q_{PL} - (Q_{PL})_S = (105 - 35) = 70 \text{ l/s}$$

is the water flux through the karst massif flowing to the Hammerbach spring. The mean discharge in the Schmelzbach spring was $Q_S = 97$ l/s giving a portion of Lurbach creek water in this spring equal to

$$(Q_{LB})_S = Q_S - (Q_{PL})_S = (97 - 35) = 62 \text{ l/s} \,.$$

The portion of the Lurbach creek in the Hammerbach spring is then equal to

$$(Q_{LB})_{HB} = Q_{LB} - (Q_{LB})_S = (184 - 62) = 122 \text{ l/s} \,.$$

Taking into account tritium concentrations measured in the **Schmelzbach spring** only when the discharge of the Hammerbach spring was lower then 200 l/s, the mean

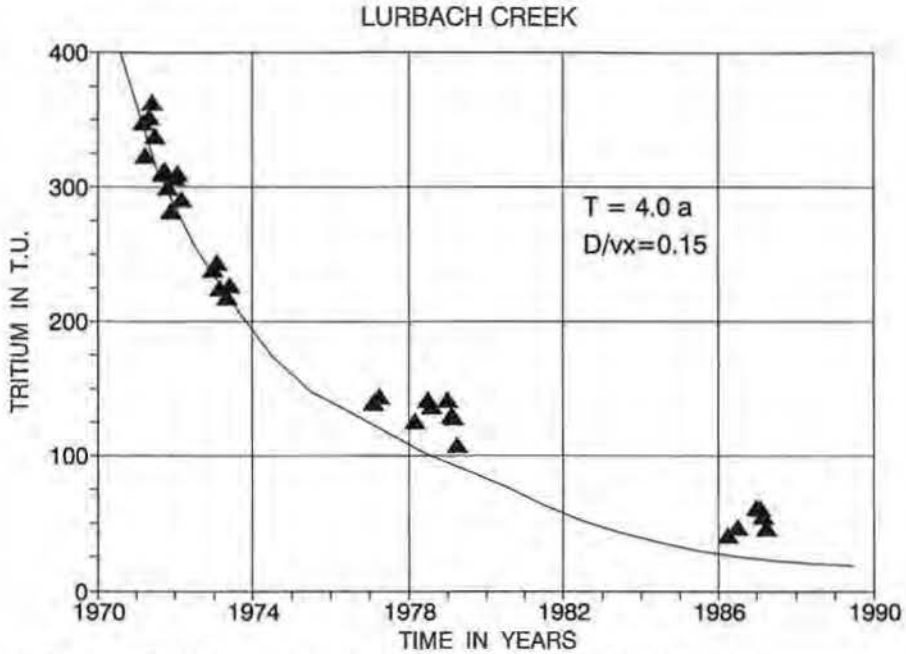

Fig. 6.23: Theoretical ^3H-output concentration curve obtained as the best fit to the concentrations measured during base flow conditions in the Lurbach creek.

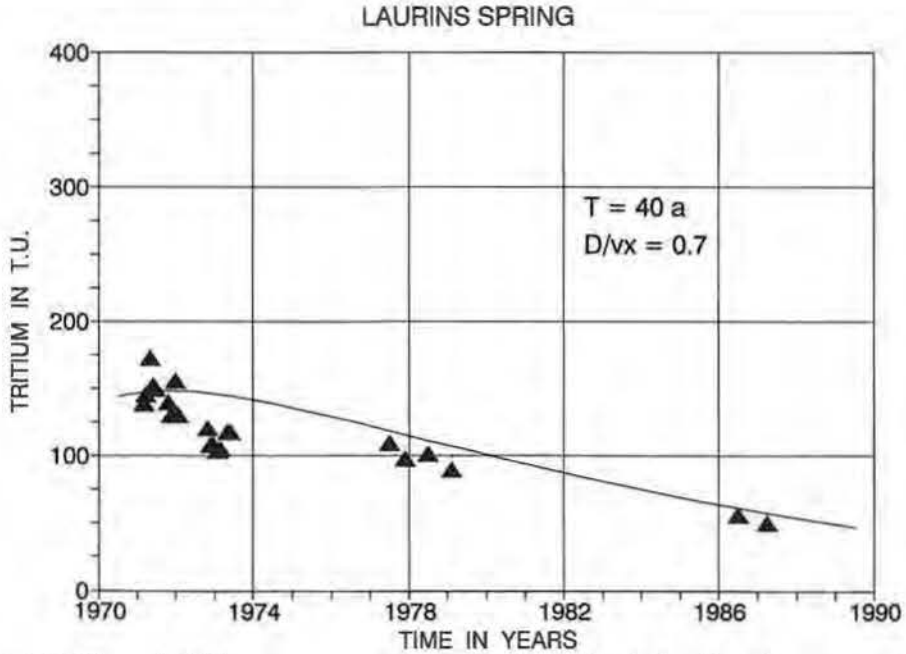

Fig. 6.24: Theoretical ^3H-output concentration curve obtained as the best fit to the concentrations measured in the Laurins spring (Schmelzbach system).

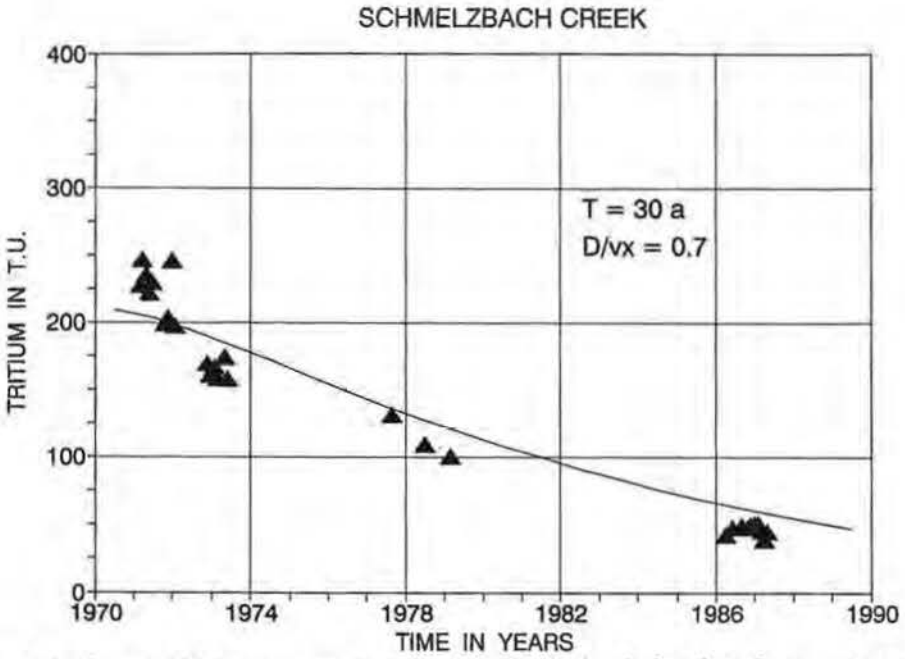

Fig. 6.25: Theoretical ^3H-output concentration curve obtained as the best fit to the concentrations measured during low flow conditions in the Schmelzbach spring (free of Lurbach component).

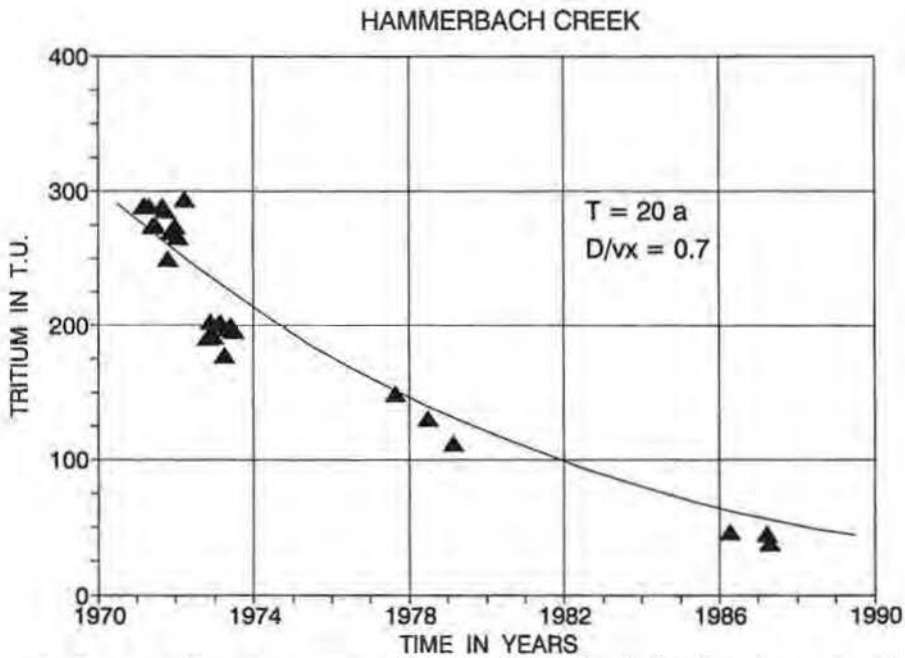

Fig. 6.26: Theoretical ^3H-output concentration curve obtained as the best fit to the concentrations measured during base flow conditions in the Hammerbach spring.

transit time of tracer equal to 30 a was found (s. fig. 6.25). It shows that the discharge of the Schmelzbach spring – which is draining the part of the karst massif like the Laurins spring – has even at low flow conditions (i.e. without connection to the Hammerbach system) a younger water component than the Laurins spring. This younger component probably consists of water from the two sinkholes Katzenbach and Eisgrube their connection with the Schmelzbach spring being proved by tracing experiments (s. chap. 5.2.).

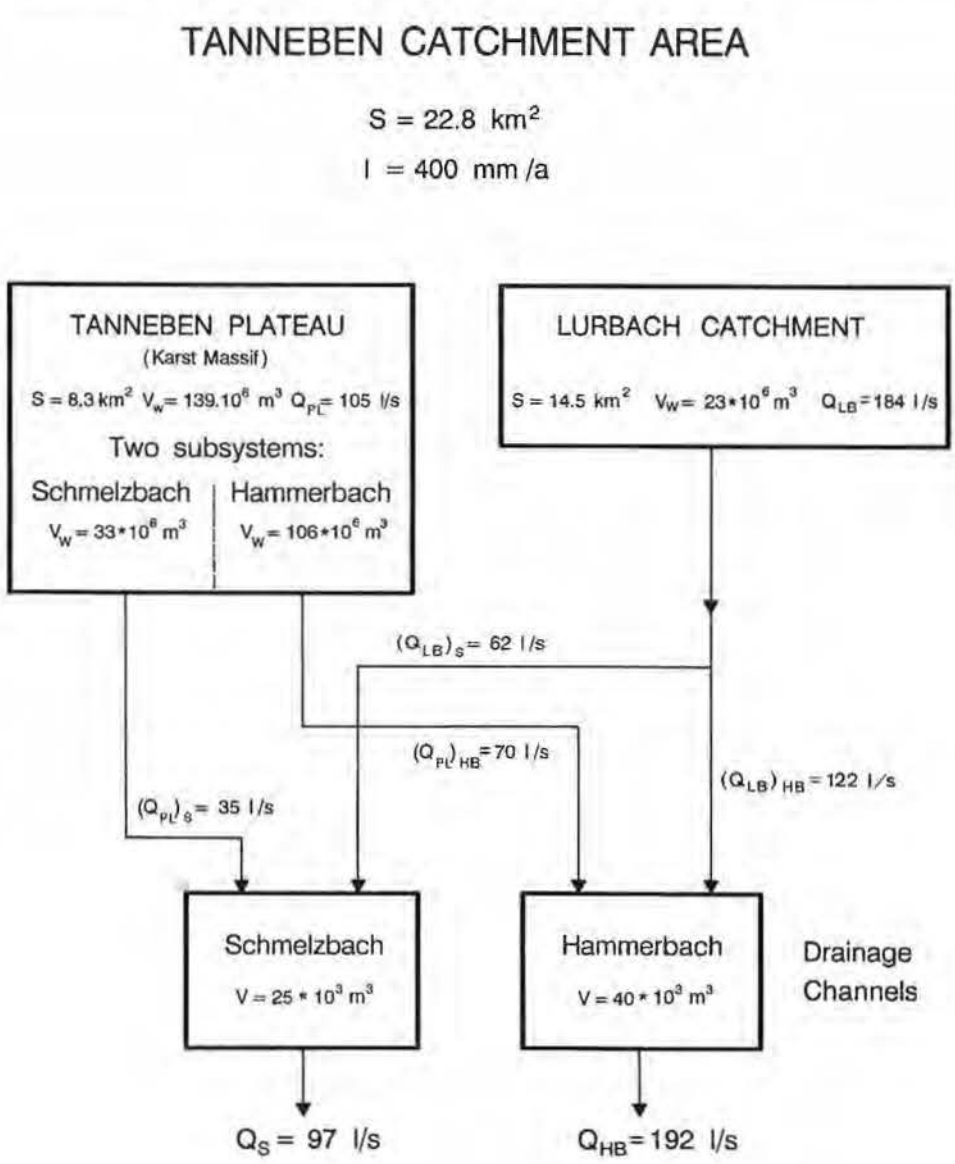

Fig. 6.27: The reservoir features of the Tanneben karstic catchment basin found using artificial and environmental tracer data (s. text).

The volume of water in the system observed from the Schmelzbach spring was then calculated to be

$$(V_{PL})_S = 33.1 \times 10^6 \text{ m}^3 .$$

In the **Hammerbach spring** the mixing of two components (Lurbach and karst massif water) is permanently observed. The mean transit time of tritium found there was equal to **20 a** (the best fit curve is shown in fig. 6.26). Assuming the good mixing of water in the spring, the mean transit time is the weighted mean value of the transit times of two water components

$$(t_t)_{HB} = [(Q_{LB})_{HB} \cdot (t_t)_{LB} + (Q_{PL})_{HB} \cdot (t_t)_{PL,HB}]/Q_{HB} . \qquad (6.26)$$

After rearrangements the mean transit time of water component flowing through the karst massif to the Hammerbach spring is

$$(t_t)_{PL,HB} = [(t_t)_{HB} \cdot Q_{HB} - (Q_{LB})_{HB} \cdot (t_t)_{LB}]/(Q_{PL})_{HB} . \qquad (6.27)$$

Putting $(t_t)_{HB} = 20$ a, $(t_t)_{LB} = 4$ a, $Q_{HB} = 192$ l/s, $(Q_{LB})_{HB} = 122$ l/s and $(Q_{PL})_{HB} = 70$ l/s one obtains finally $(t_t)_{PL,HB} = 48$ **a**. It yields from eq. (6.24) the volume of water in the karst massif system of the Hammerbach spring $(V_{PL})_{HB}$, **equal to** 106×10^6 **m³. The total volume of water in the karst massif** V_{PL}, **the sum of** $(V_{PL})_{HB}$ **and** $(V_{PL})_S$, **is about** 139×10^6 **m³.** For the mean thickness of karst massif of 340 m the **total porosity of 4.9%** (water saturated – mobile and stagnant) can be estimated from eq. (6.25).

Finally, it is interesting to point out that the ratio of water fluxes through the karst massif to the water fluxes through the drainage channels was nearly 1 : 2 (105 : 184), whereas the ratio of the water volumes in the karst massif to the water volumes in the drainage channels was about 2,000 : 1 (139,000 : 65). Figure 6.27 shows the conceptual model with the values of water fluxes and water storage volumes in the area under investigation.

7. Summary and Conclusions

7.1. General Remarks (H. ZOJER)

The common use of environmental and artificial tracer methods has been incorporated into the concept of karst water research in the investigated area. It shows very clearly, that tracer studies are important adjuncts to other more conventional methods. All these considerations lead to their methodological application in two main fields of karst hydrogeology, the calculation of subsurface water storage and the localization of recharge areas of springs and wells. In this reference quantitative aspects in karst hydrogeology can be obtained in creating tracer models expressed as a mass transport.

The results of artificial tracing experiments on the one hand and environmental tracer studies on the other simulate some contradictions, since tracers are usually injected at locations with a quick water input from the surface. This gives the impression of a short subsurface turnover time, but not representing the general infiltration conditions in the total recharge area. The environmental tracers on the other hand, measured at the outlets of the system, refer to the whole drainage and

to the total aquifer. Therefore a separation of individual recharge from local sites is not possible on the basis of natural tracers.

7.2. Geology and Karst Development (R. BENISCHKE)

The geological background of the study (s. chap. 2.1.) area with a thick sequence of very pure limestones (Schöckel limestone) offers the best presuppositions for an intense karstification. The limits of the karstification in the area are set by the surrounding geological units as in the S (Mitterbach/Taschen) or in the E (basin of Semriach) with an uplifted part of schists. Also in the underground (visible in the cave Lurgrotte) there are some parts which show that the karstification has reached at several places the geological basis.

Karstification must have at first karstifiable rocks where it acts in its initial state mainly by corrosion, later on if greater drainage paths could be developed the influence of linear erosion increases and becomes dominant over corrosion in the case of vadose flow. Such parts can be seen very well in the cave Lurgrotte.

But karstifiable rocks are not sufficient for karst development (s. chap. 2.2.). There must be also a hydraulic gradient which keeps the water in the aquifer flowing. This will happen during landscape evolution whereat the local or regional base level will be lowered (originating from tectonic movements or during tectonic stable times only by linear erosion). These alternating processes of stability and erosional phases lead to the development of altitudinal levels (plains, terraces) and therefore to the development of horizontal caves bound to distinct horizons. This can be seen very well in the precipices of the Peggauer Wand with its numerous caves. The main accessible cave galleries developed during the interglacials with their excessive amount of water during melting periods. Such processes favoured the karstification because the area never was glaciated but was within the periglacial arc at the eastern and southeastern border of the Alps. Each time a horizontal cave system was developed the next erosional phase in the foreland initiated a retrogressive underground karstification leading to a step-like development (comp. the three main levels in the Lurgrotte). Deviations from this clear process are caused by lithological differences of the bedrock (karstification acts differently on pure limestone or limestone shale) or the predominance of tectonic structures, which can stimulate the retrogressive erosion or corrosion at the time they are included into this process. In any case these processes lead after an initial phase to a **self-amplification**, i.e. that a dominant active flow path drains more and more the minor channels, therefore it can be enlarged more than the other. The Lurgrotte represents the final result of this process, whereas the Hammerbach spring with its phreatic system behind the outlet shows still a younger stage of development or became phreatic again during and after accumulation of the Würm terrace (the Mur valley was eroded to a deeper level before).

Because the karstifiable rocks reach significantly below the present valley floor and due to the observed karstification status it is possible that a part of the Hammerbach system drains directly or through deeper zones of the limestone basement to the porous aquifer of the Mur valley (s. chap. 7.3.).

The knowledge about underground karstification is limited to accessible caves – about 300 are registered and explored – but until now it was not possible to access the top of the phreatic zone, because all parts of the cave Lurgrotte and other caves going deeper are blocked by sediments or they are narrow unpassable joint-bound

passages. The Blasloch near the upper entrance of the Lurgrotte in Semriach ends about 60 m below the level of the Lurbach in a still vadose part which confirms that the phreatic zone must lie deeper. All the presently active sinkholes in the Lurbach bed or in the cave Lurgrotte cannot be followed further, but after the discovery of the Blasloch and other caves in the north-faced wooded slope of the Tanneben it seems that there exist several other cave systems with their entrances today covered by blocks or debris which are unaccessible by cavers. Some of them act easily as sinkholes (as found near the sediment barrage upstream of the upper entrance of the Lurgrotte in Semriach). The Blasloch is only a representative example for older stages of karstification in that area. It seems that the whole gorge-like part of the lower Lurbach down to the entrance of the Lurgrotte originated from successive break-down of an old cave system.

Therefore the Lurbach recharges through a number of sinkholes (older now broken-down cave passages) the karst massif. Because it springs in a schist area the type can be classified to be an **allogenic recharge**, which is probably the main source. Others at the northern slope of the Eichberg are of minor significance. On the top of the karst massif there is over extended areas a thick cover of tertiary sediments, which leads to a **diffuse recharge** into underground. Between them exist some transitional types which are not explicitely classified here. Sediment fillings with high percentage of fine grained components (clay, silt etc.) known from the Lurgrotte or from excavations in dolines show that the sediments contribute also to retardation of infiltration water as micro-fissures do. This is indicated by significantly longer transit times of tracers injected at the top of the karst massif and by the isotopic composition of percolation waters (representing much older components in the caves).

There are still open questions about the detailed development of the surface and underground drainage system during the course of time. An example is the Bassgraben, the uppermost part of the Badlgraben, which crosses a Schöckel limestone area. It is known that this small stream running in bedrock disappears often near the junction of the Mühlbachgraben (a tributary from the N) at a significant W–E running fault zone, but it is not known whether the water contributes to the Schmelzbach in the Lurgotte or only to the Badlgraben. If it contributes to the Schmelzbach this would require a revision of the water balance (but from the relatively small catchment area of the Bassgraben only to a minor extent). Other questions are about details of the beheading of the upper Lurbach in the basin of Semriach and its relationship to karst development in general and particularly to cave development at the eastern border of the karst massif.

7.3. Conclusions from the Tracing Experiments (R. BENISCHKE)

Conclusion on tracer methods:

As it was pointed out in chap. 5. and as the results of the tracing experiment 1988 show **it is absolutely necessary to standardize the analytical methods and to observe carefully analytical boundary conditions.** In some cases the variations in the results are up to 100% and more. It is clear that such variations can also be taken as examples what problems and what analytical restrictions can arise. It shows furthermore that particularly bacteriological and/or chemical contaminated waters causes a lot of problems like degradation effects, that improper storage conditions of samples or too long storage times prior to analysis give wrong results. For example,

under the assumption that only one laboratory would have analyzed one tracer probably erroneous results would be obtained. Subsequently this would lead to a wrong interpretation and later on to wrong ideas on the hydrogeological conditions of the study area, and to a wrong basis for calculations used in mathematical modelling.

Again, **standardized methods for sampling, storage, sample treatment, analytics and time of anlysis have to be established,** otherwise experiments can fail and all the effort and expenses would be senseless.

Conclusions on regional conditions:

All tracing experiments carried out since 1927 increased the knowledge about drainage paths in the underground. The results contributed to knowledge on the regional and local distribution of tracers and therefore of infiltration waters. New results from tracing experiments lead to increased efforts in speleological investigations to verify these results directly. Therefore the results of speleological research will contribute to the knowledge about the underground drainage system but is limited to accessible cave passages. But nevertheless – as the discovery of the Blasloch shows – surprises are always possible. It is of interest but still not known in detail that the diversion zone for overflow possibilities from the Hammerbach system to the Schmelzbach must be situated in the region above the Schmelzbach spring (SU). This was indicated at first by tracing experiments. What we can see directly is the existence of several overflow channels (all situated at the southern side of the cave galleries) which become successively active under increasing discharge (above 200 l/s) of the Hammerbach spring, but all attempts to access those channels failed until now. Direct explorations of the narrow siphon tubes (like Schmelzbach spring in 1967 or the Hammerbach outlet in the forties and again 1964) ended either in too narrow tubes or the water was to turbid and therefore it was too dangerous to enforce an access.

A generalized scheme is given in fig. 7.1, which summarizes all the available results of tracing experiments and the proved drainage connections between input and output points.

7.4. Karst Aquifer Hydrodynamics and Storage (T. HARUM)

The karst massif of Tanneben is being drained primarily by two karst springs, Hammerbach and Schmelzbach, which drain two karst aquifers with rather different hydrodynamic characteristics and discharge fluctuations. The results of the water balance (s. chap. 2.3.6.) show a relatively high real evapotranspiration with approx. 50% of the mean annual precipitation due to the densely forested karst plateau with dolines filled by tertiary sediments with lower infiltration capacity in comparison with alpine karst plateaus without vegetation. A deficit in the water balance of about 7% may be due to small amounts of exfiltration into the porous aquifer in the Mur valley, a too short observation period and/or errors in calculation of areal precipitation and evapotranspiration.

Concerning the hydrodynamic conditions three typical hydrological states can be deduced corresponding to three clearly distinguishable flow paths in the karst system not excluding possible minor flow systems (s. chap. 2.3.):

1) At discharges below the mean annual discharge of Hammerbach (about 200 l/s) both aquifer systems are completely separated. In this case the Hammerbach spring

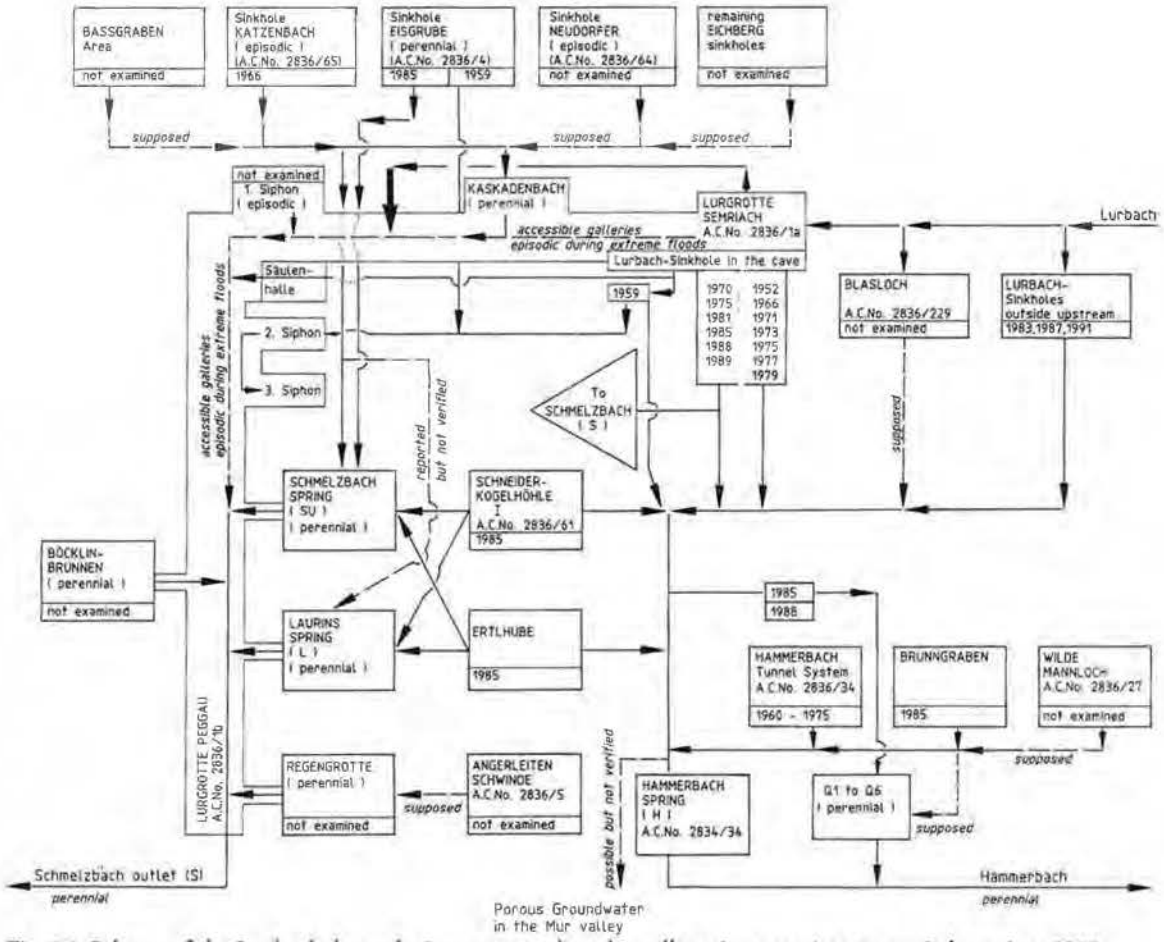

Fig. 7.1: Scheme of the Lurbach, karst drainage system based on all tracing experiments carried out since 1927.

is draining the total discharge of the Lurbach sinkhole (catchment area 14.5 km²) and the southern part of the karstified plateau of Tanneben (approx. 35% of total spring discharge). The isolated Schmelzbach aquifer drains the northern part of the plateau and two sinkholes with small discharges. **Under these conditions there exists no connection between the sinkhole of Lurbach and the two springs in the lower part of the Lurgrotte (Schmelzbach spring and Laurins spring).**

2) The overflow from the Hammerbach to the Schmelzbach aquifer becomes active at flow rates of the Hammerbach spring higher than the mean annual discharge. **Under these conditions the Schmelzbach spring is draining a portion of the water (mean portion approx. 33%) from the Lurbach catchment area (basin of Semriach).**
3) **Extreme floods take three different flow paths in the underground.** The greatest portion of Lurbach water flows directly through the accessible cave, resurges in the Schmelzbach at the cave entrance in Peggau and causes its extreme discharge fluctuations. A second portion flows through the sinkholes in the higher part of the cave to the Hammerbach aquifer where it is once more separated into two components, one flowing to the outlet of the Hammerbach spring and the other through the overflow zone to the Schmelzbach spring.

The Laurins spring being permanently isolated from Schmelzbach and Hammerbach system is draining waters from the unsaturated zone of the northern part of the karst massif.

The results of numerous tracing experiments carried out in the investigation area with injections into the Lurbach sinkhole showed that the flow velocities (V_{peak} = 0.99–3.94 km/d, $V_{centroid}$ = 0.86–2.13 km/d) depend significantly on the discharge of the Hammerbach spring (s. chap. 5.2.). Only during three experiments at high water conditions the tracers injected could also be detected in Schmelzbach spring (V_{peak} = 1.75–3.31 km/d, $V_{centroid}$ = 1.11–1.95 km/d). The total recoveries of the quasi-ideal tracers uranine and chloride increase with the discharge of the Hammerbach spring (from 15.6% at low water conditions up to 100%) which indicates that a portion of the traced water is stored over a longer time in microfissured zones and cave sediments at low water conditions and/or a nearly constant portion is flowing in a diffuse way in deeper parts of the Hammerbach aquifer into the porous aquifer in the Quaternary filling of the Mur valley.

The shape of all tracer breakthrough curves at both karst springs with long tailing parts and sometimes visible additional peaks indicates that they consist of a superposition of different curves corresponding to different flow paths (flow systems). Concerning the Schmelzbach system two different only episodically active flow paths are known (overflow zone from the Hammerbach aquifer and direct flow through the accessible part of the cave). Independent from the tracer used the results of modelling of the breakthrough curves distinguish between three and five flow paths for the Hammerbach system with different flow velocities and water volumes (s. chap. 6.1.). The last two flow paths are disputable due to the difficulties of modelling the end parts of the breakthrough curves with low concentrations close to the background.

Additional conclusions on the hydrodynamic conditions in both karst aquifers could be drawn on the occasion of a flood event during the period of the tracing experiment of the ATH-group in June/July 1988, where the contents of selected

chemical parameters and the stable isotope ^{18}O could be measured from samples taken in short intervals at the input (Lurbach sinkhole) and output (Hammerbach, Schmelzbach and Laurins spring). The fluctuations of these natural tracers during the runoff event gave informations about the processes of mixing of event water with "older" reservoir water and piston effects (s. chap. 4.). The flood of Lurbach arrived at the sinkhole one day after the injections. The tracers arrived – hydraulically stimulated – at the Hammerbach outlet in the same time as the discharge of the spring increased and exceeded after short time the "overflow level" of 200 l/s. Nevertheless all injected dissolved tracers could not be detected in Schmelzbach spring (s. chap. 5.1.). On the contrary the hydrochemical parameters measured during the runoff event and the appearance of the undissolved (floating) tracers, like microspheres and phages, in Schmelzbach spring indicated that during the flood Lurbach water was flowing to the Schmelzbach spring through the overflow zone (s. chap. 4. and 5.1.). This proves that the zone of episodically active overflow must be situated in the upper part of the Hammerbach aquifer.

The flow components in the discharges of both karst springs were separated by means of environmental isotopes and chemical parameters (s. chap. 4.4.). The volumes of event water (originating directly from Lurbach) computed for the period of the runoff event were in the range of about 42% of the total flow volume for Hammerbach and 46% for Schmelzbach. These results agree well with the volumes of the first flow path computed by modelling of the tracer breakthrough curves of all evaluable tracing experiments (s. chap. 6.1., Hammerbach 41%, Schmelzbach 29%). It can be assumed, therefore, that this event water volume calculated represents the portion of Lurbach water (input) which flows with short retardation through greater karst channels corresponding to the first flow paths FP1 of Hammerbach and also Schmelzbach system respectively to the outlets (s. chap. 6.1.). But the results with natural and artificial tracers (s. chap. 3., 4. and 5.) and of the evaluation of discharge recessions of input and output (s. chap. 2.3.4.) indicate also that an important portion of Lurbach water is stored over a longer time in microfissured zones and cave sediments.

The tracing experiments with injections into the active Lurbach sinkhole (i.e. injections directly into the karst aquifer) and the short-term investigations with natural tracers can only give informations about the flow conditions and residence times of the youngest flow components of the karst massif with relatively high flow velocities not including components with long residence times and quasistagnant water components (i.e. water which can only be discharged hydraulically stimulated) in the unsaturated zone (thickness 300–350 m). The comparison of the results of tracing experiments with those of the isotopic investigations (s. chap. 3.4. and 6.2.) show that only a small amount of precipitation water infiltrating on the forested karst plateau reaches with shorter residence time the flow channels of the saturated zone. Tracing experiments with injections in dolines on the plateau gave in spite of the long observation period only recovery rates in the range of 2–3% with flow velocities of V_{peak} = 151–168 m/d and $V_{centroid}$ = 48–106 m/d (s. chap. 5.2.). The mean residence times of the waters from the unsaturated zone computed by modelling of the tritium data (40 a for the Laurins spring, 48 a for the older flow component of the Hammerbach spring, total flow of the Hammerbach spring 20 a including the 4 a of the input of Lurbach, 30 a for the Schmelzbach spring for periods without connection with the Hammerbach system) confirm that a high portion of precipitation water infiltrated on the karst plateau is being stored over a longer time in

microfissured zones, fine-clastic cave sediments and in periodically inactive cave parts (s. chap. 6.2.). The Laurins spring representing this type of flow with high residence times computed from the tritium data after a longer observation period without fluctuations of the ^{18}O-contents on the other hand showed a sudden increasing of oxygene-18 at stable discharges during a cold winter period without karst water recharge by precipitation or snow melt. This "contradiction" to the results with tritium (if the exponential model is valid, no seasonal ^{18}O-fluctuations occur for water with mean residence times older than ~ 5 a) indicates that the different flow components in the thick unsaturated zone are not well mixed, the increasing of ^{18}O could be explained by the outflowing of older summer precipitation water.

The volume of water stored in the unsaturated zone of the karst massif is estimated by the isotopic investigations to be about 2000 times higher than the water volumes in the drainage channels. The total volume of water stored in the karst massif computed by the isotopic investigations is about 139×10^6 m^3 corresponding to a total porosity of 4.9% and the mean residence times mentioned before (s. chap. 6.2.). The analysis of discharge recessions by means of an exponential function after E. MAILLET (1905) gives as result a 93 times smaller volume of only 1.5×10^6 m^3 corresponding to a depletion time of the karst reservoirs of about 600 days (s. chap. 2.3.4.). These results seem to be contradictory but they can be well explained for two reasons:

1) In contrast to the analysis of discharge recessions including only the water volume which can flow out without hydraulic stimulation the volume computed by modelling of the isotope data includes also quasistagnant water which can only be discharged under increasing hydraulic head. Taking into account the high thickness of the unsaturated zone of the karst massif (about 300–350 m) and the fact that the volume of greater flow channels in karst massifs is usually significantly smaller than the volume of the microfissured less permeable zones the difference seems to be explicable.
2) The water volume calculated from the discharge recessions corresponds to an effective porosity of < 0.1%, a value which seems too low. An explication could be that the discharge recession periods without input due to precipitation or snow melt are usually too short in humid climates like in the area under investigation. It can be assumed, therefore, that the longest discharge recessions (30 days in the case of Lurbach system) include still parts of the karst reservoir with steeper recession limbs which do not reflect the reservoir depletion function of the reservoir parts with the highest storage capacity. The comparison of the depletion coefficients of the Lurbach system with those computed from long discharge recession limbs of karst springs in the semiaride climate of Central and Eastern Peloponnesus (A. MORFIS & H. ZOJER, 1986) shows that the depletion coefficients of these springs mentioned at last are partially about 10 times lower reflecting the depletion characteristics of the reservoir parts with higher storage capacity more significantly.

A summary of the results of the research study of the Lurbach karst aquifer shows that an intensive knowledge of the hydrodynamic conditions in karst aquifers with extremely different residence times of the flow systems is only possible by combination of various hydrogeological methods each of them giving only partial informations about the flow conditions and flow systems of the karst aquifer. Concerning future hydrogeological investigations in karst regions an intensification primarily

of sampling programs with measurement of environmental tracers (hydrochemistry, environmental isotopes) in short intervals, the execution of tracing experiments at different hydrological conditions and last but not least intensive hydrological observations with high accuracy seem necessary in order to extend our knowledge of the complex flow conditions.

7.5. Recharge Area of Springs (H. ZOJER)

The localization of recharge by means of combined tracer methods may be considered as an essential hydrogeological application. The altitude effect of the stable oxygen isotope has been used to determine – at least relatively – the mean elevation of recharge areas between the shallow groundwater of the Mur valley and the basin of Semriach. The long-term chemical analyses including the calculation of saturation indices help together with the knowledge of lithological structures to distinguish the time-dependend range of the underground distribution of Lurbach to Hammerbach and Schmelzbach system. Finally, the tracing experiments solved a number of questions with regard to local underground connections (e.g. Eisgrube, Katzenbach etc.).

The recharge area of Lurbach can be easily determined by the geological and morphological features. The mean altitude is located at about 870 m and the infiltration capacity is very limited because of fine weathered material of the underlaying schist formation effecting a high part of surface flow. These circumstances might be the reason that the mean ^{18}O-value of Lurbach cannot be supposed as representative for the whole runoff of the catchment area. The subsurface runoff of a however local NW-part of the basin is represented by the drainage outlet in the Eisgrube (Fig. 3.9) due to expected lower extent of fluctuations.

The subsurface distribution of Lurbach in the Tanneben karst massif is documented by chemical and isotopic data in a good coincidence. **Hammerbach** generally shows a mixture of infiltration from the Tanneben plateau and Lurbach input, as it is illustrated in fig. 3.7 as a mixture of surface water and karst water from the unsaturated zone. The mean altitude of Hammerbach recharge is therefore only slightly lower than that of Lurbach. Concerning the **Schmelzbach** there exist seasonal variations of the recharge dynamics. During winter time and generally at low water conditions Schmelzbach is alimentated from the karst plateau and shows similar characteristics like Laurins spring (p_{CO_2}, Ca/Mg ratio). In case of temporary overflow the hydrodynamic parameters change, Ca-content decreases due to dilution effect, the same occurs for p_{CO_2} according to the increasing influence of surface water and the oxygen-18 curves of H + S become a parallel course.

Laurins spring on the other hand shows a supersaturation with respect to calcite deriving from relatively high offer of carbon dioxide during the vegetation period. No mixture with surface water can be stated by the chemistry.

7.6. Future Aspects (H. ZOJER)

For future aspects in karst hydrogeology the combined use of tracer methods should be still more incorporated in scientific and applied studies. It is evident, that a big progress has been made in this particular field within the last decade, a critical comparison with other hydrological method is essential for the future.

Another point which has to be stressed is the development of models. As most of the tracers are dissolved solids or – like isotopes – are inserted into the atomic structure the transport of mass must be solved on a mathematical – physical basis. By modelling it can be described more detailed the undoubtly big differences in the flow dynamics expressed by various flow components.

The knowledge of regularities in karst water flow can be obtained successfully by the investigation of short-term events (storm event, snow melt event) and analysis of the hydrograph recession. Some demands on this occasion are – if possible – in situ detection of investigated parameters, or to select most appropriate time intervalls for water sampling.

References

ATKINSON, T.C. (1977): Carbon Dioxide in the Atmosphere of the Unsaturated Zone: an Important Control of Groundwater Hardness in Limestones. – Journal of Hydrology, **35**, 111–123, Amsterdam.

BARNES, B.S. (1939): The Structure of Discharge Recession Curves. – Trans. Am. Geophys. Union, **20**, 721–725, Washington.

BATH, A. (1980): TI-59-program for calculation of calcite, dolomite and gypsum saturation in solution. – Rep. No. WD/ST/80/3, Instuitute of Geological Sciences, Wallingford.

BATSCHE, H., F. BAUER, H. BEHRENS, K. BUCHTELA, F. HRIBAR, W. KÄSS, G. KNUTSSON, J. MAIRHOFER, V. MAURIN, H. MOSER, F. NEUMAIER, L. OSTANEK, V. RAJNER, W. RAUERT, H. SAGL, W.A. SCHNITZER & J. ZÖTL (1967): Ergebnisse der vergleichenden Markierungsversuche im Mittelsteirischen Karst 1966. – Steir. Beitr. z. Hydrogeologie, **18/19**, 331–404, Graz.

BAUER, F. (1972): Untersuchungen über die Verwendbarkeit von zwei Fluoreszenzfarbstoffen im Rahmen eines Färbeversuches. – Geol. Jb., **C 2**, 61–73, Hannover.

BAUER, F. (1975): Untersuchungen über die Verwendbarkeit von Tinopal CBS-X als Tracer. – Papers – 3rd Int. Symp. Underground Water Tracing (3. SUWT), Ljubljana-Bled, Sept. 27–Oct. 1, 1976, 17–25, Ljubljana.

BEHRENS, H. (1982): Verfahren zum qualitativen und quantitativen Nachweis von nebeneinander vorliegenden Fluoreszenztracern. – Beitr. z. Geologie d. Schweiz, Hydrologie, 28, 39–50, Bern.

BEHRENS, H. (1988): Quantitative Bestimmung von Uranin, Eosin und Pyranin in Gemischen mittels Fluoreszenzmessung bei definierten pH-Werten. – Steir. Beitr. z. Hydrogeologie, **39**, 117–129, Graz.

BEHRENS, H., A. BÖGLI, H. HÖTZL, W. KÄSS, Ch. LEIBUNDGUT, V. MAURIN, H. MOSER, V. RAJNER, D. RANK, W. STICHLER, H. ZOJER & J. ZÖTL (1981): Hydrogeologische Untersuchungen im Karst des hinteren Muotatales (Schweiz). – Steir. Beitr. z. Hydrogeologie, **33**, 125–264, Graz.

BEHRENS, H. & M. ZUPAN (1976): Methodik und Ergebnisse der Direktmessung der Fluoreszenztracer. – In: GOSPODARIČ, R. & J. ZÖTL (1976): Markierung unterirdischer Wässer (Untersuchungen in Slowenien 1972–1975). – Steir. Beitr. z. Hydrogeologie, **28**, 125–149, Graz.

BENISCHKE, R., J. GOLDBRUNNER & P. HACKER (1987): Postgraduate Training Course on Groundwater Tracing Techniques. Tracing Experiment 1987 Peggau–Semriach. Evaluation.– Unpubl. Rep., 26 p., Graz.

BENISCHKE, R. & P. HACKER (1989): 12th Postgraduate Training Course on Groundwater Tracing Techniques. Tracing Experiment 1989 Semriach–Peggau, Evaluation. – Unpubl. Rep., 28 p., Graz.

BENISCHKE, R. & P. HACKER (1990): Markierungsversuch Lursystem 1988. Zusammenstellung der Tracerdurchgänge. – Unpubl. Rep., 34 p., Graz.

BENISCHKE, R. & P. HACKER (1991): 13th Postgraduate Training Course on Groundwater Tracing Techniques. Tracing Experiment 1991 Semriach–Peggau, Evaluation. – Unpubl. Rep., 22 p., Graz.

BENISCHKE, R., T. HARUM & H. ZOJER (1988): Hydrogeologische Erfassung von Aquiferparametern und deren Wechselwirkung in einem Karst- und Porengrundwasserkörper, dargestellt im Bereich von Peggau, Mittelsteiermark, Teil II. – Unpubl. Rep., 72 p., Graz.

BENISCHKE, R. & T. HARUM (1990): Untersuchungsgebiet Lursystem. Kurzbericht über die Ergebnisse des Markierungsversuches im Herbst 1989. – Unpubl. Rep., 16 p., Graz.

BENISCHKE, R., H. ZOJER, P. FRITZ, P. MALOSZEWSKI & W. STICHLER (1988): Environmental and artificial tracer studies in an Alpine karst massif (Austria). Karst Hydrogeology and Karst Environmental Protection. – IAHS Publication No. 176, 938–947.

BOCK, H. (1913): Der Charakter des mittelsteirischen Karstes. – Mitt. f. Höhlenkunde, 6 (4), Juli 1913, Graz.

BOCK, H. (1917): Der Korallenfundpunkt im Lurloch.– Centralbl. f. Mineral., Geol. u. Paläont., 1917, 137–138, Stuttgart.

BRICELJ, M., G. KOSI & D. VRHOVSEK (1986): Tracing with Salmonella-phage P22H5. – In: MORFIS , A & H. ZOJER (Eds.): Karst Hydrogeology of the Central and Eastern Peloponnesus (Greece). – 269–271, Wien–New York (Springer).

DAVIES, S.N. & R. DEWIEST (1966): Hydrogeology. – 463 p, New York–London–Sydney (J. Wiley & sons).

DAVIS, G.H., T. DINCER, T. FLORKOWSKI, B. PAYNE & T. GATTINGER (1967): Seasonal variations in the tritium content of groundwaters of the Vienna basin. – Isotopes in Hydrology, I.A.E.A., 451–473, Vienna.

DECHANT, M. (1959): Das Anfärben von Lycopodiumsporen. – In: MAURIN, V. & J. ZÖTL (1959): Die Untersuchung der Zusammenhänge unterirdischer Wässer mit besonderer Berücksichtigung der Karstverhältnisse. – Steir. Beitr. z. Hydrogeologie, 10/11, 145–149, Graz.

DECHANT, M. (1967): Die Färbung der Lycopodiumsporen. – Steir. Beitr. z. Hydrogeologie, 18/19, 241–247, Graz.

DREISS, S. (1989a): Regional scale transport in a karst aquifer 1. Component separation of spring hydrographs. – Water Resour. Research, 25 (1), 117–125.

DREISS, S. (1989b): Regional scale transport in a karst aquifer 2. Linear systems and time moment analysis. – Water Resour. Research, 25 (1), 126–134.

DREYER, J. (1987): Anfärbung und Einsatz rotfluoreszierender Sporen als Grundwassermarkierungsmittel. – Unpubl. Diplomarbeit, 77 p., Freiburg/Br.

EBNER, F. & L. WEBER (1978): Die geologisch-tektonischen Verhältnisse zwischen Tannebenstock und Rötschgraben (Grazer Paläozoikum). – Mitt. Naturwiss. Ver. Stmk., 108, 95–113, Graz.

EBNER, F. (1983): Erläuterungen zur geologischen Basiskarte 1 : 50.000 der Naturraumpotentialkarte "Mittleres Murtal".– Mitt. Ges. Geol. Bergbaustud. Österr., 29, 99–131, Wien.

FANK, J. (1988): Program for calculation of calcite, dolomite and gypsum saturation in solution. – Institute for Geothermics and Hydrogeology, Joanneum Research, Graz.

FANK, J. T. HARUM, H.-P. LEDITZKY, B. STROMBERGER & H. ZOJER (1989): Nitratbelastung des Grundwassers im nordöstlichen Leibnitzer Feld (Steiermark). – Steir. Beitr. z. Hydrogeologie, 40, 5–48, Graz.

FLÜGEL, H.W. & NEUBAUER, F. (1984): Steiermark. Erläuterungen zur Geologischen Karte der Steiermark 1 : 200.000. – 127 p., 1 geol. map, Wien.

FLÜGEL, H.W. (Ed, 1975): Die Geologie des Grazer Berglandes. 2. ed. – Mitt. Abt. Geol. Paläont. Bergb. Landesmus. Joanneum, SH 1, 288 p., Graz.

FLÜGEL, H.W., V. MAURIN & K. NEBERT (1952): Zur Altersfrage von Schöckelkalk und Grenzphyllit im Grazer Paläozoikum. – Verh. Geol. B.-A., 1952, 129–142, Wien.

FRITZ, H. (1986): Zur Geologie des nordwestlichen Grazer Paläozoikums (im Bereich Schartnerkogel–Parmaseggkogel). – Unpubl. Diss., Univ. Graz, 209 p., Graz.

FRITZ, H. (1991): Stratigraphie, Fazies und Tektonik im nordwestlichen Grazer Paläozoikum (Ostalpen). – Jb. Geol. B.-A., 134 (2), 227–255, Wien.

FRITZ, P., A. CHERRY, K.U. WEYER & M. SKLASH (1976): Storm runoff analyses using environmental isotopes and major ions. – In: Interpretation of Environmental Isotope and Hydrochemical Data in Groundwater Hydrology, 111–130, IAEA, Wien.

GOLDBRUNNER, J.E. & H.-P. LEDITZKY (1979): Beitrag zur Klärung von Ionenaustauschvorgängen im Grundwasser durch die Kombination von hydrochemischen und tonmineralogischen Untersuchungen. – Steir. Beitr. z. Hydrogeologie, **31**, 151–161, Graz.

GOSPODARIČ R. & P. HABIČ (Eds., 1976): Underground Water Tracing – Investigations in Slovenia 1972–1975. – 312 p., Institute for Karst Research SAZU, Postojna, Yugoslavia.

GOSPODARIČ, R., P. HABIČ & A. KRANJC (Eds., 1976): Papers – 3rd International Symposium of Underground Water Tracing (3. SUWT), Ljubljana-Bled, Sept. 27–Oct. 1, 1976, Institute for Karst Research SAZU, Postojna. University Press Ljubljana, Yugoslavia.

GRABCZAK, J., P. MALOSZEWSKI, K. ROZANSKI & A. ZUBER (1984): Estimation of the tritium input function with the aid of stable isotopes. – Catena, **11**, 105–114.

GRAF, F. (1991): EDV-gestützte Analyse von Abflußrückgängen. – Unpubl. Diplomarbeit, Univ. Graz, 80 p., Graz.

GRAY, D.M. (1970): Handbook on the Principles of Hydrology. – Secretariat Canadian Nat. Com. for the International Hydrological Decade, Ottawa.

HARUM, T., H.P. LEDITZKY, H. ZOJER & W. STICHLER (1990): Utilisation de traceurs naturels pour la caractérisation de l'hydrodynamique et des changements temporaires dans deux systèmes aquifères karstiques. – Mémoires of the 22nd Congress of IAH, **XXII**, 392–404, Lausanne.

HERITSCH, F. & R. SCHWINNER (1932): Versteinerungen aus dem Schöckelkalk. – Verh. Geol. B.-A., **1932**, 149–152, Wien.

HILBER, V. (1912): Taltreppe. – 50 p., Graz.

HYDROGRAPHISCHES ZENTRALBÜRO (1983): Die Niederschläge, Schneeverhältnisse, Luft- und Wassertemperaturen in Österreich im Zeitraum 1971–80. – Beitr. z. Hydrographie Österreichs, **43**, 364 p., Wien (Hydrographisches Zentralbüro, Bundesministerium für Land- und Forstwirtschaft).

KÄSS, W. (Ed., 1972): 2. Internationale Fachtagung zur Untersuchung unterirdischer Wasserwege mittels künstlicher und natürlicher Markierungsmittel, Freiburg/Br. 1970. – Geol. Jb., **C 2**, Hannover.

KENNEDY, V.C., C. KENDALL, W. ZELLWEGER, T.A. WYERMAN & R.J. AVANZINO (1986): Determination of the components of stormflow using water chemistry and environmental isotopes, Mattole River Basin, California. – Journal of Hydrology, **84**, 107–140, Amsterdam.

KINDERMANN, J.C. (1779): Historischer und geographischer Abriß des Herzogthums Steyermark. – 1. Aufl., Grätz.

KOLLMANN, W. (1979): Erfahrungen bei Salzmarkierungsversuchen und deren Auswertung unter Berücksichtigung von Ionenaustauschvorgängen. – Steir. Beitr. z. Hydrogeologie, **31**, 143–150, Graz.

KOTT, Y. (1966): Estimation of low number of Escherichia coli bacteriophages by the most probable number method. – Applied Microbiology, **14**, 141–144.

KREFT, A. & A. ZUBER (1978): On the physical meaning of the dispersion equation and its solutions for different initial and boundary conditions. – Chem. Eng. Sci., **33**, 1471–1480.

KREFT, A., A. LENDA, B. TUREK, A. ZUBER & K. CZAUDERNA (1974): Determination of effective porosities by the two-well pulse method. – Isotope Techniques in Groundwater Hydrology, 295–312, IAEA, Wien.

KUSCH, H. (1972): Die Höhlen im Kugelstein bei Peggau (Steiermark). – Die Höhle, **23** (4), 145–157, Wien.

KUSCH, H. (1991): Das Blasloch (Kat.Nr. 2836/229) im Tannebenstock bei Semriach (Steiermark). – Die Höhle, **42** (1), 1–4, Wien.

KYRLE, G. (1928): Kombinierte Chlorierung von Höhlengewässern. – Speläolog. Monographien, **XII**, 94 p., Wien.

LEDITZKY, H.P. (1978): Interpretation von Ionenaustauschvorgängen beim Einsatz von Salzen zur Verfolgung unterirdischer Wasserwege durch Sedimentuntersuchungen. – Steir. Beitr. z. Hydrogeologie, **30**, 169–174, Graz.

LEDITZKY, H.P. (1981): Ionenaustauschphänomene beim Einsatz von Steinsalz als Markierungsmittel. – In: HARUM, T. & H. ZOJER (Eds., 1981): Festschrift Josef G. Zötl, 103–109, Graz (Forschungszentrum Graz).

LENDA, A. & A. ZUBER (1970): Tracer dispersion in groundwater experiments. – Isotope Hydrology **1970**, 619–641, IAEA, Wien.

MAILLET, E. (1905): Mécanique et physique du globe. – Essais d'hydraulique souterraine et fluviale.– 218 p., Paris.

MALOSZEWSKI, P. & A. ZUBER (1982): Determining the turnover time of groundwater systems with the aid of environmental tracers, 1. Models and their applicability. – Journal of Hydrology, **57**, 207–231, Amsterdam.

MALOSZEWSKI, P. & A. ZUBER (1984): Interpretation of artificial and environmental tracers in fissured rocks with a porous matrix. – Isotope Hydrology **1983**, IAEA, Wien.

MALOSZEWSKI, P. & A. ZUBER (1985): On the theory of tracer experiments in fissured rocks with a porous matrix. – Journal of Hydrology, **79**, 333–358, Amsterdam.

MALOSZEWSKI, P. & A. ZUBER (1990): On the parameter estimation from artificial tracer experiments.– ModelCARE90: Calibration and Reliability in Groundwater Modelling, IAHS Publication No. **195**, 53–62.

MALOSZEWSKI, P. & A. ZUBER (1991): Influence of matrix diffusion and exchange reactions on Radiocarbon ages in fissured carbonate aquifers. – Water Resour. Res., **27**, 1937–1945.

MALOSZEWSKI, P. & A. ZUBER (1992): On the calibration and validation of mathematical models for interpretation of tracer experiments in groundwater. – Advances in Water Resour. (in print).

MAURIN, V. & J. ZÖTL (1959): Die Untersuchung der Zusammenhänge unterirdischer Wässer mit besonderer Berücksichtigung der Karstverhältnisse. – Steir. Beitr. z. Hydrogeologie, **10/11**, 184 p., Graz.

MAURIN, V. (1951): Topographie und Geologie des Badlhöhlensystems. – In: MOTTL, M. (1951): Die Repolust-Höhle bei Peggau (Steiermark) und ihre eiszeitlichen Bewohner. – Archaeologia Austriaca, **8**, 2–15, Wien.

MAURIN, V. (1952): Ein Beitrag zur Hydrogeologie des Lurhöhlensystems. – Mitt. Nat. Wiss. Verein Stmk., **81/82**, 169–180, Graz.

MAURIN, V. (1953): Die geologischen Verhältnisse im Raum zwischen Deutschfeistritz und Semriach. – Unpubl. Phil. Diss., Univ. Graz, 117 p., Graz.

MAURIN, V. (1953): Über jüngste Bewegungen im Grazer Paläozoikum. – Verh. Geol. B.-A., **1953**, 216–220, Wien.

MAURIN, V. (1954): Das Paläozoikum im Raum zwischen Deutschfeistritz und Semriach. – Mitt. Nat. Wiss. Verein Stmk., **84**, 81–102, map 1 : 25.000, Graz.

MAURIN, V. (1960): Hydrogeologische Untersuchungen im Grazer Bergland und deren Wert für die Versorgungswasserwirtschaft. – Unpubl. Habil., Techn. Univ. Graz, 240 p., Graz.

MAURIN, V. (1975): Hydrogeologie und Verkarstung. – In: FLÜGEL, H.W. (Ed., 1975): Die Geologie des Grazer Berglandes. 2. ed. – Mitt. Abt. Geol. Paläont. Bergb. Landesmus. Joanneum, SH **1**, 223–269, Graz.

MAYER, A. sen. (1900): Tagebücher. – Archiv d. Landesver. f. Höhlenkd. i.d. Stmk.

MAYR, A. (1953): Blütenpollen und pflanzliche Sporen als Mittel zur Untersuchung von Quellen und Karstwässern. – Anz. math.-naturwiss. Kl., Österr. Akad. Wiss., **1953** (6), 94–98, Wien.

MORFIS, A. & H. ZOJER (Eds., 1986): Karst Hydrogeology of the Central and Eastern Peloponnesus (Greece). – 5th International Symposium on Underground Water Tracing, Athens 1986. – Steir. Beitr. z. Hydrogeologie, **37/38**, 301 p., Graz.

MOSER, H. & W. RAUERT (1980): Isotopenmethoden in der Hydrologie. – 400 p., Berlin–Stuttgart (Geb. Borntraeger).

MÜLLER, I. & J.G. ZÖTL (Eds.,1980): Karsthydrologische Untersuchungen mit natürlichen und künstlichen Tracern im Neuenburger Jura (Schweiz). – Steir. Beitr. z. Hydrogeologie, **32**, 5–100, Graz.

PFAFF, Th. (1987): Grundwasserumsatzräume im Karst der Südlichen Frankenalb. – GSF Rep. No. **3/87**, Munich.

QUINLAN, J.-F. & E.-C. ALEXANDER (1987): How often should samples be taken at relevant locations for reliable monitoring of pollutants from an agricultural, waste disposal, or spill site in karst terrane? First approximation. – Proc. of the 2nd multidisciplinary conference of sinkholes and the environmental impacts of karst, 277–286, Orlando, Florida 1987, (Balkema) Rotterdam.

RANK, D., G. VÖLKL, P. MALOSZEWSKI & W. STICHLER (1992): Flow dynamics in an Alpine karst massif studied by means of environmental isotopes. – The Use of Isotope Techniques in Water Resources Development, IAEA (in print).

ROGALSKI, R. (1988): Quantitative interpretation of tracer experiments performed in the karst of the Western Tatra Mts, Poland. – Proc. of the 5th Internat. Symp. on Underground Water Tracing, Athens 1986, 321–329, Institute of Geology and Mineral Exploration, Athens.

SCHICKOR, G. (1983): STEWEAG Kraftwerk Deutschfeistritz – Hydrogeologie. – Unpubl. Rep., 108 p., Bern.

SCHWINNER, R. (1925): Das Bergland nordöstlich von Graz. – Sitzungsber. Akad. Wiss., math.-naturwiss. Kl. (I) **134**, 219–276, Wien.

SEELMEIER, H. (1944): Beitrag zur Geologie des erzführenden Paläozoikums der Umgebung von Peggau–Deutschfeistritz bei Graz. – Ber. d. Reichsst. f. Bodenf., 1–25, map 1 : 50.000, Wien.

SEELY, N.D. & S.B. PRIMROSE (1982): The Isolation of Bacteriophages from the Environment.– Journal of Applied Bacteriology, **53**, 1–17.

SEILER, K.-P., P. MALOSZEWSKI & H. BEHRENS (1989): Hydrodynamic dispersion in karstified limenstones and dolomites in Upper Jura of Franconian Alb, FRG.– Journal of Hydrology, **108**, 235–247, Amsterdam.

SMITH, H.O. & M. LEVINE (1967): A Phage P22 gene controlling integration of phage. – Virology, **31**, 207–216.

STEIRISCHER GEBIRGSVEREIN, Fremdenverkehrs-Comité (Ed., 1882): Steirische Wanderbücher II. Semmering–Graz, Mürzzuschlag–Mariazell. – 66–67, Graz.

STICHLER, W. & H. ZOJER (1986): Umweltisotopenmessungen und hydrochemische Untersuchungen als Hilfsmittel für die Erfassung von Quelleinzugsgebieten. – Österr. Wasserwirtschaft, **38**, 261–266, Wien.

STOBER, I. (1988): Dispersion als Hinweis auf den Karsttypus. – Deutsche Gewässerkund. Mitt., H. **4**, 107–110.

THINNFELD, F. (1872): Die Peggauer Bäche. – Tagespost, Nr. **231**, Graz.

TSCHELAUT, W. (1985): Über das Alter der Arzberg-Schichten und der Blei-Zink-Vererzungen im Grazer Paläozoikum. – Jb. Geol. B.-A., **128** (2), 241–243, Wien.

VORMAIR, F. (1938): Studien im mittelsteirischen Karst. – Unpubl. Phil. Diss., Univ. Graz, 120 p., Graz.

VORMAIR, F. (1940): Die Dolinenwelt des mittelsteirischen Karstes. – Zeitschr. f. Geomorph., A.F., **11**, 123–150, Berlin.

WEBER, F. (1969): Die refraktionsseismischen Messungen im Murtal zwischen Peggau und Eggenfeld (Mittelsteiermark) und ihre Bedeutung für die hydrogeologische Erforschung der quartären Schotterbecken. – Steir. Beitr. z. Hydrogeologie, **21**, 5–25, Graz.

WEBER, L. (1990): Die Blei-Zinkerzlagerstätten des Grazer Paläozoikums und ihr geologischer Rahmen. – Arch. f. Lagerst.-forsch. Geol. Bundesanst., **12**, 289 p., Wien.

WEISSENSTEINER, V. (1966): Die G.W. Geßmann-Doline auf der Tanneben bei Peggau (Steiermark), Kataster-Nr. 2836/6. – Die Höhle, **17** (2), 44–48, Wien.

WEISSENSTEINER, V. (1969): Der Hammerbach bei Peggau (Steiermark, Kat.-Nr. 2836/34). – Die Höhle, **20** (4), 113–123, Wien.

WEISSENSTEINER, V. (1972): Das Wildemannloch bei Peggau (Steiermark).– Die Höhle, **23** (4), 135–144, Wien.

WINKLER-HERMADEN, A. (1955): Ergebnisse und Probleme der quartären Entwicklungsgeschichte am östlichen Alpensaum außerhalb der Vereisungsgebiete. – Denkschr. Österr. Akad. d. Wiss., math.-naturwiss. Kl., **110** (1), 180 p., Wien.

WINKLER-HERMADEN, A. (1957): Geologisches Kräftespiel und Landformung. – 822 p., Wien (Springer).

WURMBRAND, G. (1871): Ueber die Höhlen und Grotten in dem Kalkgebirge bei Peggau. – Mitt. Naturwiss. Ver. Stmk., **2** (3), 407–428, 3 Abb., Graz.

ZOJER, H. & J. ZÖTL (1974): Die Bedeutung von Isotopenmessungen im Rahmen kombinierter Karstwasseruntersuchungen. – Österr. Wasserwirtschaft, **26 (3/4)**, 62–70, annex 1–6, Wien.
ZOJER, H. (1981): Report on the Postgraduate Training Course on Groundwater Tracing Techniques. – Unpubl. Rep., 22 p., Graz.
ZOJER, H. (1983): Report on the Ninth Postgraduate Training Course on Groundwater Tracing Techniques (29 August–30 September 1983). – Unpubl. Rep., 10 p., Graz.
ZOJER, H. (1985): Report on the Tenth Postgraduate Training Course on Groundwater Tracing Techniques (26 August–27 September 1985). – Unpubl. Rep., 8 p., annex 1–7, Graz.
ZÖTL, J. (1971): Ergebnisbericht zum Forschungsprojekt "Entwicklung und Verbesserung von aktivierungsanalytischen Tracern (Markierungsstoffen) zur Verfolgung unterirdischer Wasserwege" im Jahre 1970. – Unpubl. Rep., 22–26, Graz.
ZÖTL, J. (1971): Report on the Postgraduate Training Course on Groundwater Tracing Techniques (30 August–2 October 1971). – Unpubl. Rep., 31 p., Graz.
ZÖTL, J. (1973): Report on the Postgraduate Training Course on Groundwater Tracing Techniques (27 August–29 September 1973). – Unpubl. Rep., 27 p., Graz.
ZÖTL, J. (1975): Report on the Postgraduate Training Course on Groundwater Tracing Techniques (25 August–25 September 1975). – Unpubl. Rep., 33 p., Graz.
ZÖTL, J. (1977): Report on the Postgraduate Training Course on Groundwater Tracing Techniques (29 August – 1 October 1977). – Unpubl. Rep., 24 p., Graz.
ZÖTL, J. (1979): Report on the Postgraduate Training Course on Groundwater Tracing Techniques (27 August–29 September 1979). – Unpubl. Rep., 23 p., Graz.
ZUBER, A. (1974): Theoretical possibilities of the two-well pulse method. – Isotope Techniques in Groundwater Hydrology, 277–294, IAEA, Wien.

Acknowledgements

We owe special thanks to the following institutions and organizations for their financial and organizational support:

- Bundesministerium für Wissenschaft und Forschung, Vienna, Austria;
- Grazer Stadtwerke AG, Wasserwerk, Graz, Austria;
- Joanneum Research (B. BAYER, R. URANSCHEK), Graz, Austria;
- Referat für wasserwirtschaftliche Rahmenplanung, Amt der Steiermärkischen Landesregierung, Graz, Austria;
- Steirische Wasserkraft- und Elektrizitäts-AG STEWEAG, Graz, Austria.

For providing references and data from the archives we have to thank

- Hydrographische Landesabteilung, Amt der Steiermärkischen Landesregierung, Graz, Austria;
- Landesverein für Höhlenkunde (V. WEISSENSTEINER), Graz, Austria.

Our thanks are also due to the following institutions and persons who supported the investigations with their engagement (execution of field and laboratory measurements, sampling, supplying of data, cartographic performance of the publication, translations and revisions of parts of the english text):

- B. HARUM (Leoben),
- Lehrstuhl und Referat für Wassergüte und Abfallwirtschaft (Technical University Munich),
- M. MEHLIN (GSF Munich, Institut für Hydrologie),
- S. MÜLLER (IGH Graz),
- F. REISS (IGH Graz),

- I. SCHABER (Freiburg/Br.),
- N. SCHNALZER (IGH Graz),
- P. SCHRAMEL (GSF Munich, Institut für ökologische Chemie),
- E. STELZL (IGH Graz),
- B. STROMBERGER (Hydrographische Landesabteilung Graz),
- G.M. TEICHMANN (GSF Munich, Institut für Hydrologie),
- H.R. WERNLI (Geographisches Institut Berne),
- B. ZIRNGAST (IGH Graz).